This project aimed at providing constructive and process engineering measures to guarantee sufficient melting of the flux and to avoid flux entrapment. Extensive operational investigations were carried out to identify parameters important for this flux-flow behaviour as well as to elaborate optimum set-points and SEN designs. Various methods for measuring flux layer thickness and horizontal flow velocity in the mould — important parameters influencing flux behaviour — were partly developed and applied.

Investigations covered flat and long products as well as carbon and stainless steels. Substantial physical and mathematical modelling work was carried out to provide additional information on the correlation between operational parameters and flux behaviour. Here, advanced techniques with regard to simulation of flux layer evolution and formation — also under the influence of flow conditions in the mould — were applied. Modelling results were verified by operational trials.

The research made it possible to identify certain parameters that are important for controlling flux behaviour according to goals: casting velocity, immersion depth, oscillation stroke, nozzle design and the free carbon content and viscosity of the flux. Also possible was the elaboration of statements concerning the proper adjustment of these parameters. On the other hand, parameters such as melt superheat or intensity of electromagnetic stirring have minor influence.

A very important fact is that unsteady conditions increase the risk of entrapment. Here, there is a high risk when casting begins, and until the process achieves a certain degree of stability. Moreover, a loss in mould level stability or changes in near-surface flow velocities of the melt must be avoided.

The results of this research are clearly useful for many European steel producers. To guarantee optimum flux behaviour, the parameters must be finely tuned to match the specific situation of an individual plant. The research demonstrates possible approaches to do this.

KI-NA-23182-EN-S

Price (excluding VAT) in Luxembourg: EUR 20

Publications Office
Publications.europa.eu

ISBN 978-92-79-07683-1

EC

Enhanced steel product quality and productivity through improved flux performance in the mould by optimising the multiphase flow conditions and with special regard to melting and entrapment EUR 23182

EUROPEAN COMMISSION

Community research

Enhanced steel product quality and productivity through improved flux performance in the mould by optimising the multiphase flow conditions and with special regard to melting and entrapment

PROJECT REPORT

Research Fund for Coal & Steel

Interested in European research?

RTD info is our quarterly magazine keeping you in touch with main developments (results, programmes, events, etc.). It is available in English, French and German. A free sample copy or free subscription can be obtained from:

Directorate-General for Research
Information and Communication Unit
European Commission
B-1049 Brussels
Fax (32-2) 29-58220
E-mail: research@ec.europa.eu
Internet: http://ec.europa.eu/research/rtdinfo/index_en.html

How to obtain EU publications

Our priced publications are available from EU Bookshop (http://bookshop.europa.eu/), where you can place an order with the sales agent of your choice.

The Publications Office has a worldwide network of sales agents. You can obtain their contact details by sending a fax to (352) 29 29-42758.

EUROPEAN COMMISSION
Directorate-General for Research
Research Fund for Coal and Steel Unit

Contact: RFCS publications
Address: European Commission, CDMA 0/124, B-1049 Brussels
Fax (32-2) 29-65987; e-mail: rtd-steel@ec.europa.eu

European Commission

Research Fund for Coal and Steel

Enhanced steel product quality and productivity through improved flux performance in the mould by optimising the multiphase flow conditions and with special regard to melting and entrapment

R. Striedinger ([1]), L. F. Sancho, J. Díaz ([2]), M. De Santis, M. R. Ridolfi ([3]), A. Poli, A. Bennani ([4]), J. Laraudogoitia, J. Ciriza ([5]), J. Holzhauser, L. Ernenputsch ([6])

([1]) **Betriebsforschungsinstitut (BFI) —** Sohnstraße 65, D-40237 Düsseldorf
([2]) **Arcelor España, S.A. (Arcelor España) —** P. O. Box 90, E-33480 Avilés
([3]) **Centro Sviluppo Materiali S.p.A. (CSM) —** Via di Castel Romano 100, I-00128 Rome
([4]) **Cogne Acciai Speciali S.r.l. (C.A.S.) —** Via Paravera 16, I-11100 Aosta
([5]) **Sidenor Investigation Y Desarrollo S.A. (Sidenor I+D) —** Barrio Ugarte S/N, E-48970 Basauri
([6]) **ThyssenKrupp Nirosta GmbH (TKN) —** Alleestraße 165, D-44795 Bochum

Contract No RFSR-CT-2003-00027
1 September 2003 to 28 February 2007

Final report

Directorate-General for Research

2008 EUR 23182 EN

Europe Direct is a service to help you find answers to your questions about the European Union

Freephone number (*)**:**

00 800 6 7 8 9 10 11

(*) Certain mobile telephone operators do not allow access to 00 800 numbers or these calls may be billed.

A great deal of additional information on the European Union is available on the Internet. It can be accessed through the Europa server (http://europa.eu).

Cataloguing data can be found at the end of this publication.

Luxembourg: Office for Official Publications of the European Communities, 2008

ISBN 978-92-79-07683-1

ISSN 1018-5593

Printed in Luxembourg

PRINTED ON WHITE CHLORINE-FREE PAPER

Table of contents

1. Final Summary

1.1 Introduction and objectives

Optimum melting of flux and behaviour of the molten flux pool situated above the steel melt surface as well as the avoidance of flux entrapment are important requirements to be achieved simultaneously for a stable casting process and a high product quality. The mould casting powder has to satisfy various requirements like lubrication, promotion of uniform heat-transfer, inclusion absorption, thermal insulation and chemical insulation.

The aim of the project performed by steel producers (Arcelor España, CAS, Sidenor and TKN) and research institutions (BFI and CSM) was to provide precise information on the necessary optimum constructive and process engineering measures to adjust casting conditions and as a result flow conditions in the mould in order to avoid flux entrapment into the mould and also to guarantee a sufficient thickness and behaviour of the flux layer floating on the steel melt.

The main objectives were:

- Provision of more detailed information on the interrelation between melting conditions of the flux floating on the steel melt, especially the dynamic behaviour of this flux layer and steel flow. Focus had to be given especially on what flow conditions are needed in the mould to guarantee a sufficient layer and behaviour of the flux pool and simultaneously to avoid entrapment of flux into the steel melt.
- Provision of a data base concerning optimised casting parameters (casting velocity, SEN immersion depth), SEN design to adjust the necessary flow conditions for given steel grades and selected casting powders. Also the influence of gas injection and of electromagnetic forces (EMS) had to be considered. Improvement of casting powders was also aim where necessary.
- Verification of this data base in the operational praxis.

1.2 Assembling and analysis of production plant data WP 1

Within the frame of this work package already existing data were assembled and analysed more detailed with regard to mould powder behaviour and its interrelation with operational specifications and parameters. Also supplementing data were assessed where necessary.

From all this work finally a parameter basis was set-up in order to define the most important parameters on which further investigations should aim at. So the following research activities were proposed for both modelling and industrial trials within the WP 2, 3 and 4.

Concerning **Sidenor**, it was decided to pay special attention to the following subjects:

- Characterisation of the mould powder consumption, key properties and assessment of possible trials for mould powder optimisation.
- Identification of the electromagnetic field threshold at meniscus position that leads to a significant mould level stability disturbance that could be promoting the appearance of powder entrapments.
- Plant trials with different immersion depths in order to assess thoroughly its influence on mould powder entrapment.
- Trials with nozzles with lateral ports due to its high theoretical influence on the in-mould steel flows.
- Industrial trials to characterise the mould powder liquid layer in order to provide to the CSM with the required data for the modelling activities.

At **CAS**, as a result of the data base realisation, the parameter basis for operational project investigation within WP3 was the following:

- Parameters related to powder: effect of viscosity and melting rate, also in relationship with casting speed, on incidence of slag entrapment on as-cast product. This called for a synergy with the CSM powder and flow modelling work ;
- Parameters related to fluid-dynamics: not only the effect of casting speed on quality was called for, but, since the effect of casting speed on mould flow, keeping all the other parameters constant, is to influence the steel velocity at the meniscus close to the slag layers, all the parameters potentially influencing local steel velocity at the interface steel-slag (apart of nozzle immersion depth not interesting and feasible for CAS features) were the following:
  - Effect of nozzle geometry
  - Effect of Electro Magnetic Stirring (coil current).

At **Arcelor España** the parameters to be further investigated were:

- SEN related parameters: immersion depth and geometry degradation
- Effect of mould level instabilities in downstream products
- Effect of mould level instabilities combined with superheating

For **TKN** the main conclusions of the data analysis task were the following:

- The wear of the SEN will not influence the overall steel flow pattern.
- The observed defects are related to the steel flow conditions near the meniscus
- Important factors regarding the flow field are:
  - Type of SEN
  - Casting velocity
  - Immersion depth

- Casting temperature

1.3 Operational investigations for flat products (WP 2)

In these investigations extensive trials were performed concerning parameters identified in WP 1 to be important with regard to flux melting and entrapment for flat products. Modelling results were verified and finally optimum constellations were determined.

The results achieved on plant can be generalised to refer to carbon and stainless slab casting in the following way.

The '*optimum constellation of process parameters/quantities*' concerning minimisation or avoiding of slag entrapment can be divided into two groups:

- powder features
  parameters/quantities belonging to it (plus casting temperature i.e. melt superheat) refer to the powder properties and are of most concern in determining the sintered and liquid layers thickness.
- fluid-dynamics
  parameters/quantities belonging to it refer to mechanical energy of the steel in the mould and in particular, to meniscus. They can be directly related to pouring operations (casting speed, SEN immersion depth, SEN geometry features), both in steady state and transient conditions (the latter being more critical).

Powder features

Concerning the powder features for stainless steel a *higher content of free C* increases the occurrence of defects. This seems to be due to the influence of the C-content on melting rate and thus on liquid flux layer thickness. A similar observation could be made on the long product section (see chapter 2.3.3.3.).

It was also seen that the thickness of the flux layer depends strongly on the powder used. This can lead to entrapment of powder which has a great impact on the occurrence of defects remaining on the steel surface.

From the information provided by the superheating, it can be concluded that the thermo-physical properties of the casting powder match well with the usual temperature range of the steel. If the superheat exceeds approx. 25°C an increase of entrapment seems to occur for carbon steels.

Fluid dynamics

The entrapment is more expected to be caused by local velocity variations due to unsteady flow conditions at the interface steel/flux even under steady state casting conditions.

The evolution of process variables along slab length and defects along the corresponding hot coil has been investigated for selected heats. It has been observed that the *mould level deviation* and the defects in the coil appear to be correlated along the casting length for heats with high amount of entrapment due to *high mould level fluctuations*.

Casting speed is affecting flux entrapment. Here not only the absolute value of the horizontal velocity near the interface steel melt/liquid flux has to be taken into consideration but also its fluctuation. For high casting speeds the liquid flux layer is increasing.

The fluid flow in the mould changes when *a change of SEN geometry* occurs along a casting sequence e.g. due to clogging. In order to see if, as supposed, the mentioned deterioration has impact on the entrapment context, a characterisation of clogged SENs was used in the numerical model. It has been seen that, when clogging occurs, it tends to concentrate around the SEN ports, in the well, and in the stagnant region of stream bifurcation.

Also concerning *SEN geometry* a larger SEN port leads to lower RMS-values concerning the horizontal flow velocity. Moreover the horizontal flow velocity is less sensitive with regard to SEN immersion depth.

Concerning the *SEN immersion depth* it could be stated that the flux layer thickness is decreasing with increasing immersion depth.

In case of carbon steel the SEN immersion depth within the current operational practice does not affect so significantly the occurrence of entrapment.

1.4 Operational investigations for long products (WP 3)

In these investigation extensive trials were performed concerning parameters identified in WP 1 to be important with regard to flux melting and entrapment for long products. Modelling results were verified and finally optimum constellations were determined.

The results achieved on plant can be generalised to refer to carbon and stainless steel billet casting in the following way.

Comparable to chapter 2.3.2.3. the '*optimum constellation of process parameters/quantities*' concerning minimisation or avoiding of slag entrapment can be divided into two groups:

- powder features
  parameters/quantities belonging to it (plus casting temperature i.e. melt superheat) refer to the powder properties and are of most concern in determining the sintered and liquid layers thickness.
- fluid-dynamics
  parameters/quantities belonging to it refer to mechanical energy of the steel in the mould and in

particular, to meniscus. They can be directly related to pouring operations (casting speed, SEN geometry features), both in steady state and transient conditions (the latter being more critical) or indirectly (stirring current, stroke).

First of all, the most important result in all cases is the fact that **first heats of the sequence** are more prone to slag entrapment occurrence. The most important reasons are the following:

- In-mould non-steady period at sequence beginning, basically due to the time required by the mould powder to reach stable conditions in terms of lubrication.
- Instabilities due to dummy bar withdrawal process.

The second aspect is mainly operational and needs great care. The first aspect makes the choice of the powder properties very important. The guidelines are listed below, followed by the 'flow' optimum quantities/parameters.

Powder features

Here the powder properties of most concern are the viscosity and the melting rate. Here viscosity is not the main quantity and should be properly coupled with *casting speed* and *melting rate*. In particular, carbon content, which melting rate depends strongly on, plays a strong role.

Since *the lower the steel grade carbon content*, the higher the shell shrinkage, a higher liquid slag production is required. To achieve that, *low values of free carbon content* are used to provide a higher melting rate and a homogeneous slag film between the mould and the solidified shell. The recommended content was found to *be below a critical value.* This critical value is 5% for stainless steels and 20% for carbon steels respectively.

On the other hand, *the higher the steel grade carbon content the lower should be the mould powder viscosity* in order to get a better liquid flux infiltration between billet and mould [27] indicates an optimum value of viscosity in Poise multiplied with casting speed in m/min equal to 3).

A further operating parameter related to slag entrapment occurrence was found to be *the stroke* (related to *powder consumption*) in the case of CAS casting situation. If higher (in the investigations related to CAS billet casting, exceeding 8 mm) the risk of such a defect is higher than that achievable if almost doubling the EMS coil current.

Fluid dynamics

All quantities related to steel flow at the interface steel-slag at the meniscus are involved in the phenomenon. In chapter 2.3.4 it will be shown, that a steel velocity threshold value should be exceeded to induce risks of slag entrapment. Within the operating ranges investigated for billet casting at Sidenor and CAS, these conditions were not attained. As a matter of fact, they are most likely to occur in long

product casting, where the higher flow rates can be not adequately managed with suitable nozzle geometries.

More in general, the quantities responsible for steel velocity at meniscus are *flow rate* (through *casting speed*, once fixed the as-cast format) and *nozzle geometry*, mainly through central throat diameter. As a general rule it should not be exceeded a value of 1.6 m/min as indicative ratio between volumetric flow rate and nozzle throat area to avoid the mentioned conditions risky for onset of steel-slag interface instability. Of course, *s*traight nozzles are less critical for such a problem, but lead to other quality problems as a 'cold' meniscus, affecting negatively to the mould powder working practice.

As refers to *nozzle immersion depth*, in general a deeper immersion makes the meniscus more 'quiet' and then less risky for slag entrapment, but again a 'cold' meniscus should be avoided. No general rules are here given, because how 'hot' the meniscus should be, depends on the steel grade, the casting speed and the powder on use. For example, at Basauri plant, an increase of the nozzle immersion depth up to 110-120 mm proved to be beneficial to enhance billet quality preventing mould powder entrapment.

For the configuration of the billet casters under study and for the coil current range considered, *in-mould electromagnetic stirring* was not found to play a great role in inducing risks of slag entrapment.

The above findings suggest that in general, unless the nozzle geometry is not adequate for the operating conditions, during steady-state billet casting slag entrapment is not very likely to occur. On the other hand, *unsteady conditions* (*start casting, flow oscillations due to alumina clogging flushes, improper nozzle position or local clogging in multi-hole nozzles*) can be the cause for the onset of the steel-slag interface instability. These phenomena are more common for flat product casting, due to the typical flow features induced by the bifurcated nozzles.

Nevertheless, the flow parameters should be always under control due to the fact that nowadays productivity and quality requests are higher and higher and this brings about higher casting speeds and more severe internal quality targets.

1.5 Physical and mathematical modelling (WP 4)

A further important point of view was the physical and mathematical modelling. CSM concentrated on the long products from Sidenor and CAS where as BFI concentrated on the flat products of Arcelor España and TKN.

Basing on a further analysis of operational results and on assessment of mould powder properties the numerical codes and the experimental facilities were set-up.

CSM performed investigations concerning the numerical simulation of the flux layer thickness and the flow conditions in moulds for long products. BFI performed investigations concerning formation of

liquid flux layer by physical and mathematical modelling as well as on fluid dynamic conditions at the interface steel melt/liquid flux.

Both partners investigated systematically the influence of relevant casting parameters identified in the previous work package on flux behaviour.

Finally optimum arrangements with regard to the objectives of this research were identified.

1.6 Conclusions

Extensive investigations concerning influences on and possibilities for controlling of flux melting and flux entrapment were performed.

Concerning detailed conclusions with regard to individual parameters and findings it is referred to chapters 2.3.2.3, 2.3.3.3 and 2.3.4.5. In this section here more general and summarising conclusions are drawn.

In operational trials correlations between operational trials and flux related defects could be successfully elaborated. Various methods for quality inspection as well as tools for statistical evaluation were proved to be useful to provide the necessary information basis.

Physical and mathematical modelling approaches were developed and applied successfully with regard to simulation of:

- flux in terms of melting rate and layer thickness
- 3-dimensional fluid flow in the mould also taken into consideration electromagnetic stirring
- multiphase flow in the mould in terms of
  - evolution and formation of liquid flux layer
  - separation behaviour of entrapped flux droplets

A critical horizontal melt velocity was identified, which should be avoided in order to minimise the risk of flux entrapment.

Measurement methods for assessment of flux layer thickness and flow velocity in an operational mould were provided and successfully applied.

The following mean guidelines with regard to sufficient melting of flux on the steel melt in the mould as well as to avoidance/minimisation of flux entrapment could be elaborated.

Flat products

Concerning *casting speed* and *immersion depth* an optimum could be found. In case of carbon steels the immersion depth, in the range investigated here, is not so significant.

A changing in *SEN geometry* due to wear or due to clogging has to be minimised. For the stainless steel also a larger port exit area leads to better results.

Mould level stability should be guaranteed to avoid entrapment due to fluctuations.

Concerning mould powder a sufficient low *content of free carbon* should be provided. The *superheat* of the melt has also an influence but not so significant for stainless steel within the frame of these investigations.

Long products

Concerning *casting speed* and *immersion* depth an optimum could be found.

Concerning stainless steel a *SEN geometry* with a five hole design including an enlarged bottom hole could be identified as positive.

The *electromagnetic stirring* has minor influence.

Concerning mould powder a sufficient low *content of free carbon* should be provided.

The *oszillation stroke* should be below a certain limit.

Overall the investigations showed clearly that unsteady operating conditions are the main cause for flux entrapment. Such conditions are given of course during start of casting where the process needs time to achieve a certain stability. A high risk of entrapment is given when a necessary thickness of liquid flux is not provided or temporarily this thickness falls below the necessary value. Also strong flow fluctuations e. g. caused by fluctuations of casting parameters can result e. g. in horizontal flow velocities of the melt reaching the value identified as critical for flux entrapment.

These guidelines are principle ones. Concrete values or set-points for operational parameters, SEN designs and powder types have to be adjusted to the specific production portfolio and plant constellation.

Also other production requirements could limit the application of these guidelines. This project demonstrates how this concretisation for a specific casting situation could be achieved.

1.7 Exploitation of results

The outcome of this research are guidelines for adjustment of operational parameters as well as of nozzle design with regard to a sufficient melting of the flux (e.g. sufficient liquid flux layer thickness) and to a minimisation/avoidance of flux entrapment.

Due to the fact that within the frame of these investigations producers of flat and long products casting carbon and stainless steels were involved the results should be useful for a wide range of European steel producers.

The producers involved in this project already have taken over the findings of this research where possible especially taking under consideration actual production requirements. Also plannings are now possible concerning plant or process modifications in order to exploit further results.

No patents were generated as outcome from this project.

2. Scientific and technical description of results

2.1 Objectives of the project

Optimum melting of flux and behaviour of the molten flux pool situated above the steel melt surface as well as the avoidance of flux entrapment are important requirements to be achieved simultaneously for a stable casting process and a high product quality. The mould casting powder has to satisfy various requirements like lubrication, promotion of uniform heat-transfer, inclusion absorption, thermal insulation and chemical insulation.

The aim of the project performed by steel producers (Arcelor España, CAS, Sidenor and TKN) and research institutions (BFI and CSM) was to provide precise information on the necessary optimum constructive and process engineering measures to adjust casting conditions and as a result flow conditions in the mould in order to avoid flux entrapment into the mould and also to guarantee a sufficient thickness and behaviour of the flux layer floating on the steel melt.

The main objectives were:

- Provision of more detailed information on the interrelation between melting conditions of the flux floating on the steel melt, especially the dynamic behaviour of this flux layer and steel flow. Focus had to be given especially on which flow conditions are needed in the mould to guarantee a sufficient layer and behaviour of the flux pool and simultaneously to avoid entrapment of flux into the steel melt.
- Provision of a data base concerning optimised casting parameters (casting velocity, SEN immersion depth), SEN design to adjust the necessary flow conditions for given steel grades and selected casting powders. Also the influence of gas injection and of electromagnetic forces (EMS) had to be considered. Improvement of casting powders was also considered for specific features.
- Verification of the know how assessed in the operational praxis.

The innovation proposed is the provision of detailed information on above mentioned processes and how to adjust properly the casting process with regard to casting parameters, SEN-design for given steel grades and types of fluxes.

Clear links existed between the involved steel producers and research institutions for a synergetic effect of gained results and measures for improvement of the previously mentioned objectives (**Figure 1**).

The proposed work should provide all this information for casting of flat and long products as well as for carbon and stainless steels (**Table 1**). The main slab and billet casting formats considered are listed in **Table 2**.

So a big spectrum of the production of European steel producers is covered and any of them can directly take benefit of the results of this research.

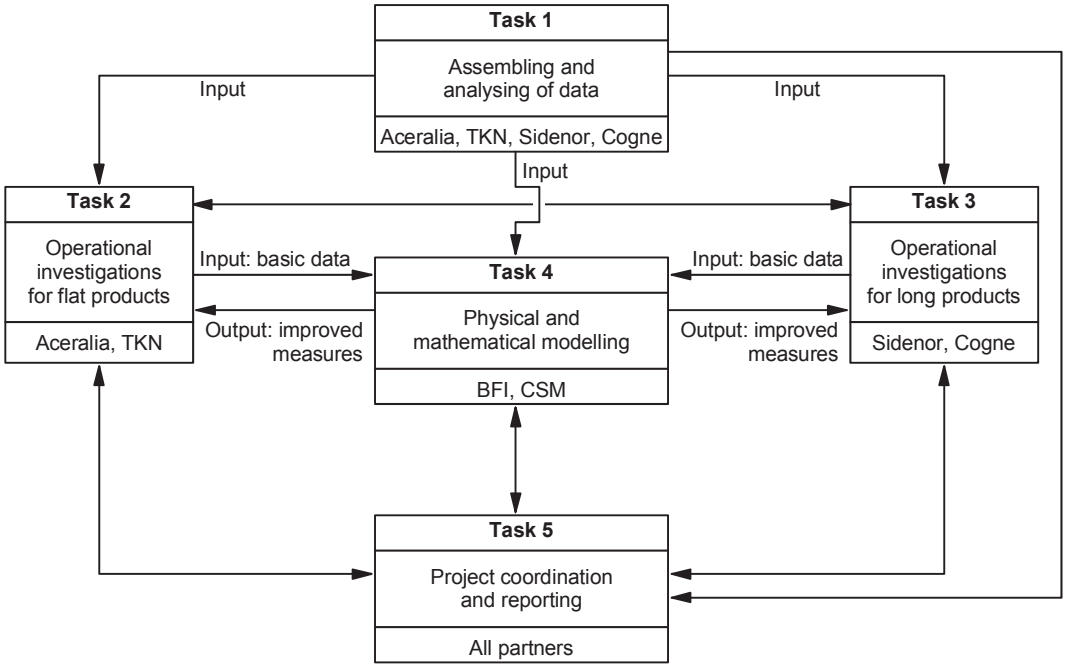

Figure 1 Structure of the project working programme

Table 1 General structure of the project

	Producers		Research institutions
	Stainless	Carbon	
Slab	TKN	Arcelor España	BFI
Billet	CAS	Sidenor	CSM

Table 2 Casting formats in this project

Producer	Width in mm	Thickness in mm
TKN	1300	240
Arcelor España	600 – 1200	220 / 280
CAS	160	
Sidenor	155 / 185	

2.2 Comparison of initially planned activities and work accomplished

All tasks were carried out according to the outlined working programme. No deviation from individual tasks is given.

2.3 Description of activities and discussion

2.3.1 Assembling and analysis of production plant data (WP 1)

The objective of this work package was to carry out an extensive analysis of plant data in order to develop a preliminary approach to the possible correlations between flux physic-chemical properties, flux melting conditions, casting parameters, lubrication, entrapment and steel grades composition. Based on the results of that preliminary approach, a starting point in terms of influential parameters for industrial trials and modelling was defined to be carried out within WP 3 and 4 respectively.

2.3.1.1 Assembling of already existing data (Task 1.1)

In this section, a description of the extensive collection of historical data related to standard heats affected with entrapments is presented. The aim was to obtain a preliminary approach to the entrapment problem and as much information as possible concerning the correlation between the standard operational parameters and the risk for mould powder entrapment. That information includes plant data related to flux types, flux properties, casting parameters, lubrication conditions, etc.

Facilities and operational data

Research has covered a wide range of steels going from carbon grades (Sidenor and Arcelor España) to stainless steels (CAS and TKN), and also both, long products (Sidenor and CAS) and flat products (Arcelor España and TKN).

The investigation concerning **Sidenor** contribution was carried out at the continuous casting machine CCM2 of Basauri Plant. **Table 3** shows its main characteristics, paying special attention to those features that play an important role in this research.

Table 3 Main characteristics of CCM2 (Sidenor)

	CCM2	
Tundish capacity	28 t	
Tundish to mould shrouding	SES	
Nozzle type	Straight nozzle	
Nozzle immersion depth	≈110 mm	
Steel flow control system	Pin-bolt stopper	
Gas injection	N_2 or Ar through stopper	
Mould tube	Parabolic, 1meter long	
Mould EMS standard intensity	270 A	
Mould section size	185 mm sq.	155 mm sq.
Average casting speed	1.25 m/min	1.70 m/min

CCM2 production programme covers a wide range of steels, going from free cutting steels to bearing steel grades, and mould powder is allocated depending on the billet format and steel carbon content according to **Table 4**. Mould powder viscosity was measured in the laboratory.

Table 4 Powder grade assignation criterion (Sidenor)

	Billet section: 185 mm sq.			
Steel carbon content in %	< 0.15	0.15 ÷ 0.35	0.35 ÷ 0.50	0.50 ÷ 1.00
Mould Powder Type	P1	P2	P3	P4
	Mould powder characteristics			
Viscosity at 1300ºC in Poise	37.9	10.0	12.7	5.5
Basicity as ratio CaO/SiO_2	0.7	0.8	0.7	0.6
Melting point in ºC	1130	1210	1220	1080

As far as **CAS** is concerned, the most important production data useful for the investigation in frame of this project is the following:

- Steel grade: stainless austenitic, martensitic, valve steel
- Main size: 160 mm square
- casting speed: 1.4 ÷ 1.6 m/min
- Strands: 4 with curved mould (780 mm long)
- Mould stroke: ±3 ÷ ±5 mm
- Frequency: up to 360 cpm
- Thermal monitoring system at meniscus: 20 k-type thermocouples
- Electro Magnetic Stirring devices as rotary in mould and final stirrer; current up to 350 A
- Level control: ± 2 mm (Berthold Co60) – METACON Tundish/Slide gate, with advanced mould monitoring system developed in the frame of a former ECSC project [1]
- Standard Nozzle: central diameter 30 mm, 5 holes: 4 inclined (+15° upwards), 1 at bottom (diameter 12 mm)
- Nozzle immersion depth: 120 mm (from port upper edge to meniscus)
- Mould water cooling flow rate: fixed, 1300 l/min
- Secondary cooling systems: air/mist, 8 segments
- Powders feeding system: mixed automatic/manual
- Flux layer thickness: 4 ÷ 5 mm for high basicity powders, 10 ÷ 15 mm for ‘acid’ powders
- Powder consumption: 0.25 ÷ 0.5 kg/ton
- Gas injected in nozzle: none
- Set of powders used: see **Table 5**. Mould powder viscosity was measured in the laboratory.

Table 5 Relevant properties of the powders considered in the database (CAS)

Powder	$T_{liquidus}$ in °C	Melting rate in mg/s	Viscosity at 1,300 °C in dPa s
A	1,190	63	1.6
B	1,215	23	6.4
C	1,190	9	3.4
D	1,180	23	1.0
E	1,190	139	3.1
F	1,190	28	0.9

As far as **Arcelor España** is concerned, the most important details concerning the facilities where this research has been carried out are the following:

- Steel grades: more than 200 different applications (API, Tin-plate, IF)
- Continuous casting: 2 Machines x 1 tundish x 2 strands
- Slab format:
  - Width: 600 ÷ 1600 mm
  - Thickness: 235/280 mm
  - Length: 5.5 ÷ 12 m
- The main features of the casters are the following:
  - Turning ladle turret with two arms
  - 60 ton tundish with sliding-gate valves
  - Tundish level control by weight
  - Mould level control by one sensor and one slide-gate valve for each mould
  - Sapsol system to prevent strand breakouts
  - Secondary cooling with air-mist spray
  - Top fed dummy bar
  - Curved mould
  - Caster with 4 radii unbending (10.5, 13.5, 19.5, 38.0 m)
  - Casting speed: 0.22 ÷ 2.2 m/min
  - Metallurgical length: 33.01 m
  - Distance between strands axes: 6 m
  - Distance between machine axes: 36 m

In the Bochum steelworks of **ThyssenKrupp Nirosta** austenitic and ferritic steel grades are produced. The steel grade 1.4301 is a mayor representation for the austenitic and the steel grade 1.4016 is a mayor representative for the ferritic steel grades. Both steel grades were investigated during the project; typically chemical composition is given in **Table 6**.

Table 6 Major steel grades - typical analyses for steel grades 1.4301 and 1.4016 (TKN)

	1.4301		1.4016	
	range of analysis %	average %	range of analysis %	average %
C	< 0.070	0.039	< 0.080	0.044
Si	< 1.00	0.41	< 1.00	0.32
Mn	< 2.00	1.23	< 1.00	0.29
Cr	17.00 – 19.50	18.13	16.00 – 18.00	16.13
Ni	8.00 – 10.50	8.54		0.20
N	< 0.1100	0.045		0.040
$T_{liquidus}$		1,459°C		1,499°C

In the Bochum melt shop an one strand bow-type casting machine is installed. This casting machine is equipped with a hydraulic driven resonance mould. The mould level and the immersion depth of the submerged entry nozzle (SEN) are automatically controlled. Two rows of 8 thermocouples in each row are installed for breakout production. The casting format covers widths from 800 – 1,650 mm and a thickness of 240 mm. Further characteristic features are listed in **Table 7**.

Table 7 Continuous casting machine in Bochum - characteristic data (TKN)

mould	length	704 mm
	narrow face taper	0.85% / 1.05 %
mould cooling	water supply	from the top
	water flow rate broad side	2 x 2800 l/min
	water flow rate narrow side	2 x 460 l/min
	$\Delta T_{broad\ side}$	5 - 6 K
	$\Delta T_{narrow\ side}$	2 - 3 K
oscillation	stroke	± 2 mm
	frequency	175 mm x casting speed ($V_{casting}$ = 1.1 m / min)
casting flux	addition	manual
	consumption	0.45 kg / to
	viscosity at 1,573 K	0.3 – 0.14 $kgm^{-1}s^{-1}$
	softening point	1,363 K
SEN	immersion depth	110 - 160 mm
	Type	50 x 70 mm 50 x 90 mm

To cast the above mentioned steel grades different casting powders as listed in **Table 8** are used. In case of the 1.4016 grade casting powders from different manufacturers are used. This powders have a similar chemical composition and also the overall casting behavior of these powders is very similar.

Table 8 Casting powders used average chemical composition and physical values (TKN)

Casting powder: Steel grades:	A 1.4016	B 1.4016	C 1.4301
Basicity (CaO/SiO_2)	0.85	0.9	1.14
Ca O+ MgO	34.0 %	34.0 %	35.5 %
SiO_2	39.5 %	37.5 %	31.0 %
Al_2O_3	4.5 %	4.5 %	6.7 %
Fe_2O_3	< 0.5 %	< 0.5 %	1.5 %
Na_2O	7.9 %	8.5 %	7.6 %
F	7.7 %	7.0 %	7.7 %
C_{free}	3.0 %	4.5 %	3.0 %
Melting temperature °C	1,100°C	1,100°C	1,120°C
Viscosity (1,200°C)	0.59 Pa·s	0.59 Pa·s	0.31 Pa·s
(1,400°C)	0.18 Pa·s	0.17 Pa·s	0.09 Pa·s

Mould powder viscosity was measured in the laboratory. All relevant process data from melting to cold rolling are stored in a company wide quality data base and can be used for analyses.

Criteria for mould powder entrapments identification

Prior to the creation of a Mould Powder Entrapment Database (MPEDB), **Sidenor** accomplished the prior definition of a set of criteria for the correct identification of a certain macroinclusion as a mould powder entrapment. Some of those identification criteria are common for every caster machine, but others depend on the specific characteristics of a certain machine in terms of refractories, slags and mould powder specifications. Below, a brief review of the different origins of a macroinclusion based on Sidenor experience is presented as well as the criteria for its correct identification based on its chemical composition.

There are different sources for macroinclusions, namely:

- Agglomeration of microinclusions
- Loose dirt, broken or wear refractory lining particles
- Interaction between steel bath and liquid slags
- Combination of some of the above sources

Agglomeration of microinclusions. It takes place at the refractory pouring duct between tundish and mould through the agglomeration of solid inclusions due to surface tension effect. Factors influencing built up phenomenon are reoxidation (oxygen sources: atmosphere, slags and refractories), steel cleanness, argon injection, steel bath temperature and refractory properties such as composition, geometry and roughness. The typical composition of that kind of macroinclusion can be one of the following ones:

- Alumina (Al_2O_3)

- Spinels ($MgO-Al_2O_3$)
- Calcium aluminates ($CaO-Al_2O_3-MgO$). See example in **Figure 2**
- Calcium sulphides (CaS)

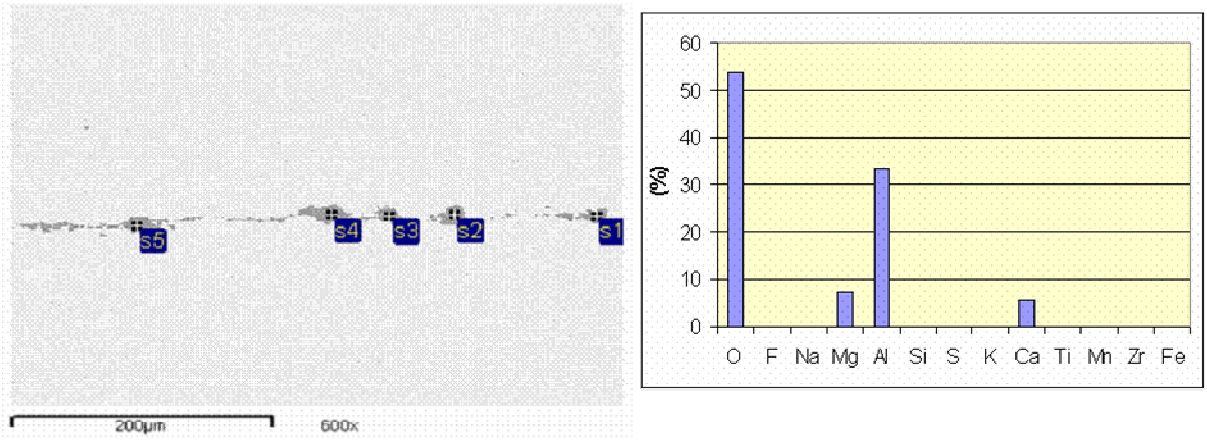

Figure 2 Example of macroinclusion – Agglomeration $CaO-MgO-Al_2O_3$ (Sidenor)

Loose dirt, broken or wear refractory lining particles. They come from ladle lining, tundish lining or tundish-to-mould refractories. Different phenomena can be responsible, namely: wear and spalling due to incorrect preheating or ageing. The typical refractory composition is the following:

- Ladle: MgO, dolomite
- Tundish: MgO
- Stopper, nozzle: Al_2O_3-C

It can be said that this is an uncommon phenomenon, except for nozzle wear at the meniscus. **Figure 3** shows an example of this type of macroinclusion. In that example the Zr content reveals the nozzle refractory as the origin of this macroinclusion. Nozzles have an external zirconia belt to diminish the refractory wear at meniscus position.

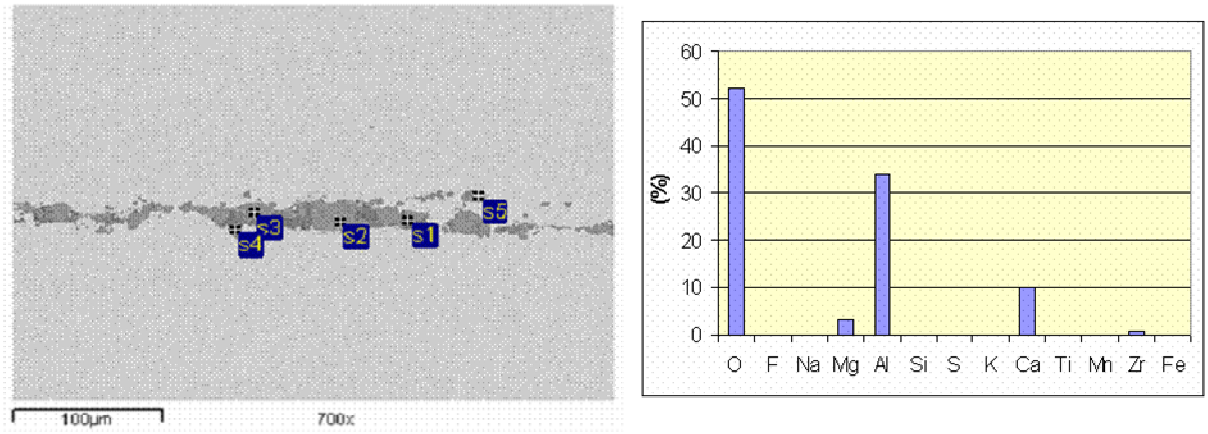

Figure 3 Example of macroinclusion – Calcium aluminate with nozzle remains (Sidenor)

Interaction between steel melt and liquid slags. This slag entrapment can take place in the ladle, tundish or mould; and there are different reasons for that phenomenon:

- Ladle:
  - Excessive stirring
  - Vortex during ladle draining process

    Figure 4 shows an example of this kind of macroinclusion. Its composition has a high resemblance with the ladle slag composition.
- Tundish:
  - Excessive turbulences (filling period)
  - Vortex during draining process
- Mould:
  - Mould level instabilities due to

    * excessive in-mould stirring conditions

    * stopper rod abnormal behaviour due to clogging or electromechanical problems
  - Malfunction of oscillation mechanism
  - Inadequate steel flows in the meniscus area due to

    * eccentric nozzle position

    * insufficient nozzle immersion depth

    * nozzle clogging

    * nozzle inner wear

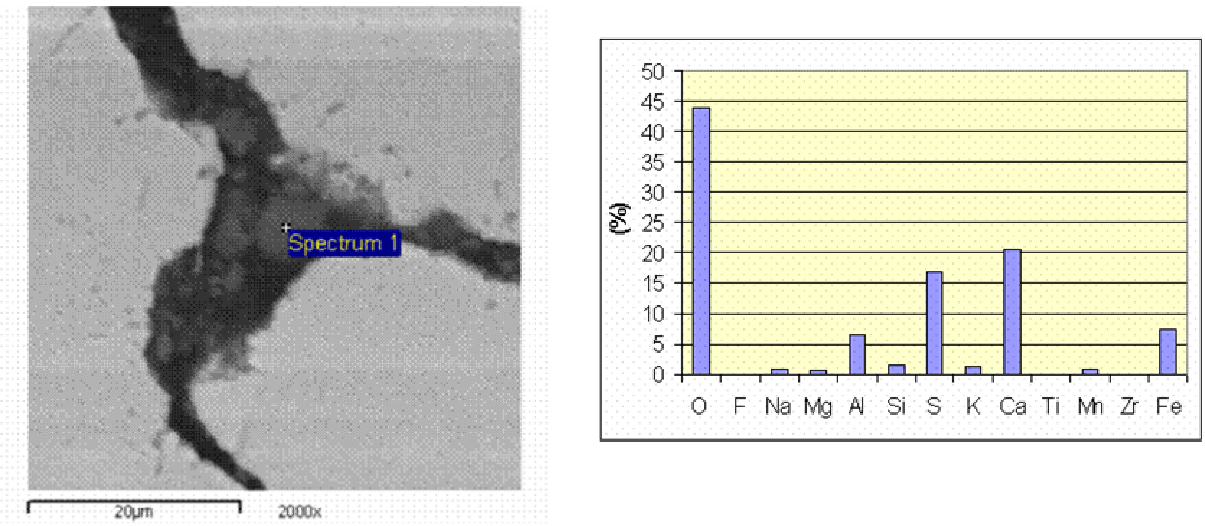

Figure 4 Example of macroinclusion – Ladle slag entrapment (Sidenor)

This kind of macroinclusion has been thoroughly analysed concerning the topic of this project, (mould powder entrapment, see example in **Figure 5**). In that case, mould powder was P6 (see Table 4). That figure also contains the mould powder chemical composition and it is possible to see an important

resemblance between macroinclusion chemical composition and mould powder P6 analysis. High contents of F and Na in the macroinclusion reveal clearly its origin as mould powder entrapment.

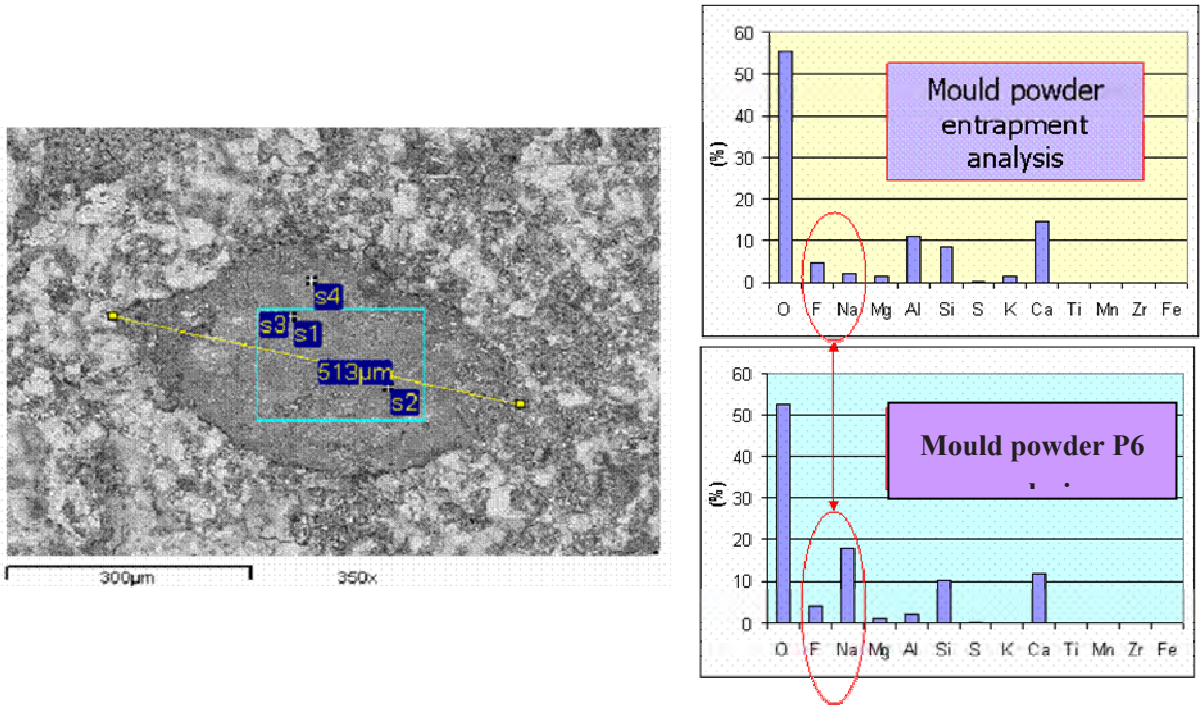

Figure 5 Example of macroinclusion – Mould powder entrapment (Sidenor)

Identification of the macroinclusion origin is usually hindered because some of the above phenomena can take place simultaneously giving rise to a complex macroinclusion structure. The most typical cases are listed below:

- Mould powder entrapment with nozzle remains. **Figure 6** shows an example of this phenomenon. This macroinclusion can be considered as mould powder entrapment.
- Calcium aluminate with nozzle remains.
- Calcium aluminate with mould powder traces. **Figure 7** shows an example. This macroinclusion can not be considered as mould powder entrapment. It is a calcium aluminate flush, dropped from the nozzle, that had some contact with mould powder. Na appears as a negligible trace.

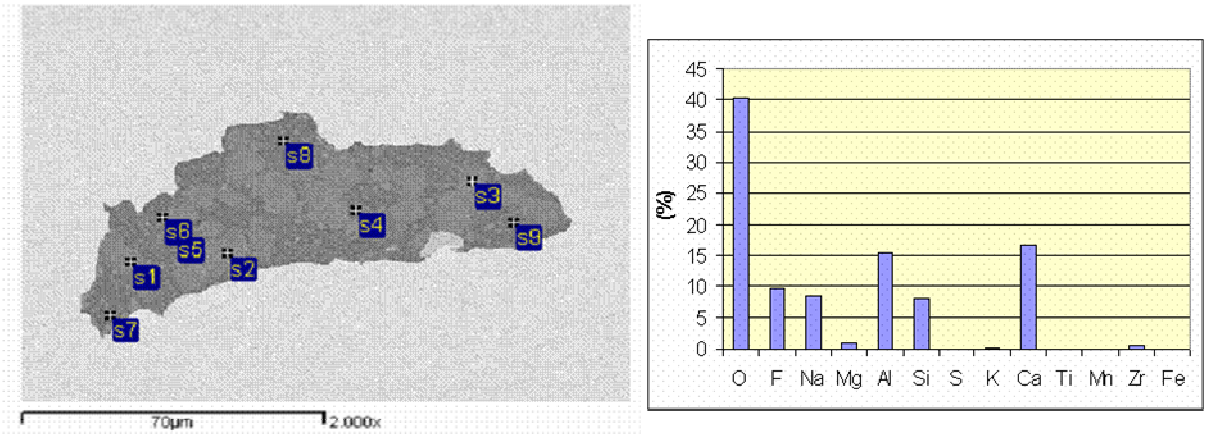

Figure 6 Example of macroinclusion – Mould powder entrapment with nozzle remains (Sidenor)

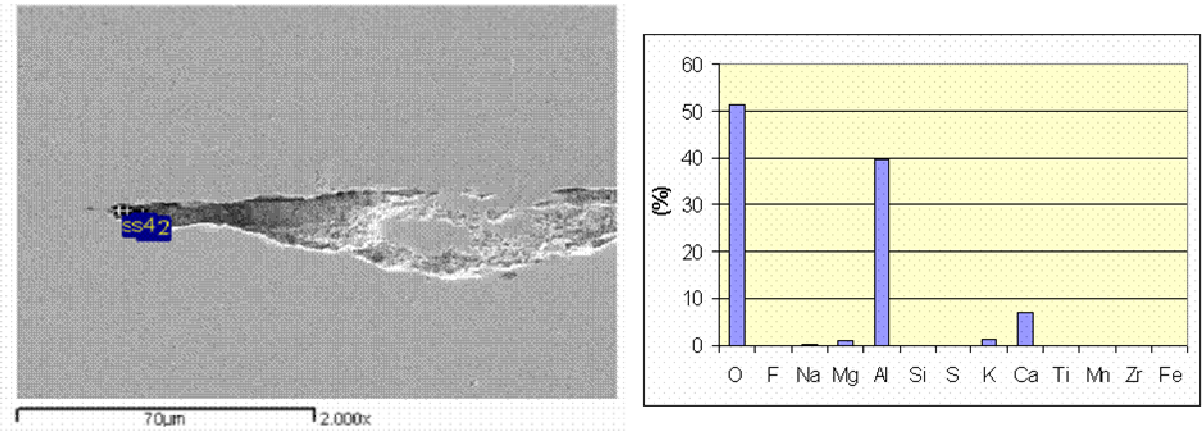

Figure 7 Example of macroinclusion – Calcium aluminate with mould powder traces (Sidenor)

Therefore, it is clear that the correct identification of the origin of the macroinclusions detected in the end product requires the proper characterisation of all the materials prone to become an exogenous macroinclusion, namely:

- Mould powders
- Tundish powders
- Refractory materials

This characterisation allows the correct identification of the macroinclusions analysed within this project. Concerning mould powder entrapment, its chemical composition gives hints for the accurate powder entrapment identification. In this respect Na, K and F can be used to identify the macroinclusions as powder entrapment (see Figure 5). Unfortunately, generally, macroinclusions have time to react with the steel melt and this leads to a modification of their composition, thus hindering the origin identification task.

At **TKN** all hot rolled and cold rolled coils produced are visually inspected with regard to surface defects. The information is stored in a data base. In case of unknown/new defects samples can be taken for metallografic and other investigations. In case of the ferritic grades (i.e. 1.4016) a surface defect near the edges can occur, which is visible as a white streak on the surface of the cold rolled coil. Metallographic examinations shows, that the defect is caused by the casting powder. The difference in chemical composition of the defective and not defective area is mainly a different carbon content (**Figure 8**). The only possible source of this additional carbon is the casting powder.

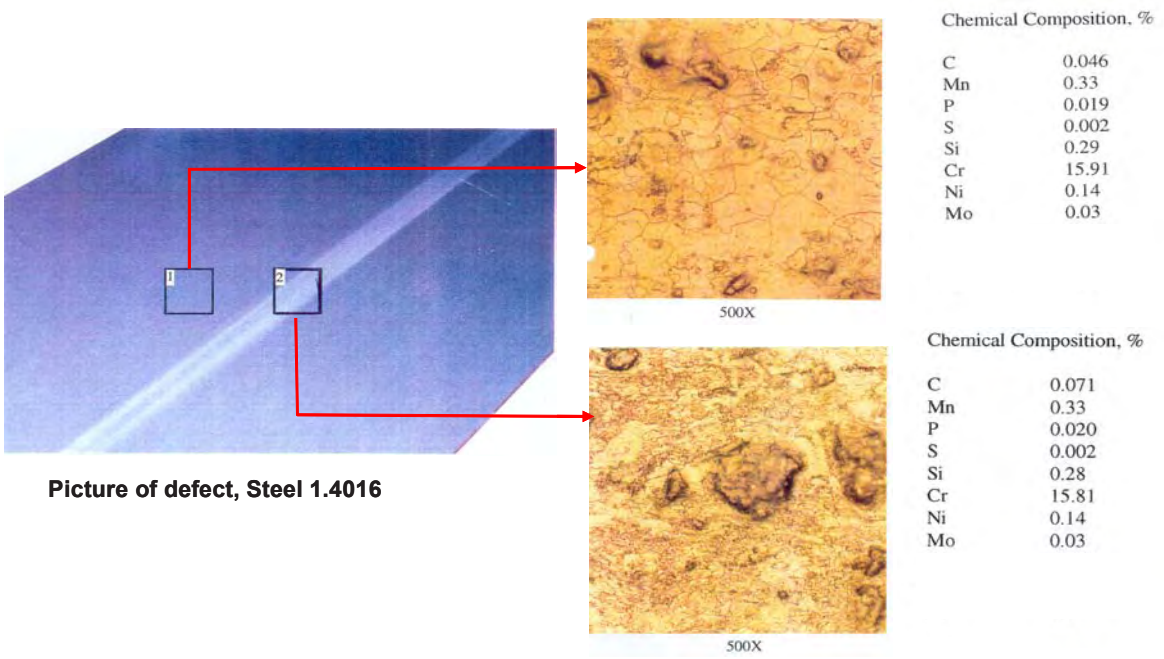

Figure 8 Casting powder related defect on steel grade 1.4016 (TKN)

2.3.1.2 Assessing of supplementing data (Task 1.2)

By means of using the identification method described in the previous section, a mould powder entrapment Data Base (MPEDB) was created by **Sidenor** based on historical data coming basically from the end product quality control inspection. Using this method, the MPEDB was fed with sixty four clear cases of mould powder entrapment. An intensive work of entrapment characterisation together with operational data collection and processing was carried out in order to collect as much information as possible related to entrapment characteristics (composition, morphology), mould powder characteristics (composition and properties) and operational parameters (casting speed, mould level position and stability, nozzle immersion depth, castability, number of heats in sequence, in-mould stirring conditions, and drawbacks related to nozzle performance such as excessive wear or nozzle breakage).

Table 9 shows the most important information concerning the MPEDB. As far as operational parameters are concerned, for this approach the most characteristic ones were selected, having an important theoretical influence over the steel flow at the meniscus and therefore on the risk for mould powder entrapment occurrence.

Table 9 MPEDB including the parameters related to the casting performance per heat (Sidenor)

Heat Number	Billet size	Steel Grade	Numb. Seq.	Tot. Seq.	Shape	Size	Macroinclusion Comp.	Powder Type	Aver. [Mould Level Std.dev.] (%)	Max. [Mould Level Std.dev.] (%)	Stopper Max-Min (mm)	Aver. [Stopper Std.dev.] (mm)	Max. [Stopper Std.dev.] (mm)	Aver [Cast. Speed] (m/min)	Aver. [Cast. Speed Std.dev.] (m/min)	Max. [Cast. Speed Std.dev.] (m/min)	Aver. [EMS Int.] (Amps)	Aver. Nozzle Inm. Depth (mm)	Gas Flow Rate (l/min)
20042	185	16MnCr5E	5	6	Amorphous	600um	Ca-Al-Si-F-Mg-Na-S	P1	0,82	1,66	2,33	0,17	0,505	1,18	0,00151	0,0249	271	106	0,8
59753	185	9SMn31	2	2	Spherical	60um	F-Mn-Ca-Zr-Si-Al-Na-Mg	P1	0,81	1,53	3,17	0,23	0,544	1,05	0,00139	0,0241	270	100	0,2
53603	185	34CrNiMo7	1	3	Elongated	230um	Al-Ca-Si-Na-Mg-K-Ti	P2	0,82	2,21	4,00	0,22	0,715	1,09	0,00190	0,0602	85	100	0,8
56266	185	20MoCr4HE	2	7	Elongated	120um	Si-Al-Mn-Na-K-Ca	P2	Data not available								271	105	0,8
57745	185	16CrNiPb5	3	3	Spherical	100um	Si-Ca-Al-Na-F-Mg-K	P2	0,93	2,45	13,40	0,45	1,251	1,25	0,00408	0,0747	250	105	0,7
18805	185	30MnV6S	5	5	Superficial crack	400um	Al-Ca-Si-Na-Mg-K-Ti	P2	0,80	1,69	3,40	0,17	0,505	1,25	0,00115	0,0346	271	105	0,8
19089	185	18CrNiMo4E	3	3	Elongated	500um	Ca-Si-Al-Na-Mg-Zr-S-K	P2	Data not available								270	104	0,8
19656	185	35CrMoPb4E	4	6	Elongated	7mm	Si-Na-Ca-Mg-Al	P2	0,75	1,39	5,20	0,15	0,506	1,31	0,00229	0,1132	271	104	0,8
20972	185	20Cr4	1	5	Amorphous	350um	Si-Al-Ca-K-Na-Mn	P2	0,89	5,67	4,83	0,21	0,995	1,15	0,00119	0,0707	271	108	0,8
21113	185	19NiMoCr6EJ	2	2	Amorphous	>60um	Al-Na-Mg-Si-K-Ca	P2	0,75	1,16	2,83	0,21	0,520	1,19	0,00101	0,0192	271	104	0,8
22132	185	20MoCrBI4E	1	6	Superficial crack	400um	Si-Ca-Al-Na-F-K-Mn-S	P2	1,00	2,15	4,50	0,30	0,744	1,14	0,00098	0,0296	271	106	0,8
22198	185	27MnCr5GR	1	4	Amorphous	600um	Si-Al-Ca-Na-Mg-Ti-K	P2	0,87	1,55	4,00	0,21	0,516	1,35	0,00016	0,0072	271	104	0,8
22810	185	19NiMoCr6EJ	6	6	Elongated	220um	Al-Na-Mg-Si-K-Ca	P2	0,81	1,29	2,83	0,14	0,508	1,10	0,00035	0,0246	271	102	0,8
23606	185	19CrMoNiV5FD	8	8	Amorphous	128um	Al-Ca-Mg-Si-S-K-Na	P2	0,83	1,70	2,83	0,14	0,525	1,15	0,00074	0,0137	270	100	0,8
24568	185	25MnCr5E	4	5	Elongated	400um	Al-Ca-Si-Na-Mg-K-Ti	P2	0,87	1,95	6,50	0,22	0,708	1,14	0,00124	0,0474	271	106	0,8
25134	185	25MnCr5E	2	6	Amorphous	128um	Si-Na-Ca-Mg-Al	P2	0,82	1,66	4,96	0,14	0,345	1,14	0,00047	0,0155	271	103	0,8
27081	185	34CrNiMo6	3	3	Superficial crack	60um	Si-Na-Ca-Mg-Al	P2	0,64	1,30	2,28	0,12	0,276	1,29	0,01487	0,1136	271	105	0,8
29844	185	19CrMoNiV5FD	1	3	Amorphous	120um	Al-Ca-Mg-Si-S-K-Na	P2	0,77	1,45	2,65	0,12	0,274	1,16	0,00585	0,0343	271	104	0,8
31671	185	18NiCrMo5E	1	3	Elongated	>5mm	F-Ca-Si-Al-Na-K-Mn	P2	0,78	1,66	10,70	0,14	0,398	1,28	0,00666	0,0540	271	105	0,8
32766	185	25MnCr5E	4	5	Amorphous	278um	Ca-Si-Al-Na-Mn	P2	Data not available								271	104	0,8
32824	185	29CrMo4FD	3	4	Spherical	100um	F-Ca-Si-Al-Na-K-Mn	P2	0,83	5,40	4,90	0,14	0,898	1,37	0,00897	0,1290	271	105	0,8
54351	185	42CrMo4AV	1	5	Elongated	7mm	Si-Al-Ca-Na-Mg-Ti-K	P3	1,05	2,21	11,50	0,56	0,721	1,32	0,00172	0,0279	221	106	0,8
17529	185	42CrMo4GRA	1	5	Elongated	5mm	Si-Al-Mn-Na-K-Ca	P3	0,78	2,44	3,33	0,17	0,598	1,25	0,00078	0,0241	269	100	0,8
18912	185	42CrMo4E	5	8	Amorphous	100um	Al-Ca-Si-Na-Mg-K-Ti	P3	0,80	1,52	5,83	0,19	0,517	1,33	0,00000	0,0000	271	103	0,8
20889	185	45Cr4E	5	5	Elongated	>150um	Al-Ca-S-Mn-Mg-F-K-Na	P3	0,78	1,25	2,67	0,15	0,509	1,34	0,00110	0,0248	271	107	0,8
21189	185	42CrMo4E	8	8	Elongated	>200um	Ca-Si-Al-Na-Mn	P3	0,92	2,10	5,00	0,22	0,712	1,31	0,00052	0,0223	271	105	0,8
27999	185	41Cr4	6	6	Superficial crack	80um	Ca-Si-Al-Na-Mn	P3	1,03	3,84	9,96	0,26	1,578	1,42	0,00496	0,0896	271	100	0,8
32519	185	C45E	4	5	Elongated	>200um	Si-Al-Ca-Na-Mg-Ti-K	P3	0,70	1,32	3,61	0,13	0,273	1,15	0,00480	0,0071	271	104	0,8
56108	185	100Cr6D	2	2	Elongated	500um	Al-Ca-Si-Mg-Na-S	P4	0,87	1,91	9,60	0,50	0,729	1,14	0,00080	0,0377	260	110	0,8
24866	185	C70E	3	3	Elongated	4mm	Al-Ca-Si-Na-Mg-K	P4	0,81	1,93	6,17	0,18	0,643	1,15	0,00000	0,0000	271	104	0,8
26634	185	C55E	2	4	Elongated	900um	Si-Na-Al-Ca-K	P4	0,72	1,17	6,80	0,19	0,523	1,15	0,00000	0,0000	271	102	0,8
31225	185	C55E	3	5	Elongated	200um	Al-Na-Mg-Si-K-Ca	P4	0,67	1,15	3,66	0,12	0,219	1,15	0,00405	0,0071	271	104	0,8
31575	185	C55E	5	5	Elongated	450um	Si-Al-Ca-K-Na-Mn	P4	0,72	1,39	4,03	0,13	0,247	1,15	0,00552	0,0080	271	104	0,8
32322	185	C55E	3	3	Elongated	>100um	Ca-Al-Si-F-Mg-Na-S	P4	0,78	1,53	4,04	0,14	0,365	1,15	0,00426	0,0149	271	103	0,8
57124	155	18NiCrMoPb6	2	3	Elongated	>4mm	Al-Mg-Ca-Na-K	P5	0,93	5,21	5,60	0,25	1,046	1,67	0,00425	0,1418	251	103	0,6
57188	155	C43NBE	2	2	Superficial crack	60um	Ca-Na-Si-F-Al-Mg-K-Zr	P5	Data not available								271	105	0,6
58570	155	DF34Cr5	4	6	Elongated	>100um	Si-Ca-Al-Na-Mn-K-Cr-Zr	P5	0,78	2,23	2,80	0,26	0,585	1,60	0,00022	0,0138	271	105	0,4
59907	155	27MnCr5HE	4	7	Elongated	>200um	Al-Ca-F-Na-Si-S-K	P5	0,79	1,31	8,17	0,19	0,515	1,62	0,00074	0,0220	270	104	0,6
51493	155	28CrMoV9E	1	1	Elongated	>400um	F-Ca-Si-Al-Na-K-Mn	P5	Data not available								271	105	0,6
21643	155	42CrMo4EA	1	5	Elongated	450um	Al-Si-Na-K-Ti-Mn-Cr	P5	0,73	1,40	3,20	0,15	0,542	1,73	0,00373	0,0525	271	105	0,6
23379	155	37Cr4FDJ	5	5	Elongated	200um	Al-Na-Mg-K-Ca-Mn	P5	0,75	1,27	3,00	0,18	0,506	1,70	0,00174	0,0251	271	105	0,3
24884	155	C43E	1	5	Spherical	100um	Al-Na-Mg-Si-K-Ca	P5	0,70	2,67	6,33	0,16	0,518	1,65	0,00259	0,0866	271	105	0,6
25006	155	C48EA	3	5	Elongated	4mm	Ca-Al-Si-Mg-S-Na-Mn	P5	1,08	5,68	6,17	0,33	1,353	1,60	0,00226	0,0962	271	105	1,0
27048	155	37Cr4E	7	7	Spherical	60um	Ca-Al-Si-F-Mg-Na-S	P5	0,64	1,11	2,26	0,11	0,206	1,79	0,00112	0,0472	271	104	0,6
55019	155	99Cr6D	2	2	Elongated	230um	Al-Na-Mg-Si-K-Ca	P6	Data not available								271	102	0,6
55338	155	56SiCrV7	1	5	Elongated	500um	Si-Ca-Al-Na-F-Mg-K	P6	Data not available								270	100	0,3
57243	155	50CrMo4E	3	3	Superficial crack	80um	Si-Ca-Al-Mn-Na-Mg-K	P6	0,77	1,13	7,50	0,24	0,543	1,81	0,00283	0,0780	270	106	0,6
57614	155	99Cr6D	2	2	Elongated	>5mm	Al-Mg-Na-K-Ca	P6	Data not available								271	100	0,6
57614	155	99Cr6D	2	2	Elongated	120um	Si-Ca-Al-Na-F-K-Mn-S	P6	Data not available								271	100	0,6
58358	155	99Cr6D	2	2	Elongated	400um	Al-Ca-Si-Mg-Na-K-Ti	P6	Data not available								271	100	0,6
58808	155	99Cr6D	2	2	Superficial crack	>2mm	Al-Ca-Si-Na-Mg	P6	0,91	2,07	3,40	0,13	0,584	1,52	0,00086	0,0264	271	105	0,4
17384	155	C50E	4	8	Elongated	>8mm	Al-Ca-Mg-Na-K-Si-S	P6	0,70	1,19	3,20	0,11	0,523	1,92	0,00151	0,0251	271	105	0,3
17783	155	55SiCr6D	1	4	Amorphous	278um	Al-Si-Mg-Ca-K-Na	P6	0,82	1,58	5,17	0,28	0,522	1,66	0,00169	0,0709	271	100	0,6
18085	155	50CrMo4E	3	7	Amorphous	1mm	Al-Ca-Si-Mg-Na-S	P6	0,92	1,62	6,33	0,22	0,515	1,80	0,00000	0,0000	271	105	0,6
19204	155	51CrVMo4FD	3	7	Elongated	500um	Ca-Al-Si-F-Na-Mg-K-S	P6	0,81	1,21	2,33	0,21	0,506	1,80	0,00073	0,0431	271	105	0,6
19301	155	53CrV5	6	6	Amorphous	4mm	Si-Na-Ca-Al-Mg-K	P6	0,95	2,96	8,33	0,56	1,949	1,76	0,00074	0,0281	272	105	0,8
21349	155	C60PbE	3	3	Elongated	>400um	Al-Ca-Mg-Si-S-K	P6	0,75	1,12	1,83	0,15	0,474	1,52	0,00025	0,0187	271	103	0,6
23634	155	62SiCr7	6	6	Amorphous	100um	Al-Mg-Ca-K-Si-Na-S	P6	0,71	1,38	1,83	0,09	0,466	1,75	0,00033	0,0182	271	103	0,3
25196	155	95Cr6D	1	6	Amorphous	200um	Al-F-Si-Ca-K-Mg-Ti	P6	0,78	2,06	4,40	0,21	0,776	1,45	0,00031	0,0158	271	105	0,0
28912	155	98Cr6E	1	3	Elongated	>400um	Ca-Na-Si-F-Al-Mg-K-Zr	P6	0,65	1,12	3,42	0,12	0,248	1,44	0,00628	0,0226	271	103	0,6
30211	155	C50E	1	4	Amorphous	4mm	Al-Ca-Si-Na-Mg-K-Ti	P6	0,67	1,21	3,63	0,12	0,287	1,70	0,00521	0,0543	291	102	0,3
31353	155	53CrMoV4FD	2	4	Amorphous	100um	Ca-Al-Si-F-Na-Mg-K-S	P6	0,66	1,03	1,63	0,13	0,228	1,86	0,00640	0,0737	291	106	0,6
31478	155	54SiCrV6F	1	7	Amorphous	200um	F-Mn-Ca-Zr-Si-Al-Na-Mg	P6	0,62	1,59	4,09	0,11	0,304	1,61	0,01425	0,0939	271	102	0,6
31876	155	C50E	2	3	Amorphous	1mm	Si-Al-Ca-K-Na-Mn	P6	0,61	0,92	2,25	0,11	0,190	1,76	0,00548	0,0780	271	106	0,3

Below, some conclusions are presented concerning the information contained in Table 9.

Mould powder types. According to the information contained in the table it is possible to say, that mould powder entrapment problems appear in both billet formats and for all the mould powder grades used at CCM2, although mould types P2, P3, P5 and P6 present a higher occurrence rate.

Mould powder entrapment morphology. Concerning mould powder entrapment morphology and composition, the following conclusions can be drawn:

- Most of the entrapments have elongated form in the rolling direction, and they are mostly internal, although there were also some superficial cases associated to surface cracks.
- The length range varies from 60 μm to 7 mm, with an average value equal to 1.4 mm in the rolling direction.

Mould powder entrapment composition. The most typical composition was [Al-Ca-Si-Na-F-Mg-K], where the percentage weight of the first three elements (Al, Ca and Si) is predominant.

Gas flow rates. The use of straight nozzles limits significantly the gas flow rates to be used through the stopper rod, otherwise gas bubbles would go very deep into the billet liquid core and they would have less chance to float to meniscus, giving rise to problems associated to pores. This is the reason why gas flow rates are very low in CCM2 and, therefore, their influence on steel flow patterns and entrapment risk can be supposed to be negligible. Those gas flow rates normally go from 0 to 0.8 l/min. In Table 9 it is possible to see that mould powder entrapments appear at any flow rate within that gas flow rate range, therefore it corroborates that entrapment phenomenon at CCM2 is independent on the gas flow rate within the standard gas flow rate working range.

In-mould electromagnetic stirring. Concerning the effect of the in-mould electromagnetic stirring on powder entrapments, stirring intensity target is the same for all the production program in CCM2 regardless of steel composition and billet format; and, for the period under consideration, 270 A was the target value. However two heats (57745 and 54351) correspond to a period of time during which extensive trials with a different EMS target value was applied. In both cases a lower EMS intensity value was used (220 and 250 A respectively). On the other hand, heat 53603 corresponds to an abnormal performance of the EMS device giving rise to an average value equal to 85 A. In the last case, the sudden stirring stoppages and following restarts could possibly have affected to the meniscus stability leading probably to the appearance of mould powder entrapment.

In order to acquire more information about the influence of the in-mould EMS on the steel flows patterns at the meniscus and the subsequent influence on mould level stability, extensive industrial trials were conducted within chapter 2.3.3, trying to identify the threshold of electromagnetic field that leads to a significant mould level instability that could promote the appearance of powder entrapments.

Number of the heat within the sequence. The first heat of the sequence has more risk to suffer powder entrapments than the rest of the heats within the sequence. **Figure 9** shows the distribution of the 64 powder entrapment cases according to that parameter together with the observed frequency of each number of the heat within the sequence according to the plant production programme. The reason for that behaviour is probably related to the transient phenomena associated to the first heat of the sequence; i.e., the time required for the mould powder to reach stable conditions in terms of lubrication (liquid pool depth) and undesirable mould level perturbations originated due to the dummy bar withdrawal process.

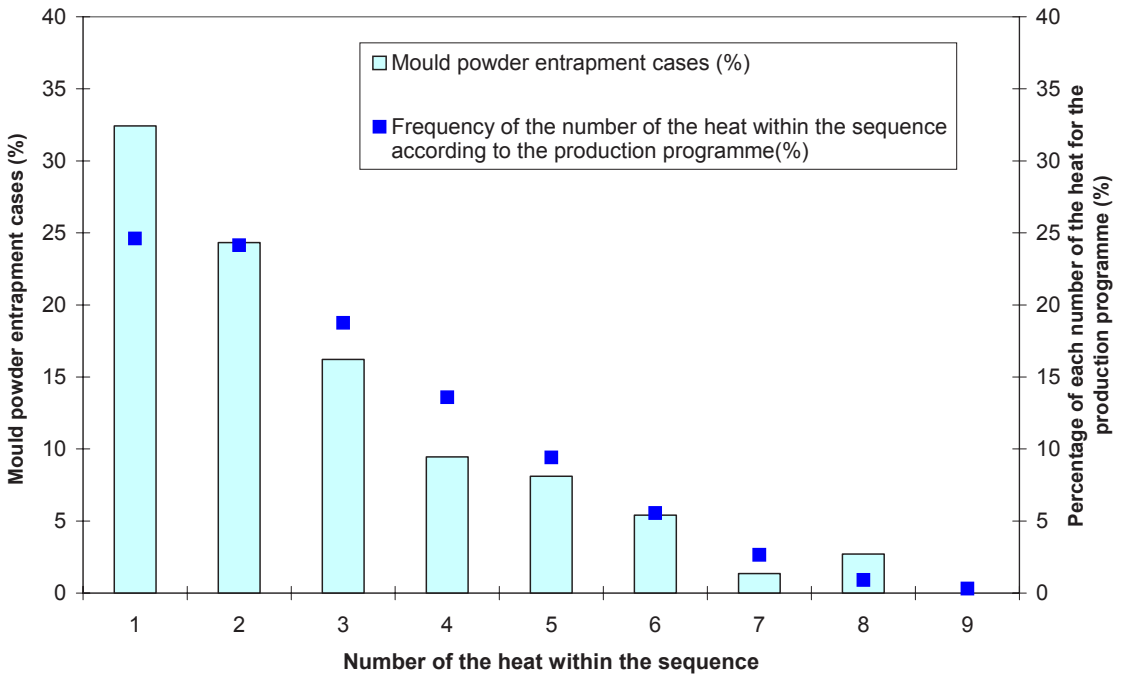

Figure 9 Relationship between the number of the heat within the sequence and the mould powder entrapment appearance (Sidenor)

Figure 10 shows how the first heat of the sequence normally gives rise to a higher mould level instability level.

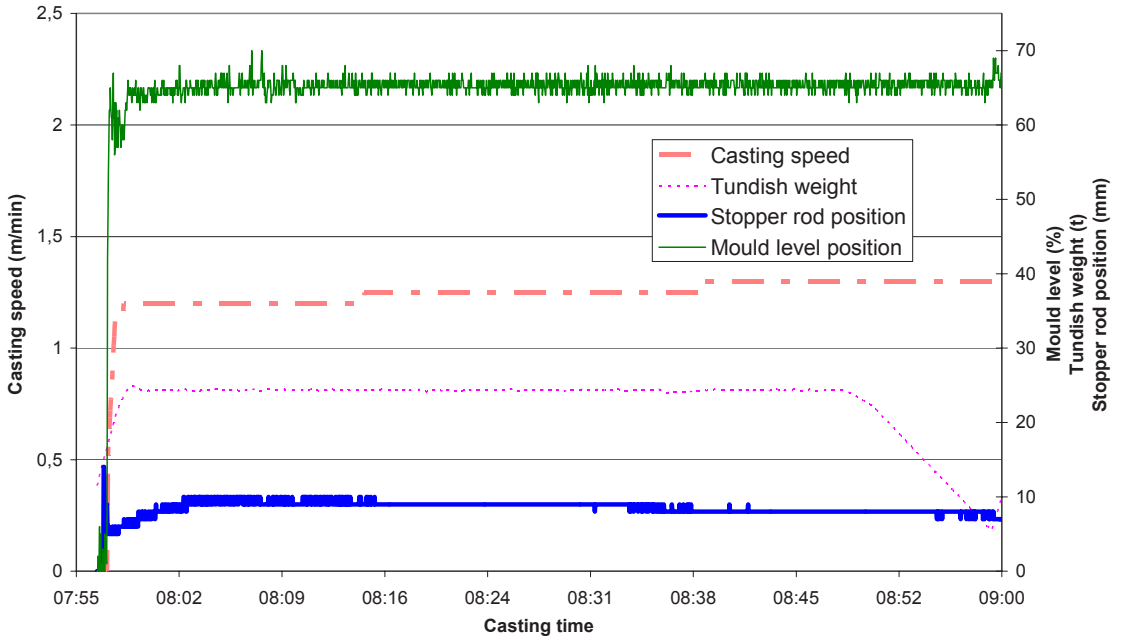

Figure 10 Example of heat with mould powder entrapment (Heat No 17529, Strand #3). Example of one heat as a first heat within the sequence (Sidenor)

Casting speed. The results show that the higher the casting speed the bigger the probability for mould powder entrapment. **Figure 11** shows the distribution of all the powder entrapment cases detected for the 185 mm squared format, and it is possible to see how, for the higher casting speed range (1.25 – 1.35 m/min), the occurrence rate of entrapment is higher than the proportion of number of heats within

that casting speed range according to the production programme. That trend was verified also for the 155 mm billet format.

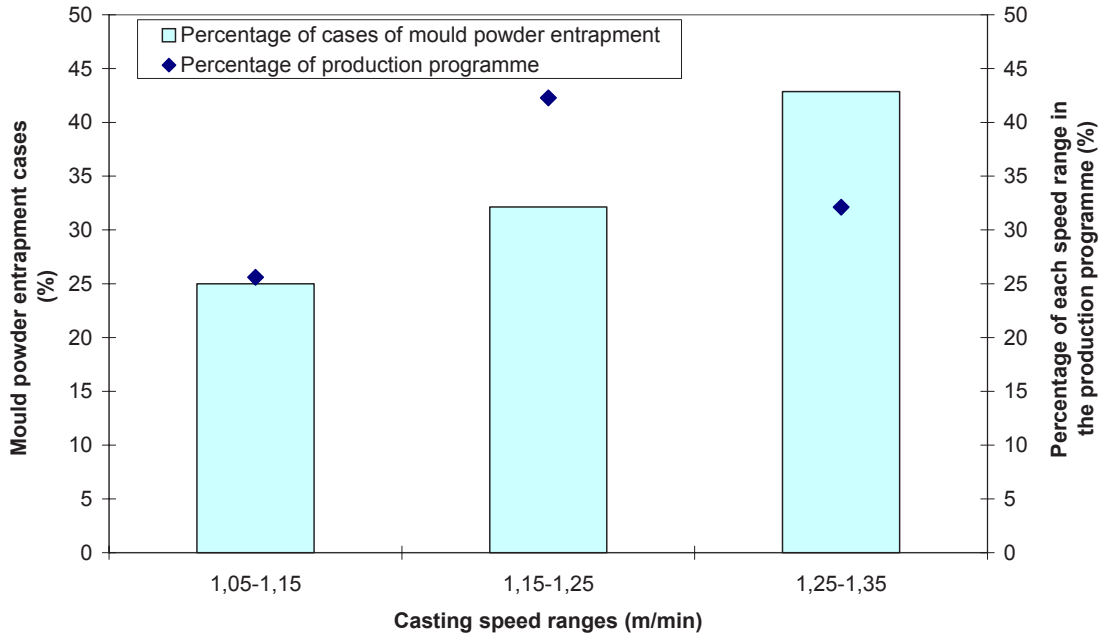

Figure 11 Assessment of the incidence of mould powder entrapments for 185 mm squared billets as a function of the casting speed (Sidenor)

At **CAS**, the billet quality index is defined in an empirical way, normally related to the 'light' or 'marked' presence of different kind of surface or subsurface defects (see **Table 10**). The visual inspection results range from 0 (no defects) to 9 (very strong defects). Defects in turn are defined empirically from the quality board 'medium' or 'light' according to its length/depth. Values equal to 2 are considered as reasonable values for a 'good' as-cast product quality.

Table 10 Empirical defect classification for the quality inspection system (CAS)

Defect classification	Value assigned
No defect	0.0
Only 1 or 2 defects	0.5
1 'Light' defect	1.5
2 'Light' defects	2.0
3 'Light' defects	2.5
1 'Medium' defect	3.0
1 'Medium' defect + 1 'Light' defect	3.5
2 'Medium' defects	4.0
3 'Medium' defects	5.0
4 'Medium' defects	6.0
Strong defects	9.0

In the current work, where the attention was focused on sub-surface defects related to slag entrapment occurrence, the percentage of billets to be conditioned due to this defect was taken. The data base was composed of about 3000 billets. The overall defect scenario included mini break-outs and traces of non-

melted powder onto the surface, mainly at the corners. Examples of these defects are shown in **Figure 12**.

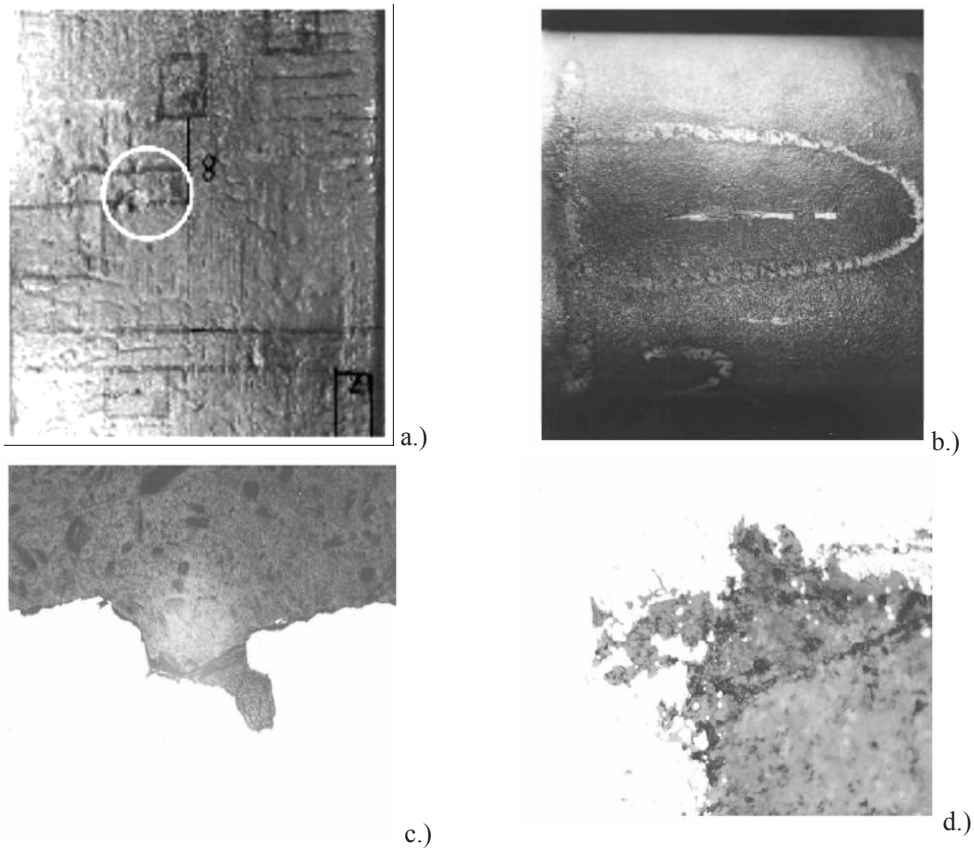

Figure 12 a.) Sample with entrapment of powder B; b.) Crack with powder entrapment (white); c.) transverse section of the defect (X 20); d.) close-up of the previous defect with CC powder entrapment (X 500) (CAS)

To have more information on the effect of mould powder properties even though only two of the five powders indicated in Table 5 are mostly used at CAS caster, the data base was fed with further data on:

- use of all different powders
- casting speed in a broader range (1.3 to 1.8 m/min) with the idea that it could have played a relevant role in determining the flow condition at the interface steel-slag at meniscus and in turn on slag entrapment incidence on as-cast product

The data base was also integrated with information concerning the level control, implemented in a logging system developed within another ECSC project [1], able to store 200 points per second (**Figure 13**).

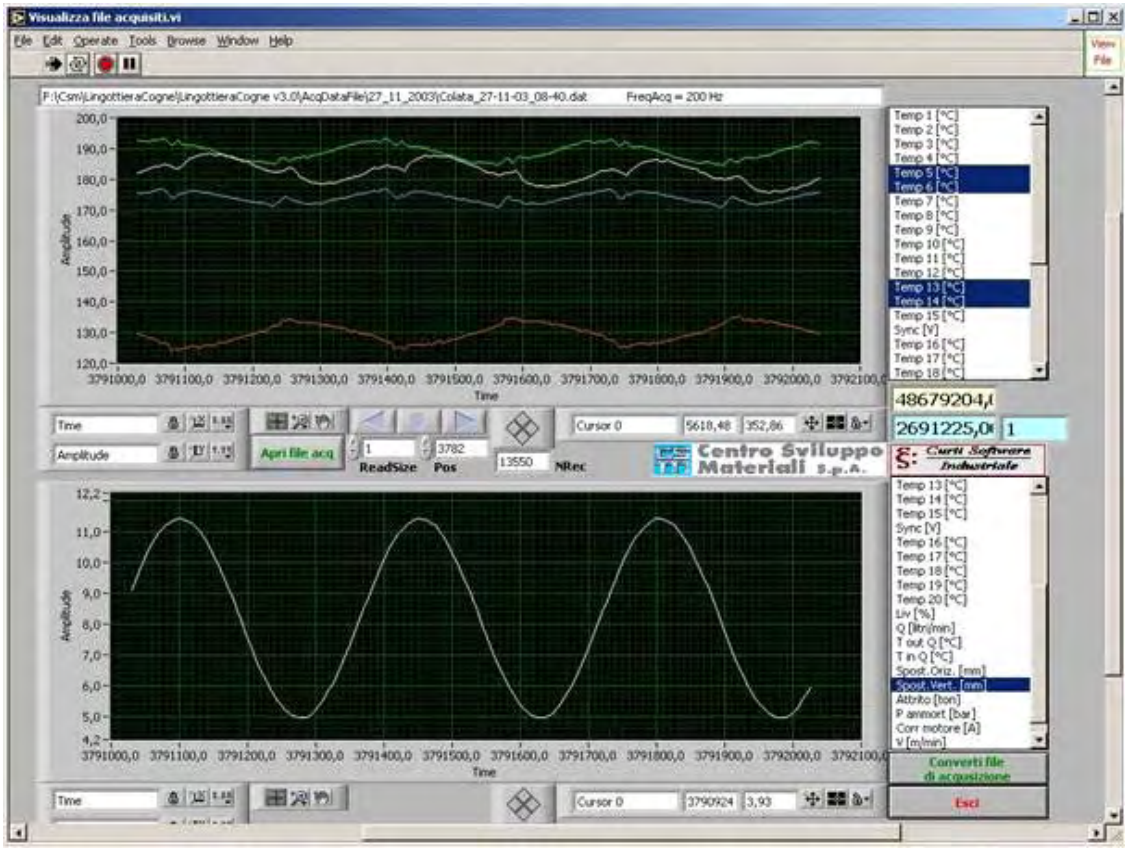

Figure 13 Typical on-line panel of the advanced mould monitoring system used at CAS billet caster

The critical analysis of the data base available allowed concentration of the operational activity on the investigations concerning the physical-chemical phenomena occurring at the interface steel-mould slag responsible for flux entrapment, namely:

- the steel fluid-dynamics at the meniscus
- the effect of powder viscosity on slag entrapment occurrence
- the effect of slag melting and consequent slag feeding rate on the local conditions at the interface

Regarding the flow conditions in the mould at **TKN**, the possible wear of the SEN was investigated. After casting longitudinal cuts were made through the SEN, see **Figure 14**.

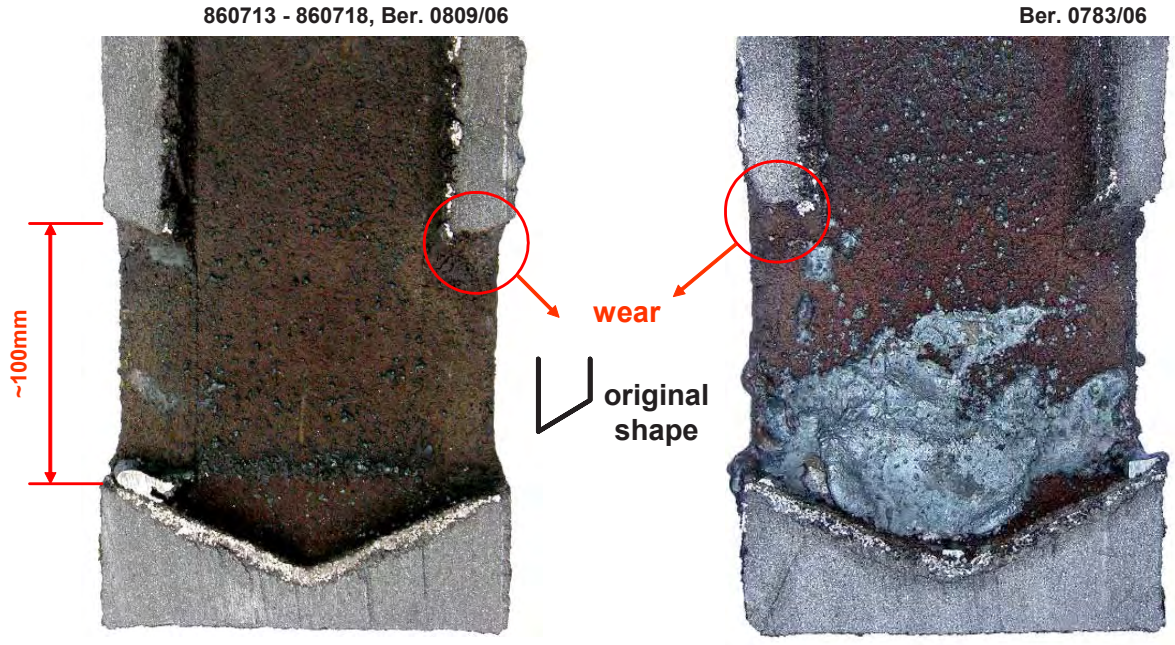

Figure 14 Wear of operational SEN type 50 mm x 90 mm, after casting 1.4016 (TKN)

It can be seen, that there is some wear at the upper edge of the entry area. Due to the strong vortex in this area and the fact, that the steel flow is directed somewhat downwards. It is assumed that this wear will not influence the overall steel flow pattern.

2.3.1.3 Extensive analyses of data and elaboration of correlation (Task 1.3)

At **Sidenor**, in order to study the influence of certain operational parameters such as mould level stability, casting speed stability and stopper rod evolution and stability, a random period of time (RP: Reference Period), comprising thirty five heats without entrapment problems, was taken as a standard operational reference. By that way, a comparison between the standard operational conditions and those obtained in the heats with mould powder entrapments was performed.

Table 11 shows the results concerning the comparison between the MPEDB and the RP, and the following conclusions can be drawn:

Mould level stability. Mould level stability, assessed in terms of average stability 'Aver. [Mould Level Std. dev]' is slightly worse for the cases with entrapments; and, additionally, the assessment in terms of maximum instability 'Max. [Mould Level Std. dev]' shows clearly, that the cases with entrapments presented a higher amplitude concerning mould level punctual perturbations.

Table 11 Comparison between the groups of heats with mould powder entrapment (MPEDB) and the reference period (RP) in terms of casting operational performance. (Sidenor)

	Mould level		Stopper rod			Casting speed	
	Aver. [Mould Level Std. dev.] in %	Max. [Mould Level Std. dev.] in %	Aver. [Stopper Max-Min] in mm	Aver. [Stopper Std. dev.] in mm	Max. [Stopper Std. dev.] in mm	Aver. [Cast. Speed Std. dev.] in m/min	Max. [Cast. Speed Std. dev.] in m/min
Mould Powder Entrapment Database (MPEDB)	0.797	1.84	4.87	0.213	0.582	0.00284	0.0409
Reference Period (RP)	0.775	1.64	4.85	0.186	0.578	0.00127	0.0388

Stopper rod evolution and stability. Stopper rod evolution and stability is another aspect with an important theoretical influence on meniscus stability. **Figure 15** and **Figure 16** show that, amongst the heats with mould powder entrapment problems, there was a very big difference in stopper rod behaviour. Figure 15 shows the stopper rod behaviour when having castability problems and how it clearly affects to the mould level stability. Additionally, Figure 16 shows that mould powder entrapment is also possible in spite of having very good stability in terms of mould level and stopper rod behaviour.

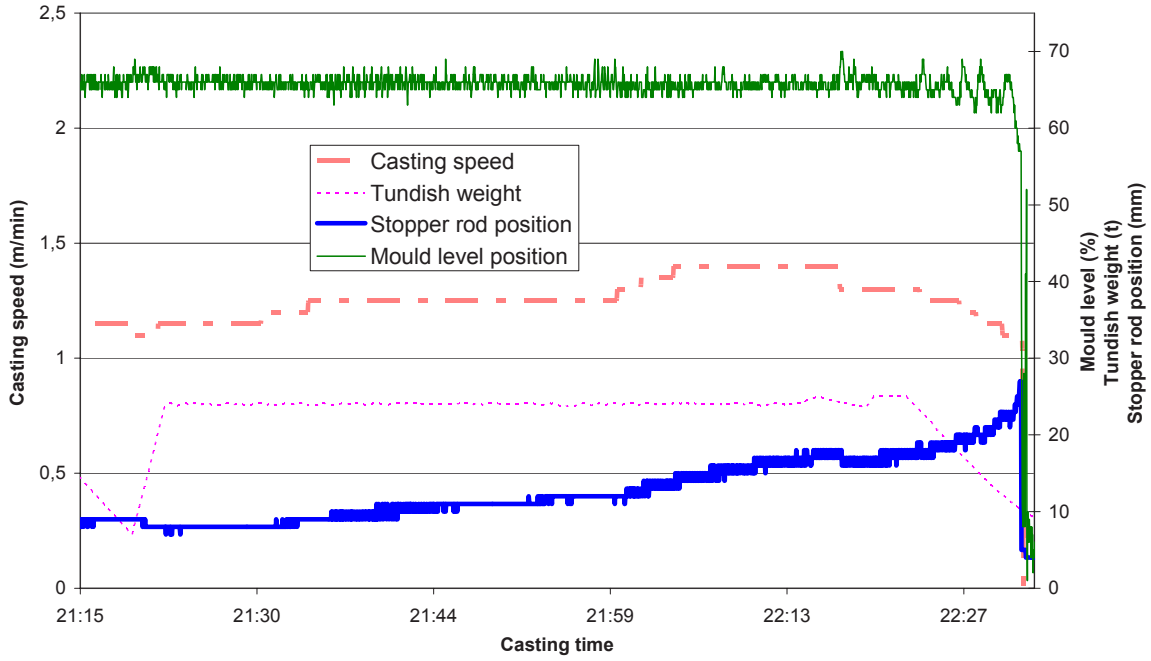

Figure 15 Example of heat with mould powder entrapment (Heat No 57745, Strand #1) – Example of one heat with bad operational parameters stability (Sidenor)

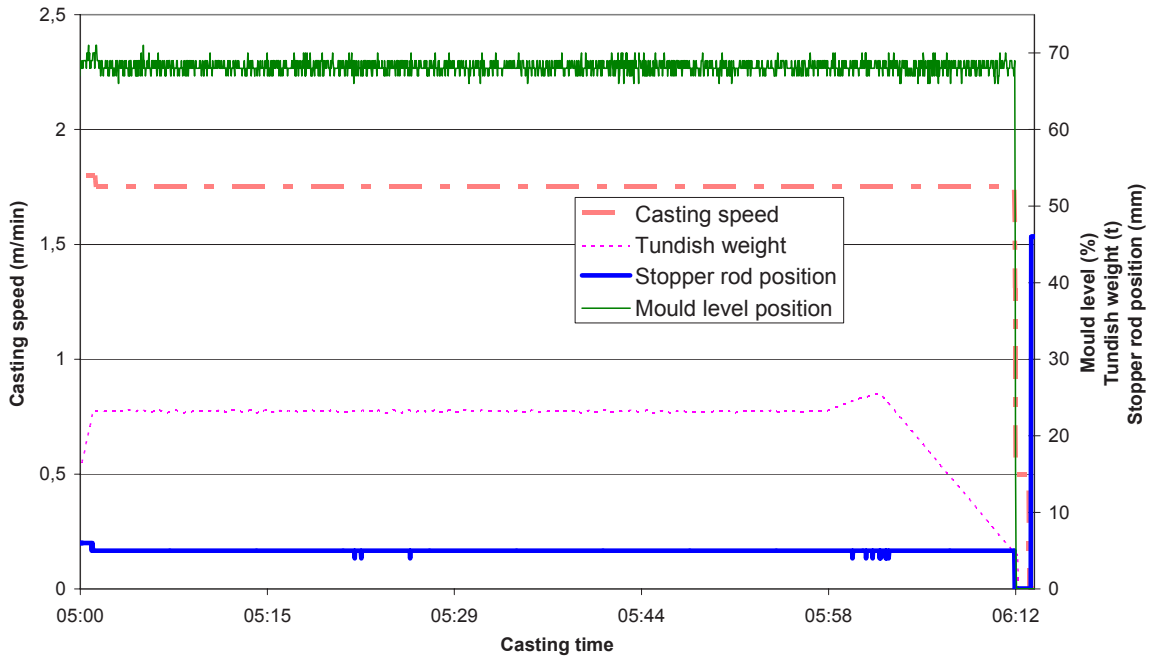

Figure 16 Example of heat with mould powder entrapment (Heat No 23634, Strand #3) – Example with a fairly good result concerning meniscus stability (Sidenor)

Concerning the rest of parameters, stopper rod stability 'Aver.[Stopper Std. dev.]', as expected, is also clearly worse for the group of heats within the MPEDB. On the contrary, castability condition, assessed by means of the total relative movement of the stopper throughout the heat 'Aver. [Stopper Max-Min] almost does not present any difference between both groups.

Casting speed stability. Heats with entrapment also present a worse casting speed stability than the standard practice in terms of average stability 'Aver. [Cast. Speed Std. dev.]' and in terms of maximum instability 'Max.[Cast. Speed Std. dev.]'. To support this, some heats with entrapments were found to have some abnormally abrupt casting speed changes.

Nozzle immersion depth. Nozzle immersion depth average value [Aver. Nozzle Imm. Depth (mm)] is very similar in both groups (MPEDB: 104 mm and RP: 105 mm); therefore, no relationship of this parameter with mould powder entrapment was found within the normal variation range (100 – 109 mm). But, due to the theoretically high influence of this parameter on entrapment, extensive experimental trials were carried out within WP3 changing the immersion depth range in order to assess thoroughly its influence on mould powder entrapment.

Therefore, based on this preliminary approach, performed over the historical data concerning mould powder entrapment (MPEDB) and using also a reference period (RP), the following conclusions were drawn:

- It is clear that any instability affecting mould level or stopper rod and a high casting speed variability are negative factors influencing the risk of mould powder entrapment. On the one hand, unfortunately, the stability of both, mould level and stopper rod, are determined to a high extent by

castability conditions, which cannot be adjusted freely. On the other hand, it is clear that the longer the sequence the worse the castability; therefore, shorter sequences would reduce the risk of entrapment. But this opposes to the productivity needs. Therefore a compromise has to be reached between entrapment risk and productivity.

- Casting speed stability is another parameter influencing the entrapment risk, calling for its minimisation by means of applying smaller increments when any change is made in the casting speed value. By this way, entrapment risk can be minimised reducing as much as possible the casting speed variability.

At **CAS**, the analysis of data brought about the following results in terms of correlations between operational parameters and defect incidence on product. In **Figure 17** it is shown for powders A and B the corresponding defect index found. Here, from all defects those concerning powder entrapment were considered (precisely, 'non-melted powder entrapment' was found).

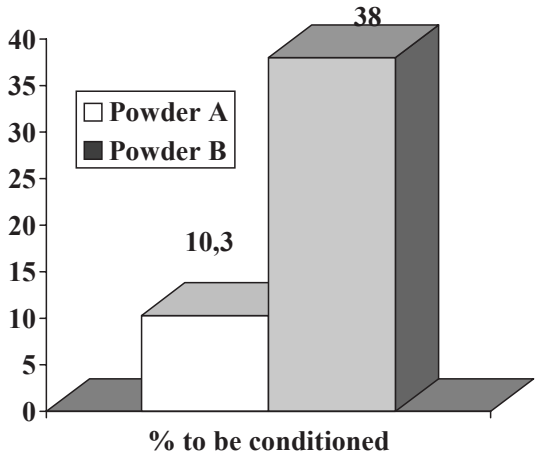

Figure 17 Powder entrapment incidence for the reference caster mould powders (CAS)

Furthermore, **Figure 18** shows, as interesting aspect involving different mould powders that a different viscosity with similar melting rate can bring about different quality results.

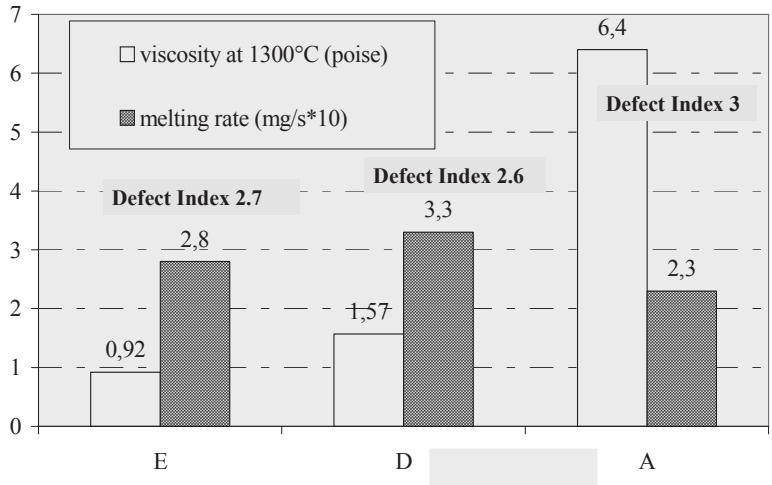

Figure 18 Preliminary plant data: correlation between defect index, powder viscosity and melting rate (CAS)

In particular,

- being ascribed the undesired behaviour of high-viscosity powder to lack of lubrication;
- being noticed a strong dependence of the powder behaviour from casting speed;

the information gained for the next investigations was to have in mind solutions aiming at facing the risks of slag entrapment also taking into account the basic request for a proper powder working (lubrication action, good feeding …).

Further relevant information gained was the main occurrence of slag entrapment in the first heats of the sequence, suggesting some interrelations with unsteady conditions in terms of flow and powder layer conditions.

The final information was the occurrence of slag entrapment in form of non-melted powder, leading to local steel recarburisation. This suggested the potential role of a poor meniscus feeding with liquid powder, due to powder feeding itself, to melting rate or to powder consumption. This aspect was investigated in more detail in chapter 2.3.3.1.

At **Arcelor España**, the original set of production plant data consisted on process variables with one value per heat. In order to refine the analysis this original dataset was improved, at the beginning with process values defined per slab, and then with process data coming from caster instrumentation sampled at 0.2 Hz. Special routines where developed in order to correlate timestamp with casting length and slab number.

For quality results (i.e. information on entrapment) it was necessary to build a new data base, used for evaluating the impact of the different variables. The database was obtained from human inspection of slabs. The inspection consisted of manual counting near-surface inclusions after scarfing. A value of entrapment density was calculated from this data.

The first step was to gather existing production data and to provide supplementary information coming from different sources like process data registers or handwritten reports. All this information was grouped in a database that has been continuously updated and improved. The analysis of data and the search of relevant correlations have been conducted following CRISP-DM methodology [2] using different statistical tools (Matlab, Clementine, etc.).

Study of entrapment distribution. In order to identify situations where entrapment problems are more relevant, a study on defect distribution was conducted. Results are shown in **Figure 19**, **Figure 20** and **Figure 21**.

Figure 19 shows the occurrence of entrapment on 2000 slabs during year 2005 for the steel grade of reference (ULC1). It can be concluded that entrapment phenomena are randomly distributed along time without relevant peaks or marked tendencies. The graph also shows the frequency of slabs falling into

each entrapment density category. Two or three normal populations could be identified in the graph. Anyhow, it can be seen that the main part of the slabs present a null or low entrapment density. This distribution is almost constant along time. Similar distributions of entrapment defects are found when individual casters and strands are taken into account.

The distribution of entrapments by slab face (upper-wide face, lower-wide face and narrow faces) was studied. Results are summarised in Figure 20(a) were it is clearly shown that the upper face is the least problematic and the distribution of entrapments by levels (low > medium > high) is very similar, regardless the considered face.

Comparing Figure 20(a) with Figure 20(b), a decrease in entrapment defects appears. This improvement was only obtained via a change in the mould level set point described later in more detail. The attained reduction in entrapment has been kept for all the year 2006 and the most important reductions have been observed in the lower and narrow faces.

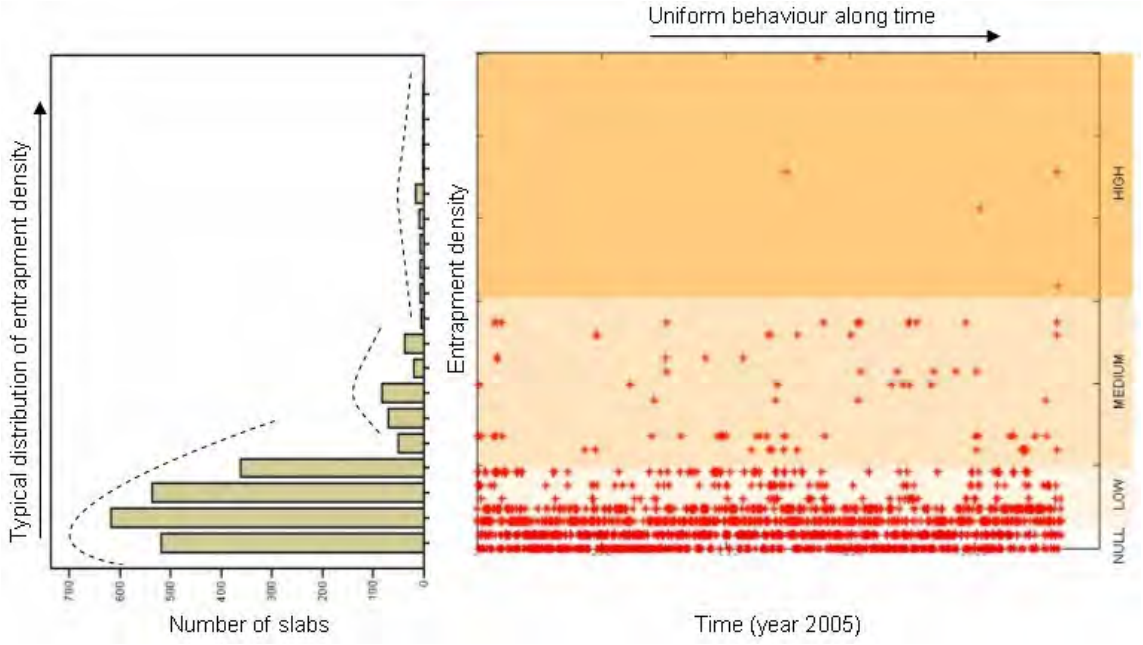

Figure 19 Distribution of entrapment for ULC1 – entrapment density along time where each point represents one slab (right); distribution of slabs by entrapment density (left) (Arcelor Espana)

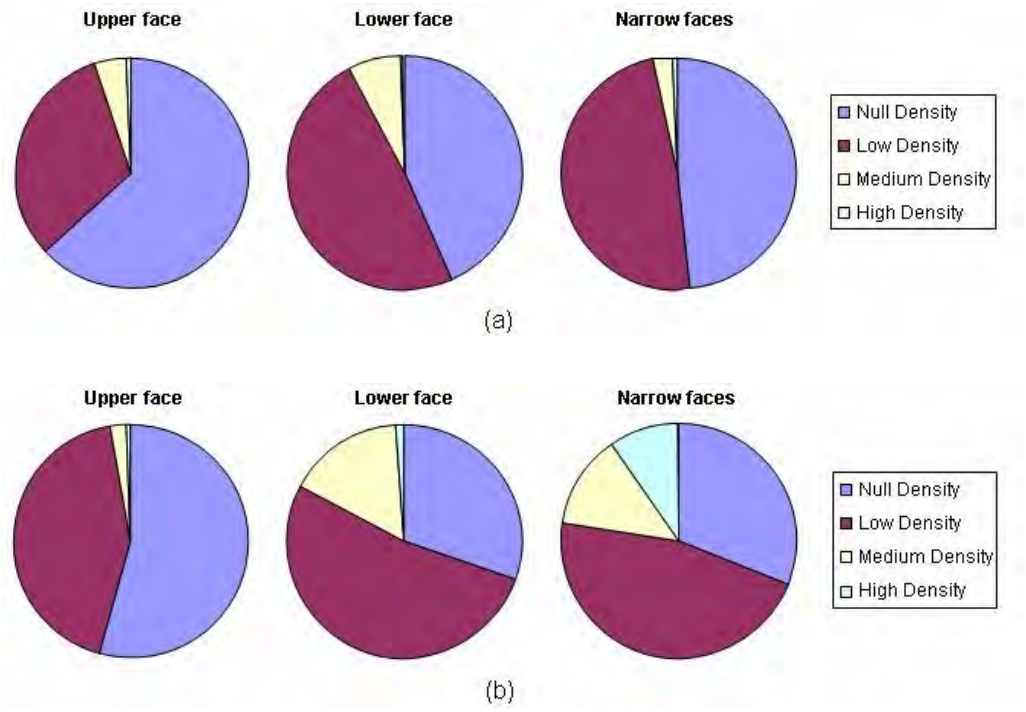

Figure 20 Distribution of entrapment by slab face. Results for ULC1 in 2005 (a), and previous results (b) (Arcelor España)

The preference of entrapment in the lower face can be explained from a particle-flotation point of view and taking into account the curvature of the mould. As illustrated in Figure 21, a near-surface entrapment is formed in the upper part of the mould where the film of solid steel is thinner. When a particle of slag has been entrained by the liquid steel and then floats in the vicinity of the lower face of the mould (left part of the picture) it can be retained by the curved wall of the mould, and hence, entrapped. By contrast, when the flotation of the particle occurs near the upper face of the mould (right side in the picture) it is more probable that the particle can float, and then be absorbed by the molten flux pool in the upper part of the mould. However, it should be noted that in the case of deeper inclusions (typically endogenous inclusions) the preferred side of deposition is the upper one. Moreover, it must be mentioned that the geometry of the mould is not the only relevant factor as the quality and shape of the front of solidification should also play an important role.

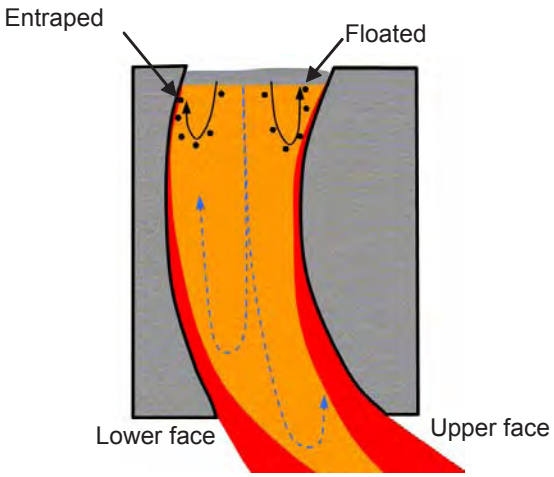

Figure 21 Mould section (not drawn at scale) illustrating the preferential deposition of near-surface entrapments in the lower face of the slab (trajectories in black). By contrast deeper inclusions result preferably entrapped in the upper part of the slab (trajectories in blue) (Arcelor España)

It was also found that the entrapment on a given face is not strongly correlated with the entrapment on another. The obtained correlation coefficients were 0.25 (upper-lower), 0.25 (narrow-lower) and 0.21 (narrow-upper).

Powder type and batch. The mould powder type (see **Table 12**, viscosity was measured in the laboratory) has been maintained almost unchanged along the project duration, making more emphasis in the investigation of other process parameters. However, for operational reasons, a different powder was used for some casts. From the correlation analyses and visualization techniques applied to heat-averaged values of process variables, it was observed a clear correlation between entrapment and powder type. The results pointed to a better performance in the entrapment context of the new powder. However, other aspects as lubrication behaviour made not advisable the adoption of them. In addition, a slight effect of the powder batch on entrapment was observed. This result is probably due to the natural variability of powder prime matters and storing conditions.

Table 12 Description of mould powder for ULC1. (Arcelor España)

Element	Powder for ULC
SiO_2	38.0 – 40.0 %
CaO	32.5 – 34.5 %
MgO	5.0 – 6.0 %
Al_2O_3	3.5 – 5.0 %
Na_2O	4.0 – 5.5 %
K_2O	0.5 – 1.5 %
MnO	<0.1 %
Fe_2O_3	1.5 – 3.0 %
C_{FREE}	1.0 – 2.5 %
CO_2	3.5 – 4.5 %
C_{TOTAL}	2.5 – 3.5 %
F	5.0 – 6.5 %
H_2O at 600°C	<1 %
Softening point	1170 °C
Melting point	1220 °C
Fluidity point	1250 °C
Viscosity at 1300°C	3.3 dPas·s
Viscosity at 1400°C	1.9 dPas·s
Basicity	0.80 – 0.92 %

Mould level set point. It was detected a relevant correlation between the mean value of the mould level and the entrapment density in the slab. These two variables are plotted together in **Figure 22**, being the slabs ordered chronologically; an increase of 10 mm in mould level set point can be observed by slab number 450.

The obtained correlation coefficient between mould level and total entrapments was 0.346. In addition, the analysis was done differentiating the faces of the slabs. The effect of the mould level on entrapments is localized mainly on narrow faces. The obtained correlation coefficient was 0.410 while was 0.073 and 0.060 for the upper face and the lower face, respectively. We can conclude that the narrow faces of the mould are being a preferential location for entrapment and they are very influenced by significant changes in the mould level set point.

The observed relation between mould level and powder entrapments in the narrow face can be explained as follows. An increase in the mould level, keeping unchanged the rest of the parameters, results in an increase in the thickness of the solidified steel film and consequently the entrapments are fixed more deep in the slab. Therefore, the slab is free of surface and near-surface powder entrapments. The diminution of powder entrapment was assessed by subsurface inclusion inspection on the slab. In order to see the effect of this entrapment reduction on downstream quality, the related defects were observed with Parsytec system on the pickled coil. Only a part of the coils could be analysed and the

results are indicated in Figure 22. It can be seen that, in principle, the reduction of defects in the slab has not a corresponding reduction of defects in the pickled coil, but neither implies an increment. It would have been desirable to further validate this conclusion by means of a more extensive study of downstream quality data. Unfortunately, it is difficult to have both extensive and reliable quality data from coils because a thorough verification of the possible defects detected by automatic detection systems is very time-consuming.

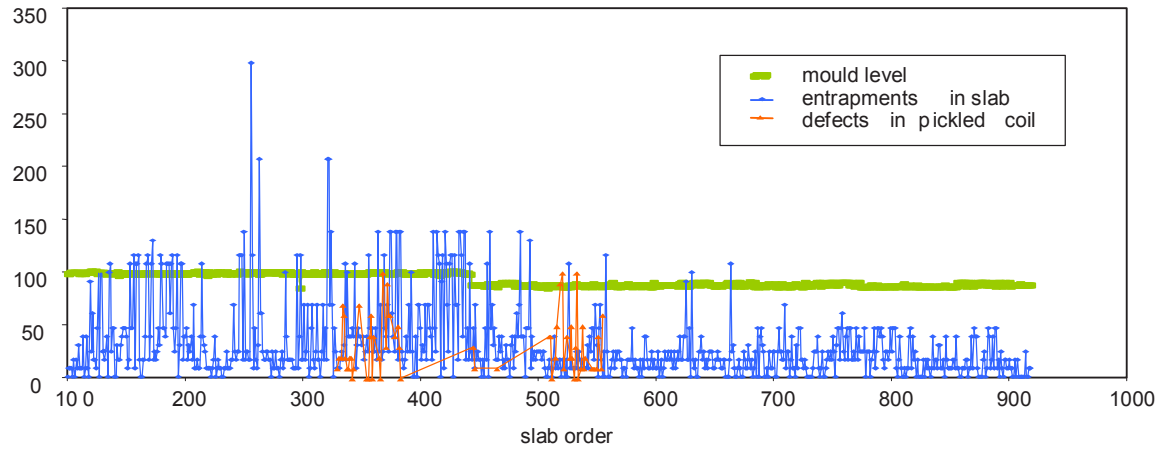

Figure 22 Evolution of entrapments after increasing by 10 mm the mould level set point (around slab number 450). The depth of steel surface in mould is represented in green (Arcelor España)

Mould level stability. Mould level set point was found to have a strong effect on entrapment on narrow faces. The stability of mould level has been also studied and typical results are shown in **Figure 23**, which represents the data of a series of slabs from the same heat; the different slabs are represented with distinct colours and they are ordered by decreasing entrapment density.

The data represented in Figure 23 are the entrapment density (Figure 23-a) of the slab and the mould level mean value (Figure 23-b) and deviation (Figure 23-c), both calculated in a 5 seconds basis. It can be seen that the slab with most defects is that with most important mould level deviations. It is also interesting to note that the time scale of the harmful oscillations is smaller than 5 seconds: The slab with biggest deviation in the mould level (Figure 23-c) is not necessarily the slab with biggest variation of the mean mould level (Figure 23-b).

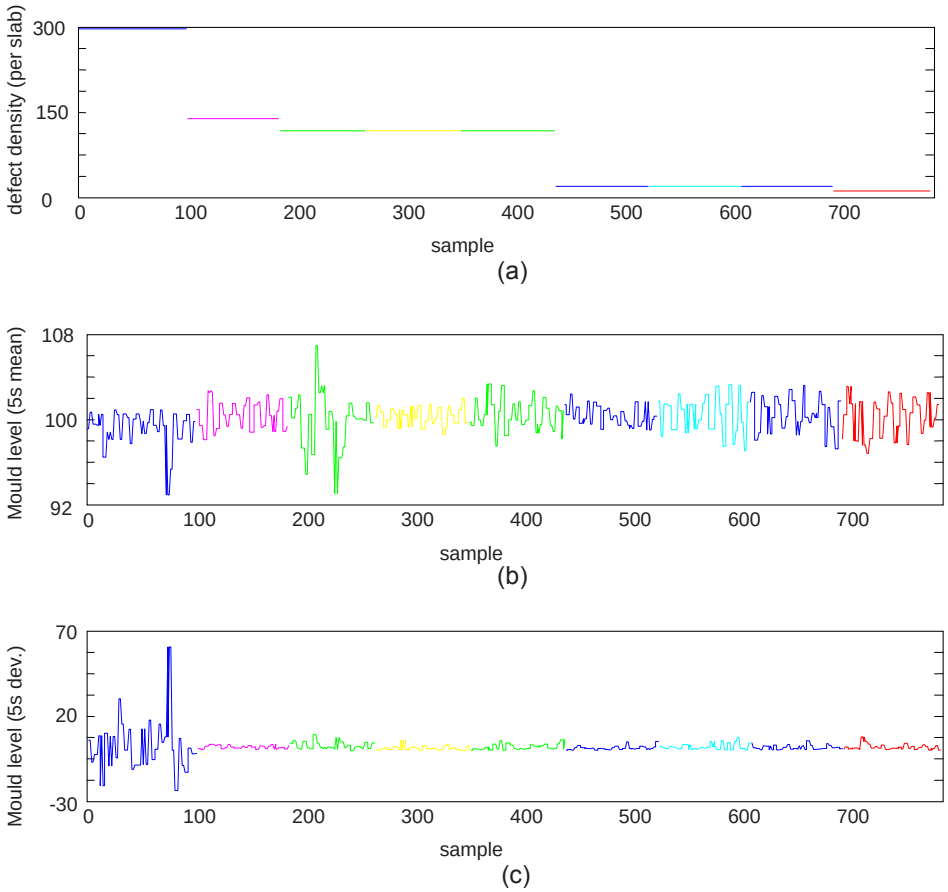

Figure 23 Comparison of defects in slabs with the mould level curves for several slabs of the same heat. Each slab is represented with a different colour. The slab with most defects has also the most important mould level instabilities (Arcelor España)
a) entrapment density; b) mould level mean value; c) mould level mean deviation

Casting speed and oscillation frequency. Any significant correlation between the casting speed and the powder entrapments could not be found. The coefficient of correlation was in this case only 0.010. In a similar way, it has been investigated the effect of the oscillation frequency of the mould on powder entrapments. The results did not give a significant correlation between both variables (correlation coefficient of 0.020).

Additionally, the application of special data visualization techniques permitted to analyse the combined effect of several factors acting simultaneously and to search those combinations of variables which are more related to entrapment problems. For this purpose, Self Organizing Maps (SOM) were applied in the project. SOM is a kind of neural network, whose main advantage is, that it allows a 2D representation of spaces of higher dimensionality [3]. The general idea is to project the high dimensional input data onto a two-dimensional grid. SOM allows different ways of knowledge representation. One of the most useful is the characteristic map that represents a map for each input variable. They are calculated by plotting the values of the weight vector corresponding to the selected variable with a colour scale.

The analysis was concentrated on the ULC grade of the previous studies taking a total number of 2000 slabs corresponding to the year 2005 that were fully inspected after scarfing. The results of the inspection (counting of surface entrapments) allowed classifying the entrapment severity of each slab type of face (upper, lower and narrow) in four levels of entrapment density with an associated numeric value: null (0), low (1), medium (2) and high (3). The analysis was made both differentiating by faces and also taking a total value per slab.

The SOM analysis was made for a 40x40 grid and the vicinity ratio was 0.8 with 20 iterations. All variable values were normalized to a (-1, 1) range. The results obtained with this configuration can be seen in **Figure 24**. From this figure several conclusions can be extracted:

- A certain number of variables are representing the same special event for this particular set of data: that means that the SOM map is very similar for the case of mould level related variables (Figure 24: graphs 1, 2, 10 and 11). The major part of the slabs presenting “very high” mould level fluctuations correspond to that cases of mould level control in non-automatic mode or presenting change of SEN (Figure 24: graphs 3 and 8).
- In addition, there is a group of slabs where the mould level fluctuations are “high”, but not “very high” (Figure 24: graphs 1 and 2). These slabs are not affected by SEN change nor mould level control in non-automatic mode. As is evident, the group with “very high” fluctuations is contained in the “high” group.
- No correlation can be detected for the case of superheating, the ageing of the mould plates, ladle change or argon flow rate (Figure 24: graphs 5, 6, 7 and 9).
- It can be clearly stated that almost all the slabs presenting high mould level fluctuations result in a medium-high level of entrapment (Figure 24: graphs 2 and 12).
- There is also a big group of slabs with medium-high level of entrapment that, in principle, cannot be related to any of the represented variables.

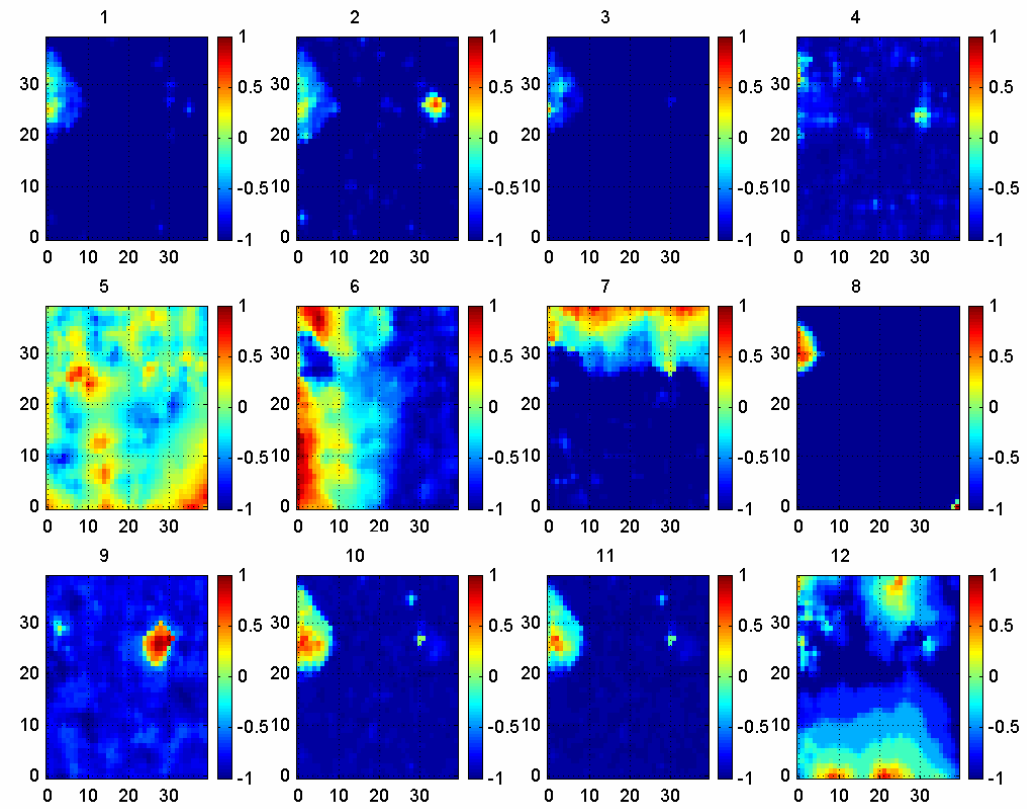

Figure 24 SOM 2-D representation of the 12 variable problem formed by:

1. Percentage of slab affected by a very quick variation of mould level;
2. Percentage of slab affected by a quick variation of mould level;
3. Percentage of slab with non-automatic level control;
4. Velocity gradient of casting speed;
5. Superheating in tundish;
6. Life of the mould plates (number of heats);
7. Percentage of slab affected by ladle change;
8. Percentage of slab affected by SEN change;
9. Flow rate of gas injected at slide gate system;
10. Max-min mould level variation;
11. Mean-min mould level variation;
12. Entrapment density (Arcelor España)

At **TKN** a complex correlation analysis of process data and surface inspection data shows that the following process parameters have a significant influence for the entrapment of casting powder, see **Figure 25**.

- exit area of the SEN
- type of casting powder
- superheat of the melt

The influence of the immersion depth of the SEN was also seen, but not in a clear way.

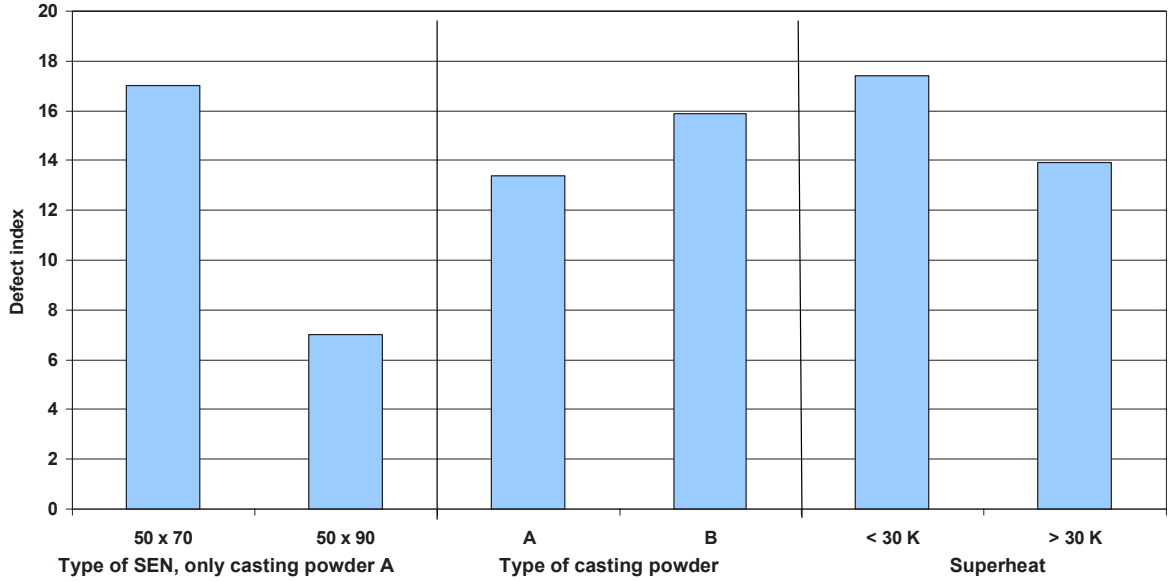

Figure 25 Statistic correlations between process parameters and occurrence of surface cracks for steel grade 1.4016 (TKN)

From this findings it can be concluded, that the defect is strongly related to the flow conditions in the mould near the meniscus.

Also the casting powder and its melting behavior have an influence on the occurrence of the defect. Other process parameters seems to be not important.

2.3.1.4 Set-up of a parameter basis (Task 1.4)

Based on the outcome of this preliminary approach, the following research activities were proposed for both modelling and industrial trials within the chapters 2.3.2 to 2.3.4.

Concerning **Sidenor**, it was decided to pay special attention to the following subjects:

- Characterisation of the mould powder consumption, key properties and assessment of possible trials for mould powder optimisation.
- Identification of the electromagnetic field threshold at meniscus position that leads to a significant mould level stability disturbance that could promote the appearance of powder entrapments.
- Plant trials with different immersion depths in order to assess thoroughly its influence on mould powder entrapment.
- Trials with nozzles with lateral ports due to its high theoretical influence on the in-mould steel flows.
- Industrial trials to characterise the mould powder liquid layer in order to provide to the CSM with the required data for the modelling activities.

At **CAS**, as a result of the data base realisation, the parameter basis for operational project investigation within WP3 was the following:

- parameters related to powder: effect of viscosity and melting rate, also in relationship with casting speed, on incidence of slag entrapment on as-cast product. This called for a synergy with the CSM powder and flow modelling work ;
- parameters related to fluid-dynamics: not only the effect of casting speed on quality was called for, but, since the effect of casting speed on mould flow, keeping all the other parameters constant, is to influence the steel velocity at meniscus close to the slag layers, all the parameters potentially influencing local steel velocity at the interface steel-slag (apart of nozzle immersion depth not interesting and feasible for CAS features) were the following:
  - effect of nozzle geometry
  - effect of Electro Magnetic Stirring (coil current).

At **Arcelor España** it was decided to investigate some parameters that were difficult to analyse by only using database information but were important for a better understanding of the involved phenomena and the reduction of powder entrapment:

- SEN related parameters: immersion depth and geometry degradation
- Effect of mould level instabilities in downstream products
- Effect of mould level instabilities combined with superheating

For **TKN** the main conclusions of the data analysis task were the following:

- The wear of the SEN will not influence the overall steel flow pattern.
- The observed defects are related to the steel flow conditions near the meniscus
- Important factors regarding the flow field are:
  - Type of SEN
  - Casting velocity
  - Immersion depth
  - Casting temperature

2.3.2 Operational investigations for flat products (WP 2)

In this chapter plant activity was performed on flat product casters of Arcelor España and TKN to identify optimum constellations of operating parameters and mould powder properties to reduce slag entrapment occurrence in the steel.

The approach was the following:

- at first *performance of parameter studies* were made (Task 2.1). The work was complementary to that of WP1, where a reference process quantities data base was set up and related to slag entrapment occurrence on the product;
- on the other hand, *verification of the modelling results* was accomplished (Task 2.2);

- *determination of optimum constellations* (Task 2.3) were finally achieved.

Arcelor España and TKN cared the WP activity. But from the approach shown, synergy between partners, also in interrelation with the work performed in chapter 2.3.4 was exploited, especially with BFI modelling activity.

2.3.2.1 Performance of parameter studies (Task 2.1)

The main objective of the operational investigations at **Arcelor España,** starting from historical data analysis, was to study more in detail the effect of different process variables on powder entrapment occurrence in the slab. This task was carried out in connection with numerical modelling of mould by lab partners, since both approaches (modelling and plant investigations) are complementary.

Three main working guidelines were followed:

- Study of process parameters in selected casts
- Study of SEN impact on entrapment, including the effect of the degradation of its geometry.
- Assembling of supplementary data for CFD modelling.

The following additional tasks have been done:

- Sampling and characterization of the SEN ageing along a casting sequence.
- Measurement of flux layer thickness.
- Detailed surface and near-surface examination and inspection of slabs.
- Sampling and chemical analysis of the as-cast product in order to confirm the nature of the near-surface inclusions that are detected.

An off-line system (developed in another project) has been used in this project mainly for sampling surface longitudinal strips on the hot slab. The chemical analyses of these samples helped to confirm that the main origin of the inspected near-surface inclusions is powder entrapment (**Figure 26**).

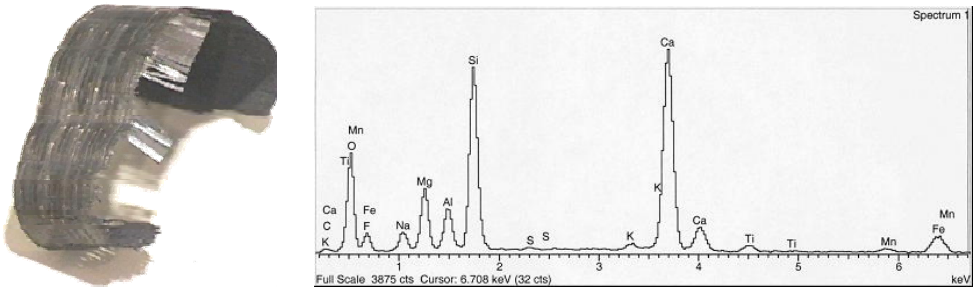

Figure 26 Strip of steel sampled from a slab and chemical analysis of the near-surface entrapments. The near-surface inclusion can be seen in the sampled strip while chemical analysis reveals the presence of casting powder (Arcelor España)

At Arcelor España some interesting heats have been selected and the evolution of process variables along slab length and defects along the corresponding hot coil has been investigated. The steps for obtaining the quality data of the hot coil are the following:

- Identification of the coil number from slab number, using Mityca, a tool developed by Arcelor España which provides detailed information about product traceability.
- Coil searching in the Parsytec's database and list filtering of possible defects found in order to select only those defects more probably related with powder entrapment.
- Individual precise verification (defect by defect) by an expert (not always possible) or merely approximate verification. This step is clearly very time-consuming, but very necessary in order to have reliable quality results.
- Incorporation of these verified quality results to the existing database of this project.

An example of the results obtained is shown in **Figure 27**. The standard deviation of the mould level along the length of a slab is represented in Figure 27-a. The position of relevant defects along the length of the top face of the resulting hot coil is marked in Figure 27-b. The top face of the coil corresponds to the bottom face of the slab.

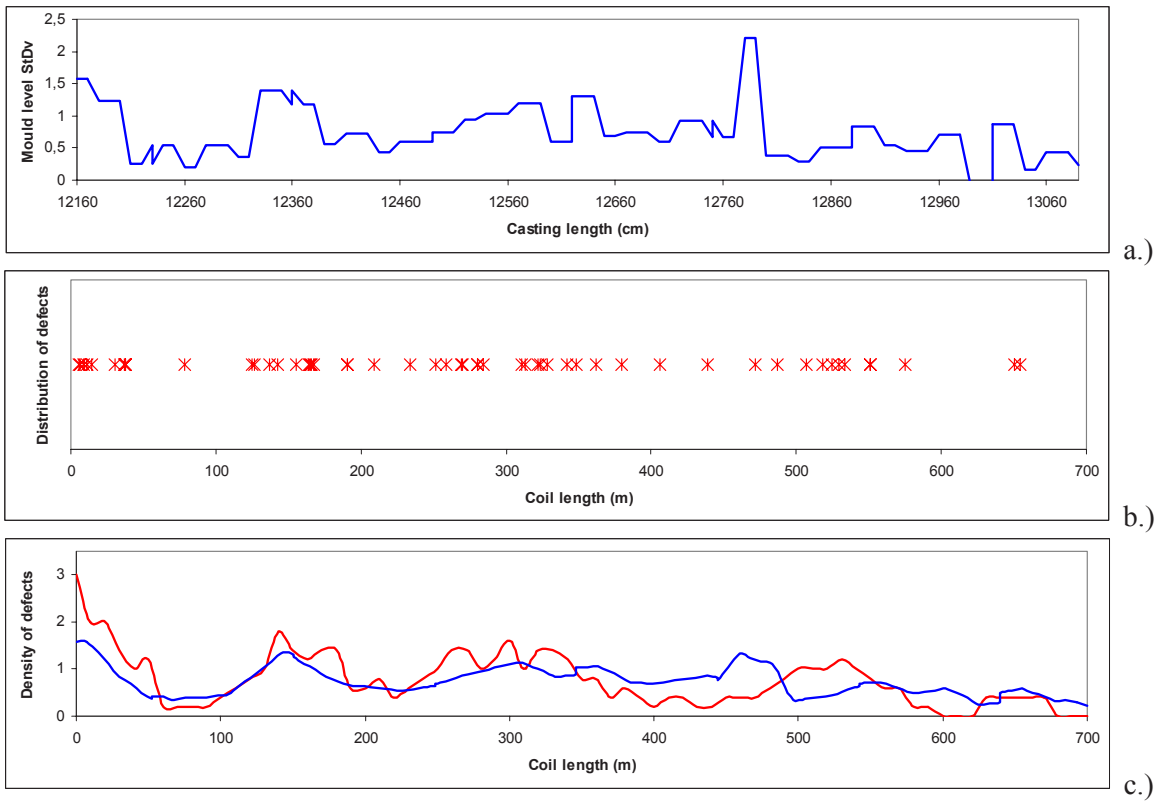

Figure 27 Results for a slab from one heat selected for detailed study: Mould standard deviation along slab length (a), appearance of defects along the obtained hot coil (b), and comparison of mould level standard deviation (blue) with defect density, both referred to coil length (c). (Arcelor España)

Comparing Figure 27-a and Figure 27-b it is noteworthy that the peaks in the standard deviation of the mould level are correlated with the presence of relevant defects in the hot coil. This result can be better

seen in Figure 27-c where the mould level standard deviation and the defect density are represented in the same graph versus coil length. In order to take into account that an instant perturbation of the mould level can produce entrapment in an interval of the strand length, a Savitzky-Golay filter has been applied to the original curve of level standard deviation.

Summing up, the mould level deviation and the defects in the coil appear in corresponding positions along the casting length. This behaviour has been observed in several slabs; however, it is observed typically in heats with high amount of entrapments due to high mould level fluctuations.

In order to assess the importance of the thermal status in the mould, the possible effect of superheat has been studied for selected heats discriminating between slab faces. The results are shown in **Figure 28** and **Table 13**.

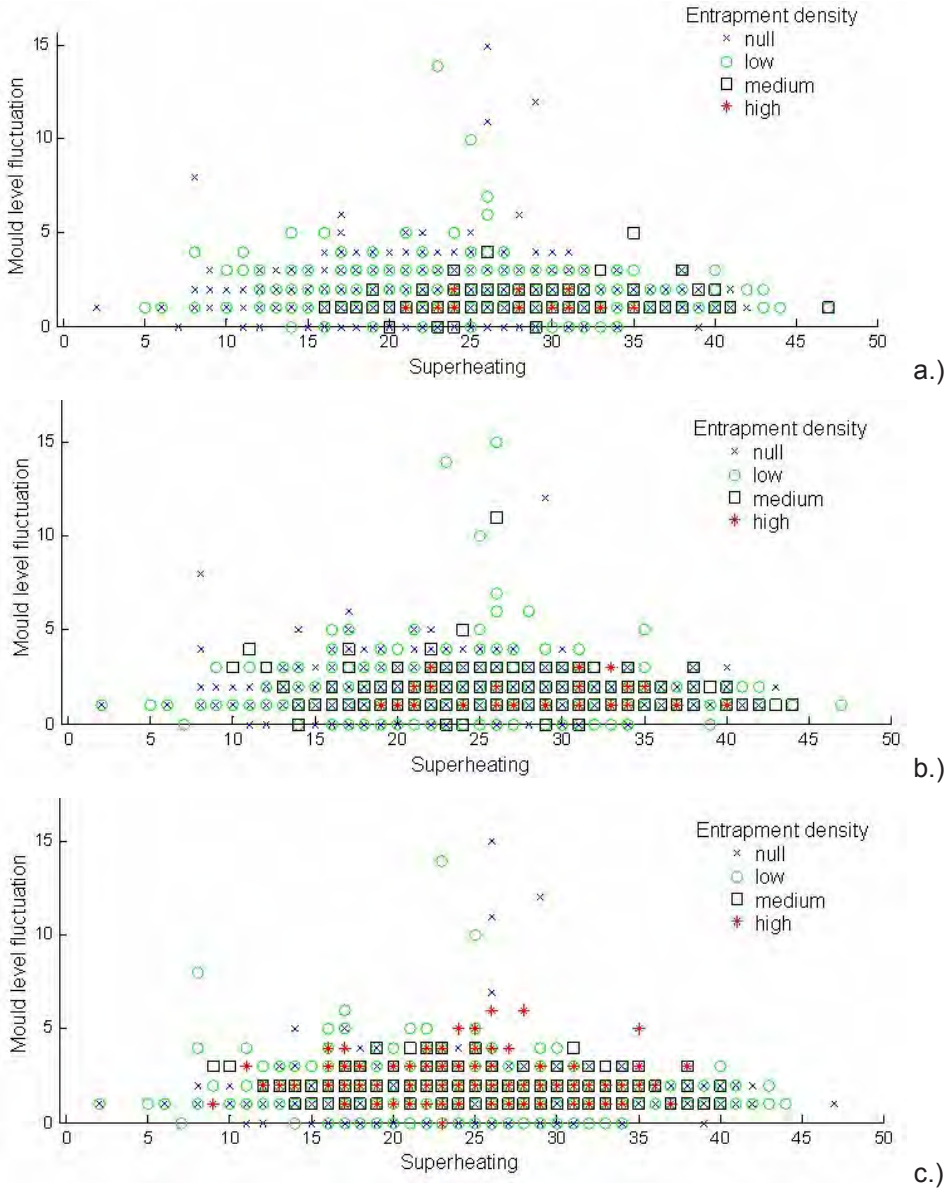

Figure 28 Distribution of slabs by entrapment density with regard to mould level fluctuations and superheating measured in tundish: (a) top face, (b) bottom face and (c) narrow face. (Arcelor España)

Table 13 Percentage of slabs with medium-high entrapment density (Arcelor España)

Mould level fluctuations	Top Face		Bottom Face		Narrow Faces	
	SH < 25ºC	SH > 25ºC	SH < 25ºC	SH > 25ºC	SH < 25ºC	SH > 25ºC
low	2.8 %	2.8 %	3.8 %	10.5 %	1.8 %	3.7 %
medium	2.6 %	2.6 %	5.3 %	6.9 %	2.6 %	6.9 %
high	2.8 %	2.8 %	8.3 %	7.5 %	2.8 %	3.8 %

Focusing on the slabs with medium-high level of entrapment in the top face it can be seen a tendency to increase as the superheat increases above 25ºC, even with low mould level oscillations. This effect is also noticeable in the bottom face and in the narrow faces which are more affected by mould level oscillations when the superheat is below 25ºC.

From the information provided by the checks on the effect of superheat parameter on slag entrapment occurrence in slab, it can be concluded that the thermo-physical properties of the casting powder fits well with the usual temperature range of the steel.

Influence of SEN immersion depth

As the mould level is an influencing operational factor, it has been investigated if the SEN immersion depth affects the occurrence of entrapment. The current standard practice, as illustrated in **Figure 29**, is to vary SEN immersion depth in order to distribute the wear caused by powder layers. For the steel grade under consideration the casting sequence starts with a SEN depth of 210 mm which is maintained for 150 minutes and then reduced to 180 mm, remaining at this depth during 150 minutes. With the standard steel flow rate, it implies 3 + 3 heats for a single SEN.

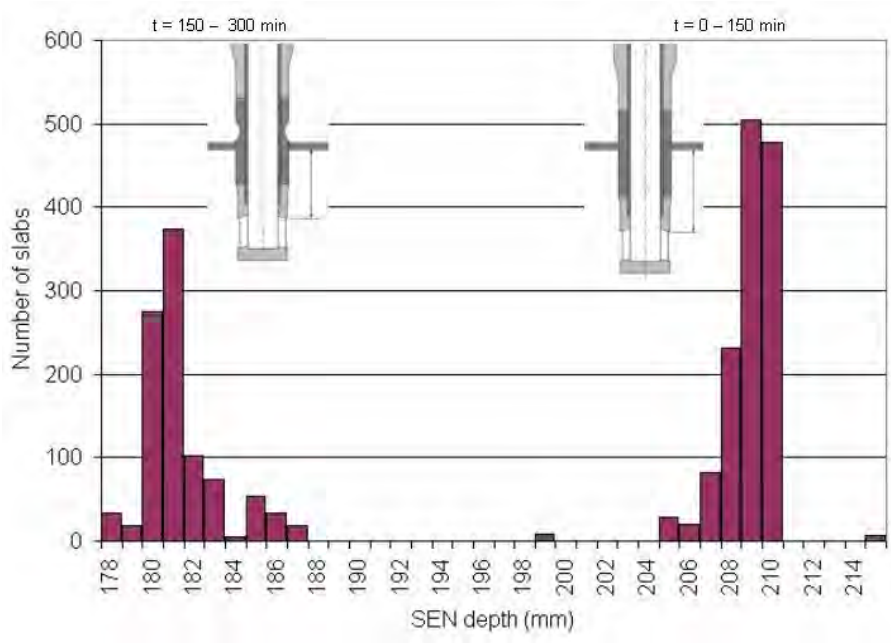

Figure 29 SEN immersion depth: operational practice and distribution of slabs by SEN depth (Arcelor España)

Figure 30 permits to analyse the impact of SEN immersion depth on entrapments. The SEN depth is represented in the horizontal axis and the entrapment density in the vertical axis. The colour scale indicates the number of slabs with a given SEN depth and entrapment density. It can be seen that the defect distribution is almost the same regardless the depth in use. The totals are around 85 % of slabs with null – low entrapment density and 15 % with medium – high for both immersion depths. From these results it can be concluded within the current operational practice the SEN depth does not affect appreciably the occurrence of entrapment.

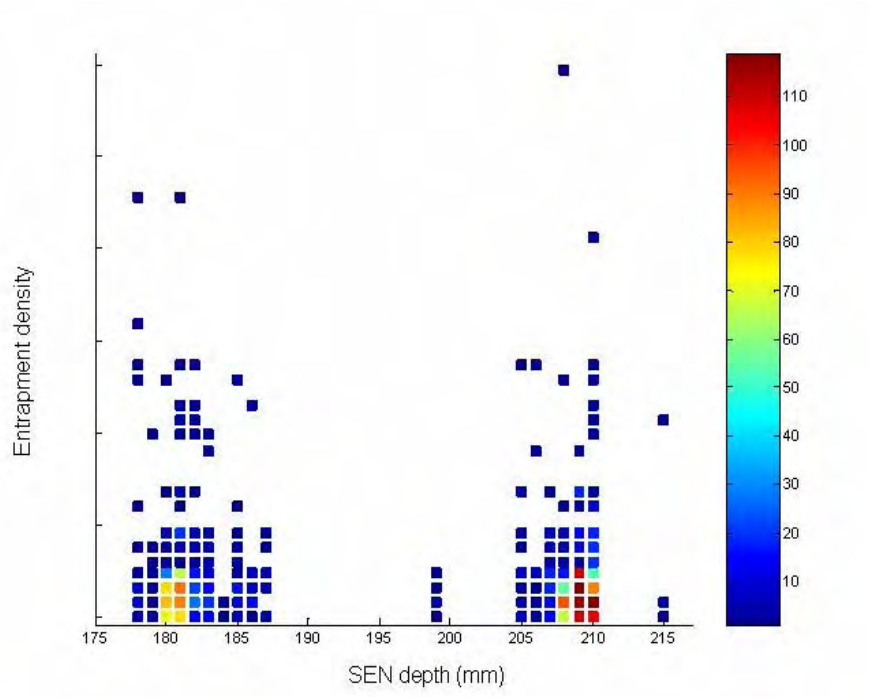

Figure 30 Slab frequency as a function of entrapment density and SEN depth for analysing possible effect of SEN immersion depth on the resulting entrapment density (Arcelor España)

Influence of SEN conditions

Fluid flow in the mould can change due to a change in the SEN geometry because of wear during a casting sequence. Some studies have shown that the major impact of the SEN geometry on the entrapment phenomena takes place through the instability of the streams of steel inside the mould [4] and [5] and through the modification of the front of solidification. Moreover, as emphasized by numerical and physical modelling in the frame of this project, a not stable flow field near the meniscus can also cause entrapment.

The alterations in the front of solidification and in the meniscus velocities are not always detectable by common mould instrumentation (mould level or sliding gate oscillations). By contrast, a characterization of the typical ranges of variation of SEN geometry is possible and can be used as a modelling input. The modelling results will provide an assessment of the impact of this factor on mould powder entrapment.

The mould wall thermocouples give some indirect information on the meniscus temperature and steel flow asymmetry [6]; as a consequence, only weak correlation with the entrapment in the mould is expected. Mould wall temperatures have been represented and compared with other process variables and entrapment occurrence through quality results both in slab and in coil after hot rolling, but with no stringent correlations. **Figure 31** represents the time evolution of mould wall temperatures along a casting sequence. Although asymmetry is observed in certain intervals, the related slabs did not present a noticeable increase in entrapped powder occurrence.

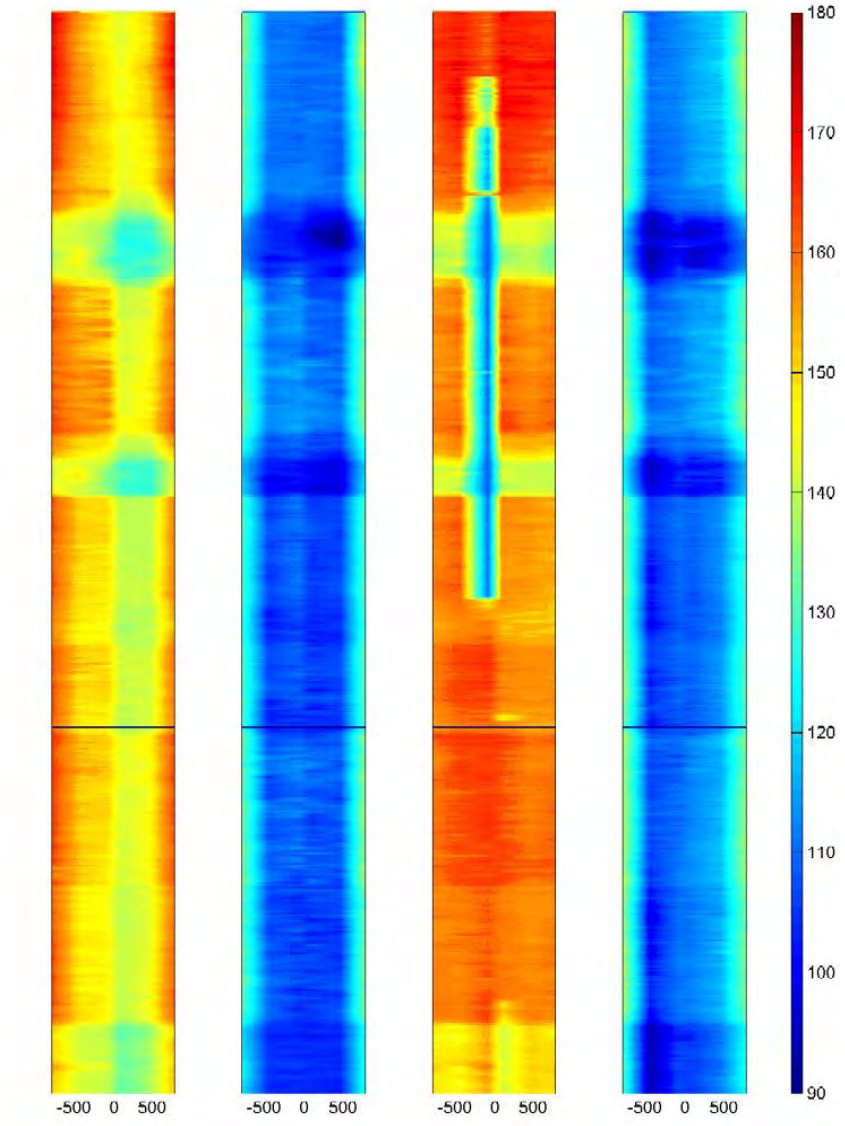

Figure 31 Representation of mould wall temperature evolution along a casting sequence: (a) temperatures in º C at 90 mm below meniscus (top face), (b) temperatures in º C at 226 mm below meniscus (top face), (c) temperatures in º C at 90 mm below meniscus (bottom face), (d) temperatures in º C at 226 mm below meniscus (bottom face) (Arcelor España)

Existing studies show that the two causes of geometry modification, clogging and erosion, occur mainly in the inner part and near the outlet ports of the SEN [7]. In general, the shape of the clog appears to follow the contour of the steel flow through the nozzle where clog material tends to collect in the more stagnant regions with the presence of eddies. The heat losses from the stagnant steel within the clog

matrix in these regions might allow it to solidify, thereby strengthening the clog and helping it to grow further. So, the bulk of the deposit is composed of oxide particles (usually alumina) with voids partially or totally filled with steel [8], [9] and [10]. Sometimes, the deposit is very fragile, so care has to be taken while handling and cutting the SENs in order to obtain valid results.

A representative set of twelve used SENs has been analyzed. They have been sampled in order to cover different casting time, number of heats, etc. Its main characteristics are summarized in **Table 14**. The sampled nozzles have been cut and prepared for measuring the diameter and thickness at different positions (**Figure 32**). Due to technical limitations, it was necessary to divide each nozzle before performing the longitudinal sections.

Figure 32 Preparation and measurement of used SENs in order to assess geometry degradation along casting sequence Comparison (Arcelor España)

From the SENs analyses (**Figure 33**) it was concluded that, when clogging is present, a bulk deposit is mainly observed in the zone that is submerged inside the melt, mainly

- around the ports
- in the well
- in the stagnant region of stream bifurcation

By contrast, the straight part of the SEN above the meniscus level is essentially clean. The level of erosion in the observed samples seems to be not very important.

Based on the observed samples, a typical clogged SEN has been defined.

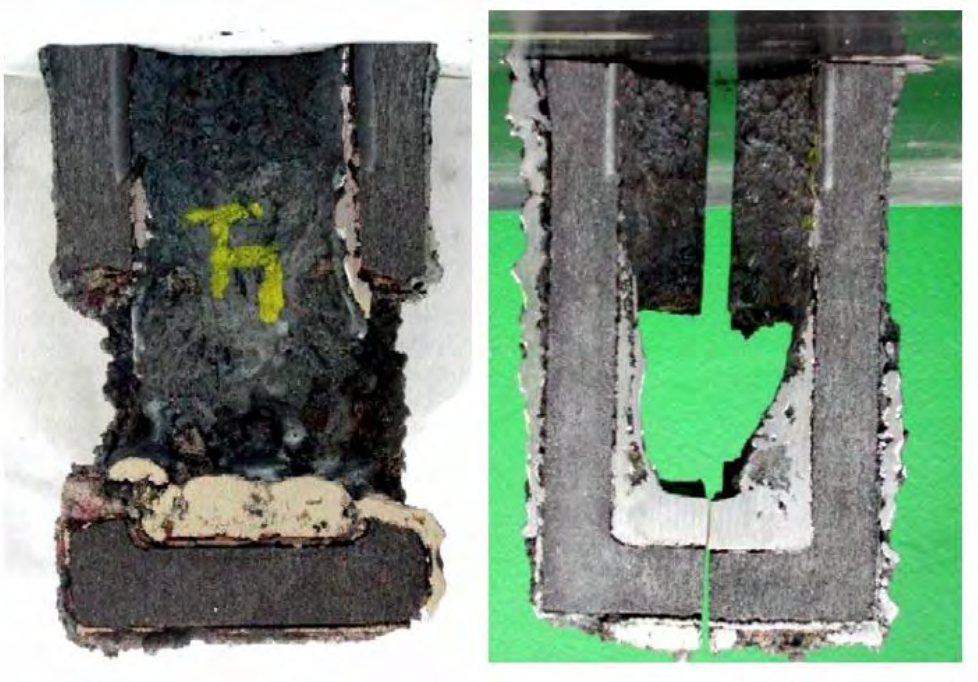

Figure 33 Examples of clogged SENS used in the definition of the geometry for numerical modelling (Arcelor España)

Figure 34 shows a technical drawing of standard mould and SEN used at Arcelor España.

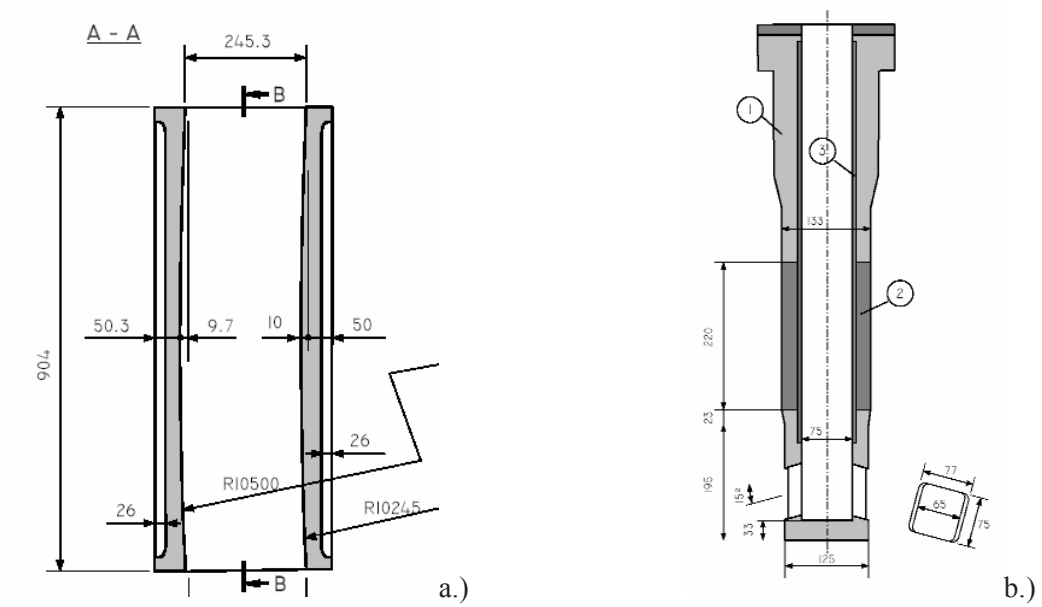

Figure 34 Geometrical description of the mould (a) and the SEN (b) provided to BFI in order to set up the model for Arcelor España process. In addition, the physical properties of the materials have been provided as well as other operational information (Arcelor España)

Table 14 Percentage of slabs with medium-high entrapment density (Arcelor España)

sample	date	casting time	number of heats	order in sequence
FLX01	30/10/2005	182’	4.0	1
FLX02	03/11/2005	271’	4.5	2
FLX03	03/11/2005	119’	2.0	3
FLX04	31/10/2005	148’	2.0	1
FLX05	26/10/2005	122’	2.0	1
FLX06	03/11/2005	206’	3.5	1
FLX07	29/10/2005	232’	4.0	1
FLX08	30/10/2005	182’	4.0	1
FLX09	03/11/2005	201’	3.5	1
FLX10	22/10/2005	122’	2.0	3
FLX11	26/10/2005	122’	2.0	1
FLX12	29/10/2005	118’	2.0	2

At **TKN** further operational parameter studies were aiming at the influence of:

- casting speed
- super heat
- SEN immersion depth

on the behaviour of the flux in form of layer formation (i.e. thickness) and on the horizontal velocity of the steel melt near the interface steel melt/liquid flux.

To measure the slag thickness the following different methods can be used [11]:

- immersion of a lockable tube
- wire method
- sheet method

The method with immersion of a lockable tube was used in a former work [12]. One disadvantage is, that the different layers are disturbed due to the movement of the tube by lowering in into the slag/steel. Therefore it is very difficult to get results regarding the slag thickness. So it was decided to use the other methods.

For the measurement of the slag layer the wire-method with a pair of two wires of different melting temperatures has been tested. Due to the different melting temperatures one wire melts down at the phase border solid-to-liquid in the flux powder and one wire at the phase border liquid flux-to-steel-melt. The difference in length of the two wires is equivalent to the thickness of the liquid flux layer. For the measurement of the slag layer at different positions in the mould the measuring device is equipped with six pairs of wire, **Figure 35**.

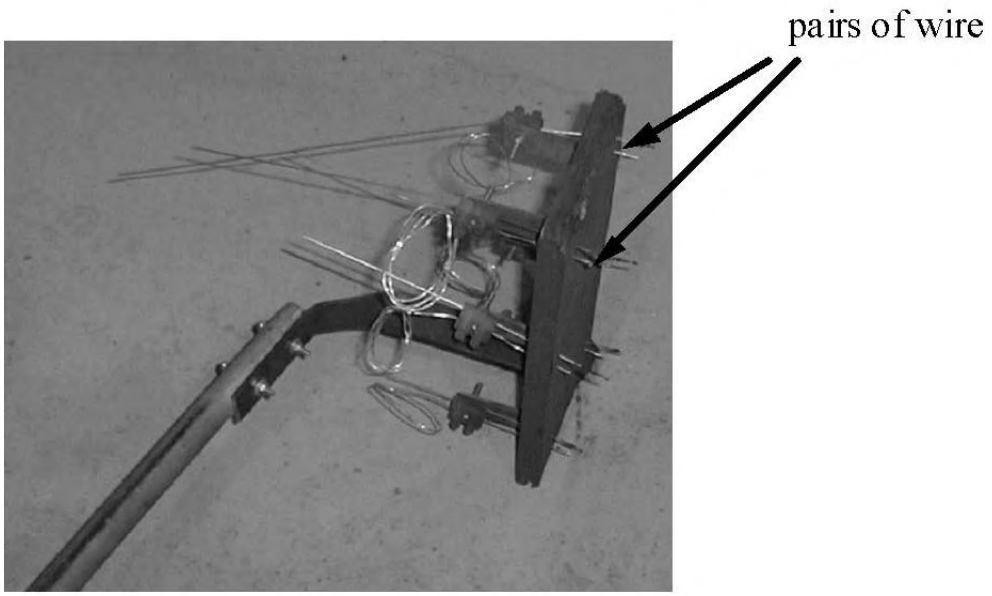

Figure 35 Measuring device for the measurement of the liquid slag layer at TKN

The disadvantage of this method is that only the thickness of the liquid flux layer can be estimated and not the thickness of the whole casting powder. Therefore it is not possible to get any information about the contour of the different phase borders powder – flux – melt.

The disadvantages of the wire-method can be avoided using the sheet-method. This method is very similar to the wire-method and also easy to use. A thin steel sheet is lowered into the melt and will melt down just at the phase border liquid steel-to-liquid flux. The phase border liquid flux-to-sintered-powder can be identified by the change of the temper colour of the steel sheet. The thickness of the solid powder layer can roughly be evaluated by powder particles sticking on the sheet.

The sheet measuring device consists of the following components as shown in **Figure 36**:

- Fix point for the measuring tool (installation on the ladle turret)
- Measuring tool (steel pipe with sheet fastening device)
- Steel sheet (100 mm x 200 mm x 1 mm)

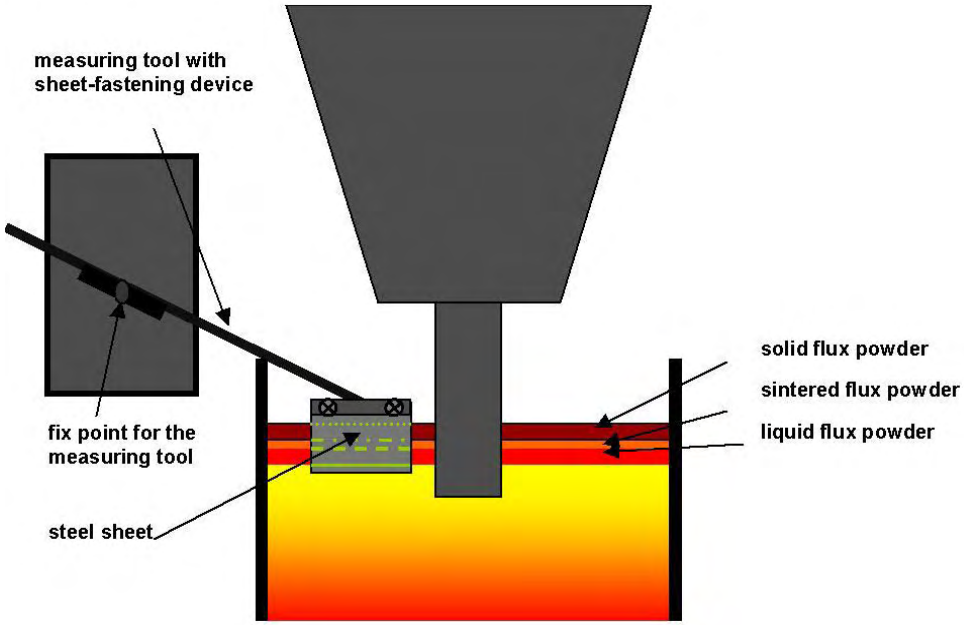

Figure 36 Construction of the sheet measuring device at TKN

In dependence of the steel grade to be investigated an appropriate sheet material has to be used. The sheet has to melt down just at the phase border flux – melt in a short time.

The following sheet materials have been chosen:
steel grade 1.4301: sheet material 1.4565 with T_L = 1,400°C
steel grade 1.4016: sheet material 1.4301 with T_L = 1,455°C

The chemical composition and the liquidus temperature of the mentioned steel grades were already shown in Table 6.

To get an appropriate melt down of the sheet at the phase border to the steel, the sheet with a thickness of ~ 1mm is lowered into the mould for 10 – 15 seconds.

To measure the flow velocity in the mould, different possibilities are described in the literature. One can measure the mass-loss of an immersed body [13] - [15], the detaching frequency of a vortex tube acting after Karman's principle [16] - [17] or inductive methods [18] - [19]. Very often the movement or the torque of an immersed body is measured [20] - [25].

The measurement of the torque is a comparable simple measurement device which can be used in the rough surrounding of a continuous casting machine.

Using the following equation

$$v = \sqrt{\frac{M/l}{\rho/2 \cdot A \cdot c_w}} \tag{1}$$

one can estimate the horizontal mean velocity v acting on the immersed body.

Here M is the measured moment, l the distance between half of the immersion depth of the immersion body and the rotation axis, ρ the density of the fluid, A the projected area of the immersion body the flow is directed against, and c_w the drag coefficient for the immersion body, which was determined by aid of physical model trials performed by BFI (see chapter 2.3.4.3).

Figure 37 shows the principle of the measurement and the installation in the mould.

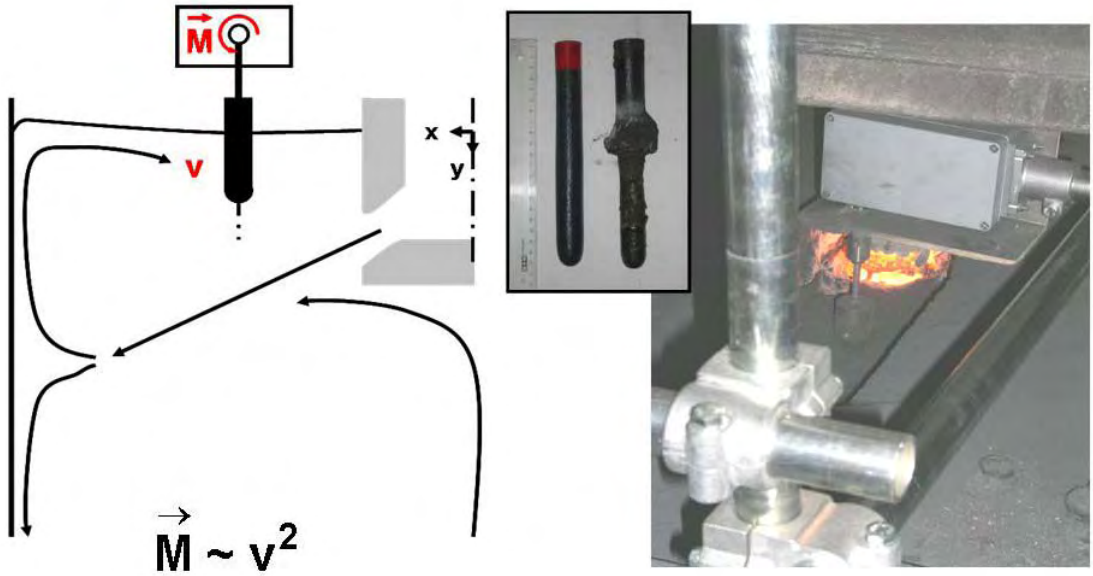

Figure 37 Estimation of flow velocity near the mould level surface at TKN

A round bar, made from alumina graphite, fixed on a device for measuring the momentum, is lowered into the steel. The fluid flow will lead to a momentum, which is according to equation (1) proportional to the squared velocity.

Due to the aggressive character of the casting flux alumina graphite was chosen as a material for the body. This material shows sufficient thermal shock resistance and also the thermo chemical wear was small enough to assure a serving life long enough for a measuring campaign.

The equipment is cooled with compressed air to avoid overheating of the electronic installation build in the measuring device.

During the calibration trials at BFI additional trials were performed in order to be able to recalculate different immersion depths of the bar to an immersion of 50 mm. For more details on physical model trials see chapter 2.3.4.3.

During casting of steel grade 1.4301 the measurements were carried out with the wire method at constant measuring parameters. So the influence of the measuring position, the casting speed and temperature and the immersion depth of the submerged entry nozzle (SEN) on the thickness of the liquid flux layer could be investigated.

The average liquid flux thickness has been determined at the measuring positions:

- close to the narrow face to 9 – 11 mm
- in the middle between the SEN and the narrow face to 12 – 17 mm
- close to the SEN to 13 – 20 mm

Influence of casting speed

Figure 38 shows the influence of casting speed on the flux layer thickness. At a low casting speed, i.e. 0.8 m/min, the liquid flux layer tends to be thinner than at high casting speed.

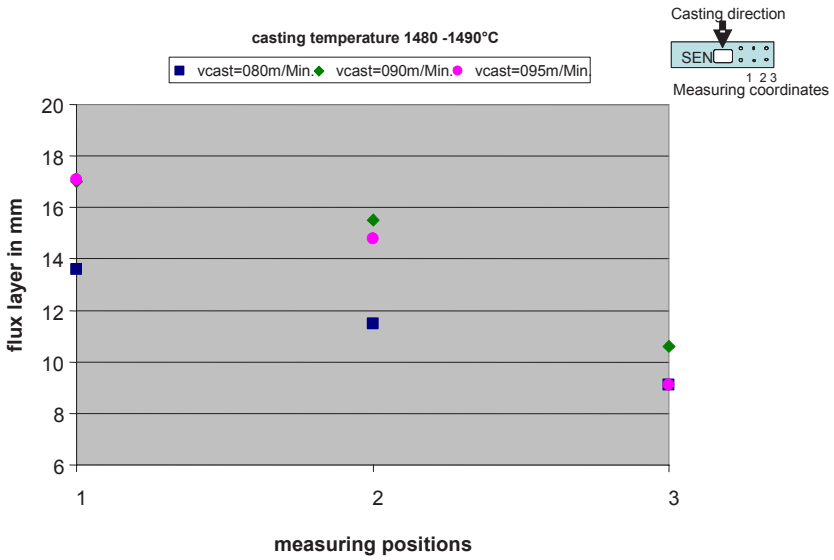

Figure 38 Average flux layer in dependence of casting speed at TKN

Influence of casting temperature

Figure 39 shows the influence of superheat on the flux layer thickness. It can be seen that there is for the temperatures investigated no correlation with the layer thickness.

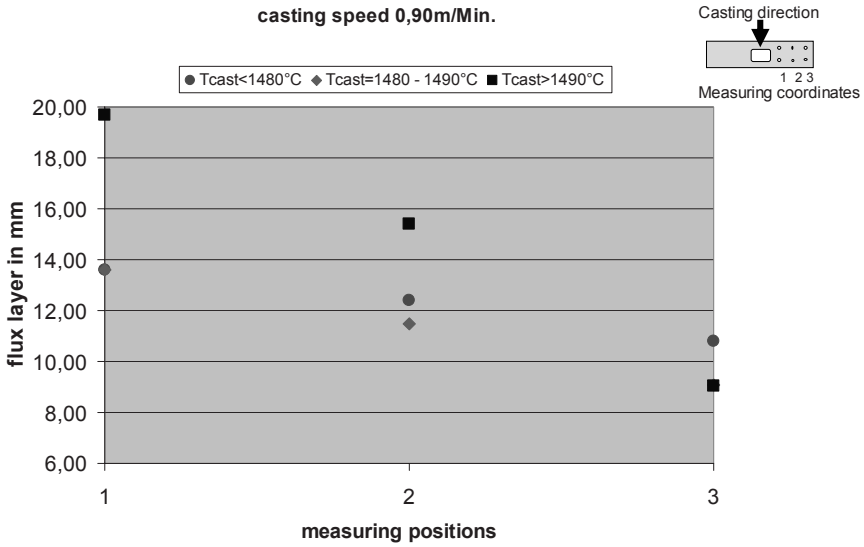

Figure 39 Average flux layer in dependence of casting temperature at TKN

Influence of SEN immersion depth

Figure 40 shows the influence of the immersion depth on the flux layer thickness. For the high immersion depth of 140 mm the layer tends to be thinner than for the low immersion depth of 120 mm.

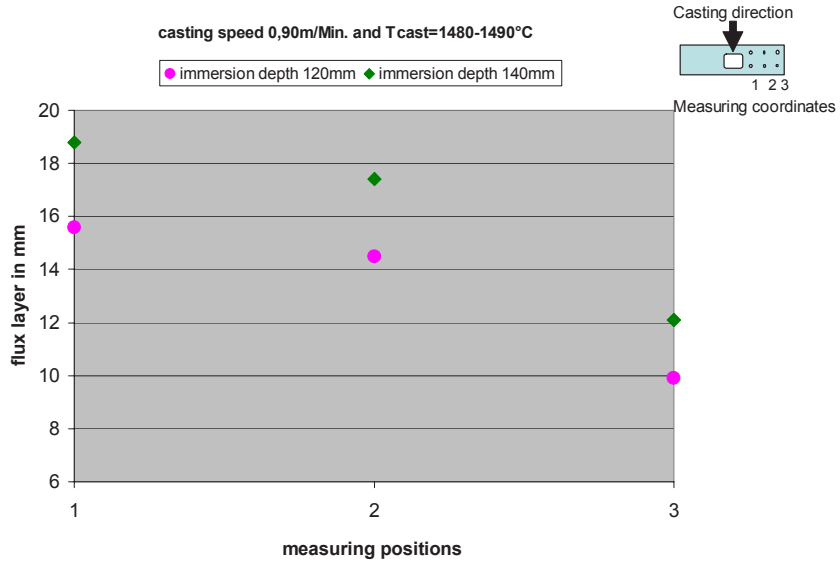

Figure 40 Average flux layer in dependence of SEN immersion at TKN

The above reported dependencies of process parameters give only a tendency due to the big variations in the single measurement.

Further measurement were performed with the sheet method for steel grade 1.4301. The steel sheet made from 1.4565 one with a size of 100x200 mm was inserted in the mould for 10 -15 sec, with a distance of 20 – 25 cm from the narrow face. During this time the sheet in contact with the steel melted down to the interface melt-slag. From the colour of the remaining sheet the boundary slag – powder

could be also measured and from traces of the powder remaining on the sheet, the thickness of the powder layer also could additionally be estimated.

Figure 41 and **Figure 42** show typical results of a measuring campaign in one sequence of casting. The average thickness of the total casting powder layer, i.e. powder and slag is approximately 37 mm near the narrow side and around 42 mm towards the SEN. The thickness of the liquid pool is 14 mm and 17 mm respectively. The thickness of the slag layer and more pronounced the slag and powder layer differs strongly at different times during a sequence. In case of the powder layer, this can be explained by the manual feeding of casting powder.

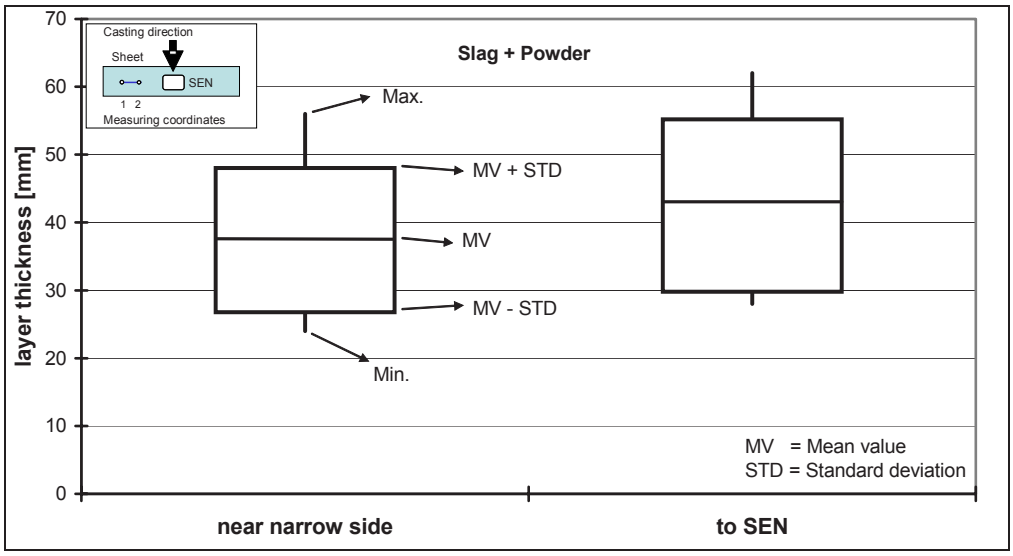

Figure 41 Measurement of melting of mould powder at TKN for steel grade 1.4301 using mould powder C

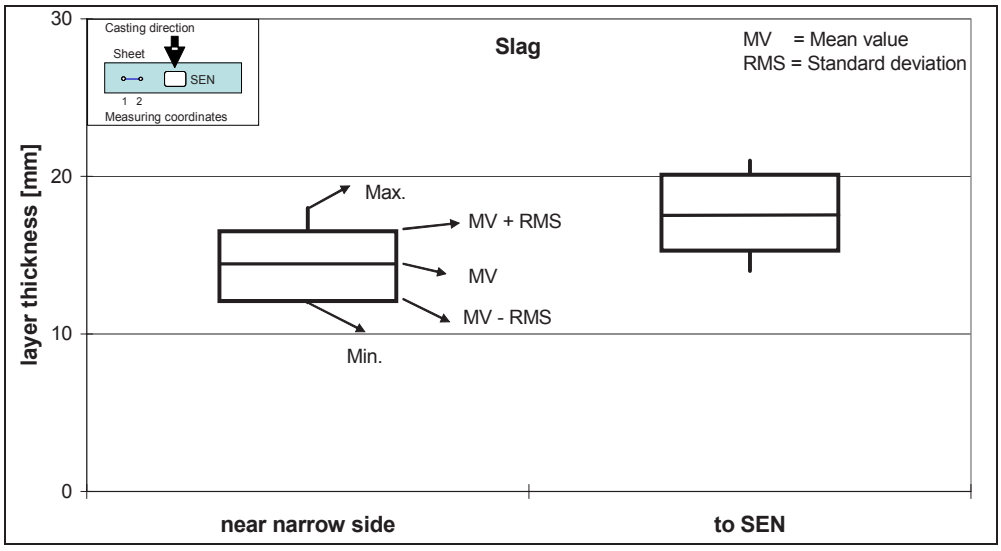

Figure 42 Measurement of the melting of mould powder at TKN for steel grade 1.4301 using mould powder C

In case of the slag layer an influence of the turbulent flow of steel near the meniscus exists. Therefore, like in the trials with the wire-method, just a tendency of the influence of casting velocity and casting temperature is shown (see **Figure 43**).

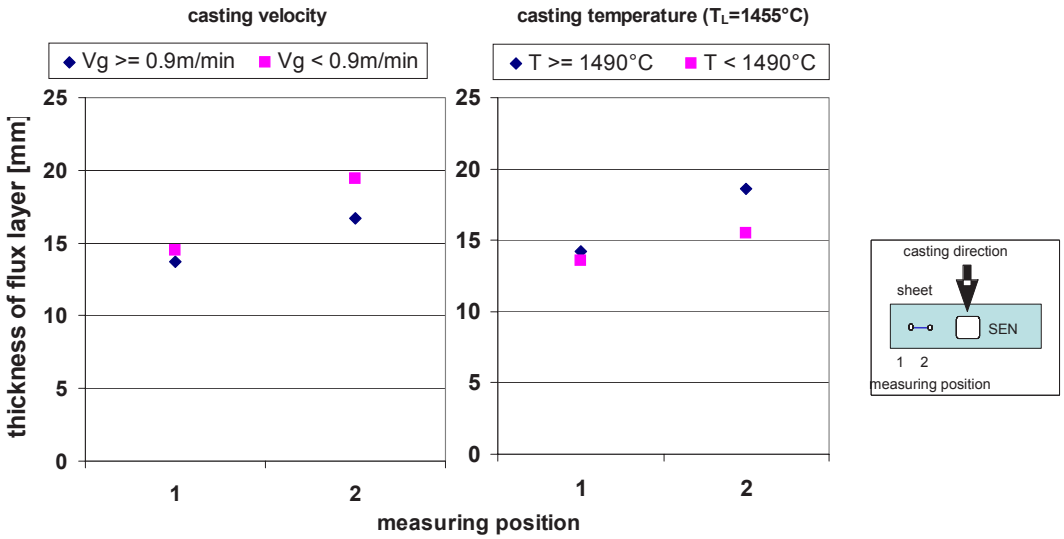

Figure 43 Average flux layer at TKN for steel grade 1.4301 using mould powder C

In the same way trials were also performed using the steel grade 1.4016, which is cast with the casting powders A and B.

Additionally some trials were performed with two connected sheets. In this case, the distance to the narrow face was about 5 cm. With this short distance to the narrow side, the standing wave of the steel surface can be weakly seen at the boundary steel - slag and slag – powder, assuming the powder surface as a horizontal plane, see **Figure 44**.

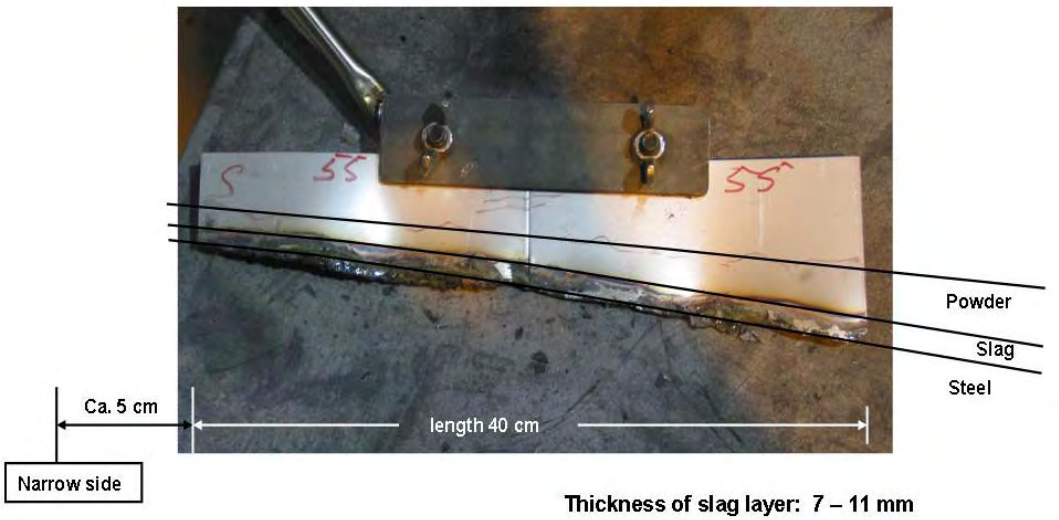

Figure 44 Measurement of slag layer at TKN for at steel grade 1.4016 using mould powder B, sample of sheet

This also shows that the powder layer near the submerged entry nozzle (SEN) is thicker than near the narrow side.

It can be seen that according the turbulent and random flow of the steel melt the interfaces steel – slag and slag – powder are very uneven.

These different layer thicknesses in one sample at different points are also observed in different samples at the same measuring point. Here one must have in mind, that the manual addition of casting powder will amplify these differences.

Figure 45 and **Figure 46** show the evaluation of the measured thickness in the different measuring campaigns. The slag layer near the narrow side has an average thickness of 8.8 mm, towards the SEN the thickness is around 12 mm. The average thickness of the total layer (i.e. slag and powder) is 37 mm near the narrow side and 47 mm closer to the SEN.

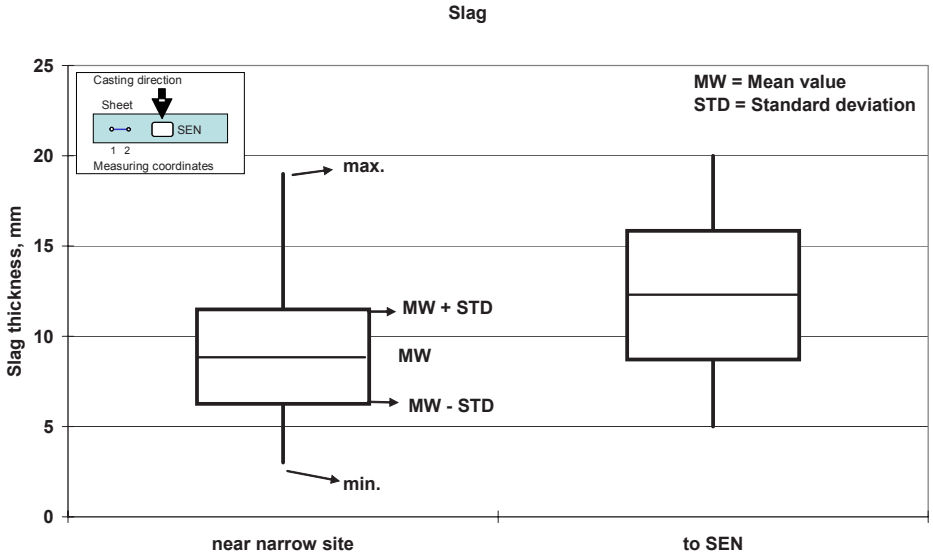

Figure 45 Measurement of the melting of mould powder at TKN for steel grade 1.4016

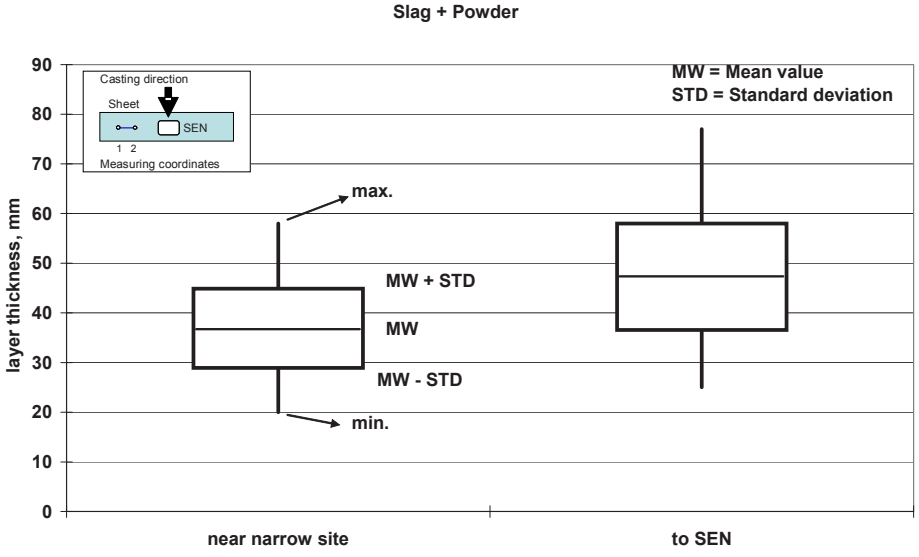

Figure 46 Measurement of melting of mould powder at TKN for steel grade 1.4016

In case of the trials with the steel grade 1.4016 it was of special interest to see, if there is a difference between the two casting powders used, as this is indicated by the examination of the process data. But there are only minor differences like the differences observed with the other process parameter casting velocity, temperature and immersion depth as **Figure 47** indicates.

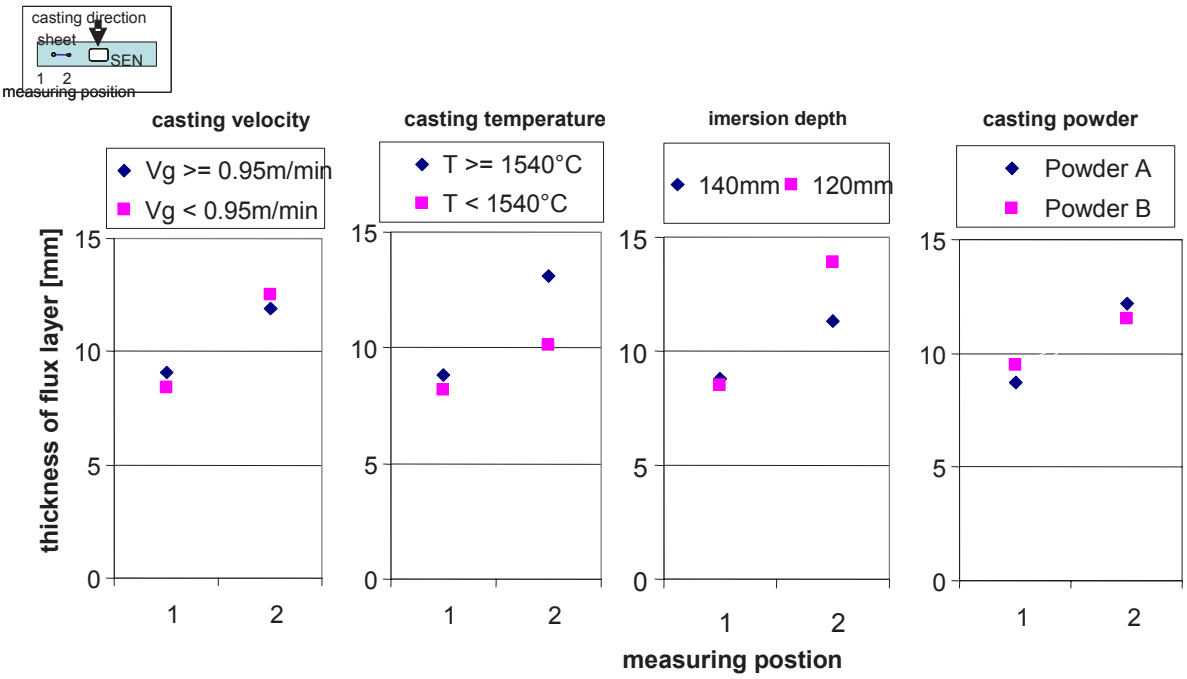

Figure 47 Average thickness of flux layer in dependency of different parameter at TKN for steel grade 1.4016

The wire-method and the sheet-method are both able to measure the thickness of the liquid flux layer at the meniscus. With the sheet-method additionally the thickness of the powder layer can be estimated. Assuming a 'flat' reference powder surface, steel meniscus near the narrow face is around 1- 2 cm higher than towards the SEN.

The total slag thickness of all casting powders is approximately equal and differs between 35 and 45 mm; anyway, manual feeding during time can lead to greater differences in layer thickness.

Figure 48 shows the flux layer thickness during casting the different steel grades (1.4016 and 1.4301) with the different casting powder types (Powder A/B and powder C). It is clearly seen that the flux layer in case of casting 1.4016/powder A/B is significantly lower than casting 1.4301/powder C.

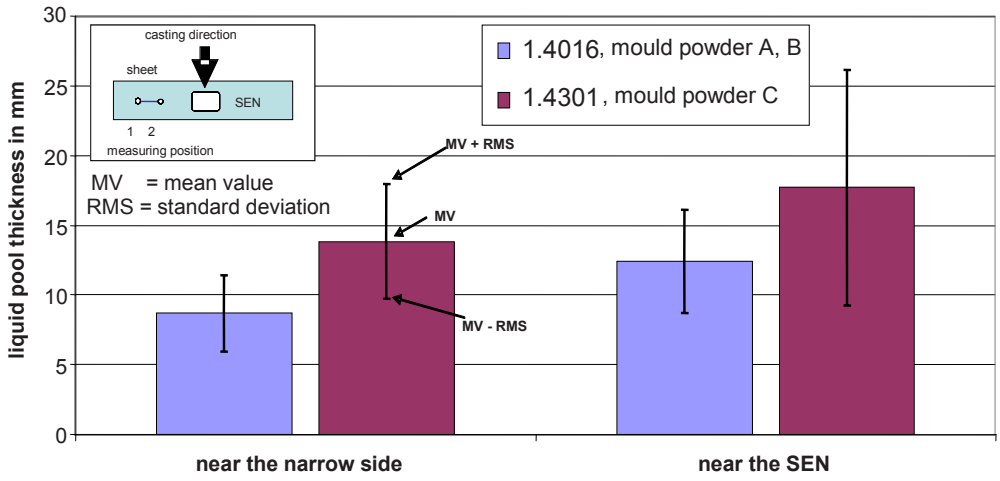

Figure 48 Measurement of liquid flux thickness in TKN investigations

Moreover, it can be seen that

- the liquid pool is much thicker towards the SEN than near the narrow face,
- the thickness of the liquid pool depth is strongly fluctuating,
- for the austenite / mould powder “C” the thickness of the liquid pool is much thicker.

It can be then concluded, that the different behaviour is related mainly to different casting powders and not to different steel grades. The thinner flux layer may be one of the causes of the observed defect, see chapter 2.3.1 for more details.

The measurement device for measuring the horizontal flow velocity is mounted on tubes at the tundish and adjusted above the mould. Then the measuring bar is lowered into the steel. One measuring campaign is approximately 10 min long. **Figure 49** shows a typical result of a measuring campaign. Parallel to the horizontal flow velocity the casting velocity, mould level and stopper rod position are recorded.

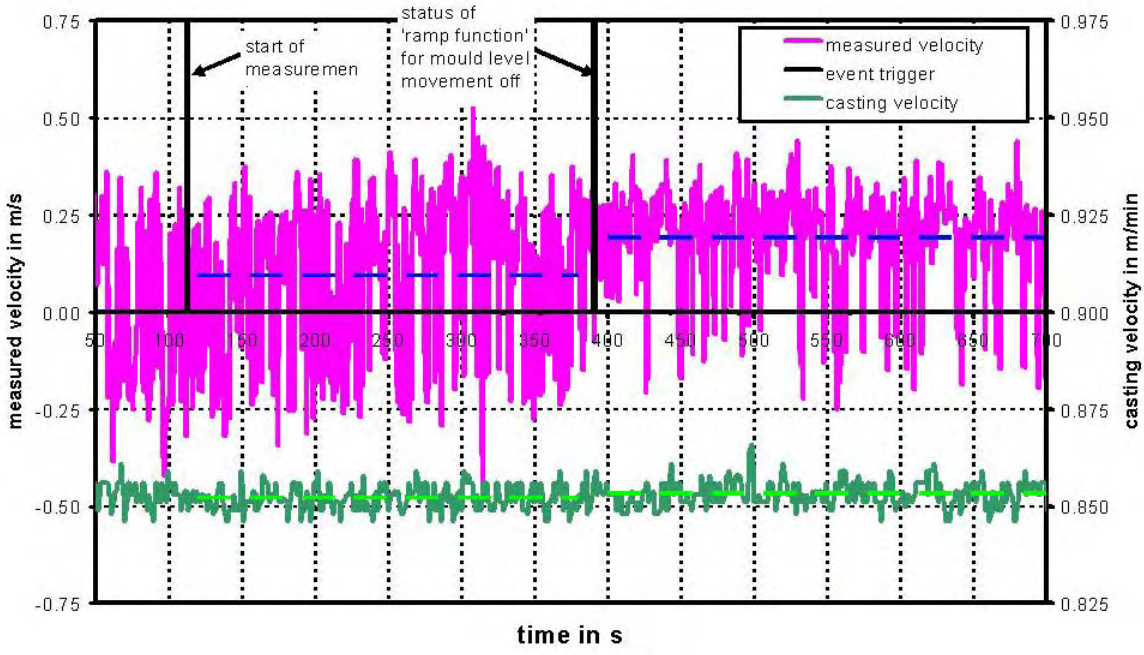

Figure 49 Estimation of the velocity near the meniscus. Immersion depth of measuring body 35 mm format: 1,500 x 240 mm², SEN immersion depth: 120 mm (TKN)

The magnitude of the measured velocity and the fluctuations are as expected from the physical model It shows that even under steady state casting conditions the flow is strongly fluctuating. During the first period the steel level in the mould had been altered by a ramp like movement with amplitudes of ± 10 mm during 20 minutes around the nominal mould level. This is an operational practice at the TKN-Bochum continuous caster to minimize the wear of the SEN. During the second period the ramp function has been switched off. One can clearly see that the range of measured velocities is smaller during the second period, resulting in a higher mean value and a lower RMS value of the horizontal velocity.

Different trials were performed to measure the flow velocity regarding steel grade, immersion depth of the SEN (ID), casting velocity and also to observe the influence of the ramp (GSR).

Not all measurements were reliable, due to

- too high temperature in the box of the measurement device,
- too high bar immersion depth,
- bar breaking during the measurement.

All measurements were performed 430 mm away from the marrow face, i.e. around 210 mm respectively 350 mm away from the centre of the mould (depending on the width). In this region the models indicate the highest values of the velocity.

Table 15 and **Table 16** show the results of the measurements.

Table 15 Results of flow velocity measurements at TKN, 1.4301 steel, SEN 50 x 70 mm^2

Format	Casting velocity in m/min ID	GSR	0.82/0.85 v in m/s	0.82/0.85 RMS in m/s	0.90 v in m/s	0.90 RMS in m/s	1.00 v in m/s	1.00 RMS in m/s
1265 x 240	120	off	0.246	0.063	0.280	0.091		
		on			0.303	0.103	0.336	0.084
	140	off			0.321	0.063	0.358	0.074
		on			0.379	0.061	0.359	0.071
1550 x 240	120	off	0.311	0.064	0.374	0.065		
		on			0.423	0.213		

Table 16 Results of flow velocity measurements at TKN, 1.4016 steel, SEN 50 x 90 mm^2

Format	Casting velocity in m/min ID	GSR	0.80 v in m/s	0.80 RMS in m/s	0.90 v in m/s	0.90 RMS in m/s	1.00 v in m/s	1.00 RMS in m/s
1280 x 240 1305 x 240	120	off			0.276	0.065	0.363	0.055
		on	0.248	0.063	0.268	0.083	0.350	0.069
	140	off			0.309	0.057		
		on			0.282	0.126		
	160	off			0.306	0.085		
		on			0.339	0.091		
1560 x 240	140	off			0.388	0.090		
		on	0.378	0.081			0.393	0.121

In both cases, 1.406 steel with exit-area of the SEN of 50 x 90 mm^2 and 1.4301 steel with 50 x 70 mm^2 exit of SEN, it can be stated what follows.

- With higher casting velocity the horizontal flow velocity increases.

- With ramp function of liquid metal level ‘on’, the horizontal flow velocity is nearly equal but the standard deviation (RMS) is higher.
- With higher immersion depth the horizontal flow velocity increases.
- Greater width values lead in turn to higher horizontal flow velocity values.

The comparison of both types of SEN shows that

- the average horizontal flow velocity does not increase, and the RMS is higher, in case of the smaller exit area of the SEN. This result was not expected, but also seen in the LDA measurements at the physical model (see chapter 2.3.4.3).
- the flow field is more reliable in case of the bigger exit-area, because the influence of the immersion depth is lower and leads to smaller RMS values of the horizontal flow velocity. This may be the reason of lower defect rate by using this type of SEN.

2.3.2.2 Verification of modelling results (Task 2.2)

Due to the turbulent steel flow at the meniscus and turbulent changes at the interface flux–melt, the differences between the measured values are high. These differences are much higher than the differences due to the process parameters. The physical model trials indicate, that a low immersion depth has a strong influence on the stability of the steel flow at the meniscus, but such values are outside of the range of the operational window.

These findings are in accordance with the numerical simulations as shown in **Figure 50**.

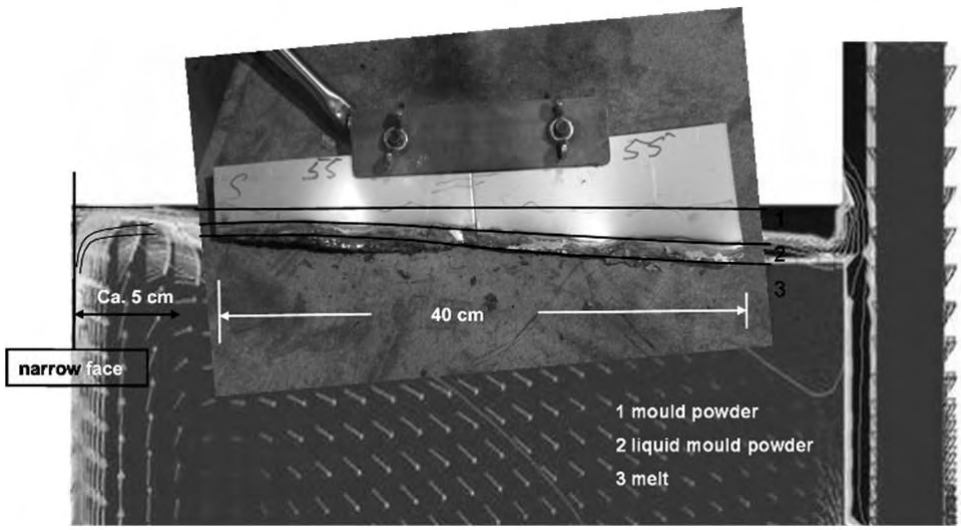

Figure 50 Comparison between numerical simulated and measured flux thickness

Figure 51 shows a comparison between the velocity measured and estimated in the physical and numerical models, showing data in good agreement. The differences according the physical model can be explained by a secondary vortex at the port exit, which influences the flow direction of the “steel” (see chapter 2.3.4.3).

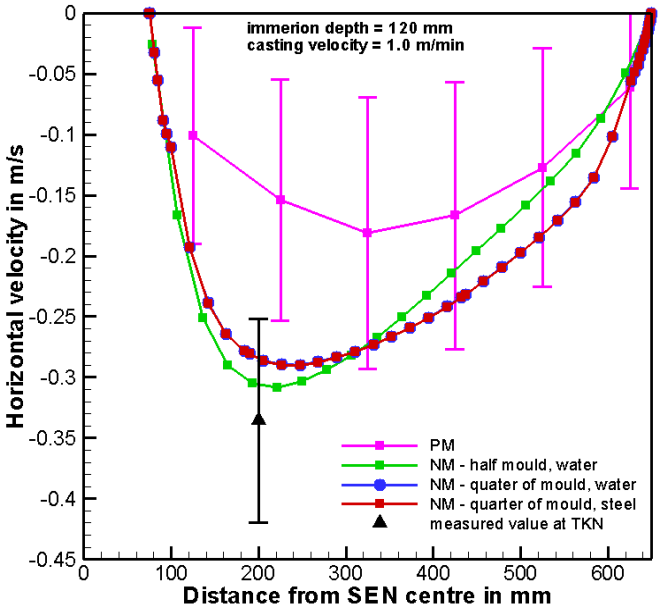

Figure 51 Comparison of operational and modelling results with SEN type 50 x 70 mm^2

The influence of the ramp function of liquid metal level is also confirmed by the physical model. The trials indicate that the casting velocity is influencing the horizontal flow velocity stronger than the SEN immersion depth.

Arcelor España performed investigation also concerning the influence of a change in SEN geometry in terms of clogging. As a result it could be found that a clogged SEN leads to more defects due to powder entrapment. Also numerical computations of BFI related to the operational situation of Arcelor España shows for a clogged SEN a clear increase of the horizontal velocity near the interface steel melt/liquid flux. This increases also the risk for flux entrapment. So the operational findings were verified. For a detailed description of the relevant numerical computations see chapter 2.3.4.4.

2.3.2.3 Determination of optimum constellations (Task 2.3)

The results achieved on plant can be generalised to refer to carbon and stainless slab casting in the following way.

The '*optimum constellation of process parameters/quantities*' concerning minimisation or avoiding of slag entrapment can be divided into two groups:

- powder features

  parameters/quantities belonging to it (plus casting temperature i.e. melt superheat) refer to the powder properties and are of most concern in determining the sintered and liquid layers thickness.
- fluid-dynamics

  parameters/quantities belonging to it refer to mechanical energy of the steel in the mould and in particular, to the meniscus. They can be directly related to casting operation (casting speed, SEN

immersion depth, SEN geometry features), both in steady state and transient conditions (the latter being more critical).

Powder features

Concerning the powder features for stainless steel a *higher content of free C* increases the occurrence of defects. This seems to be due to the influence of the C-content on melting rate and thus on liquid flux layer thickness. A similar observation could be made on the long product section (see chapter 2.3.3.3.).

It was also seen that the thickness of the flux layer depends strongly on the powder used. This can lead to entrapment of powder which has a great impact on the occurrence of defects remaining on the steel surface.

From the information provided by the superheating, it can be concluded that the thermo-physical properties of the casting powder match well with the usual temperature range of the steel. If the superheat exceeds approx. 25°C an increase of entrapment seems to occur for carbon steels.

Fluid dynamics

The entrapment is more expected to be caused by local velocity variations due to unsteady flow conditions at the interface steel/flux even under steady state casting conditions.

The evolution of process variables along slab length and defects along the corresponding hot coil has been investigated for selected heats. It has been observed that the *mould level deviation* and the defects in the coil appear to be correlated along the casting length for heats with high amount of entrapment due to *high mould level fluctuations*.

Casting speed is affecting flux entrapment. Here not only the absolute value of the horizontal velocity near the interface steel melt/liquid flux has to be taken into consideration but also its fluctuation. For high casting speeds the liquid flux layer is increasing.

The fluid flow in the mould changes when *a change of SEN geometry* occurs along a casting sequence e.g. due to clogging. In order to see if, as supposed, the mentioned deterioration has impact on the entrapment context, a characterisation of clogged SENs has been done to be used in the numerical model. It has been seen that, when clogging occurs, it tends to concentrate around the SEN ports, in the well, and in the stagnant region of stream bifurcation.

Also concerning *SEN geometry* a larger SEN port leads to lower RMS-values concerning the horizontal flow velocity. Moreover the horizontal flow velocity is less sensitive with regard to SEN immersion depth.

Concerning the *SEN immersion depth* it could be stated that the flux layer thickness is decreasing with increasing immersion depth.

In care of carbon steel the SEN immersion depth within the current operational practice does not affect the occurrence of entrapment so significantly.

2.3.3 Operational investigations for long products (WP 3)

In this chapter plant activity was performed on long product casters of CAS and Sidenor to identify optimum constellations of operating parameters and mould powder properties to reduce slag entrapment occurrence in the steel.

The approach was the following:

- at first *performance of parameter studies* were made (Task 3.1). The work was complementary to that of WP1, where a reference process quantities data base was set up and related to slag entrapment occurrence on the product;
- on the other hand, *verification of the modelling results* was accomplished (Task 3.2);
- *determination of optimum constellations* (Task 3.3) were finally achieved.

CAS and Sidenor cared the WP activity. But from the approach shown, synergy between partners, also in interrelation with the work performed in chapter 2.3.4 was exploited, especially with CSM modelling activity.

2.3.3.1 Performance of parameter studies (Task 3.1)

The operational results achieved in chapter 2.3.1 were used as a suitable basis for model approaches to set up the numerical codes, the experimental facilities and the measuring systems. This work allowed to identify both, the physical system to be investigated and the parameters to be reasonably varied.

Taking into account the guidelines for plant investigations derived from the preliminary approach to the entrapment problem (see chapter 2.3.1), industrial trials focusing on the influence of the following items over the mould powder entrapment risk were scheduled per partner as follows:

- At Basauri carbon steel caster (Sidenor):
  - powder properties;
  - in-mould EMS intensity;
  - nozzle type influence using experimental nozzles with lateral ports;
  - nozzle immersion depth.

Moreover, as a part of the collaborative work with CSM, industrial trials were developed in order to characterise the liquid pool depth for the 185 mm square billet and the four different mould powders on use at the Basauri billet caster; this work can be ascribed to the '*Verification of modelling result*' part;

- At Cogne stainless steel billet caster (CAS)
  - Powder features
  - In-mould EMS intensity
  - Nozzle geometry/immersion depth

and, similar to Sidenor, validation of the CSM model of liquid pool depth formation was accomplished with measurements on plant.

Characterisation and optimisation of mould powder concerning lubrication

At **Sidenor**, in order to optimise the mould powder performance in terms of lubrication, the following steps were scheduled for the 185 mm square billet format:

- Characterisation of the standard mould powder consumption.
- Plant trials using experimental mould powders.
- Assessment of the experimental mould powder performance (consumption, billet surface quality, entrapment).

At first, industrial trials have been carried out in order to characterise the consumption of the four different mould powder grades used for the 185 mm billet format at CCM2. This kind of assessment was performed in one strand by means of measuring the powder consumption for each trial during the entire heat. **Table 17** sums up the results of those trials in terms of number of heats, average casting speed and mould powder consumption expressed in different units.

Table 17 Main results of mould powder consumption trials for the 185 mm billet format (Sidenor).

Mould powder	Steel Grade in % C content	No. of heats	Casting speed in m/min	Mould powder consumption			Viscosity at 1300° in Poise	C free content in powder in %
				in kg/min	in kg/ton	in kg/m^2		
P1	< 0.15	4	1.18	0.0875	0.279	0.0925	37.40	12.50
P2	0.15 – 0.35	69	1.26	0.0774	0.237	0.0857	9.93	19.75
P3	0.35 – 0.50	17	1.30	0.0717	0.215	0.0776	13.51	18.30
P4	0.50 – 1.05	22	1.15	0.0452	0.150	0.0541	7.04	22.40

As indicative example, **Figure 52** shows the specific mould powder consumption for mould powder P2 as a function of the casting speed. As expected, the higher the casting speed the lower the specific powder consumption (kg/ton). The same holds for all the powders considered. Moreover, **Figure 53** shows the data concerning mould powder P4 performance, with a distinction between two quite different heat groups concerning the steel grade carbon content (with a carbon content around 0.5%, right hand side, and around 1.0%, left hand side).

In the figure, the strong influence of shrinkage on mould powder consumption is shown: mould powder consumption is very low for the highest carbon grades according to the casting speed values.

Mould powder P4 liquid flux infiltration could be improved because it is quite low compared with the others (see Table 17), and mainly for steel grades with a carbon content around 1.0%. In fact, those steel grades with carbon content around 1%C normally present high billet-mould friction values and surface defects associated to an insufficient lubrication (longitudinal bleeds). The next step was therefore to improve the performances of powder P4.

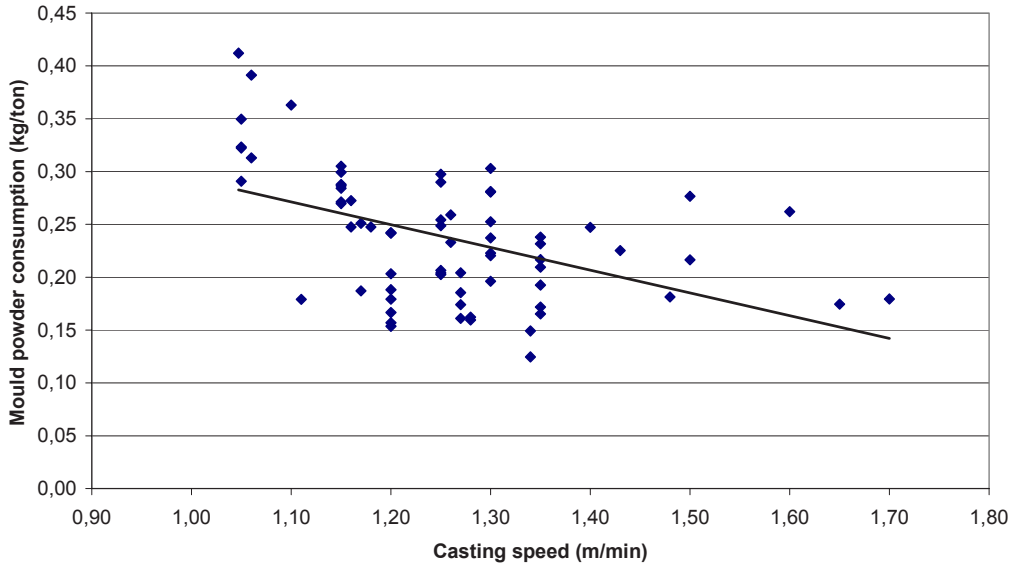

Figure 52 Mould powder P2 (0.15 < %C < 0.35) consumption as a function of the casting speed (Sidenor)

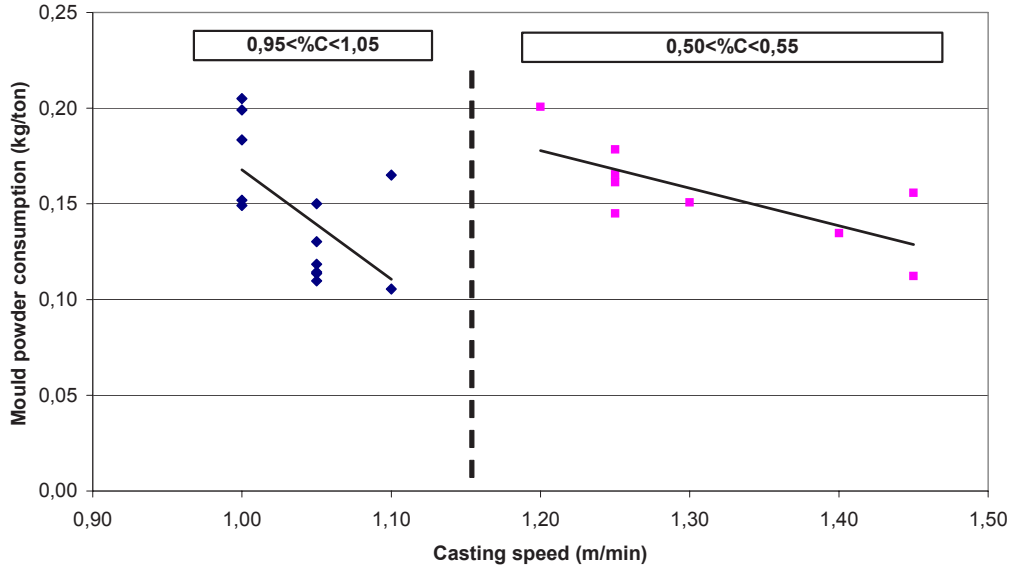

Figure 53 Mould powder P4 (0.50 < %C < 1.50) consumption as a function of the casting speed making a distinction between two different carbon ranges (Sidenor)

To favour consumption without affecting a high enough liquid pool layer, a modified P4 powder was designed with a lower viscosity (countermeasure beneficial for consumption) and a lower free carbon

content (beneficial to attain a reliable liquid pool thickness). 'P4 experimental' powder features compared with P4 ones are shown in **Table 18**.

Table 18 Comparison between mould powders P4 and P4exp (Sidenor)

Mould powder grade	Basicity index	Viscosity at 1300°C in Poise	C free in %	Melting point in °C
P4	0.58	5.5	22.4	1080
P4exp	0.63	1.8	13.5	1060

Three heats were performed with the new powder with steel carbon content in the range (0.95<%C<1.05), using P4exp on one strand and P4 in the others. As a result, the *mould powder consumption increased* of about 40%. In terms of *billet surface quality*, P4exp lead to a worse surface quality (surface cracks after rolling), but concerning powder entrapment, no significant difference was observed. The interesting result of this unsuccessful approach was, that mould powder consumption is a relevant factor for the assessment of the mould powder performance, but a more complete assessment is required concerning the mould powder properties correlated with steel grade and operating conditions.

At **CAS**, for a set of powder currently used, two representative powders, A and B, were considered for the investigations. Their properties are summarised in **Table 19**. The relevant feature consists of a significant viscosity difference at 1300 °C.

Table 19 Main characteristics of the powder used for investigation on the powder viscosity effect on slag entrapment occurrence on as-cast product at CAS billet caster

%	Powder A	Powder B
CaO + MgO	30.6	31.5
SiO_2	40.8	33.5
Basicity index	0.75	0.95
Al_2O_3	3.47	5.83
Na + K	8.50	12.0
F^-	4.6	7.0
C_{free}	5.4	2.1
C_{tot}	7.4	4.0
Melting point in °C	1130	1090
Viscosity at 1300 °C	6.5	1.6

Then a campaign of heats leading to a number of about 3000 austenitic inspected steel billets was made using both the powders for comparison. Standard operating conditions were kept the same (5-holes nozzle with angle +15° for the lateral ports, 120 mm immersion depth). Moreover, the tests were made at different casting speeds, ranging from 1.3 to 1.7 m/min.

As a result of this campaign, the quality results on as-cast products shown in **Figure 54** were achieved.

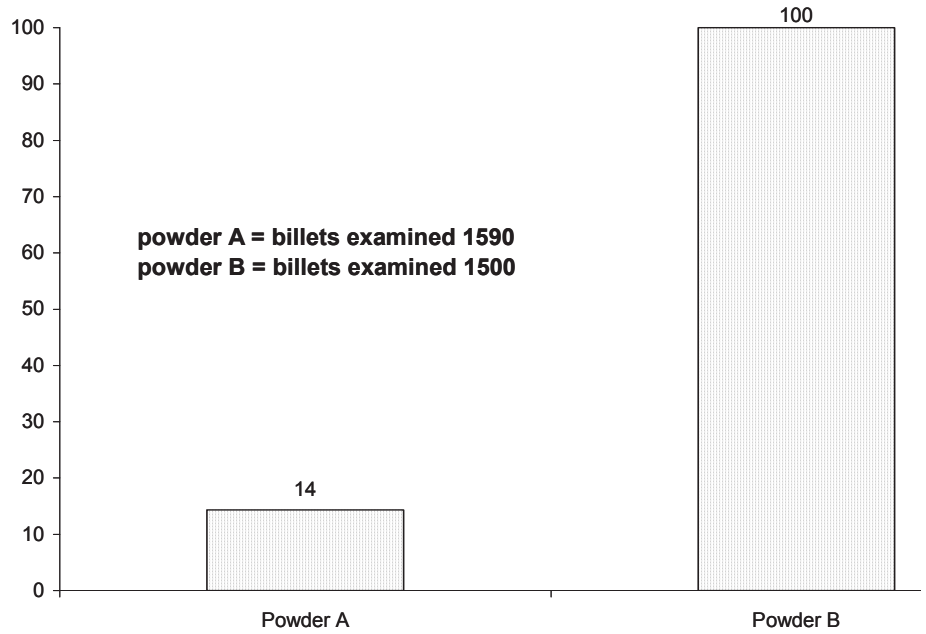

Figure 54 Relative mould powder entrapment occurrence on product after inspection in the CAS plant campaign

As a result, a relevant relative incidence of slag entrapment occurrence with powder B use with respect to powder A was found. The defect seemed to be more remarkable for the 'low' velocity range (below 1.5 m/min). Such a result was explained with the combined effect of liquid pool consumption and melting rate according to [26] for powder B (see **Figure 55**). From the figure, derived from plant data, powder B seems to present 'a lack of liquid pool depth', so entrapment can be more easily occur at the steel-slag interface.

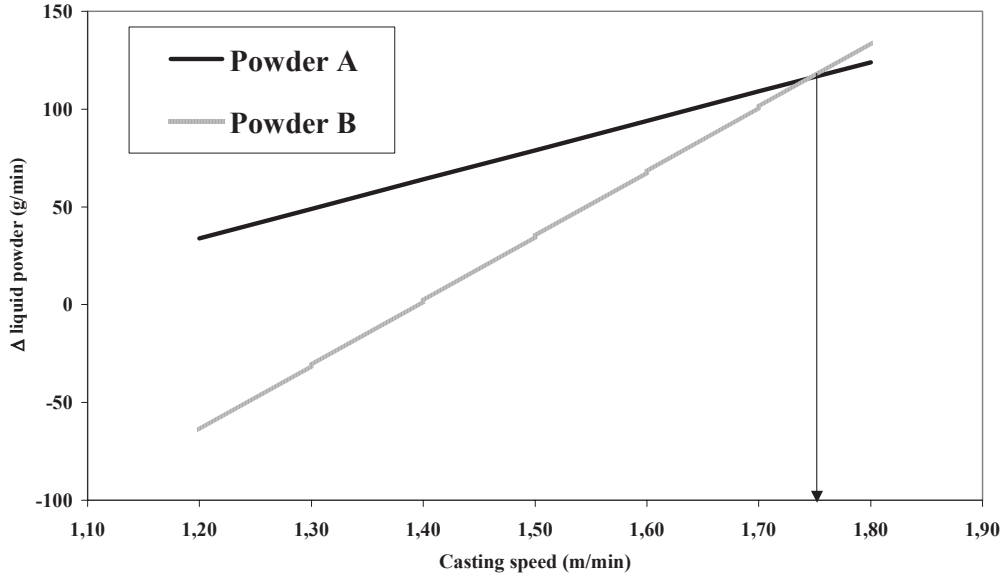

Figure 55 Liquid powder variation at mould steel surface – Trials at CAS caster

As a matter of fact, the lower viscosity and the very low free carbon content, below 4 % in the powder, can lead according to [27] (see **Figure 56**) to an excessive infiltration together with an insufficient liquid pool depth. Therefore, the interplay between these parameters, on the basis of common empirical

and analytical relationships[1] can lead to an excess of consumption with respect to the melting rate and the subsequent non-melted powder entrapment.

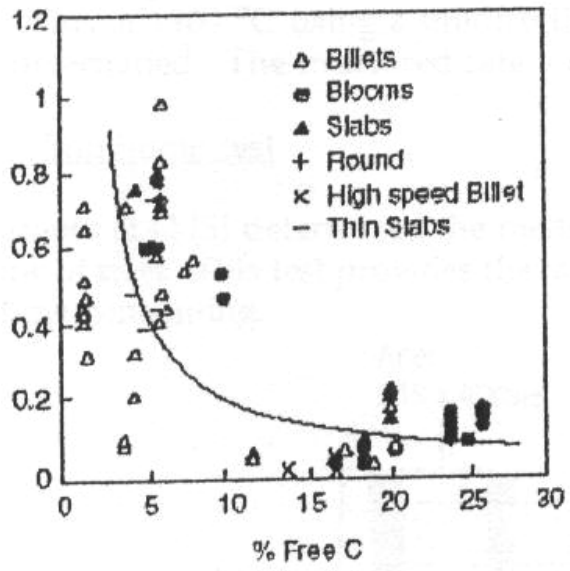

Figure 56 Plant data on melting rate versus free C content of powders according to [27]

As a result, it was find out that, to increase productivity, powders should be fitted, and in particular this finding for CAS caster resulted in a significant improvement of quality as refers to slag entrapment occurrence in the as-cast product.

As a general result for this topic, both for Sidenor and CAS investigations, apart from the specific findings, viscosity is not the most important property, and should be fitted with powder carbon content (related to melting rate) and operating conditions like casting speed to fit the proper consumption/feeding policy for the quality target on concern.

Effect of in-mould EMS intensity

The in-mould EMS is in theory, due to its well known influence on the in-mould steel flows, a key factor influencing meniscus stability; therefore, an important influence on the risk for mould powder entrapment was expected.

According to the mould powder entrapment Database (MPEDB), the influence of in-mould EMS on entrapment risk was not clear at **Sidenor**, because the in-mould EMS intensity at CCM2 is the same (270 A) for the whole production programme.

Based on Basauri plant experience, the standard in-mould EMS (270 A) of CCM2 provides a good efficiency in terms of in-mould stirring conditions without involving appreciable meniscus instabilities. Anyway, the identification of the EMS electrical intensity threshold leading to a significant impairing of mould level stability, promoting in theory the appearance of mould powder entrapment, was a matter of considerable interest. Therefore, investigations were carried out in order to compare the effect of the

standard EMS target (270 A) with regard to the non stirring conditions (0 A) and higher EMS intensity targets (290 and 310 A).

Taking into account the preliminary approach, based on the entrapment data base analysis, mould level stability turned out to be the most important parameter influencing mould powder entrapment, and this is the reason why this parameter was selected to judge the risk for mould powder entrapment when increasing the in-mould EMS intensity (see chapter 2.3.1.3.).

Therefore at the beginning three trials were carried out changing during casting the EMS current intensity from 270 A to 0 A during at least 10 minutes in all the strands.

Figure 57 shows the graph concerning Trial A, strand #3. During the period 24 min to 38 min (period B) the EMS was disconnected. Three different casting periods were considered:

- Period A: 270 A
- Period B: 0 A
- Period C: 270 A

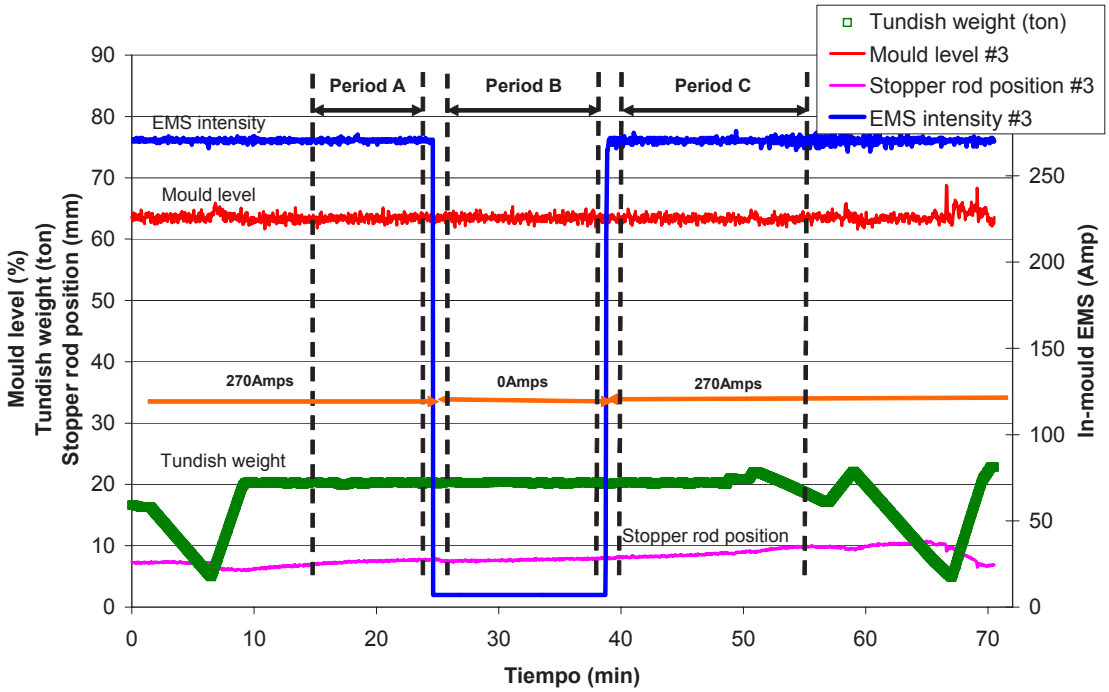

Figure 57 Sidenor investigation on effect of EMS current on slag entrapment occurrence (trial A, strand #3) – Comparison between in-mould 270 A EMS and no EMS

Figure 58 represents the results of the mould level stability assessment for the three periods of time under consideration as an average value of the six strands. As a conclusion of that trial, it could be stated that the current in-mould EMS target (270 A) does not generate any impairing of the mould level stability with regard to the 'no stirring' working conditions.

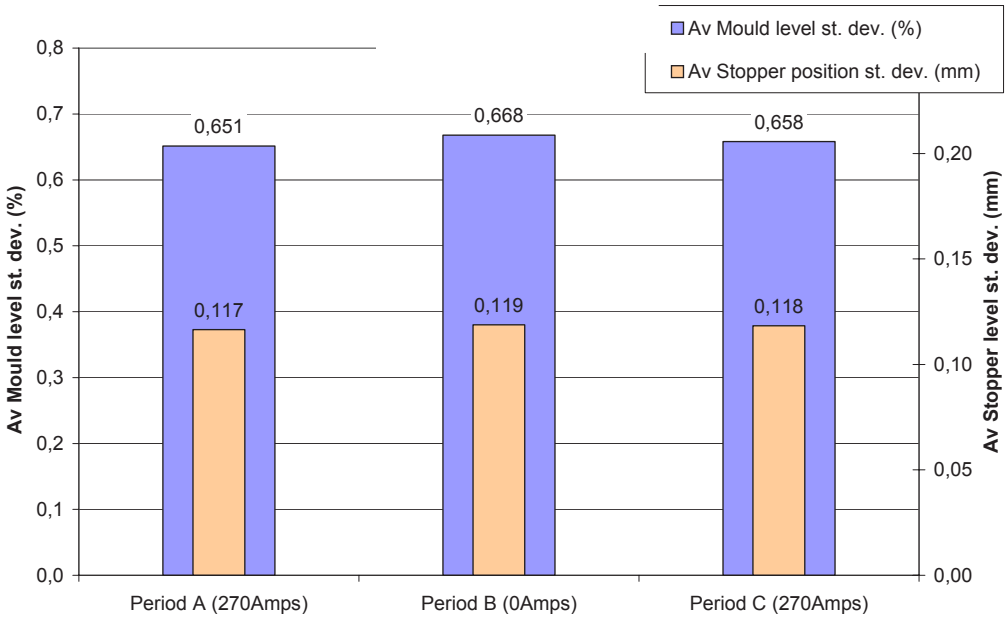

Figure 58 Sidenor investigation on effect of EMS current on slag entrapment occurrence – Mould level stability index within mould (270 A EMS and no EMS)

The differences between 270 A and no stirring are negligible and they are due to slight differences in castability conditions between the periods of time under consideration.

According to the ultrasound control, and the ulterior macroinclusion assessment procedure, no difference was found between both EMS conditions in terms of mould powder entrapment; therefore, the EMS threshold for entrapment seems to be higher than the standard EMS target (270 A). A reason for this result is the EMS coil location at the end of the mould, resulting in a very low electromagnetic field at the meniscus position. Therefore, the steel movement at the meniscus due to the EMS field can be considered as negligible when using the standard EMS target.

Additional trials using 290 and 310 A – maximum intensity of industrial interest - coil current were then scheduled. Two campaigns were performed with:

- 48 heats using 290 A
- 38 heats using 310 A
- additionally a group of 38 heats were selected from the standard practice as representative of the results using 270 A.

Figure 59 shows the results of the assessment of those three groups of heats in terms of mould level stability, as the average of the mould level standard deviation calculated each minute. The three groups are the following:

- 270 A (38 heats → 223 strands); Standard EMS
- 290 A (48 heats → 285 strands)
- 310 A (38 heats → 223 strands)

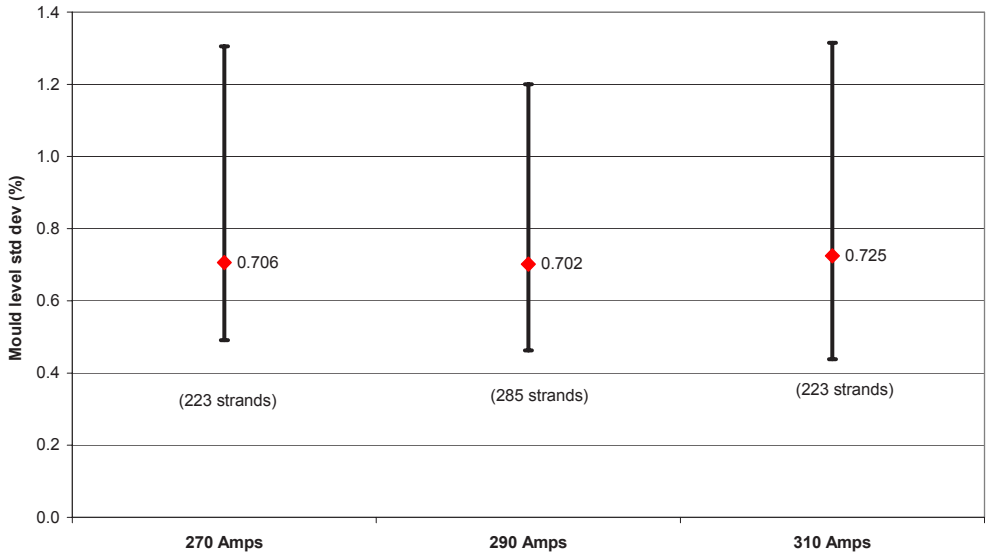

Figure 59 Comparison in terms of mould level stability for the three groups of heats using different in-mould EMS intensities of 270, 290 and 310 A (Sidenor)

Again, the slightly worse average value for the trials with 310 A (2.7 % and 3.3 % higher than the value for 270 and 290 A respectively), was explained with the influence of castability conditions on mould level stability. Considering the stopper rod standard deviation, and its effect on mould level stability, **Figure 60** was obtained. Then, comparing the effect of the three EMS targets, after withdrawing the castability effect, the mould level stability seems to be not affected by the EMS target within the intensity range under study.

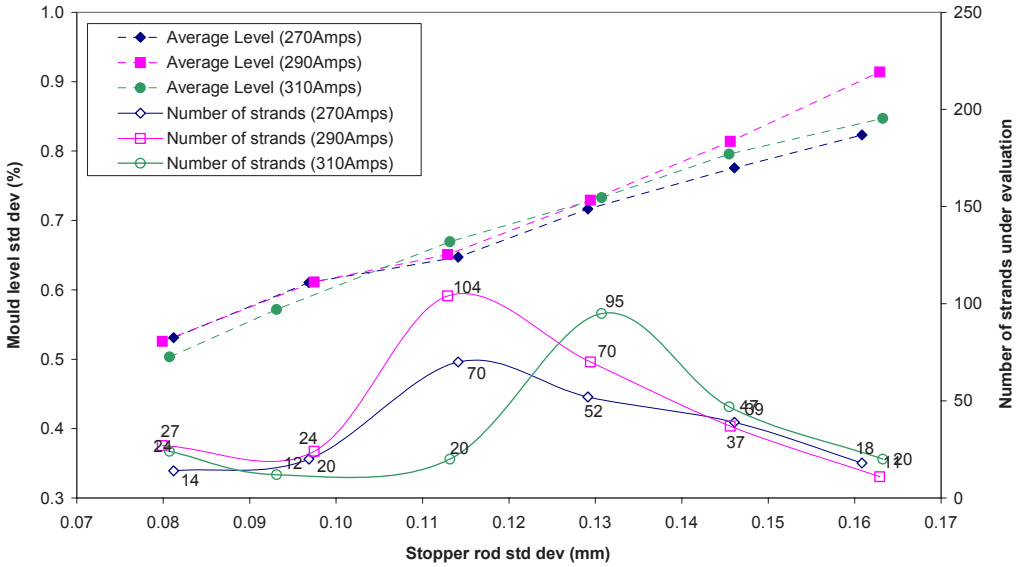

Figure 60 Comparison in terms of mould level stability for heats using different in-mould EMS intensity as a function of the stopper rod stability withdrawing the castability effect (Sidenor)

This result has been corroborated by the fact that, concerning the end product quality control, it was not found any worsening when using 290 A nor 310 A as far as mould powder entrapment is concerned.

Therefore, for the EMS intensities under consideration in this study, no effect on slag entrapment was found.

At **CAS** tests were made by varying the coil current between 150 – 350 A when casting austenitic steel in standard conditions (casting speed 1.5 m/min, 5-holes nozzle, nozzle immersion depth 120 mm). Also different mould strokes (from 6 to 10 mm) were used. Powder A was used as a reference.

A typical level control chart is shown in **Figure 61**.

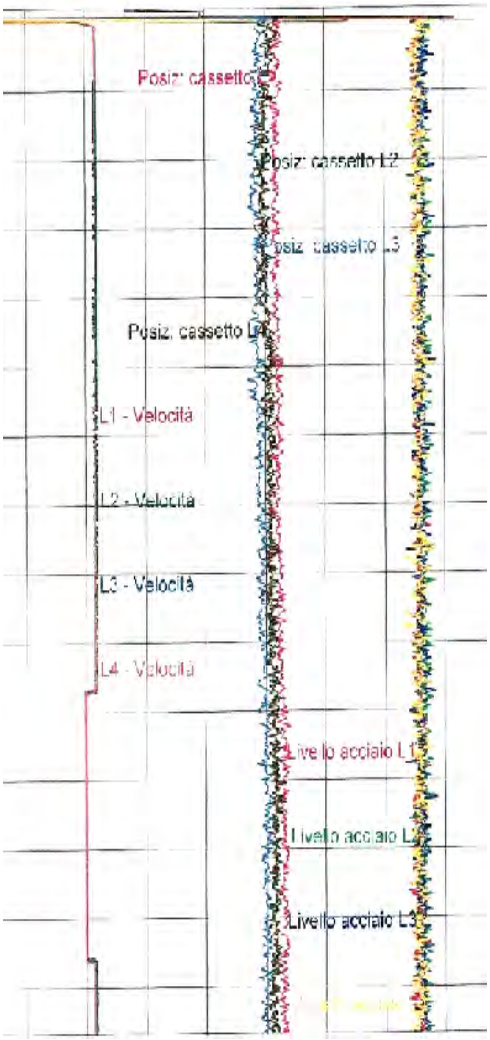

Figure 61 CAS investigation on effect of EMS coil current on slag entrapment occurrence. Level control chart in a case with 150 A coil current (arrow indicating level)

About 1000 billets had been inspected in two different campaigns and the results, in terms of normalised mould entrapment occurrence, are shown in **Figure 62**. In fact, the absolute number of slag entrapment defect (example in **Figure 63**) was not in general very high. In any case the defects were found to increase with the coil current. This was reasonable as higher coil currents are in principle associated to higher steel velocity at meniscus. But it should be also noted that the nozzle used is a 5-holes nozzle and therefore a good meniscus feeding apart from the EMS effect is expected (see chapters 2.3.3.1 and 2.3.4).

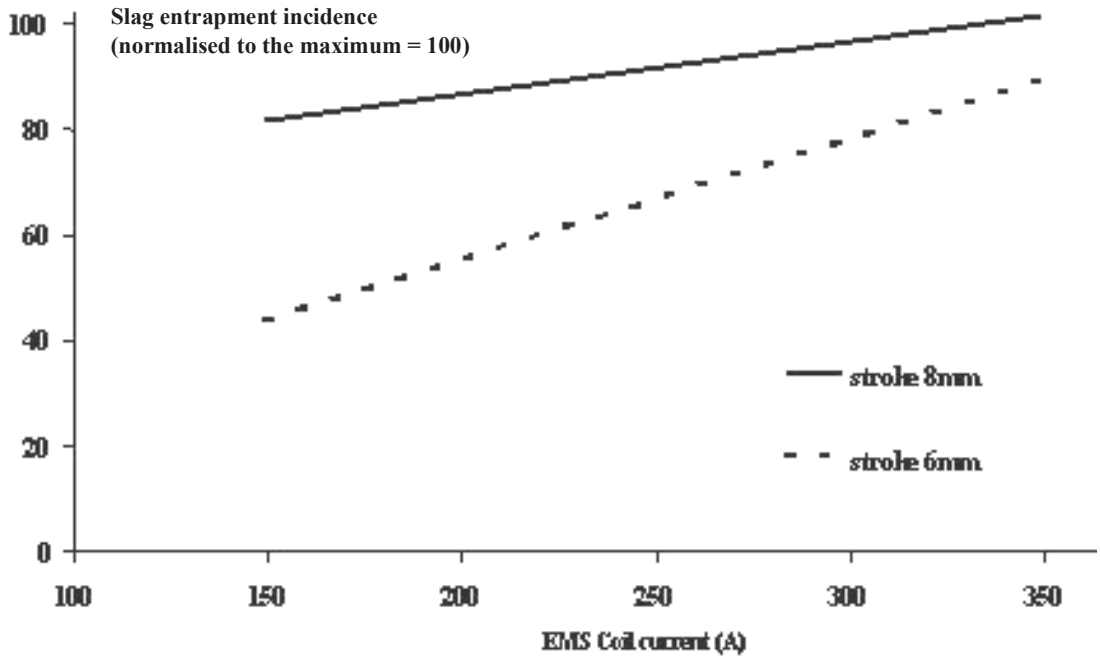

Figure 62 Plant trials at CAS billet caster – Effect of oscillation stroke and EMS coil current on occurrence of slag entrapment

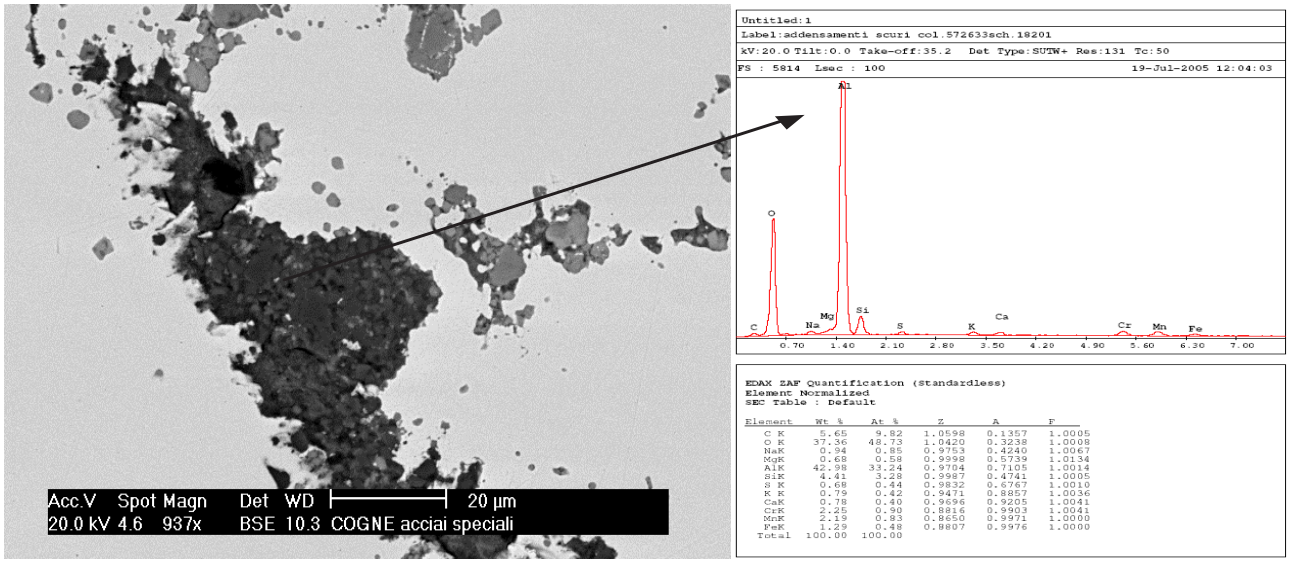

Figure 63 Plant trials at CAS billet caster – Example of slag entrapment occurrence in as-cast product in case of 350 A EMS coil current

A very interesting aspect found is the stronger dependence between slag entrapment defect occurrence and mould stroke.

As a matter of fact, from Figure 62 appears that the stroke 'weight' on slag entrapment occurrence prevails on EMS current. For example, the relative defect incidence is higher for 150 A current, 8 mm stroke than 250 A current, 6 mm stroke. This can be explained by the fact that according to most authors in [27] powder consumption increases with increased stroke, and this can lead to operating conditions for the powder liquid pool similar to those indicated in Figure 55.

In general, it could be concluded that, although worse conditions can be expected for slag entrapment risk, EMS coil current is not a parameter of most concern to be monitored within the intensity range under study for both casters. Stroke and powder characteristics seem to play a much stronger role in affecting as-cast quality from this point of view.

But the most interesting aspect arising from the experimental trials at CAS plant is the occurrence of slag entrapment defects in correspondence with the *first one-two bars casting*. This can be *correlated with the first 15-20 minutes of casting sequence*, being in turn associated to the *time needed at start casting to attain the 'regime' liquid pool height*.

This can represent a fundamental key for a definite description of the occurrence of slag entrapment phenomena for both casters, since it appeared in CAS's conditions (and also in Sidenor's conditions, supported from the investigations concerning nozzle geometry and modelling in chapter 2.3.4) that meniscus flow conditions at the interface steel-slag were not so critical in steady-state operation to give rise to clear risk of slag entrapment.

Effect of nozzle geometry and immersion depth

Nozzle configuration, i.e. straight nozzles or nozzles with lateral ports, has a strong influence on the in-mould steel flows, especially at meniscus, where flow conditions are of most concern in slag entrapment occurrence. To this purpose, industrial trials were set up at Sidenor and CAS plants.

Sidenor started with the investigation of nozzles with four lateral ports orientated towards the centre of the mould tube faces to establish a comparison with regard to the standard straight nozzle used at the continuous casting machine of Basauri Plant. **Figure 64** shows the sketch of the experimental nozzle with four lateral ports, and the relative position of the lateral ports with regard to the mould level control window.

The use of such an experimental nozzle with lateral ports was not successful. As a matter of fact, this nozzle was tested in strand #6, but problems appeared at sequence beginning during initial mould filling process because steel stream impacted directly into the mould level control area not allowing a appropriate start of the mould level regulation process, and in turn, a wrong response of the stopper rod and an aborted start due to a too fast mould level increase.

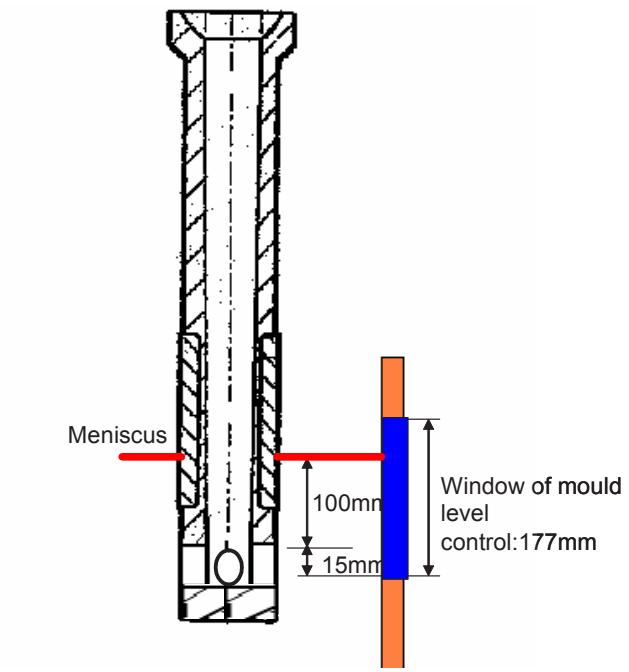

Figure 64 Sketch of the experimental nozzle and the relative position of the lateral ports with regard to the mould level control window (Sidenor)

Therefore, the trials using nozzles with lateral ports had to be cancelled due to their incompatibility to the mould level control system used at the billet caster of Basauri Plant. The next step was then to vary the flow conditions at meniscus changing nozzle immersion depth within a greater range than that in the data base (100 ÷ 109 mm).

Industrial trials were then carried out modifying the standard nozzle immersion depth by means of using nozzles with different length with regard to the standard one and varying the mould level target regarding the mould top. Standard working conditions at CCM2 are the following:

- SES nozzle length: 470 mm
- Mould level position: 65 %
- Average nozzle immersion depth: 105 mm

Table 20 presents the operational parameters used in the industrial trials (20 heats) in terms of SES nozzle length, mould level position target and the arising nozzle immersion depth. That table also includes the results of the ultrasound control by means of a parameter called 'Severity Index'. This index stands for the amount of inclusions detected per volume unit of the rolled bar sample.

Figure 65 summarises the results in terms of Severity Index as a function of nozzle immersion depth. A nozzle immersion depth lower than 100 mm yields to a worse internal steel cleanliness. Although this method doesn't distinguish between inclusions coming from mould powder entrapment and coming from alumina flushes, since all the heats belong to the same steel grade and all other operational parameters are constant. The mould powder entrapment can be considered as the main factor spoiling the 'Severity Index' for nozzle immersion depths lower than 100 mm.

Table 20 Sidenor plant trials concerning effect of nozzle immersion depth geometry on slag entrapment occurrence

Heat number	Mould level position target in %	Nozzle length in mm	Nozzle immersion depth in mm	Severity Index
19197	40	470	62	7.3
19198	45	470	70	7.8
19392	46	470	72	124.0
19488	40	470	62	16.0
19489	40	470	62	56.0
20947	45	470	70	137.0
20948	50	470	79	22.5
21251	55	470	88	21.5
21381	50	470	79	0.0
21382	50	470	79	1.7
21734	50	500	109	16.3
21947	50	500	109	4.3
21948	50	500	109	3.0
22091	45	500	100	18.0
22092	58	500	123	7.0
22237	50	500	109	12.0
22238	50	500	109	6.0
22269	50	500	109	6.7
22270	50	500	109	0.0
22520	50	500	109	4.5

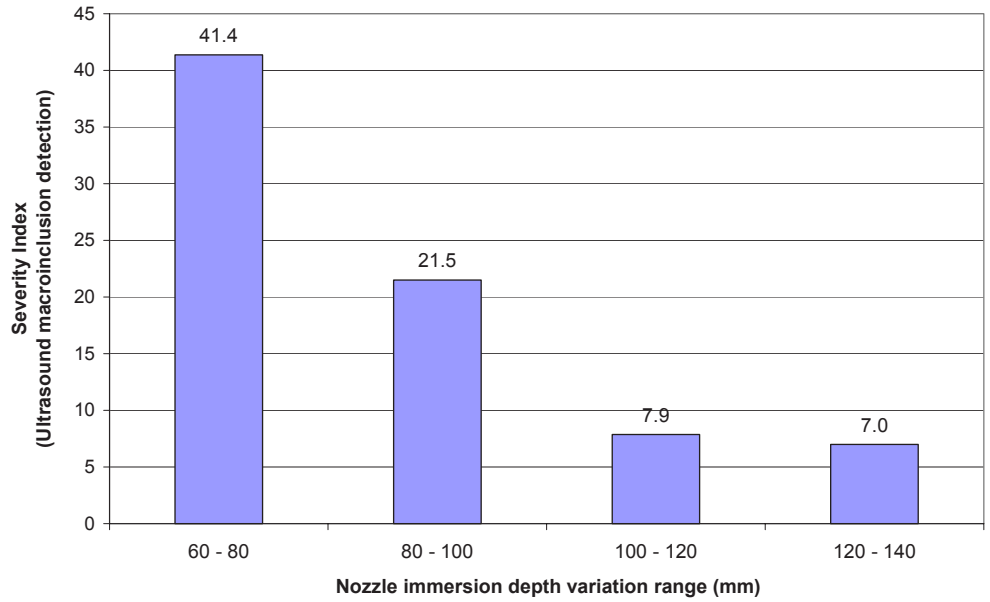

Figure 65 Sidenor investigations on effect of nozzle immersion depth on slag entrapment – Relationship between nozzle immersion depth and mould powder entrapment risk

Nozzle immersion depth on the mould powder entrapment risk was found to be critical, then leading to the decision to increase the nozzle immersion depth from the range 100 – 110 mm to 110 – 120 mm (by means of working with a lower tundish position, after checking that this change had no a significant influence on the mould powder melting behaviour).

At **CAS**, taking into account that straight nozzles are not longer used for a long time in order to avoid risk of mini break outs, trials were performed with multi-hole nozzles as indicated in **Table 21**. The larger bottom hole used for the prototype had the aim of reducing the kinetic energy of the stream coming from the lateral port to reduce risks of mini break outs. The geometry for the different prototypes and the reference nozzle tested are shown in **Figure 66**. Casting speed considered was 1.5 m/min, immersion depth 120 mm, EMS coil current 150 A. The results achieved on 160 mm square product are shown in **Figure 67** in terms of average index of defects for austenitic steels related to SEN geometry. The meaning of the index is, that the lower the index value is, the better is the as-cast quality.

Table 21 Nozzles used in CAS plant investigation concerning effect of nozzle geometry on slag entrapment occurrence

Nozzle type	Central diameter in mm	Bottom hole diameter in mm	Lateral Port features
5- holes (standard)	30	12	Inclined + 15°
5- holes	30	12	Inclined - 15°
5- holes	30	14	Inclined + 15°

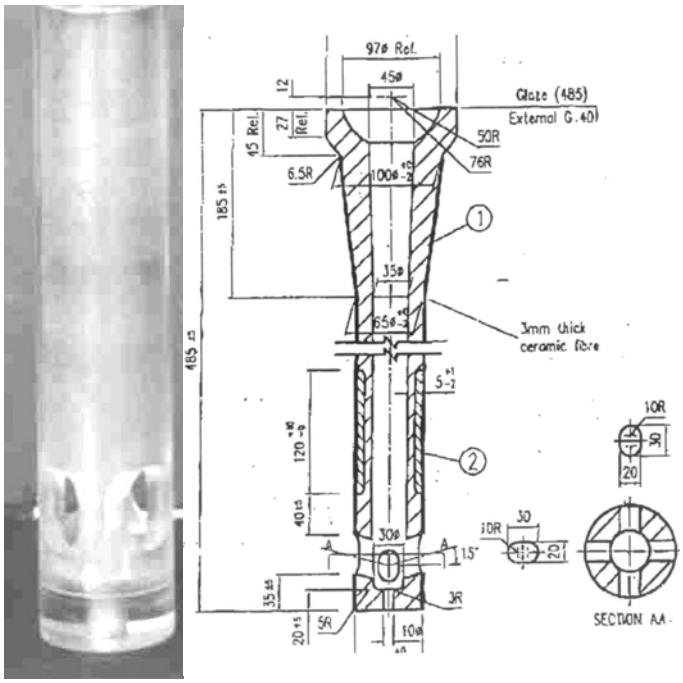

Figure 66 Investigated nozzle geometries at CAS – Perspex prototypes of 5-holes nozzle, lateral holes inclined +15° (left) and straight nozzle (right)

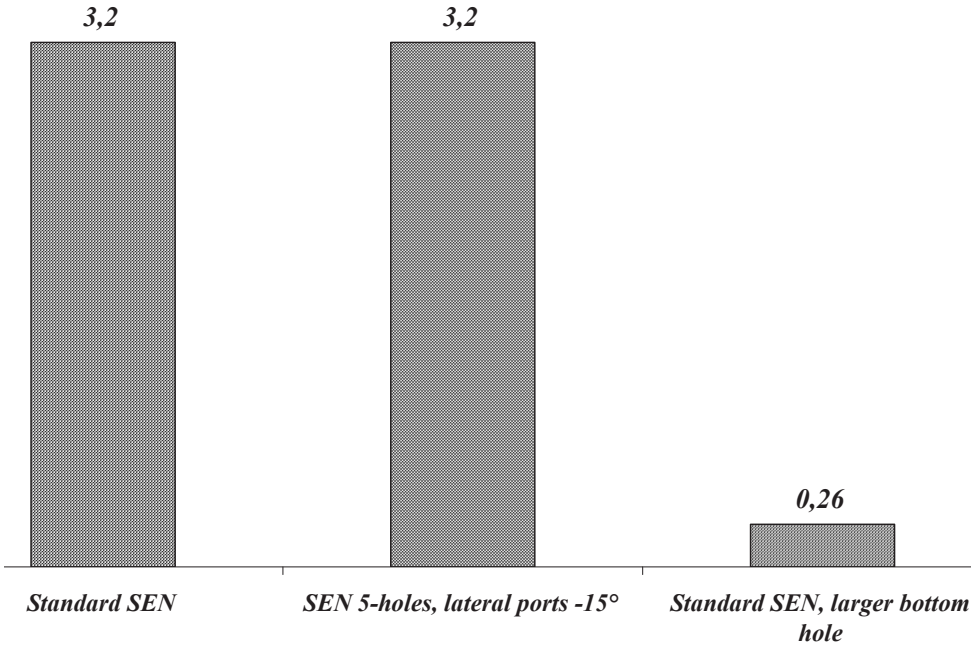

Figure 67 CAS plant investigation results concerning effect of nozzle geometry on slag entrapment occurrence on as-cast products

The main aspects arising from the quality inspection on the as-cast product achieved from the trials were the following:

- the effect of the lateral port angle on the steel behaviour at the meniscus, intended as the cause leading to slag entrapment, appears to be the same. This can be explained by the fact that in any case the kinetic energy of the stream coming from the lateral port in both cases is so high that the contribution to the upper recirculation (towards the meniscus) is not significantly affected;
- the effect of enlarging the bottom hole appears to be very significant in reducing the slag entrapment occurrence. This is due to the reduction of the flow rate available for the lateral holes, and in turn to the reduction of the steel velocity at the lateral port exit and, after impingement of the stream at lateral walls and subsequent recirculation upwards at the meniscus, of a weaker steel flow at the interface with the slag.

The net effect of such a flow in 5-holes nozzle with enlarged bottom hole is similar to have the former 5-holes nozzle, cast at higher casting speed. Strictly speaking, the steel velocity achieved at meniscus under these conditions are the same occurring at higher casting speed with a 5-holes nozzle with smaller bottom exit port, but without the potential risk of excessive steel kinetic energy at the exit port leading to subsequent shell remelting risk.

As a consequence of the results achieved, the modified nozzle became the standard for 160 mm square CAS billet caster. As a confirmation of the previous investigation results, the defect occurrence involved only the first bars of the sequence.

This suggested that the flow conditions related to nozzle geometry were a parameter to keep into account but not of outmost importance in determining the defect – otherwise it should have occurred

independently from the heat number of the sequence– but that the start casting conditions in attaining the liquid powder layer are of most importance, and that within this period (15 – 20 min) a flow more 'vivacious' can make easier the occurrence of the drawback.

2.3.3.2 Verification of modelling results (Task 3.2)

Verification of modelling results was made on the basis of CSM powder melting and flow modelling results as follows.

Liquid pool depth characterisation

In order to provide CSM with additional data for the modelling activities concerning the in-mould EMS influence on mould level stability and the entrapment risk, extensive plant trials were carried out at **Sidenor** using the wire dipping method for the assessment of the liquid pool depth.

Preliminary trials were focused on the procedure optimisation to determine the optimum wire diameter and immersion time so as to obtain reliable results. **Figure 68** shows on the left a sketch of the wire dipping test using three different wire materials (iron, copper and aluminium), and on the right how those materials get melted at the different interfaces between the different layers within the casting mould. Optimum diameters were found to be 1.2 mm for Fe, 1.0 mm for Cu, 1.5 mm for Al, for a immersion time of 3 sec. On the right one can see an example for the three different wires after a test using optimum wire diameters and immersion time.

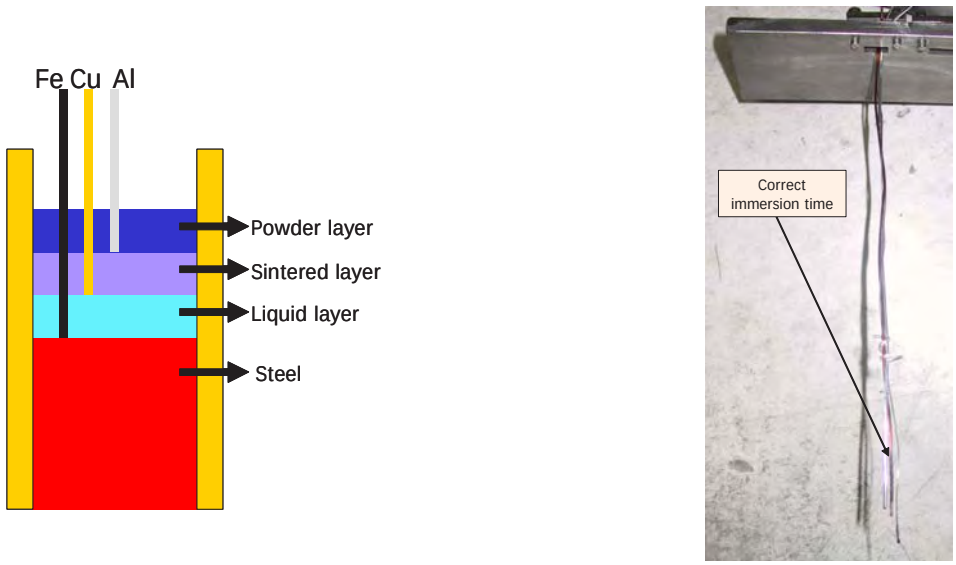

Figure 68 Measurement of liquid pool depth at Sidenor – Sketch of the wire dipping method (left) and an example of the wire dipping test results (right)

Table 22 shows the results of the slag layer thickness average measurement for the four mould powders on use at the billet caster of Basauri Plant for the 185 mm billet format. An important scattering was found in the results, highlighting the existence of quite different conditions in terms of slag layer

thickness, especially due to the manual powder addition. Anyway, the modelling results were in good agreement with the measured data (see chapter 2.3.4).

Table 22 Slag layer thickness characterisation using the wire dipping test (Sidenor)

Mould powder	Liquid pool depth in mm	Sintered layer in mm
P1	9	7
P2	12	11
P3	14	7
P4	15	10

CAS measured slag layer thickness with a technique similar to that shown by Sidenor. In the section concerning modelling a comparison will be found between these values arising from CAS plant measurements and CSM modelling results, showing good agreement between both data.

This allowed CSM using the model results to identify the mechanism of slag entrapment of most concern, the interaction between steel and slag at start casting when the non-melted powder is close to the interface. Within this casting period, occasional flow conditions with velocity inducing onset of interface instability leads to waves able to favour slag entrapment in the steel and this is found on the as-cast product in form of local recarburisation. Moreover, some studies highlighted that a thin liquid slag layer favours more rapid attainment of steel-slag instability [28].

Flow characterisation

Indirectly, the main occurrence of slag entrapment defect on billet only at start casting confirmed the indications of flow modelling (BFI and CSM, see chapter 2.3.4). That is to say, it is very difficult to have slag entrapment in steel during steady-state flow conditions at the meniscus, unless:

- wrong nozzle design occurs (able to induce steel velocity at meniscus exceeding a threshold);
- local flow perturbation occurs (formation of harmful flow oscillation due to clogging impairing flow symmetry at port exit in multi-hole nozzles or wrong nozzle positioning).

Moreover, as also resulting from modelling and shown before the EMS current values in the ranges examined were not relevant for inducing slag entrapment.

2.3.3.3 Determination of optimum constellations (Task 3.3)

The results achieved on plant can be generalised to refer to carbon and stainless steel billet casting in the following way.

Comparable to chapter 2.3.2.3. , the '*optimum constellation of process parameters/quantities*' concerning minimisation or avoiding of slag entrapment can be divided into two groups:

- powder features

  parameters/quantities belonging to it (plus casting temperature i.e. melt superheat) refer to the powder properties and are of most concern in determining the sintered and liquid layers thickness.
- fluid-dynamics

  parameters/quantities belonging to it refer to mechanical energy of the steel in the mould and in particular, to meniscus. They can be directly related to pouring operations (casting speed, SEN geometry features), both in steady state and transient conditions (the latter being more critical) or indirectly (stirring current, stroke).

First of all, the most important result in all cases is the fact that **first heats of the sequence** are more prone to slag entrapment occurrence. The most important reasons are the following:

- In-mould non-steady period at sequence beginning, basically due to the time required by the mould powder to reach stable conditions in terms of lubrication.
- Instabilities due to dummy bar withdrawal process.

The second aspect is mainly operational and needs great care. The first aspect makes the choice of the powder properties very important. The guidelines are listed below, followed by the 'flow' optimum quantities/parameters.

Powder features

Here the powder properties of most concern are the viscosity and the melting rate. Here viscosity is not the main quantity and should be properly coupled with *casting speed* and *melting rate*. In particular, carbon content, which melting rate depends strongly on, plays a strong role.

Since *the lower the steel grade carbon content*, the higher the shell shrinkage (0.10<%C<=1.0), a higher liquid slag production is required. To achieve that, *low values of free carbon content* are used to provide a higher melting rate and a homogeneous slag film between the mould and the solidified shell. The recommended content was found to *be below a critical value.* This critical value is 5% for stainless steels and 20% for carbon steels respectively.

On the other hand, *the higher the steel grade carbon content the lower should be the mould powder viscosity* in order to get a better liquid flux infiltration between billet and mould [27] indicates an optimum value of viscosity in Poise multiplied with casting speed in m/min equal to 3).

A further operating parameter related to slag entrapment occurrence was found to be *the stroke* (related to *powder consumption*) in the case of CAS casting situation. If higher (in the investigations related to CAS billet casting, exceeding 8 mm) the risk of such a defect is higher than that achievable if almost doubling the EMS coil current.

Fluid dynamics

All quantities related to the steel flow at the interface steel-slag at the meniscus are involved in the phenomenon. In chapter 2.3.4 it will be shown, that a steel velocity threshold value should be exceeded to induce risks of slag entrapment. Within the operating ranges investigated for billet casting at Sidenor and CAS, these conditions were not attained. As a matter of fact, they are most likely to occur in long product casting, where the higher flow rates can be not adequately managed with suitable nozzle geometries.

More in general, the quantities responsible for steel velocity at meniscus are *flow rate* (through *casting speed*, once fixed the as-cast format) and *nozzle geometry*, mainly through central throat diameter. As a general rule suggested by [29], it should not be exceeded a value of 1.6 m/min as indicative ratio between volumetric flow rate and nozzle throat area to avoid the mentioned conditions risky for onset of steel-slag interface instability. Of course, *s*traight nozzles are less critical for such a problem, but lead to other quality problems as a 'cold' meniscus, affecting negatively to the mould powder working practice.

As refers to *nozzle immersion depth*, in general a deeper immersion makes the meniscus more 'quiet' and then less risky for slag entrapment, but again a 'cold' meniscus should be avoided. No general rules are here given, because how 'hot' the meniscus should be, depends on the steel grade, the casting speed and the powder on use. For example, at Basauri plant, an increase of the nozzle immersion depth up to 110-120 mm proved to be beneficial to enhance billet quality preventing mould powder entrapment.

For the configuration of the billet casters under study and for the coil current range considered, *in-mould electromagnetic stirring* was not found to play a great role in inducing risks of slag entrapment.

The above findings suggest that in general, unless the nozzle geometry is not adequate for the operating conditions, during steady-state billet casting slag entrapment is not very likely to occur. On the other hand, *unsteady conditions* (*start casting, flow oscillations due to alumina clogging flushes, improper nozzle position or local clogging in multi-hole nozzles*) can be the cause for the onset of the steel-slag interface instability. These phenomena are more common for flat product casting, due to the typical flow features induced by the bifurcated nozzles.

Nevertheless, the flow parameters should be always under control due to the fact that nowadays productivity and quality requests are higher and higher and this brings about higher casting speeds and more severe internal quality targets.

2.3.4 Physical and mathematical modelling (WP 4)

Aim of this modelling part was the estimation of optimum constellations concerning the operating parameters and mould powder properties to improve flux performance in terms of reduced slag entrapment in the steel.

In order to do so the approach was the following:

- *the operational results* were analysed first. This work was complementary to that of chapter 2.3.1 where a reference process data base had been set up and related to slag entrapment occurrence on the product;
- parallel, *mould powder properties* were assessed, in order to have the complete scenario in terms of chemical-physical properties to be investigated and correlated to the defect found, and then to allow a well targeted modelling investigation;
- *codes/models* (for fluid flow description and powder melting), *and experimental facilities were set up* and/or adapted, in order to allow investigations on process quality indicators when varying operating parameters;
- *modelling activity* was then accomplished. These results were used together with the interrelated operational results to obtain the deliverables in form of

  identifying optimum constellations of process parameters with the related typical range to have in mind when aiming at facing the problem of slag entrapment in the steel.

  In this way, operational work as described in chapter 2.3.2 and 2.3.3 was supported leading to the *definition of the optimum constellations of process quantities* and range as *a final deliverable of the project*.

BFI and CSM were involved in this part. But from the approach shown, synergy between partners, also in interrelation with the 'operational' partners was exploited.

In particular, synergy and interrelation within WPs brought about the following work steps where information from mould powder and steel fluid flow investigation were combined:

- CAS and Sidenor provided powder characteristics and related casting operating conditions;
- CSM evaluated the liquid pool height resulting from the above conditions with the liquid pool model;
- CSM (long products) and BFI (flat products) evaluated at the same time the flow field at the surface with numerical model in the same conditions;
- In particular, BFI made thorough investigation of the multiphase flow at steel-slag interface with use of numerical and physical modelling of slab casting;
- CSM, highlighting on the caused inducing slag emulsification, namely, velocity above a threshold (around 0.35 m/s) evaluated with the numerical model the expected maximum height at the surface in the casting conditions of concern (variables: EMS coil current, casting speed, nozzle geometry)
- CAS and Sidenor provided data on the product to favour correlations between entrapment/recarburisation and operating conditions;
- A correlation between product data and modelling information allow the link between process and product aspects and the definition of criteria to reduce the drawbacks (conditions leading to the

proper pool liquid height able to avoid waves able to embed sintered powder, or, at start casting, indication of 'gentle' casting speed strategies to minimise risks of dangerous waves when liquid pool is not completely assessed).

- BFI analysed the information concerning the operational situation of TKN. Here especially data concerning liquid flux layer thickness and the horizontal velocity near the interface steel melt/liquid flux were in the focus.
- BFI furthermore performed additional numerical modelling concerning the situation at Arcelor España. Here the difference between a clogged and a not clogged SEN was under investigation following the results from chapter 2.3.2.1.

Details on the work performed are discussed below.

2.3.4.1 Analysis of operational results (Task 4.1)

The operational results achieved in chapter 2.3.1 were used as a suitable basis for model approaches to set up the numerical codes, the experimental facilities and the measuring systems. The task allowed identifying both the physical system to be investigated and the parameters to be reasonably varied.

The work performed in this frame consisted therefore in the identification of the physical system to be investigated in order to drag properly the modelling work, concerning the numerical approach and the lab investigation.

The physical representation was found by the 'modelling partners' (CSM – BFI) in close cooperation, on the basis of their experience and tools, and as it is detailed below.

Concerning the slag entrapment and retaining in the metal affecting cleanliness, the physical system under investigation consists of a liquid slag layer with its own physical properties (viscosity, melting temperature and powder composition both influencing the melting rate) and the steel layer flowing with a velocity depending in turn on mould feeding conditions (flow rate, casting speed, nozzle geometry and immersion depth).

Referring to the interface conditions on the 'slag side', the physical and chemical properties of the powder which undergoes melting are influenced by the following two main aspects:

- the existence of a liquid pool high enough to allow slag feeding for the lubricating action.
  In lack of this, not only lubrication and in turn heat transfer between shell and mould is affected, but powder can be in contact with steel and if particle 'entrapment' occurs, second phase retaining in the melt is easier than after liquid slag entrapment;
- via the slag viscosity, the shear stress field in the liquid slag layer at the interface with the steel layer.

As a matter of fact, influencing the interface instability starting from which slag drops can be detached and carried down in the steel.

As a result, the investigations on this topic will also concern the effect of the chemical and physical properties of the slag (viscosity versus temperature, melting rate) on the tendency of slag entrapment at meniscus in the operating conditions.

To have information on the condition leading to the instability of a slag-steel surface, most helpful is the work of Oeters concerning gas stirred ladles [30]. Here, the source of mechanical energy is the power transferred to the metal liquid by inert gas injected from porous plugs on the bottom (the frame considered is a ladle). As a result of the transferred power, melt recirculates at the interface with the slag and, in case of shear stress conditions leading to interface instability exceeding a threshold, emulsification occurs and slag penetrates in the melt. At this stage, if the fluid-dynamics conditions do not favour the second phase floatation from the steel, 'entrapment' has been accomplished.

The physical phenomena at the interface slag-steel in a gas stirred ladle can be considered similar to that at the mould meniscus in continuous casting (and, in particular, in billet casting). In the first case **(Figure 69, left)**, steel velocity at the interface arises from the momentum transferred by the gas. In the second, **(**Figure 69**, right)** steel velocity at the interface arises by the fluid-dynamics induced by the submerged entry nozzle (SEN). But the onset of the instability conditions and in turn of slag entrapment occurrence should be the same in both cases.

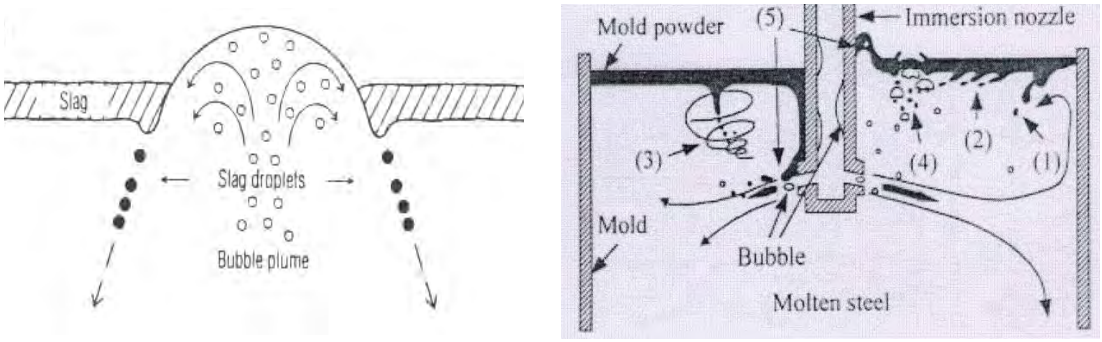

Figure 69 Typical slag-metal interface in bottom stirred ladle according to Oeters [30] (left) and in mould meniscus (right)

The 'threshold' condition was studied by Oeters [30] via relationships involving the steel velocity at the interface being critical for emulsification, metal and slag density, steel-slag interface tension σ and contact angle α. To this parameter-set a critical emulsified drop is associated. The amount of emulsified slag depends on slag viscosity.

According to this physical schematisation, emulsification starts if the local steel velocity exceeds the emulsification onset velocity. Afterwards, the 'simple' emulsification becomes 'slag retaining' and therefore entrapment if the particles formed cannot float at the surface. This occurs depending on the fluid-dynamics conditions of the system steel-slag.

As a result, the investigations on this topic concerned

- the effect of the feeding fluid-dynamics parameters (nozzle geometry and immersion depth, flow rate, casting speed) on the steel velocity profile at the interface;
- the definition of the meniscus zone where emulsification onset velocity is exceeded;
- the definition of the conditions for which entrapped slag is definitively retained in the melt or not, according to its density and characteristic size (the latter derived again from Oeters).

The above findings led to the following approach:

- fluid-dynamics modelling focusing on the velocity field at the surface, resulting from the operating conditions (flow rate, SEN geometry), and on the behaviour of a second phase dispersed at the interface steel-slag;
- powder melting modelling, focusing on the evaluation of the liquid layer thickness at the interface steel-slag;
- merging both information, assuming that a wave formed at the meniscus can entrap powder in the melt which can float or be fixed onto the solidified shell.

To this purposes:

- CSM and BFI set up numerical fluid-dynamic simulation tools to investigate the physical frames under concern. They are detailed in the next section;
- CSM adapted an existing numerical model to describe powder melting and liquids layer formation;
- BFI supported the numerical modelling approach with physical model trials in order to obtain velocity information near the mould level surface using Laser-Doppler-Anemometry (LDA) and Particle-Imaging-Velocimetry (PIV) and entrapment behaviour performing model trials using oil as surrogate for the liquid mould powder.

2.3.4.2 Assessment of mould powder properties (Task 4.2)

As refers to this task, the work was shared between CSM and BFI as follows:

- ***CSM work*** was targeted at determining the physical and chemical properties of the mould powders involved (for long products, CAS and Sidenor of concern) in order to give adequate input to the model calculating the liquid pool thickness.

  Therefore the 'relevant mould powder properties' considered are those of the powder as resulting from lab tests, in the same way as suppliers give information to steelmakers;

- ***BFI work*** consisted in contributing to assess a system for the adequate measurement of liquid pool thickness at TKN slab casting. The method developed and the results obtained with the measuring device have already been described in more detail in chapter 2.3.2.

As a 'relevant mould powder property' it was considered a parameter strictly related to the powder behaviour during casting and found to be of relevance in slag entrapment occurrence.

CSM facilities **(Figure 70)**, used in an earlier project [31] allowed to achieve information on powders about their:

- melting range (with thermo-balance from Differential Thermal Analysis (DTA); gives information on powder homogeneity;
- melting rate (calculated from chemical analysis and model), responsible for the liquid pool height;
- viscosity (calculated from models); related to slag feeding in the gap between steel and mould;
- crystallization range (from DTA analysis); gives indication about the melt flux tendency to crystallize; the start crystallization temperature gives indication on the mould abscissa from meniscus at which crystal slag layer can form, affecting thermal exchange;
- amount of crystalline phase (from DTA analysis), responsible for thermal-conductive behaviour of the powder.

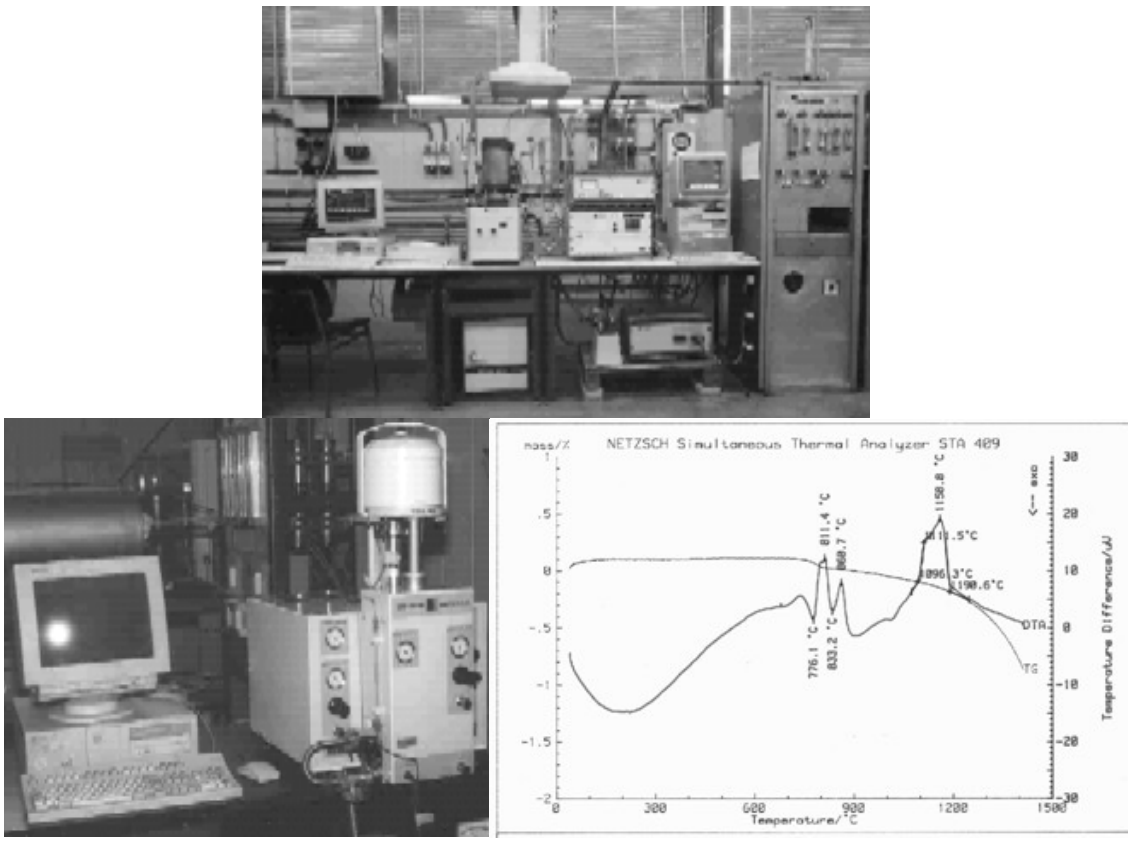

Figure 70 Laboratory facilities for characterisation of mould powders: thermo-balance (up); thermal analysis equipment (down left) with a typical DTA result (down right)

Molten pool depth is also affected by the consumption rate and by the mould dimensions [32]**.** The factors controlling the amount of liquid slag were found to be:

- thickness of the solid powder layer;
- particle size of the powder;

- variation of the powder apparent density;
- variation in the graphite content.

The assessment of the properties of the most interesting mould powder involved in the CAS investigations was made by CSM via laboratory tests. For the topics investigated in this project, great relevance is given to viscosity and melting rate. Viscosity is determined by roto-viscosimeters; melting rate is identified from Differential Thermal Analysis (DTA). Properties for Sidenor and CAS mould powder used are shown in **Table 23** and **Table 24**.

Table 23 CAS relevant powder mould properties after CSM laboratory characterisation

Powder	$T_{liquidus}$ in °C	Melting rate in mg/s	Viscosity at 1300 °C in dPa s
A	1190	63	1.6
B	1215	23	6.4
C	1190	9	3.4
D	1180	23	1.0
E	1190	139	3.1
F	1190	28	0.9

Table 24 Sidenor mould powder properties, chemical composition included

		P1	P2	P3	P4
% SiO2		32.50	25.00	33.60	31.40
% CaO		22.80	21.00	22.80	18.20
% MgO		2.10	1.50	3.98	1.06
% Al2O3		14.30	10.25	6.28	5.20
% Na2O		3.60	3.25	6.17	9.98
% K2O		1.40	1.00	0.37	0.78
% MnO		0.00	0.10	0.24	0.04
% FeO		3.50	3.75	0.81	1.76
% F		2.60	5.25	1.82	4.42
Viscosity	Riboud	37.40	9.93	13.51	7.04
	Suplier data	37.90	10.00	12.70	5.50
Basicity		0.70	0.64	0.67	0.53
Density (Kg/dm3)		0.85	0.65	0.87	0.83
Melting behaviour	Soft. Point	1100	1140	1120	1000
	Melt. Point	1130	1210	1220	1080
	Fluid. Point	1190	1250	1260	1130
C free		12.50	19.75	18.30	22.40
C total		13.20	22.00	19.50	23.90
% Carbon range per mould powder		C < 0.15	0.15 < C < 0.35	0.35 < C < 0.5	C > 0.5

These values were used as input for the model describing powder melting and liquid pool thickness assessment (concerning chapter 2.3.4.3) and as a reference to compare the results achieved in operational trials (concerning chapter 2.3.3) with modelling (concerning chapter 2.3.4.4) allowing at the end to give indications on the ‘optimum’ conditions.

2.3.4.3 Set-up of codes and experimental facilities (Task 4.3)

The modelling facilities used were the following:

- CSM numerical model to have indication on thickness layers (sintered, liquid) of mould powders;
- CSM Computational Fluid Dynamics code to describe flow field in the mould and at the interface steel-slag; also electromagnetic forces are taken into account being simulations focused on long product casting operations;
- BFI Computational Fluid Dynamics code, to describe multiphase flow in slab casting;
- BFI multiphase cold model of the mould system steel-slag, represented respectively with water and oil.

CSM numerical model for mould powder melting description

A finite difference model set up to simulate the heat transfer through the different layers over the liquid steel level in the mould and developed in other ECSC projects [31] has been adapted for the project.

The model, adapted to CAS casting features (mould and operating conditions), has been implemented on a dedicated routine within the frame on finite difference MARC code and deal with the description of the meniscus perimeter.

The schematic of the physical frame the model is based on is shown in **Figure 71**.

Heat transfer is described via the Fourier equation, discretised adopting a one-dimensional mesh. Boundary conditions are:

- temperature, taken from the closest thermocouples to meniscus,
- radiation and convection with air at room temperature, at the free powder layer surface.

The model was conceived to represent thermal state versus time with description of the evolution of thickness, both of the whole system and of the single layers. Thermal and geometric conditions change during time according to the material physical characteristics and liquid flux consumption.

Time is subdivided in a large number of time steps, for each of which the Fourier equations are solved, with arising problems of achieving convergence.

For our purposes, liquid flux consumption is represented as a lump of material which disappears at the start of each time step, corresponding to a reduction of the liquid layer thickness.

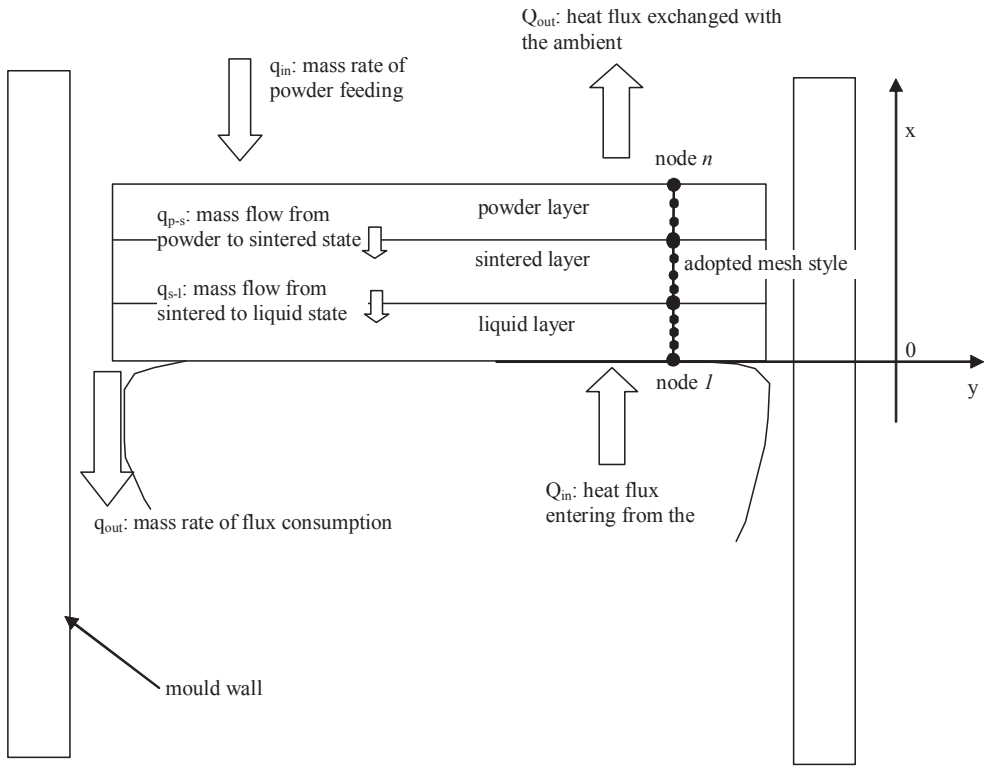

Figure 71 Physical frame the CSM model for powder melting is based on

A typical output of the model is shown in **Figure 72** for powder type B used at Sidenor.

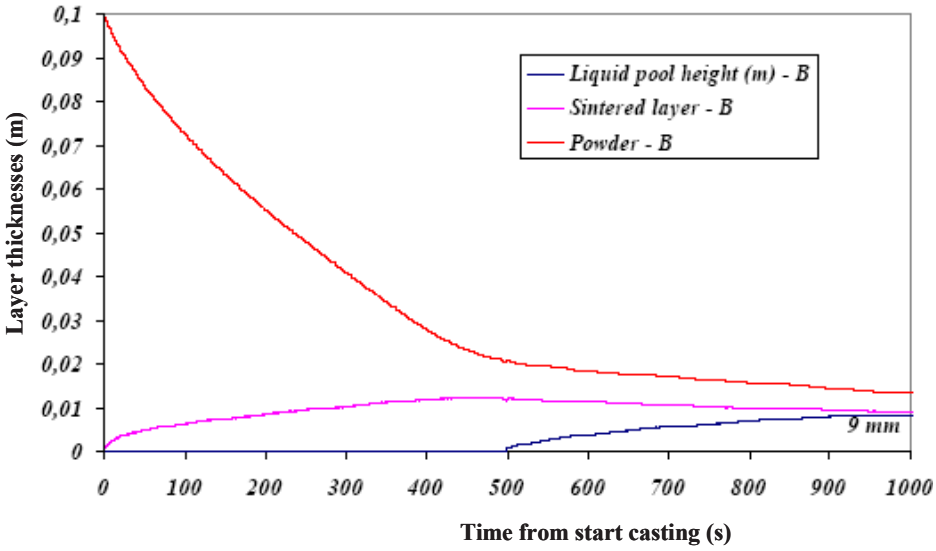

Figure 72 Typical output of the model describing mould powder melting of type B from Sidenor

Codes for fluid flow description

The aim of the modelling in frame of this project is to provide a reliable representation of the transport phenomena at the interface steel-slag, as refers to slag entrapment occurrence.

Modelling of multiphase flow in mould was exploited, based on Computational Fluid-Dynamics commercial codes validated in previous works, also supported by ECSC [33]. The packages used by

CSM (Phoenics) and BFI (Fluent) include both Navier-Stokes' equation, k-ε model options for turbulence description and two phase representation via suitable techniques

- Volume of Fluid (VoF) method, with domain cells associated to a percentage of first and second phase mass,
- particle tracking, with second phase assumed to be composed by spherical particles with well defined diameter and density, and moving in a converged single phase flow field using a 'Lagrangian approach'.

Stop tracking can be imposed at well defined boundaries, for example at surfaces in case of floatation or at exit in case of flow sink. The two phases considered are represented by the steel melt and the slag entrapped in form of emulsified particles, i.e.:

- to be spherical, with a diameter equal to the characteristic emulsified drop diameter [30];
- to have a density equal to that of the slag (this value can be changed, for example, considering a composition variation due to chemical reactions with species dissolved in the metal bath);
- to start moving at the meniscus in the steel where emulsification is likely to occur, i.e., where the local velocity value, achieved from the numerical simulation, exceeds the threshold. For many purposes, even though as previously mentioned, this limit velocity depends on the slag chemical-physical properties, this value is approximately 0.35 m/s [34];
- stop tracking is imposed once the particle reaches the meniscus (physical meaning, floatation) or the nozzle wall (removal) or the lateral wall (sticking on the shell).

BFI physical model for steel-slag system in the mould

Physical model trials are often subject to limitations due to the specific circumstances in operational plants. In steel production large dimensions, thermal conditions and real fluid properties often restrict laboratory work. Realistic conditions can be approximated using similarity theory. With the aid of dimensionless numbers model conditions can be adjusted to obtain appropriate results.

For physical modelling of fluid dynamic processes, following relevant dimensionless numbers have to be taken into account. For isothermal modelling of single-phase melt flow, these are the Reynolds (*Re*) and the Froude number (*Fr*):

$$\mathrm{Re} = \frac{\text{inertial forces}}{\text{viscous forces}} = \frac{c \cdot \rho \cdot l}{\mu} = \frac{c \cdot l}{\upsilon} \tag{2}$$

$$\mathrm{Fr} = \frac{\text{inertial forces}}{\text{body forces}} = \frac{c^2}{g \cdot l} \tag{3}$$

Here c represents the flow velocity, ρ the density, μ the dynamic viscosity, υ the kinematic viscosity, l a characteristic length and g the gravitational acceleration.

Another dimensionless number for similarity of flow is the Weber number (*We*). This number describes the ratio between inertial force to the surface tension σ and reads:

$$\mathrm{We} = \frac{\text{inertial forces}}{\text{surface tension}} = \frac{c^2 \cdot \rho \cdot l}{\sigma} \tag{4}$$

When similarity of flow is approximated with respect to *Re* and *Fr* the Weber number differs for air-water and liquid steel-liquid mould powder system respectively. This has to be considered when phenomena regarding free surfaces are discussed.

Due to the similarity criteria discussed above the physical modelling work is carried out for full scale dimensions, i.e. Reynolds and Froude number are the same as in the operational plant. Therefore an existing physical model was adapted to the TKN casting conditions, i.e. mould format of 1300 x 240 mm^2.

In **Figure 73** the physical model is shown. Oil was used as fluid simulating slag.

The following tools were used for measurements:

- flow visualisation trials using colour injection method:
  The flow visualisation using colour injection trials gives information about the structure of the flow field quantitatively, i.e. the propagation of the jet out of the port of the SEN as well as the symmetry of the flow field can be evaluated. Especially a more symmetric flow field will ensure a low amount of flux being entrapped.

  Figure 74 shows exemplarily the colour propagation for different casting velocities at special time steps for a mould format of 1300 x 240 mm^2 using TKN Standard-SEN at constant immersion depth of 120 mm. One can see, that the colour injection is very symmetric and that the colour propagation increases with casting speed as expected.

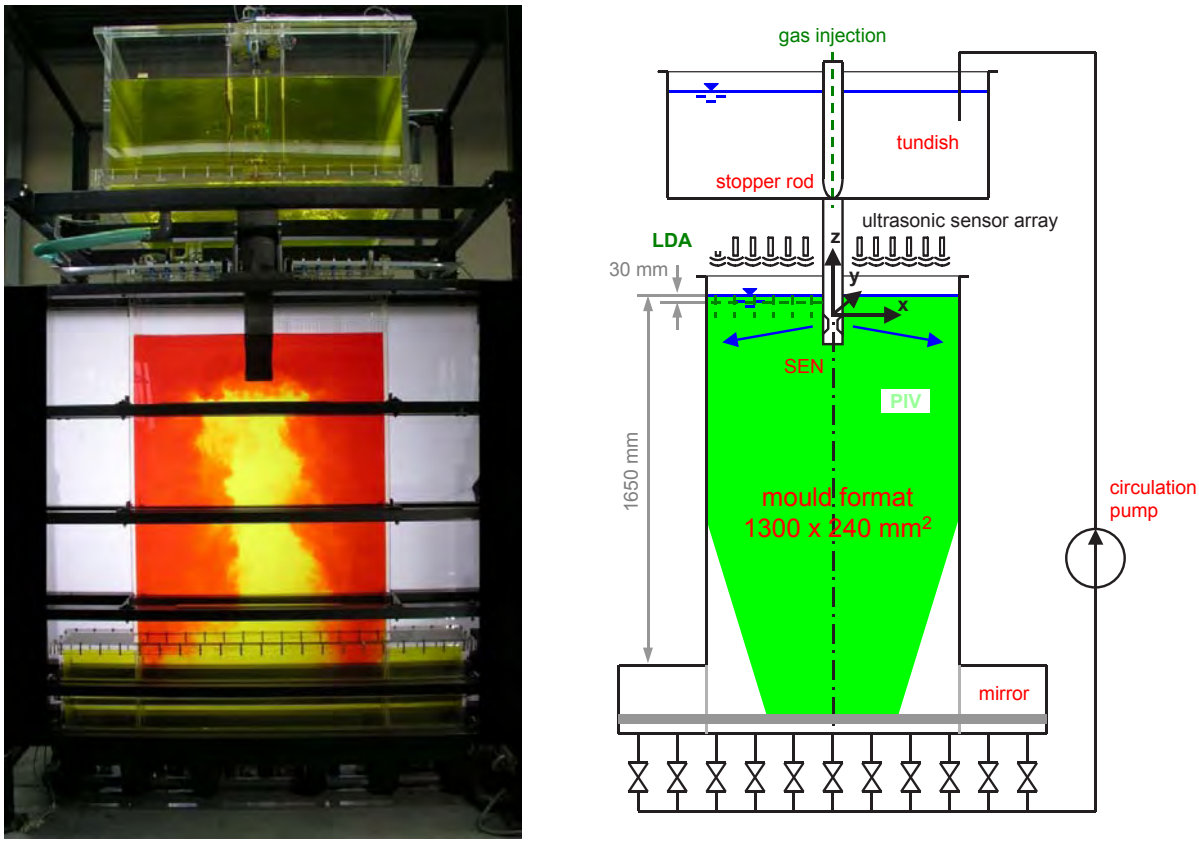

Figure 73 BFIs physical model – modified for TKN casting format using the TKN-Standard SEN geometry

For quantification of the flow symmetry a special developed post processing algorithm was used. For the post processing the original picture of the flow field of interest has first to be divided into two halves. Then for both halves all equivalent pixel colour values are compared. So it can be judged, if the flow in both halves is coloured in the same way or not. If both are coloured in the same way the pixel colour value of both pixels is set to the value of green, if one is coloured and one not the pixel colour value of the coloured one is set to "red" and the other to "white" and if both are not coloured both are set to "white". Taking into account the alteration with time one can estimate the propagation time of the colour tracer.

In **Figure 75** a typical result of the post processing described before is shown for the mould format of 1300 x 240 mm^2 at a casting velocity of 1.0 m/min using TKN Standard-SEN at constant immersion depth of 120 mm. Here the previous stated flow symmetry is proved. For the other investigated casting velocities as well as immersion depths no significant flow asymmetry has been observed.

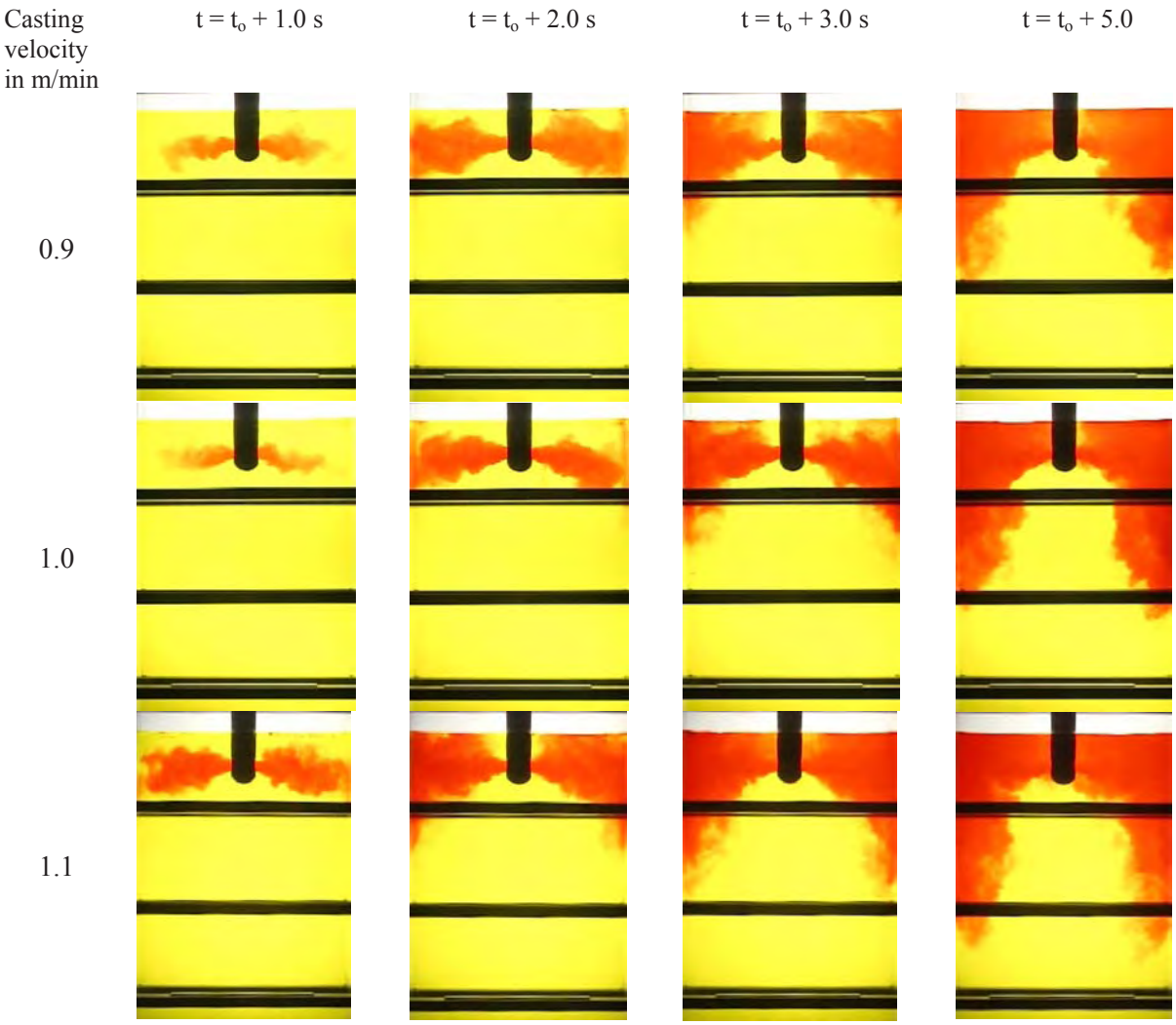

Figure 74 Flow visualisation with colour injection
Casting format 1300 mm x 240 mm; immersion depth 120 mm; TKN Standard-SEN (BFI)

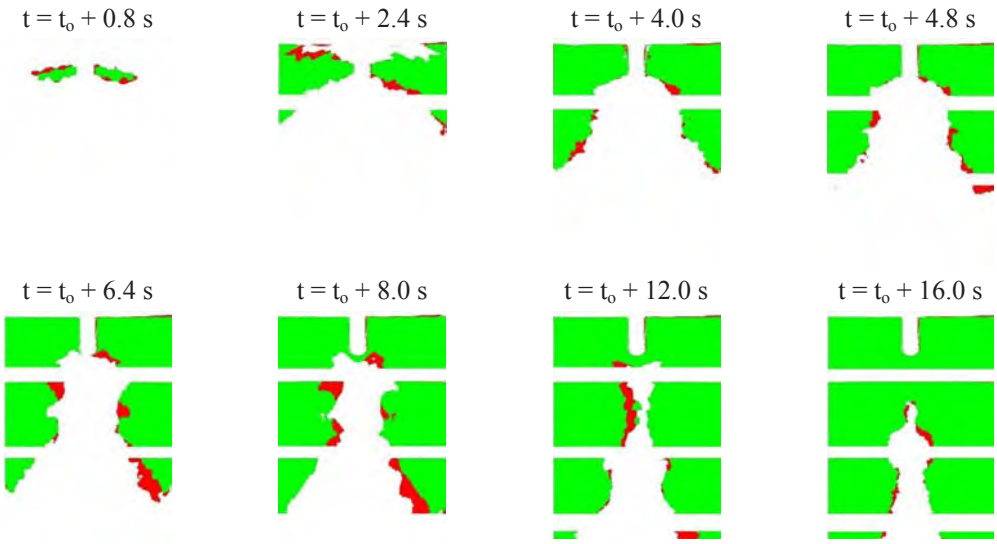

Figure 75 Flow visualisation with colour injection – flow symmetry:
Casting format 1300 mm x 240 mm; casting velocity 1.0 m/min; TKN Standard-SEN; immersion depth: 120 mm (BFI)

- velocity measurements close to the meniscus using LDA and PIV:

  The LDA was used for the non-intrusive measurement of the time-dependent local flow velocity close to the meniscus. The time-dependent flow conditions close to the mould surface are of particular importance regarding to the melting behaviour of the mould powder as well as to the flux entrapment. The horizontal velocity component is an important quantity for elaboration of guidelines concerning the optimal casting conditions. **Figure 76** shows exemplarily the influence of immersion depth and casting speed on the velocity near mould level surface in the middle plane. A first analysis of the performed LDA-measurements can be summarised in the following ways:

  - Near the mould level surface exists a horizontal velocity component which always point to the SEN, i.e. negative values. This explains the observation at TKN that the average thickness of the liquid flux layer varies along the width of the mould.
  - Increasing the casting velocity leads to higher absolute values in the horizontal velocity component near the mould level surface, whereas the vertical velocity component keeps nearly constant.

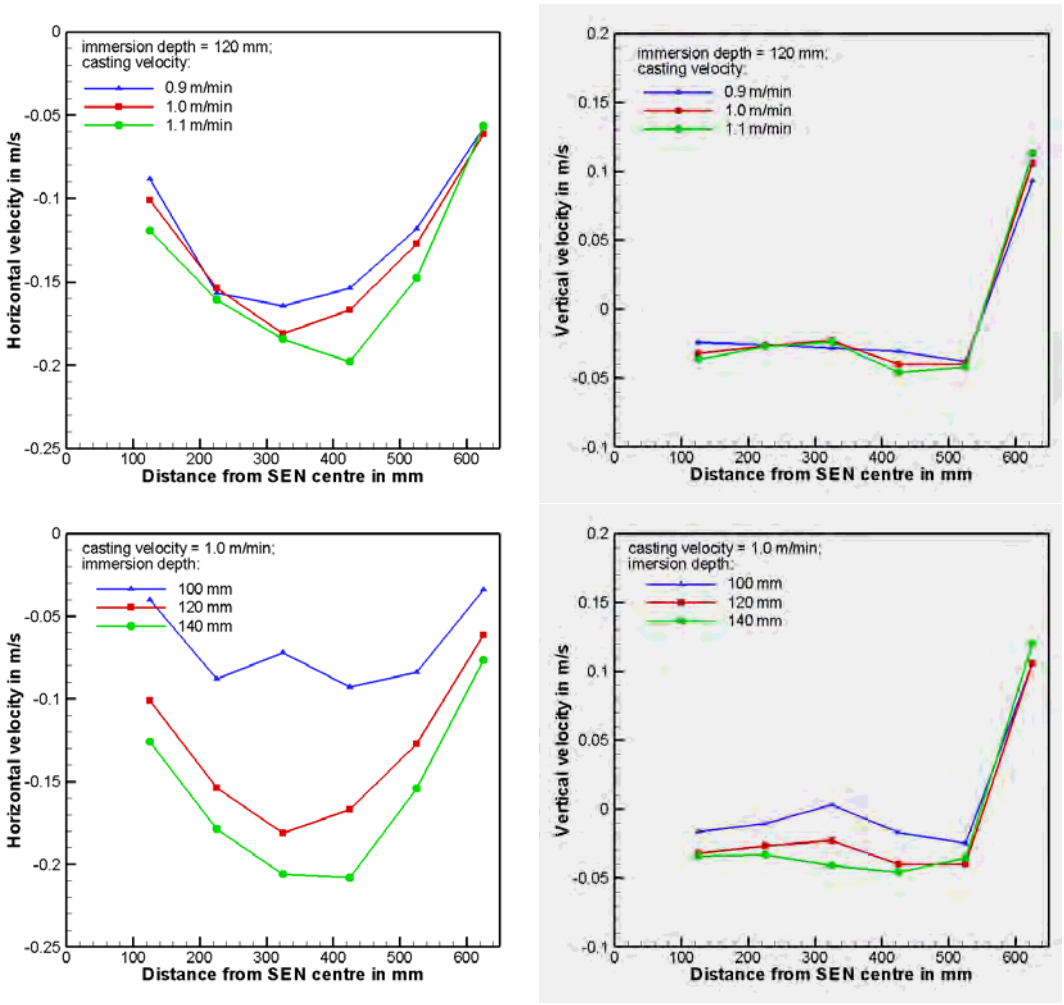

Figure 76 Measured velocity components at BFI using TKN Standard-SEN
upper line: influence of casting velocity at constant immersion depth of 120 mm, lower line: influence of immersion depth at constant casting velocity of 1.0 m/min

If a higher horizontal velocity would result in a better melting of the mould powder, this would be in good accordance with the observations made at TKN. But the critical horizontal velocity for entrapment has to be avoided.

- Increasing the immersion depth leads to higher values of the absolute horizontal velocity and smaller absolute values of the vertical velocity. This should result in higher thickness of the liquid flux layer due to better thermal conditions which was also observed at TKN. Again the critical horizontal velocity for entrapment has to be kept in mind.

Due to the fact that the LDA measurements could only be performed 30 mm beneath the mould level surface, additional PIV measurements were conducted. So it was possible to get information about flow velocity direct at the steel-slag interface. The investigated region is shown in **Figure 77** on the left schematically. On the right of Figure 77 the velocity information obtained for the TKN-standard case, i.e. casting with the SEN with the small port outlet geometry using a casting velocity of 1.0 m/min at an immersion depth of 120 mm is shown. In this figure some vectors along the interface are indicated. The corresponding velocity information is given in the table. The maximal velocities observed are approximately in the range of 0.24 to 0.28 m/s which is not to far away from the critical velocity according to Oeters [30].

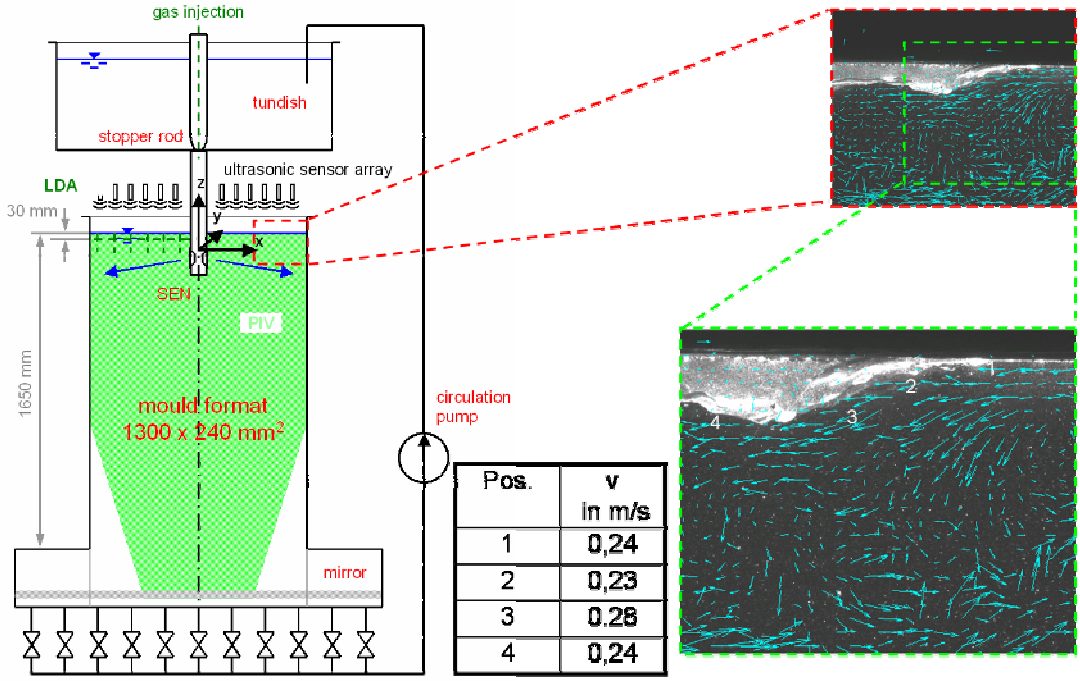

Figure 77 Physical model trials – PIV measurements at BFI for estimation of velocity near mould level surface considering liquid mould powder

- model trials using oil as surrogate for the liquid mould powder in order to characterise entrapment behaviour.

In order to estimate the influence of immersion depth and casting velocity on liquid mould powder entrapment behaviour physical model trials have been conducted. In preliminary trials the measuring configuration being necessary to obtain realistic results has been estimated. Finally a liquid mould

powder thickness of 30 mm in combination with a plate of Styrofoam covering the liquid mould powder has been chosen. In this configuration the casting velocity and the immersion depth was changed and the behaviour recorded with a video camera. In order to get a better contrast of obtained entrapment information the oil representing the liquid mould powder was dyed red and the water representing the steel melt in yellow. In a first step representative flow situations have been extracted from the recording for each casting condition and this information has been compared for different casting conditions.

In **Figure 78** one can see for example one typical entrapment situation and its schematic interpretation. The entrapment situation for a casting velocity of 0.9 m/ min is shown in the upper right of Figure 78 and for 1.0 and 1.1 m/min in the lower left and lower right respectively. One can clearly see that the entrapment behaviour degrades with increasing casting velocity as expected.

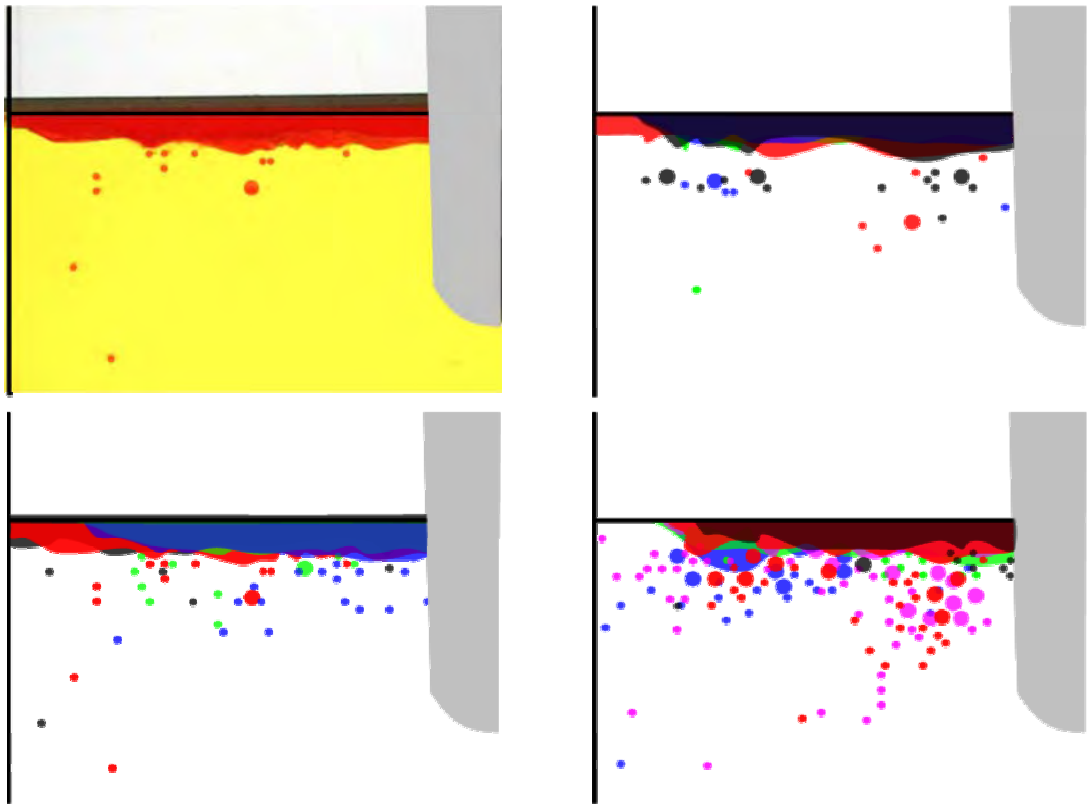

Figure 78 Influence of casting velocity on liquid mould powder entrapment – exemplary photo of a typical entrapment situation and the schematic information included (upper left), entrapment behaviour for 0.9 (upper right), 1.0 (lower left) and 1.1 m/min (lower right) (BFI)

In **Figure 79** the influence of immersion depth is shown in the same manner as described before. The investigated range of immersion depth was 80 mm (upper left) to 200 mm (lower right). Here one can clearly see that the entrapment behaviour changes for the better with increasing immersion depth as expected.

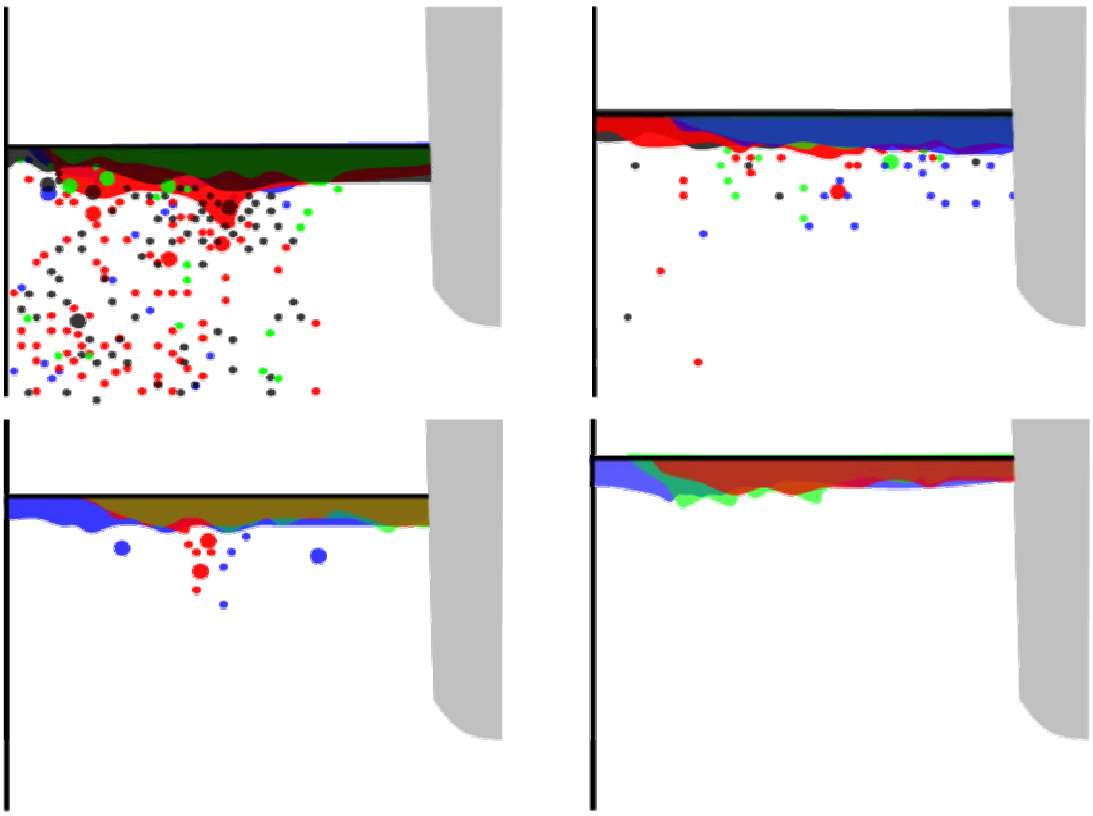

Figure 79 Influence of SEN immersion on liquid mould powder entrapment – entrapment behaviour for 80 (upper left), 120 (upper right), 160 (lower left) and 200 mm (lower right) (BFI)

Finally the information obtained was analysed with respect to entrapment intensity and frequency. Therefore the following classes of entrapment intensity had been defined:

- none: case without any mould powder entrapment
- incipient: case where first single mould powder spheres are being entrained
- advanced: case where first single mould powder spheres are being entrained by the port stream
- pronounced: case with intense mould powder entrapment

and the video-sequences analysed. **Figure 80** shows on the left the influence of casting velocity on mould powder entrapment. With increasing casting velocity the quantity as well as the intensity of the mould powder entrapment cases increases. Concerning the influence of immersion depth (right) one can see that entrapment quantity and intensity decrease with immersion depth.
In both cases there seems to be a critical value beneath which no mould powder entrapment occurs.

As already mentioned in chapter 2.3.2 BFI also performed supplementing model trials in order to calibrate the measuring device for the estimation of the velocity near the meniscus. Therefore the velocity field around the immersion body has been estimated using LDA (**Figure 81**, upper left).

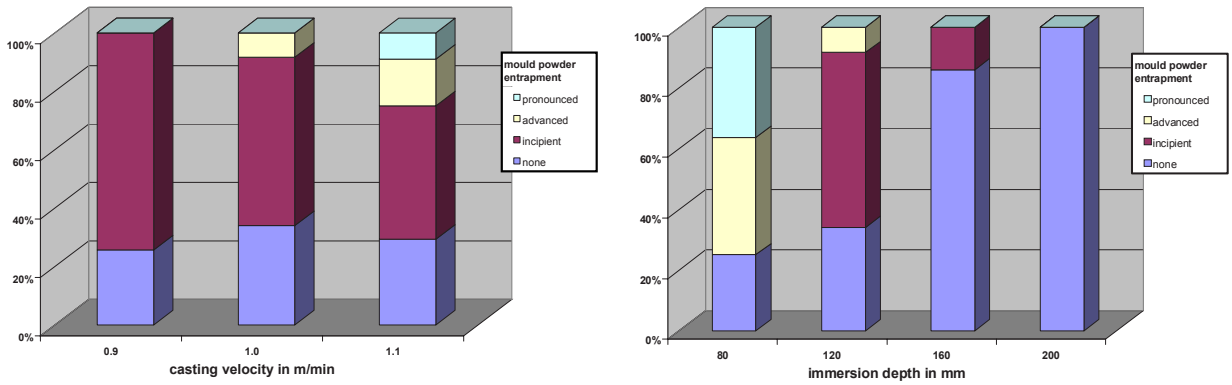

Figure 80 Influence of casting velocity (left) and SEN immersion (right) on intensity and frequency of liquid mould powder entrapment (BFI)

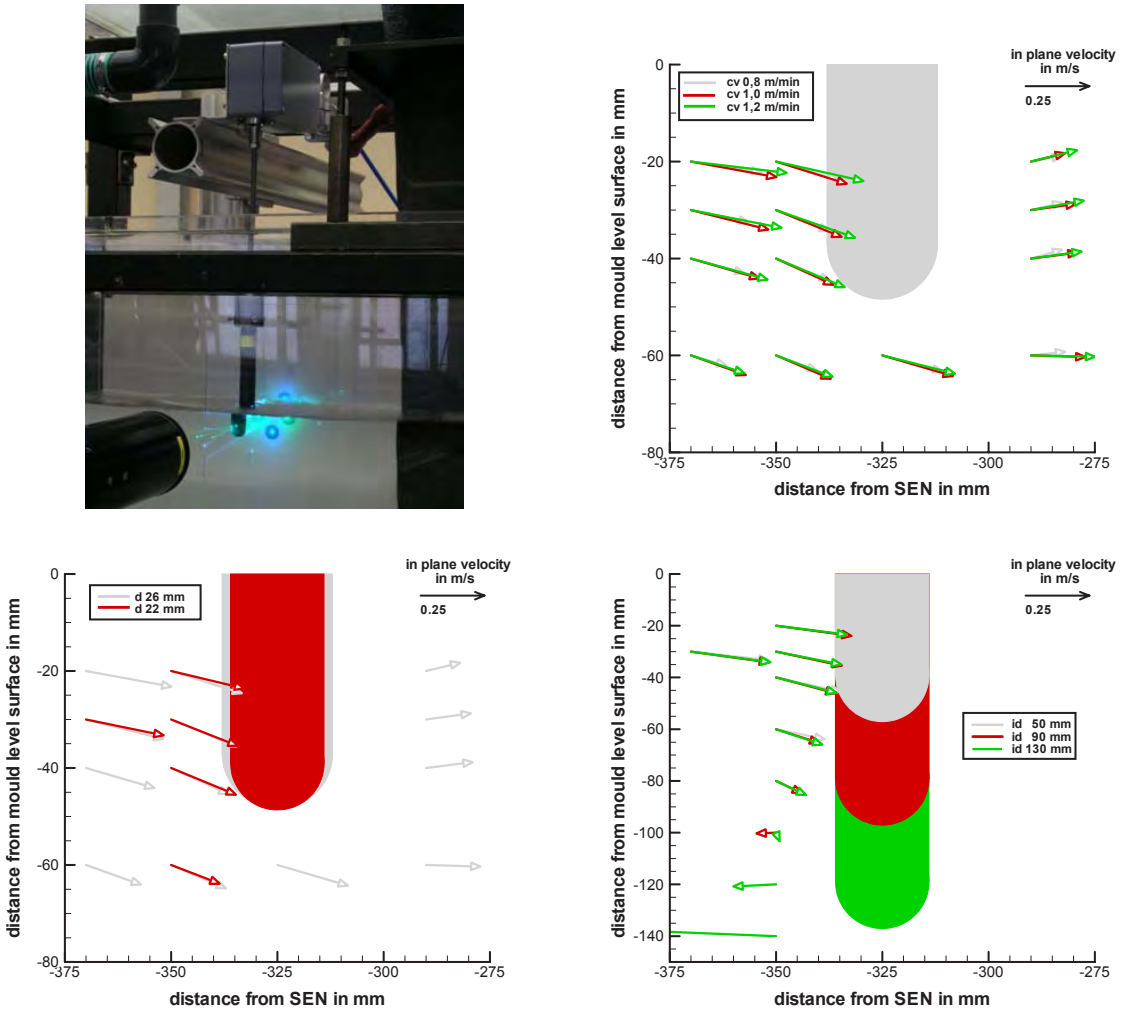

Figure 81 Calibration of the measuring device at the physical model of BFI via Laser-Doppler-Anemometry (upper left) – influence of flow velocity (upper right), diameter of the immersion body (lower left) and immersion depth of immersion body (lower right)

Knowing the mean velocity one can estimate the drag coefficient for the immersion body from the following equation:

$$c_w = \frac{M/l}{\rho/2 \cdot A \cdot u^2} \tag{5}$$

Here M is the measured moment, l the distance between half of the immersion depth of the immersion body and the rotation axis, ρ the density of the fluid, A the projected area of the immersion body, which is flown against, and u the measured horizontal velocity component.

In the same way the influence of the casting velocity (Figure 81, upper right), the diameter of the immersion body (Figure 81, lower left) and the immersion depth of the immersion body (Figure 81, lower right) had been considered.
Finally a revaluation formula has been elaborated to estimate the velocity at a reference mould height for different immersion depths of the immersion body. This is necessary to compare the results obtained in the physical model with the ones obtained in the operational praxis, because the velocity decreases with higher displacement from mould level surface.

2.3.4.4 Modelling of the relevant multiphase flow conditions in the mould with special regard to flux melting and entrapment (Task 4.4)

According to the physical scheme already described in the section dedicated to this WP, it was considered of most concern:

- on one hand, with the CFD code, the identification of the conditions of possible excess of the steel velocity threshold at the interface steel-slag to induce risky waves at the meniscus and slag emulsification occurrence;
- on the other hand, the evaluation
  - with the CSM powder melting model of the thickness of the liquid pool.
  - with the enhanced Fluent model considering the melting behaviour developed by BFI.

  As a matter of fact, the data on the defect occurrence on product (see chapter 2.3.1 to 2.3.3) highlights the presence of slag entrapment in form of recarburised zones in the first as-cast products (slabs, long products). This phenomenon could be ascribed to powder or sintered powder entrapment, so that the physical scenario associated to such a defect assuming stable casting conditions were the following:

  - at first, liquid pool is very thin and then recarburised layer is very close to steel interface;
  - at the same time, velocity conditions at the meniscus are such that instability occurs, interface steel-slag breaks, waves forms whose amplitude is high enough to embed powder or sintered layer;
  - sintered particles are more difficult to float with respect to liquid ones, and can be trapped onto the first solidified skin forming at the early stage of solidification.

The work performed at **CSM** then concerned:

- for fluid flow modelling, the investigation of variation of casting parameters on velocity field at meniscus and the ‘potential wave height’;

- for mould powder modelling, the evaluation of liquid pool thickness in function of the different properties,

to correlate the expected conditions- risky or not –expected to arise from modelling with the results on the plant results on product.

Modelling work was therefore made describing long products' plant partner casting operation (CAS and Sidenor) as follows:

- CAS 160 mm square caster: effect of casting speed, electromagnetic stirring coil current, nozzle geometry on velocity at meniscus;
- Sidenor 185 mm square caster: effect of Electro Magnetic Stirring coil current and nozzle immersion depth on velocity at meniscus.

As refers to investigations concerning CAS casting conditions, the investigations included:

- nozzles geometry basically of two types, straight and with 5 holes (4 lateral and one at the bottom). Cases with holes inclined of ± 15° were considered. This was justified by the fact that nozzle geometry is mostly responsible of steel velocity in the mould, and therefore steel velocity at the interface with the slag is strongly dependent on the steel velocity in the nozzle. In particular, the CAS aim was to redistribute the kinetic energy of the inlet stream among the holes in such a way to ensure good meniscus feeding without risks of shell remelting at hot spot.
- EMS current of 150 – 250 – 350 A.

At first, the flow conditions were investigated in order to find if velocity field at the meniscus could lead to emulsification onset according to Oeters indications. Being this information simply related to metal velocity field, single-phase flow was simulated.

The most relevant results obtained are shown in **Figure 82**. The most relevant result achieved is the fact, that the threshold limit for slag entrapment occurrence, via the phenomenon of emulsification onset previously described, is never attained in the conditions examined, also considering nozzles with four lateral holes.

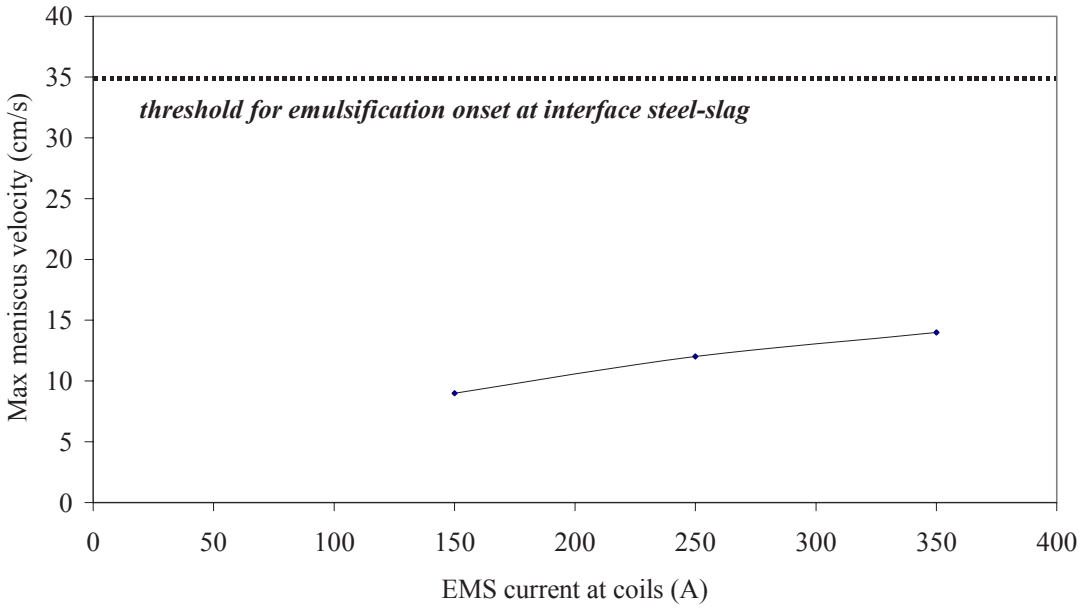

Figure 82 Maximum velocity at meniscus achieved from CSM numerical modelling of flow in CAS mould casting with EMS at a casting speed of 1.5 m/min using the standard nozzle

With the highest coil current intensity considered, velocity is not greater than about 0.15 m/s, according to CSM experience index of good meniscus feeding but for sure not risky for perturbing the interface steel-slag. This aspect is also confirmed by the 'multiphase' investigation made by means of the Particle tracking facility in the code (**Figure 83**).

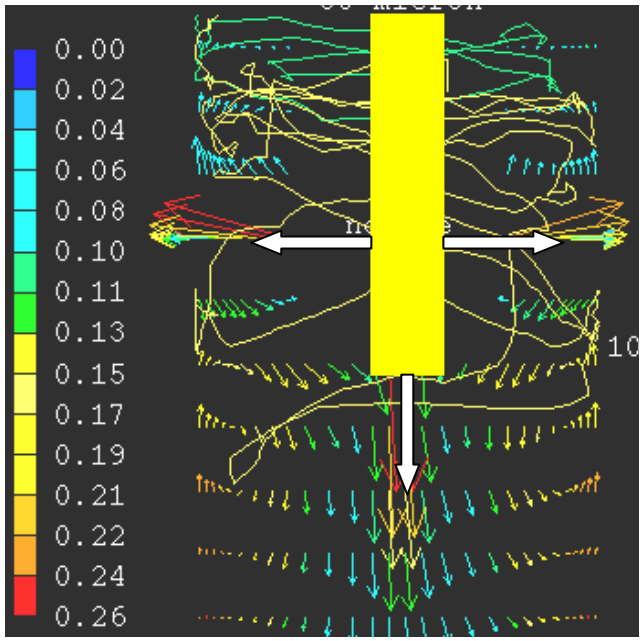

Figure 83 Numerical simulation of steel and particle flow in the centre plane of the CAS mould (velocity in m/s) – Multihole nozzle, port exit angle +15°, coil current 250 A (Particles : 50 µm diameter (blue) and 100 µm diameter, (green) 3000 kg/m^3.) Nozzle position in yellow (CSM)

Here, it is assumed that eventually liquid slag is carried away at the interface, with a typical size given by Oeters [30] and its path is described close to the meniscus. As confirmed also by BFI modelling results, the particle tendency is to float at the surface, therefore suggesting that the mechanism proposed

even physically reasonable is not related to the steady-state casting condition occurring in the processes of our concern.

The same results were achieved simulating Sidenor casting conditions (**Figure 84**). Due to the straight nozzle, velocity values at meniscus are well beyond the threshold for emulsification onset.

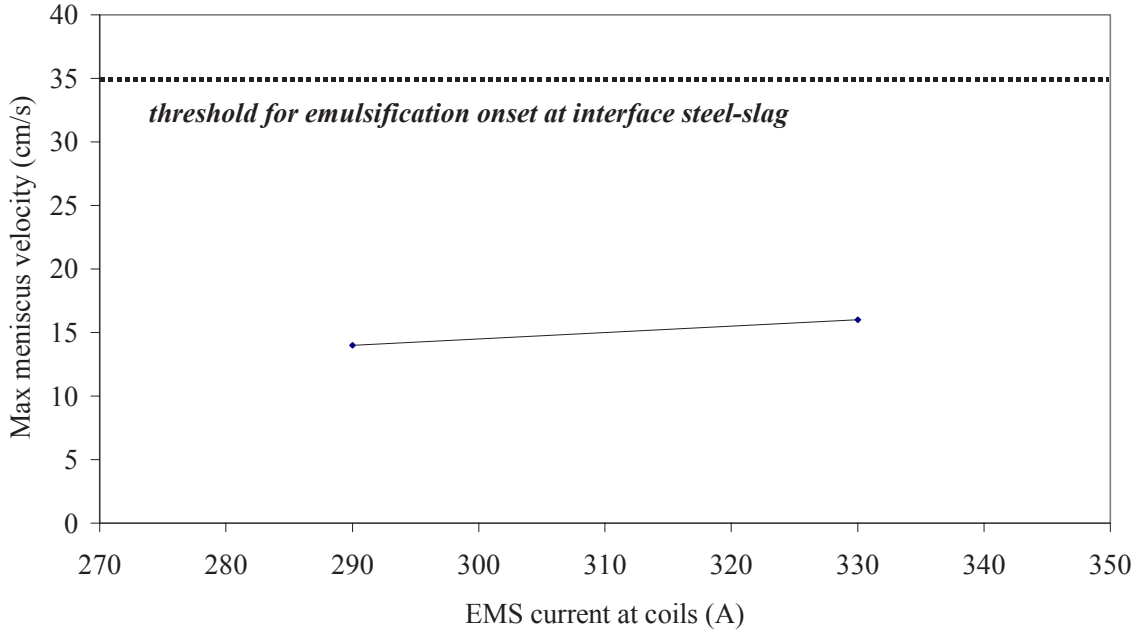

Figure 84 Results of CSM numerical modelling of Sidenor billet casting with EMS at a casting speed of 1.0 m/min using the standard nozzle – Effect of electromagnetic stirring coil current on maximum velocity at meniscus

The results on the product (see chapters 2.3.1 to 2.3.3) clearly indicating that cases of slag entrapment on as-cast products were found anyway, and the main occurrence were related to the start casting period, suggested:

- to concentrate on the interrelation between liquid pool height and wave height formed due to flow at meniscus. A potential wave height h can be associated to a point where steel velocity is v on the basis of the relationship $h = v2/2g$ (all the local kinetic energy is transformed into potential energy), with 2*h potential peak-to-peak wave amplitude;
- to consider, if also very weak waves can be achieved from the velocity fields obtained, unlikely to entrap sintered powder according to the mechanism described before, unsteady flow conditions that give rise to local and momentary velocity values high enough to allow emulsification onset.

The first aspect will be described in the part related to powder modelling. Here, the second aspect is highlighted.

Two main *unsteady flow conditions* can be identified in casting operations:

- those due to improper lay-out arrangement:
  a typical example is represented by the presence of a nozzle inclined or misaligned with respect to

the mould axis. In this case double roll recirculation toward the surface is not symmetric but there is a local reinforcement that can give rise to undesired flow conditions at meniscus;

- those due to improper nozzle design:
  is the case of flow instability at the exit ports due to lateral port oversize [35] and occurrence of cross flow due to impact at the broad face before reaching the narrow faces [36].

The first aspect is common to both flat and long product. For long product it can be the main source of instability, due to the fact that in most cases straight nozzles are used and for curved casters an asymmetric ascending flow to the meniscus occurs, that on the loose side and that on the fixed side (**Figure 85**). The second results in flow oscillations which very seldom occur in long product moulds. These oscillations are more common in slab casters and can lead to 'trumpets' [37] (see **Figure 86**).

CSM achieved information from water modelling concerning flow stability varying SEN operating conditions (SEN mould axis misalignment in long products) and design (SEN lateral port area and angle).
For long products SEN geometry (generally mould feeding with straight nozzles) and stirring action (leading to flow homogenisation) hinder occurrence of flow instabilities. In this case, the improper positioning of the nozzle (e.g. misaligned with respect to the mould axis – effect amplified in presence of a curved mould) could lead to problems. But generally the velocity induced at meniscus, although in an asymmetrical frame, is not high enough to generate dangerous waves at meniscus.

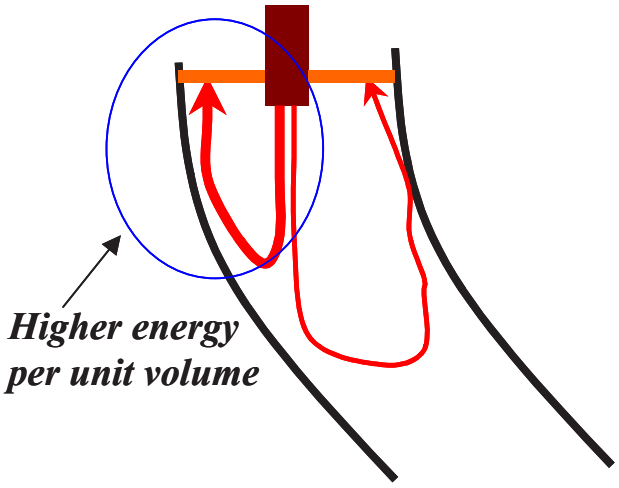

Figure 85 Flow asymmetry induced by geometrical misalignment between nozzle axis and mould curvature (typical for billet casting)

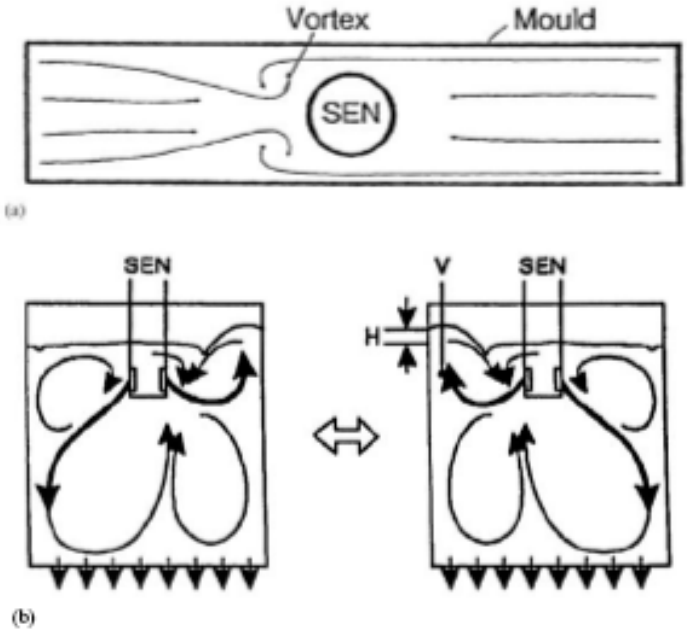

Figure 86 Flow oscillations induce also slag entrapment through vortices [37]

Figure 87 shows exemplarily the situation where a 160 mm diameter round mould is fed by a straight nozzle with an inner diameter of 40 mm also considering the caster curvature (radius 10 m). One can see that the effect of asymmetry exists, but that the velocity at meniscus is low anyway. So finally it is more dangerous that the effect of 'local shell washing' at the hot spot occurs.

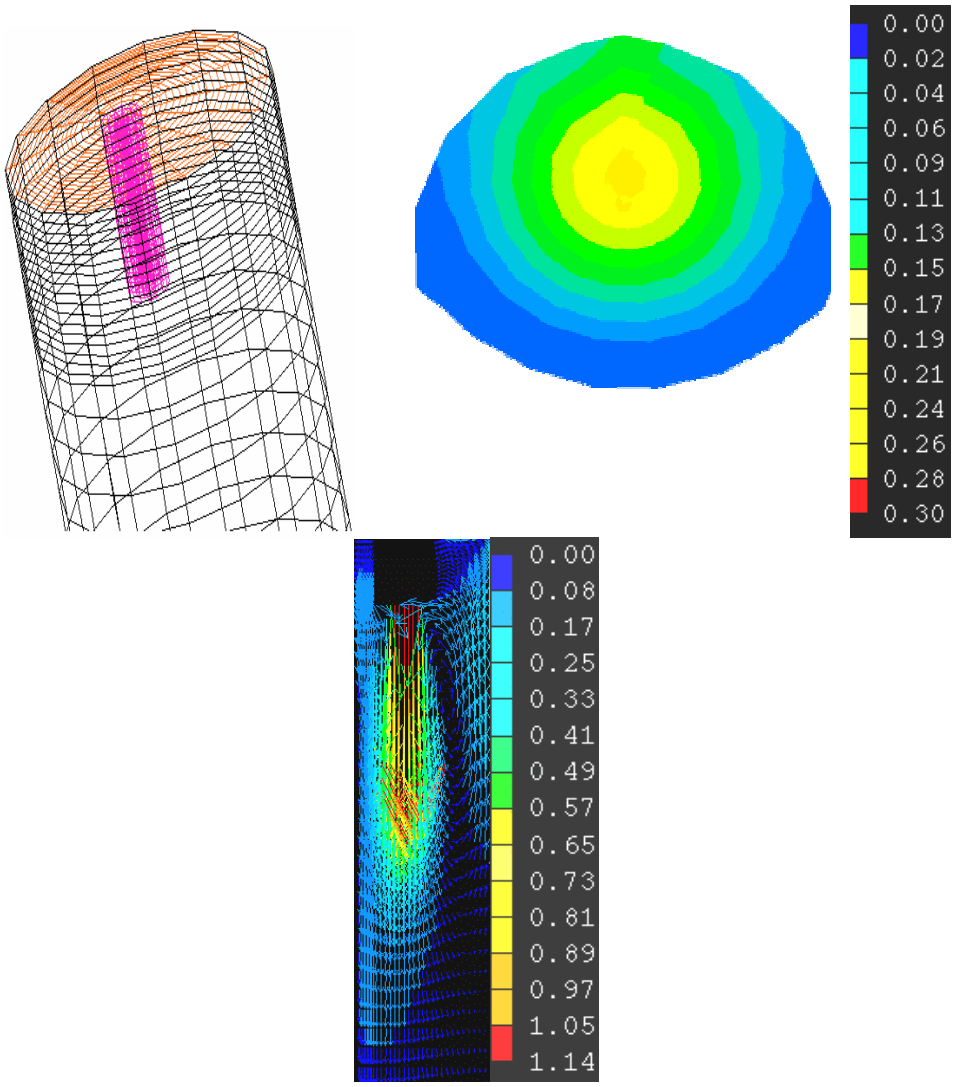

Figure 87 160 mm diameter round mould fed at 2.8 m/min by a straight nozzle (40 mm diameter) with 20 mm misaligned axis with respect to the mould axis (left); velocity map in m/s at hot spot (centre) and meniscus (right) (CSM)

For flat products, the situation is different. Using traditional bifurcated nozzles, the need of feeding moulds with high flow rates (over 2 ton/min) without generating too marked velocity at meniscus brought about a big SEN geometry design work involving the central section and the lateral ports size and angle. Data from CSM on effect of nozzle parameters on instability include SEN port angle and size.

In particular, instability was found to occur especially for positive angles (stream directed upwards), starting from +15°. **Figure 88** shows a typical case for nozzle with a diameter of 55 mm and a port angle of +15°. Here, a flow results (arrows) directed to the centre of the meniscus, close to the nozzle, due to the upwards angle. The undesired effect one obtains is the overlapping of such a flow with the 'typical' one directed from the meniscus corner to the centre. As a result of this induced instability, oscillations are achieved able to give rise to very high waves and local flow reinforcement with velocity of about 0.50 m/s

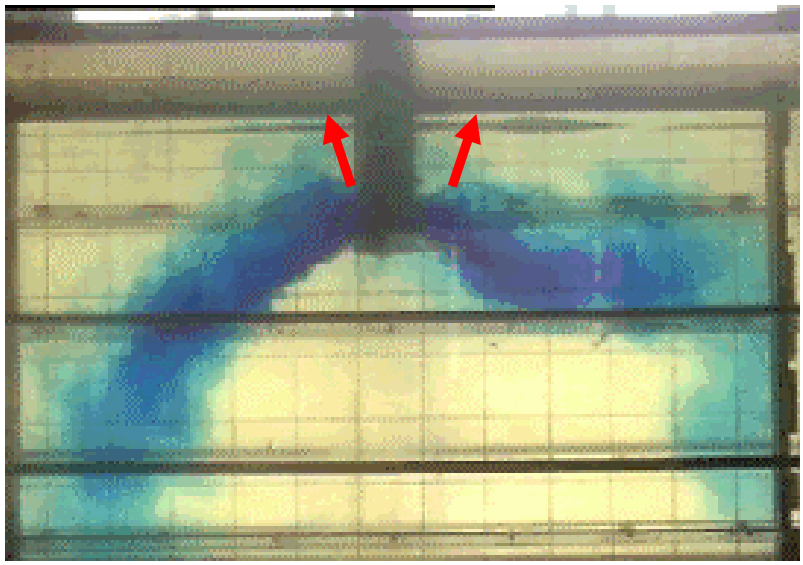

Figure 88 Flow instability oscillations induced by improper nozzle geometry. The arrows indicate flow towards the meniscus center – Nozzle with a diameter of 55 mm and a port angle of +15° using a casting speed of 1.0 m/min at a format of 1300 x 210 mm^2 (CSM)

The same instability was found when the port size exceeded the central diameter. The effect is greater if the port height is enlarged.

The general series of results achieved are summarised in **Figure 89** (effect of port angle) and **Figure 90** (effect of nozzle misalignment with respect to mould axis). A positive port angle (flow directed upwards) and an improper nozzle position (not centred in mould) seems to be harmful for flow stability. Furthermore, nozzle ports area greater than the nozzle central section area is commonly considered 'oversized' and a further cause of nozzle instability.

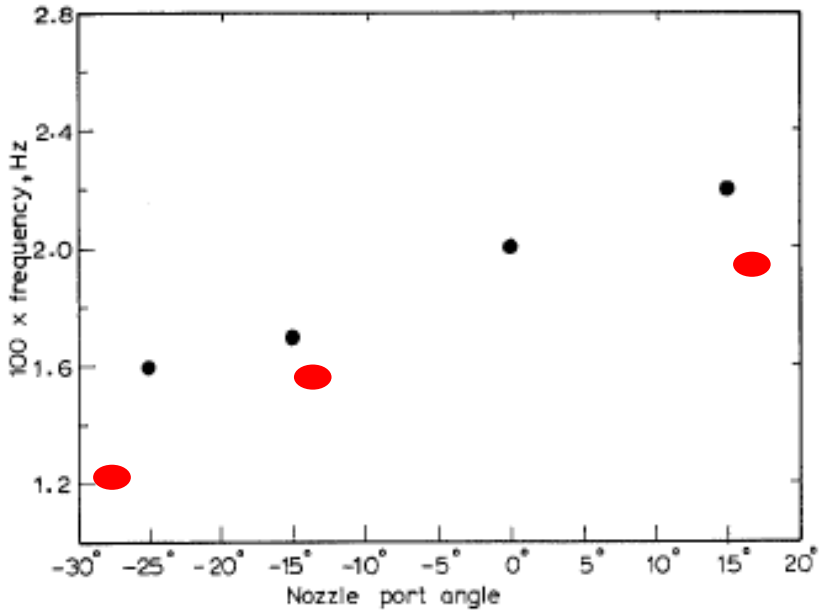

Figure 89 Data achieved with CSM water modelling (slabs, flow rate 2 ton/min, nozzle central diameter 55 mm, nozzle exit ports 55 x 70 mm^2) in the same conditions as in [36] concerning frequency of flow oscillations in function of nozzle port angle. Positive angle = flow directed upwards

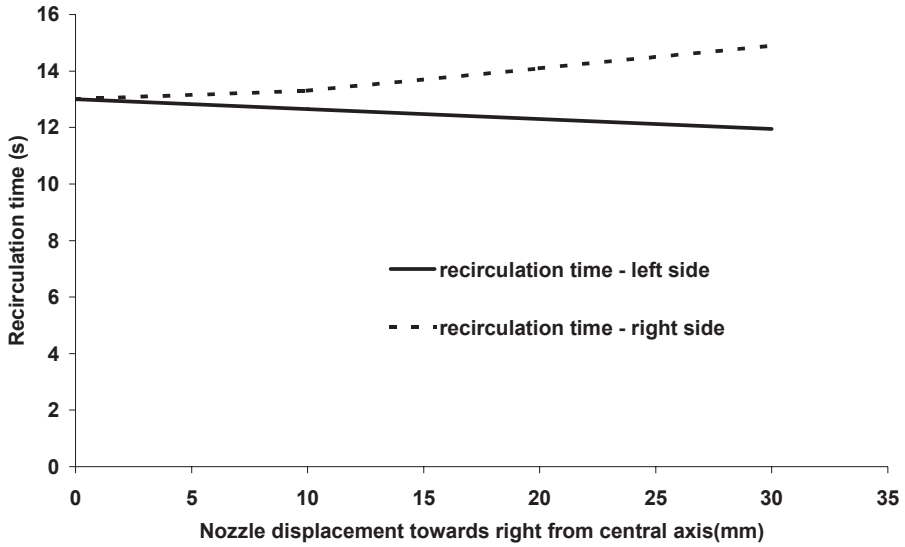

Figure 90 Data achieved with CSM water modelling (slabs, flow rate 2 ton/min, nozzle central diameter 55 mm, nozzle exit ports 55 x 70 mm^2) in the same conditions as in [36] in case of nozzle displacement from centre

The CSM work concerning *powder melting modelling* consisted in evaluating the liquid powder thickness during time from start casting to regime conditions.

The regime conditions were in general attained after 15 min casting (see example of output in Figure 72).

The information concerned CAS powders as well as Sidenor powders, whose properties were already summarised in Table 23 and Table 24. The results achieved in terms of liquid pool thickness are shown in **Table 25**.

Table 25 Results of powder melting modelling (CSM)

Powder	Liquid layer thickness at regime in mm	
	Model	Experimental data
P1 – Sidenor	9.0	9.0
P2 – Sidenor	10.5	12.0
P3 – Sidenor	13.0	14.0
P4 – Sidenor	13.5	15.0
A – CAS	9.0	10.0
B – CAS	12.0	13.0

One can find:

- good agreement between experimental and model data, so leading to further validation of the model;
- dependence of the liquid pool from the powder characteristics;
- the fact that in general powder liquid layers are of the order of magnitude of 10 mm.

It should be observed that to keep a certain liquid level, apart from the suitable mould powder properties, adequate feeding should be provided balancing the ongoing consumption with further powder to be melted. But the results arising from operational work (see chapter 2.3.3), in general seems to be independent from the powder, especially for CAS conditions. As a matter of fact, defects ascribed to slag entrapment seems to occur only in correspondence with the first bars at start casting, corresponding to the time during which liquid pool is being attained.

Therefore, the most relevant cause for the occurrence of slag entrapment should be related more on the poor liquid layer itself at start casting than to problems of excessive consumption with respect to the melting rate.

From the information that the mould powder layers are of the order of magnitude of 10 mm, it can be derived, that the centripetal force acting on the meniscus, related the stirring effect, has no significant effect on the interface instability. In the cases with the 'maximum current' at the coils (over 250 A in both cases for CAS and Sidenor conditions) the velocity imposed at the meniscus reaches the order of magnitude of 0.10 m/s. Also in this case, the liquid edge raising (obtained by equating the centripetal force related to steel velocity v and to the level raising along the radius r needed to compensate this force) is very negligible (below 1 mm).

Therefore, the only factor risky for slag entrapment in steel occurrence, apart from instability phenomena due to asymmetric flow, is the presence of a very low liquid pool causing direct contact between steel and non-melted powder.

In this case, also wave amplitudes of very few millimetres (considering velocity at meniscus of 0.15 m/s as in the 'strongest stirring cases') can break the liquid layer not completely formed in the first 5 min of casting. Moreover, after negative strip, with gap feeding with liquid slag, a depression forms in the liquid powder layer causing 'liquid metal sucking'. This phenomenon is more marked when the stroke is higher. As a result, further slag is entrapped in the molten metal.

This calls for the need of using as low stirring current as possible in the first 15 minutes of casting, and to keep the stroke as low as possible compatible with the overall casting parameters.

Considerations referring to melting rate control in order to avoid lack of powder feeding were already made in chapter 2.3.3 and were used, together with the modelling information achieved, to assess the deliverables on optimum arrangements of parameters to avoid slag entrapment.

The numerically work performed at **BFI** concerned

- for fluid flow modelling, the investigation of variation of casting parameters on velocity field at meniscus and the 'potential wave height';
- for mould powder modelling, the relative influence of casting parameters on melting behaviour

to correlate the expected conditions- risky or not –expected to arise from modelling with the results on the plant results on product.

Modelling work was therefore made describing slab products' plant partner casting operation (Arcelor España and TKN) as follows:

- TKN standard format of 1300 x 240 mm^2: casting speed, nozzle immersion depth and mould powder properties on the velocity at meniscus and the melting behaviour
- Arcelor España standard format of 1400 x 235 mm^2: effect of casting speed and nozzle wear on the velocity at meniscus.

The investigations started with the investigation of the flow conditions in order to check if velocity field at the meniscus could lead to emulsification onset according to Oeters indications.

So for the TKN standard configuration, i.e. casting format of 1300 x 240 mm^2 casting with a casting velocity of 1.0 m/min using a bifurcated SEN with a port inclination 25° upwards with an port exit of 50 x 70 mm^2, a numerical simulation was set-up to appropriately represent the conditions in the test facility, i.e. two phases (water and air) were considered. **Figure 91** shows the discretised domain.

Such two phase simulation is based on the VoF-Method and requires transient computation of the flow. Turbulence was treated by the Realizable k-ε turbulence model. The transport equations were discretised by the Power-Law-Scheme, a scheme which is first order accurate (First-order-upwind) when the flow is dominated by advection. Diffusion dominated regions of the domain are discretised using second-order-schemes. The Power-Law-Scheme is computational inexpensive and reduces cross-stream-diffusion.

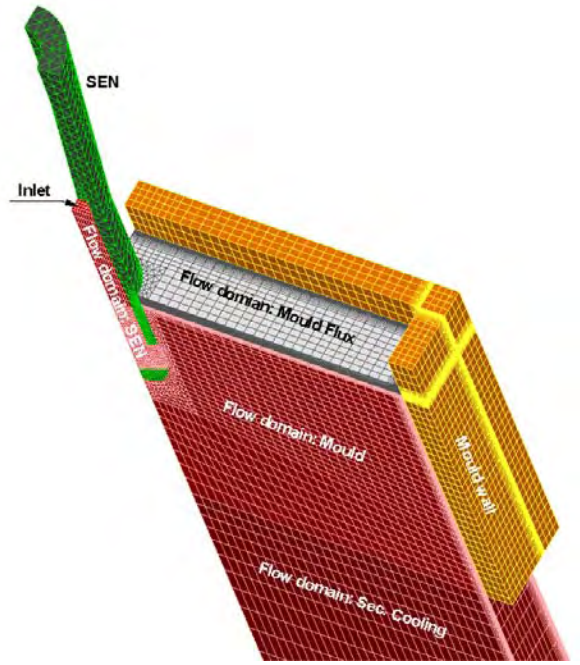

Figure 91 Discretised domain for numerical computations of TKN standard configuration at BFI

Figure 92 shows a comparison between the numerically predicted velocity vectors and the visualised flow by the colour injection in the symmetry plane between the wide faces. The red colour was injected through the stopper rod of the mould in BFI's perspex mould. One can see that the macroscopic flow field is calculated correct, i.e. the flow close to the mould surface is directed towards the SEN, which indicates a double roll pattern in the mould. SENs with upwards orientated ports are suspected to lead the injection jet towards the mould level and cause a single roll pattern. The jets coming out of the ports are orientated downwards.

Figure 93 shows on the left a comparison between numerically (NM) obtained and measured (PM) velocities in horizontal direction 30 mm below the mould level and on the right for vertical velocity direction respectively. Blue lines represent numerical data and red lines show measured ones. The bars attached to the red lines represent the RMS of the velocities estimated experimentally.

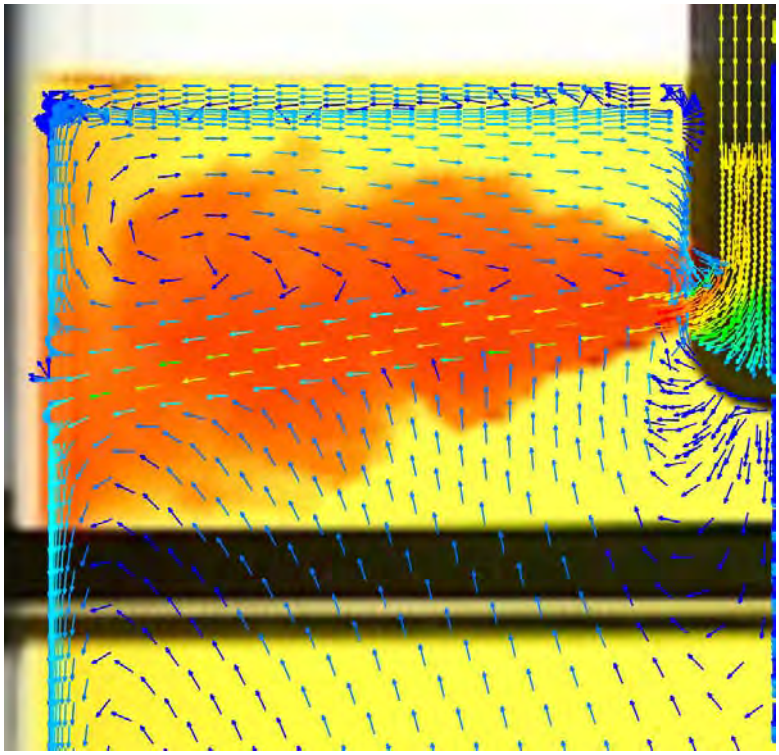

Figure 92 Flow field in the symmetry plane between the wide faces – numerically predicted velocity vectors and visualised flow by the colour injection (BFI)

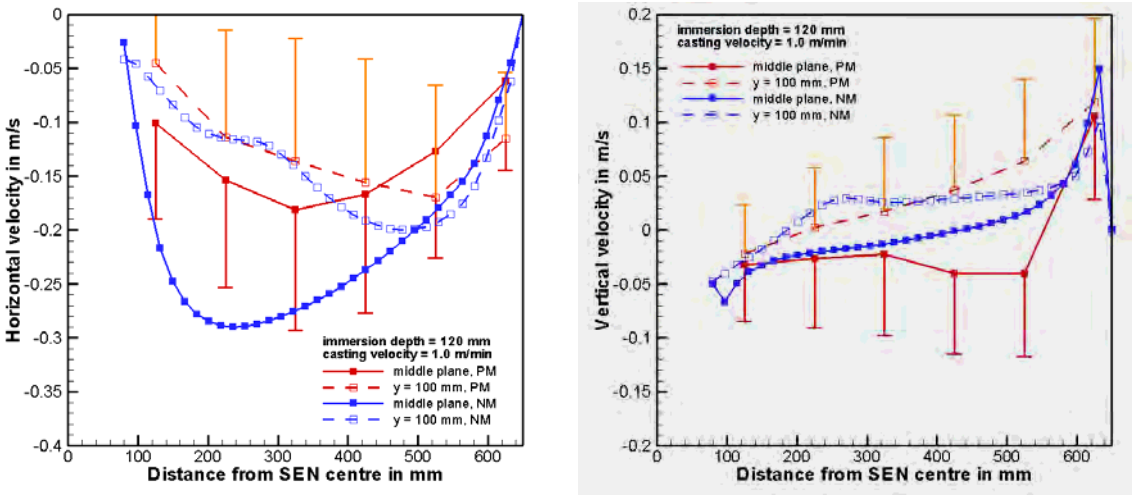

Figure 93 Comparison of numerically and experimentally obtained horizontal (left) and vertical velocities (right) as well as the corresponding RMS of the experimentally measured velocity fluctuations (BFI)

Along the middle plane good agreement between predictions and the averaged experimental data is shown for both directions. Divergence between the experiment and prediction can be observed closer to wide face (y = 100 mm) for the horizontal flow direction. The magnitude of the calculated velocities is differing from measured ones. The amplitude of the RMS of the experimentally obtained instantaneous velocities indicate highly transient flow conditions along the mould level and this may cause energy dissipation which in turn may cause the reduction of the mean velocity in the experiment. This phenomenon can not be accounted for with only modelling a quarter of a mould.

In order to see, if diffusion of momentum occurs due to unsteady flow conditions where the flow pattern fluctuates as observed in the model plants, two more numerical models were created by mirroring the original '1/4-model' along the symmetry planes. **Figure 94** shows on the right the model which was extended in narrow face direction (x-direction) and on the left the model which was extended in broad face direction (y-direction).

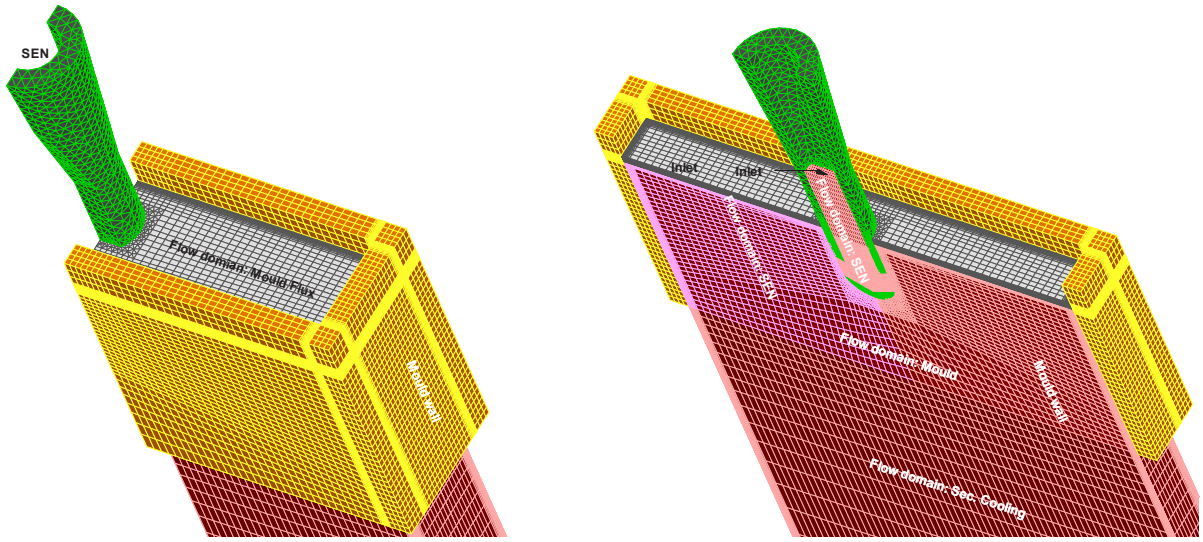

Figure 94 Mould model extended at BFI in y-direction (left) and in x-direction (right)

Fluctuation of flow pattern was predicted for the model extended in x-direction, as shown in **Figure 95** in the upper part. The transient computation showed the typical sequential increase and decrease of near meniscus velocity with time and this is caused by the unsteady flow field. Consequently, trumpets formed in the wake of the SEN, which is shown in Figure 95 in the lower part. It is not clear what causes the oscillating flow pattern. The most likely cause is due to shear of fluid entering the mould (port jet) and the fluid in the re-circulation zones. The unsteadiness develops only when symmetry conditions are not applied between the narrow faces.

Extending the computational domain, i.e. the mould in the y-direction, did not support unsteady flow pattern. However, in both cases the magnitude of near meniscus velocities are met not exactly, which is shown in **Figure 96** for the middle plane. Here the curve obtained for operational properties as well as the measured information at TKN (see chapter 2.3.2 for more details) are additionally plotted. One can clearly see that the numerically obtained information meets better the operational estimated horizontal velocity than the information obtained at the physical model. Reason for the difference of the velocity estimated in the physical model seems to be a different port stream outlet angle, generated artificially by the vortex generated in the SEN bottom. This vortex extends deeply into the mould (see **Figure 97**).

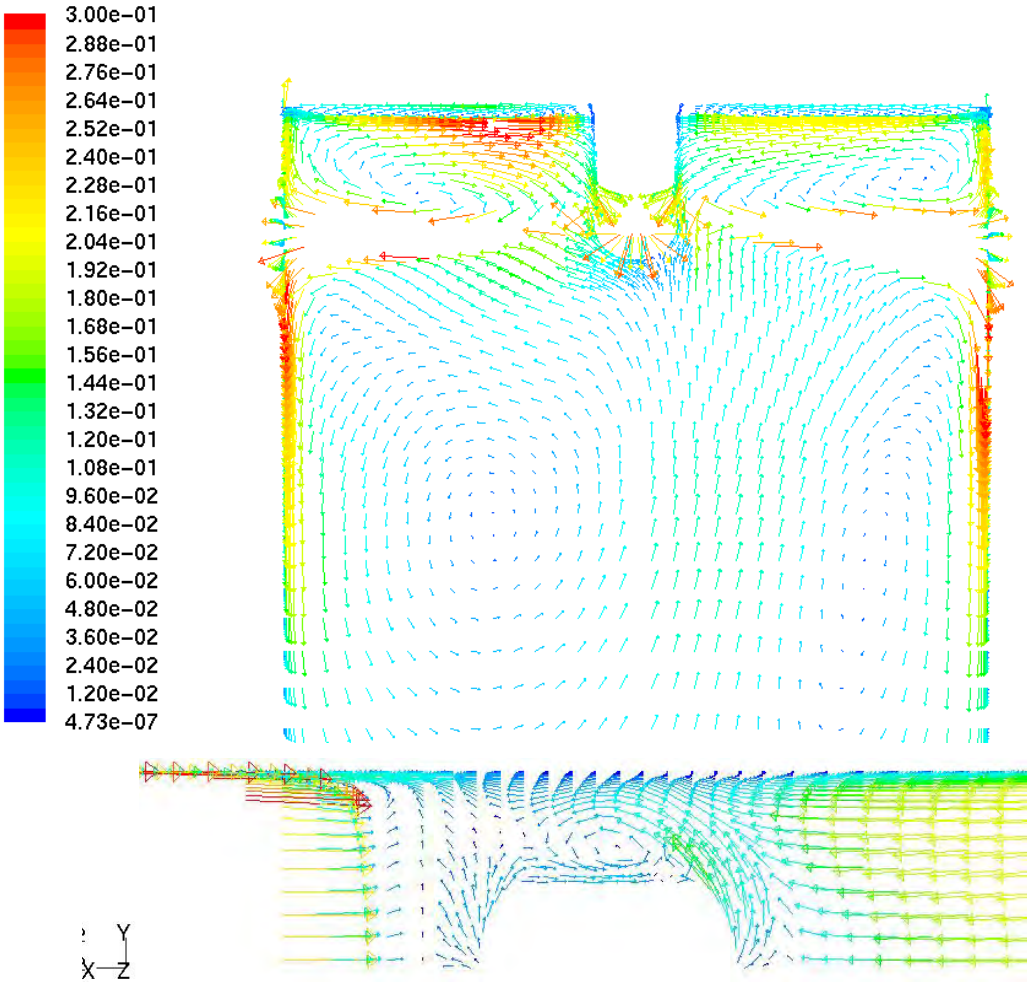

Figure 95 Velocity vector showing oscillating flow pattern in extended mould model (x-direction) for TKN standard configuration (BFI)

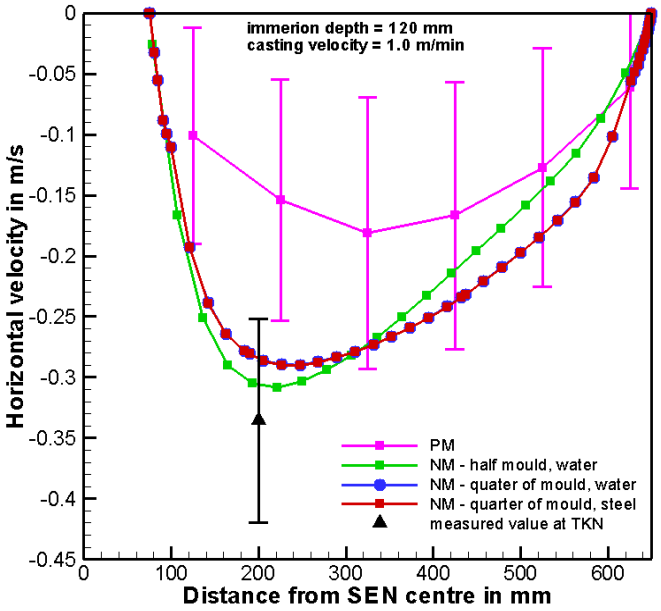

Figure 96 Comparison of estimated horizontal velocities for TKN standard configuration (BFI)

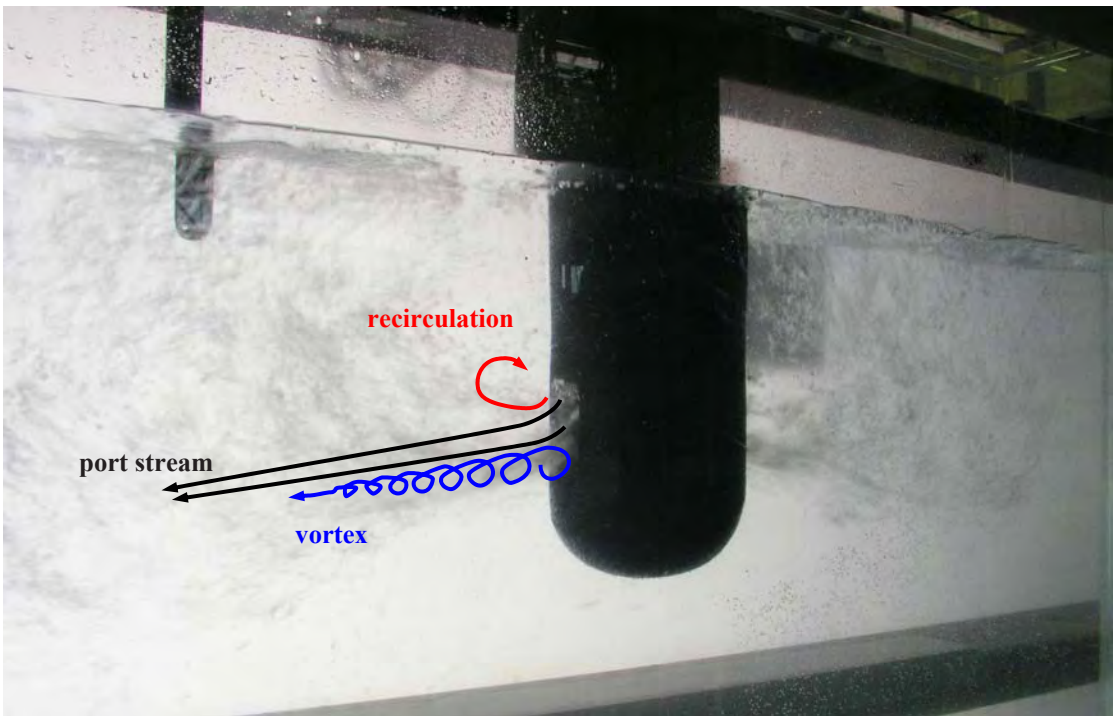

Figure 97 Flow phenomena in the water model for TKN standard configuration (BFI)

So it could be shown that the more accurate way for the simulation is to model half of the mould extended in x-direction, but that the modelling only a quarter of the mould also gives quite 'validated' results, i.e. in good accordance to the operational ones. If one additionally considers the computational effort being necessary for the numerical simulation, in some cases only a quarter of the mould had been simulated.

In the following set-up of the quarter of the mould has been used for comparative studies of the variation of casting conditions such as casting speed and immersion depth. Solution was obtained for three different casting velocities and three different immersion depth.

Figure 98 show the horizontal velocity profiles along the middle plane and y = 100 mm for casting velocities of 0.9 m/min, 1.0 m/min and 1.1 m/min, respectively. In each diagram the velocity profiles for three different immersion depths (100 mm, 120 mm and 140 mm) are compared. The immersion depth affects the velocity profile close to the wide face (y = 100 mm) only marginally. More pronounced is the variation due to a changed immersion depth along the centre line of the mould (y = 0 mm). In both measuring rakes an increase of the horizontal velocity was observed. A stronger influence on the flow field close to the mould level was caused by the variation of the casting velocity.

Similar trends were observed by physical model trials (see chapter 2.3.4.3) and in the measurements performed at TKN considering the small format (see chapter 2.3.2.2).

However all horizontal velocities calculated, are lower than the critical ones according to Oeters [30], but quite in the critical range according to [34] for the highest casting velocity.

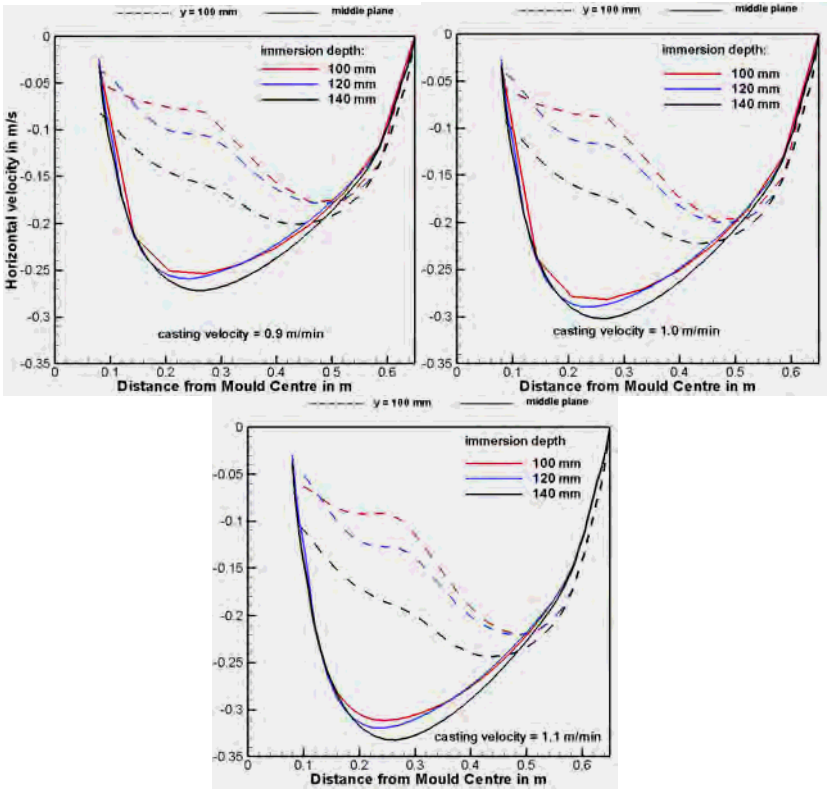

Figure 98 Comparison of numerically obtained horizontal velocities near the mould level for a casting velocity of 0.9 (left), 1.0 (middle) and 1.1 m/min (right) and different immersion depths (BFI)

In the course of this project melting of casting powder and the resulting formation of the interface between mould powder and steel were investigated. Due to the mentioned time consuming aspects of calculation (especially, multiphase flows are difficult to treat numerically and this requires a lot of computational time), such a transient computation concerned a ‘quarter’ of the mould.

Initially, a 20 mm thick layer of solid casting powder was modelled above the melt. Physical properties of the mould powder were taken from a data sheet from TKN. From literature the melting heat was taken. **Table 26** shows the physical specifications of the mould powders.

Table 26 Specifications of the TKN mould powders

Powder Type – No.	1	2
Steel grade	1.4301	1.4016
Density in kg/m³	2500	2500
Heat capacity in J/kgK	1230	1230
Thermal conductivity in W/mK	1.7	1.7
Viscosity in kg/ms	0.15	0.3
Basicity	1.11	0.89
Melting Heat J/kg	530 000	530 000
Solidus temperature in K	1398	1383
Liquidus temperature in K	1470	1455

Figure 99 shows the mould powder layer at the beginning of the computation along the symmetry plane between the wide faces. Blue colour of the horizontal layer indicated the mould powder. The horizontal iso-lines close to the SEN mark the interface between solid and liquid mould powder. Most of the mould powder is solid only a small liquid pool developed between SEN and narrow side.

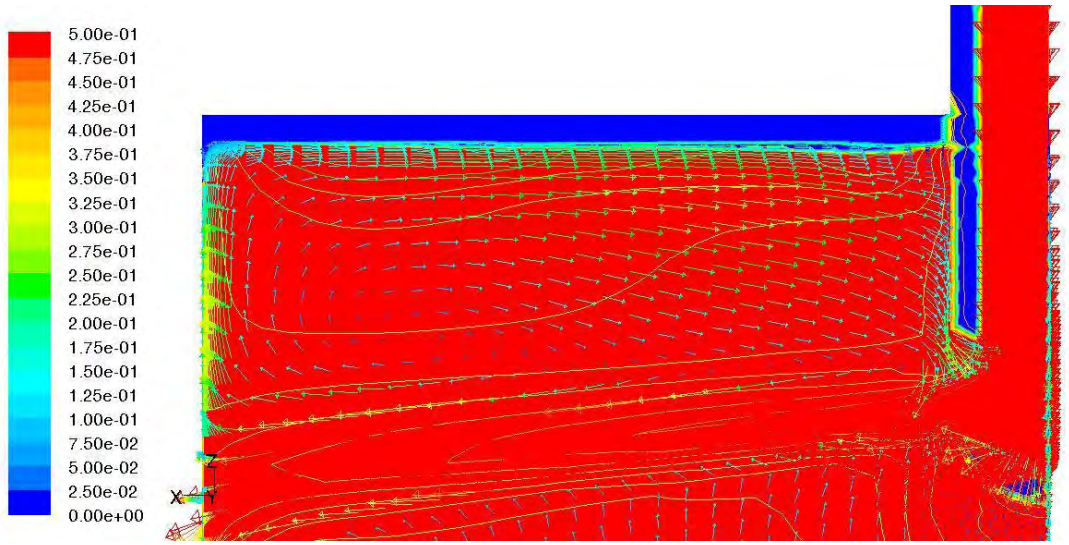

Figure 99 Layer of solid mould powder at the beginning of the computation of the TKN standard configuration (BFI)

Figure 100 shows the melting of mould powder after 4 and 20 seconds respectively. After 4 seconds a large liquid pool developed. Melt travelling with the upper roll of the mould flow reach the solid mould powder and produce more molten casting powder which is than pushed towards the SEN. The melting of mould powder continues until only a small area remains where steel and solid mould powder are in contact. However, the smaller this area, the steeper the flow recirculation angle at the meniscus corner (labelled *alpha* in the figure) and this may promote mould powder entrapment according to Oeters [30].

In Figure 100 there are three vertical lines indicated at which the development of the liquid and solid mould powder was measured over time. The measuring positions were at a distance of 150, 325 and 575 mm from the mould centre respectively. A fourth measuring position closer to the wide face (100 mm distance from the mould centre) was chosen for the position of 325 mm. Both the interface between liquid and solid mould powder and the interface between liquid mould powder and steel converge towards a certain height. In the middle plane the maximum liquid pool depth is in the centre, i.e. x = 325 mm. In the centre of the mould (y = 0) the liquid pool depth is greater and extends further in both vertical directions than the liquid layer closer to the wide face. This thought to be due to the greater influence of the upper roll in the centre of the mould (see **Figure 101**).

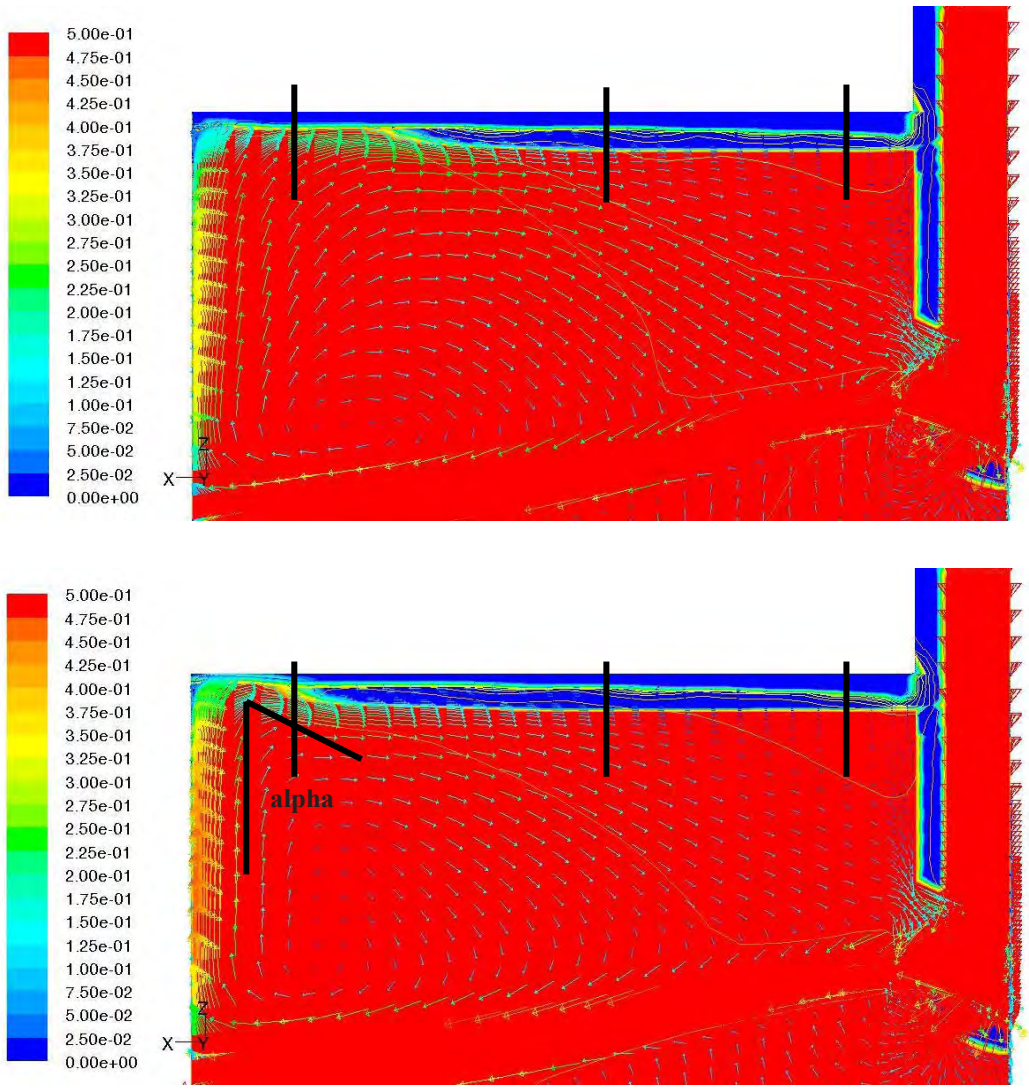

Figure 100 Layer of solid mould powder after approximately 4 (top) and 20 seconds (bottom) for TKN standard configuration (BFI)

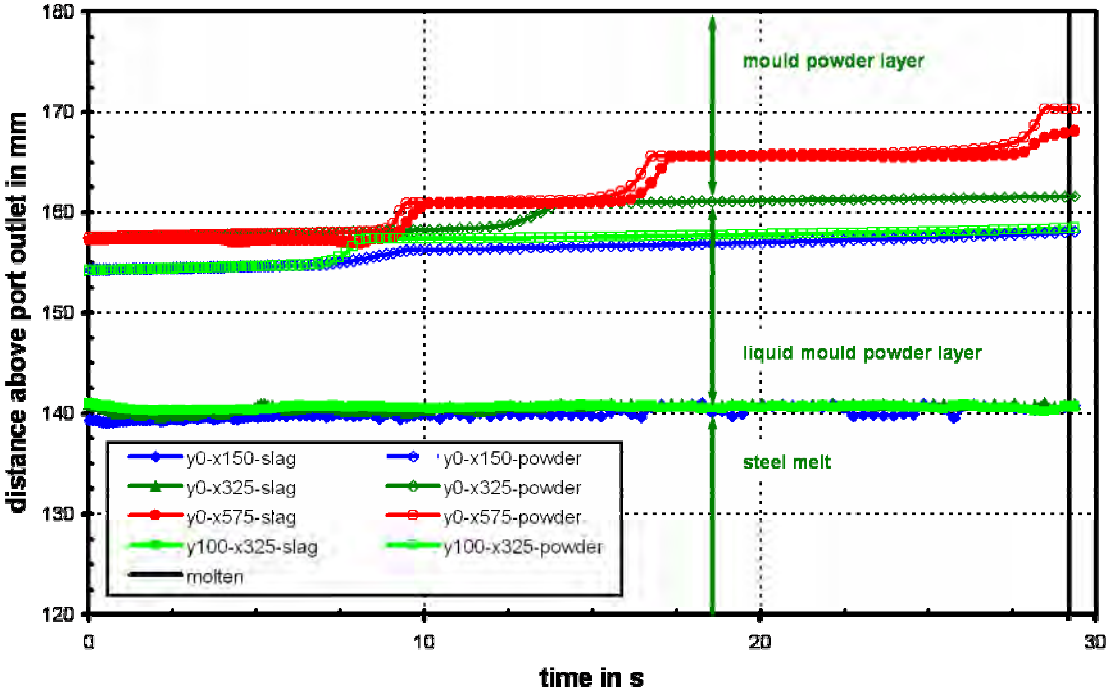

Figure 101 Development of mould powder layers with time for TKN standard configuration (BFI)

Further investigations concerned liquid mould powder entrapment occurrence. A study was made about the causes of mould powder droplet entrapment under steady state casting conditions. Therefore, starting from previous converged solution of velocity field, droplets were injected at location prone for entrapment. The density of the droplets was 3,500 kg/m³.

In the first trial, droplets with a diameter of 1 mm were introduced in the computational domain and their trajectories visualised. **Figure 102** shows the result for this computation. Droplets with a diameter of 1 mm move hardly towards the lower part of the mould where they may be caught by the strand shell. Thus the droplets have to be smaller. In further computations, the droplet size was reduced until they were sufficiently small to travel with the flow into lower regions of the mould (some hundreds □m diameter). **Figure 103** shows the trajectories for droplets with a diameter of 0.2 mm. However, it appeared to be unlikely that such small droplets are separated from liquid pool. The information obtained from numerical and physical modelling showed that mould powder entrapment is very unlikely to occur in continuous casting process of slabs at steady state conditions.

Then, a parameter variation had been performed considering influence of casting velocity, temperature at SEN inlet and casting powder properties according to Table 26. From the results obtained the following information was extracted at the four positions already described in Figure 100:

- time of first mould powder layer complete melting up to the surface. This can occur anywhere in the patched powder domain. Up to this time, the simplified simulation should be comparable for the different casting conditions;

- total wave height, defined as maximum difference between highest and lowest position of interface steel melt/liquid mould powder
- liquid mould powder thickness
- horizontal velocity 10 mm beneath the mould level surface

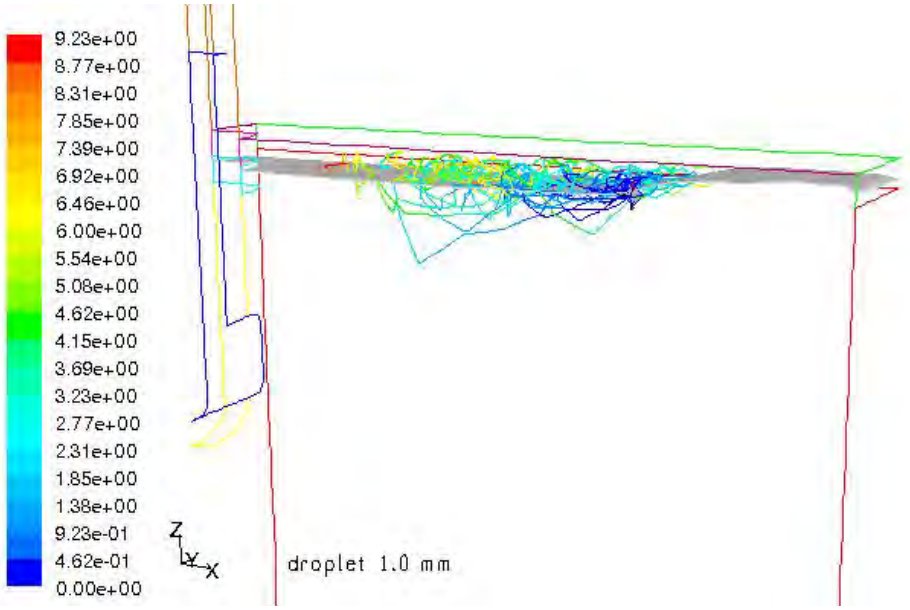

Figure 102 Trajectories for droplets with a diameter of 1 mm for TKN standard configuration (BFI)

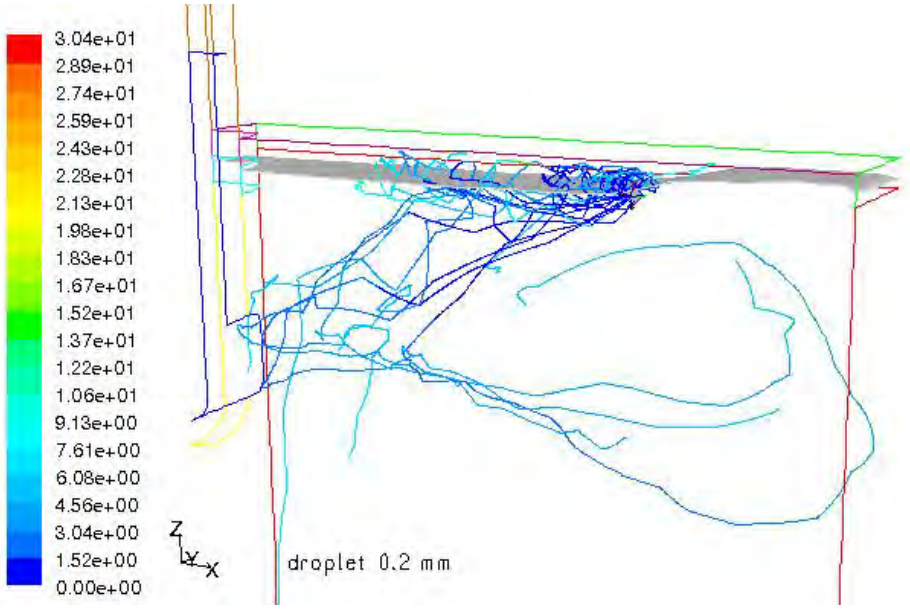

Figure 103 Trajectories for droplets with a diameter of 0.2 mm for TKN standard configuration (BFI)

Figure 104 shows the influence of the parameters on the time when powder molten first time completely (solid line) and the change of wave height (dashed line). The wave height for each case has been normalised with the value obtained for the TKN standard configuration, i.e. 25.8 mm.

As expected, at higher casting velocity mould powder melts more quickly due to the enhanced transport of the steel melt with higher temperature. Also the expected decrease in melting time with higher temperatures at SEN inlet can be seen. But this effect is smaller than that of casting velocity. Mould

powder properties have only minor influence on melting time, but melting point is not very different for the two powders. As expected, estimated wave height increases with increasing casting velocity, whereas temperature at SEN inlet and mould powder properties have nearly no influence. Higher wave heights are supposed to be more critical with respect to mould powder entrapment.

Figure 105 shows the influence of the mentioned parameters on the change of liquid mould powder thickness at different measuring positions considered. Again, the liquid mould powder thickness value for each case has been normalised with respect to that obtained for the TKN standard condition, i.e. 17.2 mm at the position x = 150 mm and 20.2 mm at the position x = 325 mm in the middle plane and 17.5 mm at the position x = 325 mm in the axis y = 100 mm. The values for the position in the region of the narrow face in the middle plane were not printed, because they scattered widely due to the very small liquid mould powder values (smaller than 1 mm) in this region.
As expected is the influence of casting velocity on change of liquid mould powder thickness quite strong, because this quantity should correlate with wave height. However, influence of casting velocity on liquid mould powder level is higher at the middle position than on wave top. Temperature at SEN inlet and mould powder properties have no significant influence.

Figure 106 shows finally the influence of the parameters on the change of the horizontal velocity at different measuring positions. Again, the horizontal velocity for each case has been normalised with respect to that found for the TKN standard condition, i.e. -0.015 m/s at the position x = 150 mm, -0.081 m/s at the position x = 325 mm and -0.183 m/s at the position x = 575 mm in the middle plane and -0.080 m/s at the position x = 325 mm in the axis y = 100 mm. Here one should consider that the value of horizontal velocity is not the maximum value. This lies closer to the narrow face.
As expected is the influence of casting velocity on change of horizontal velocity quite strong, i.e. horizontal velocity increases with casting speed. However, influence of casting velocity seems to be stronger for lower velocity values. Influence of temperature at SEN inlet is quite not so clear. Considering that the high velocities are only obtained at an x-position of 575 mm one can conclude that influence is small. Similar information is obtained for influence of mould powder properties.

But again after the estimated velocity changes, mould powder entrapment occurrence is not expected.

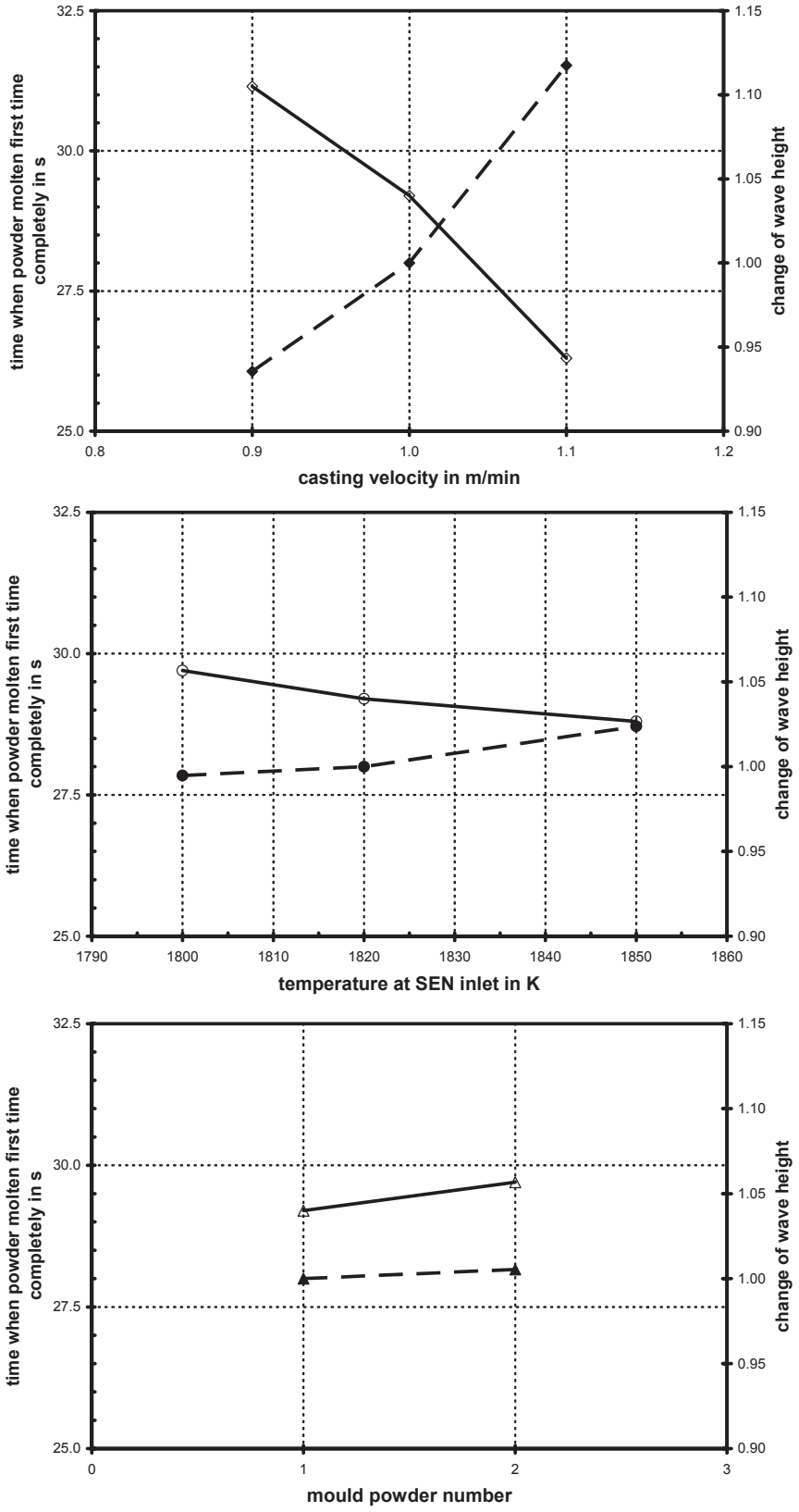

Figure 104 Numerical parameter variation performed at BFI – time when powder molten first time completely (solid line) and change of wave height (dashed line): influence of casting velocity (upper line), temperature at SEN inlet (middle) and mould powder number (lower line)

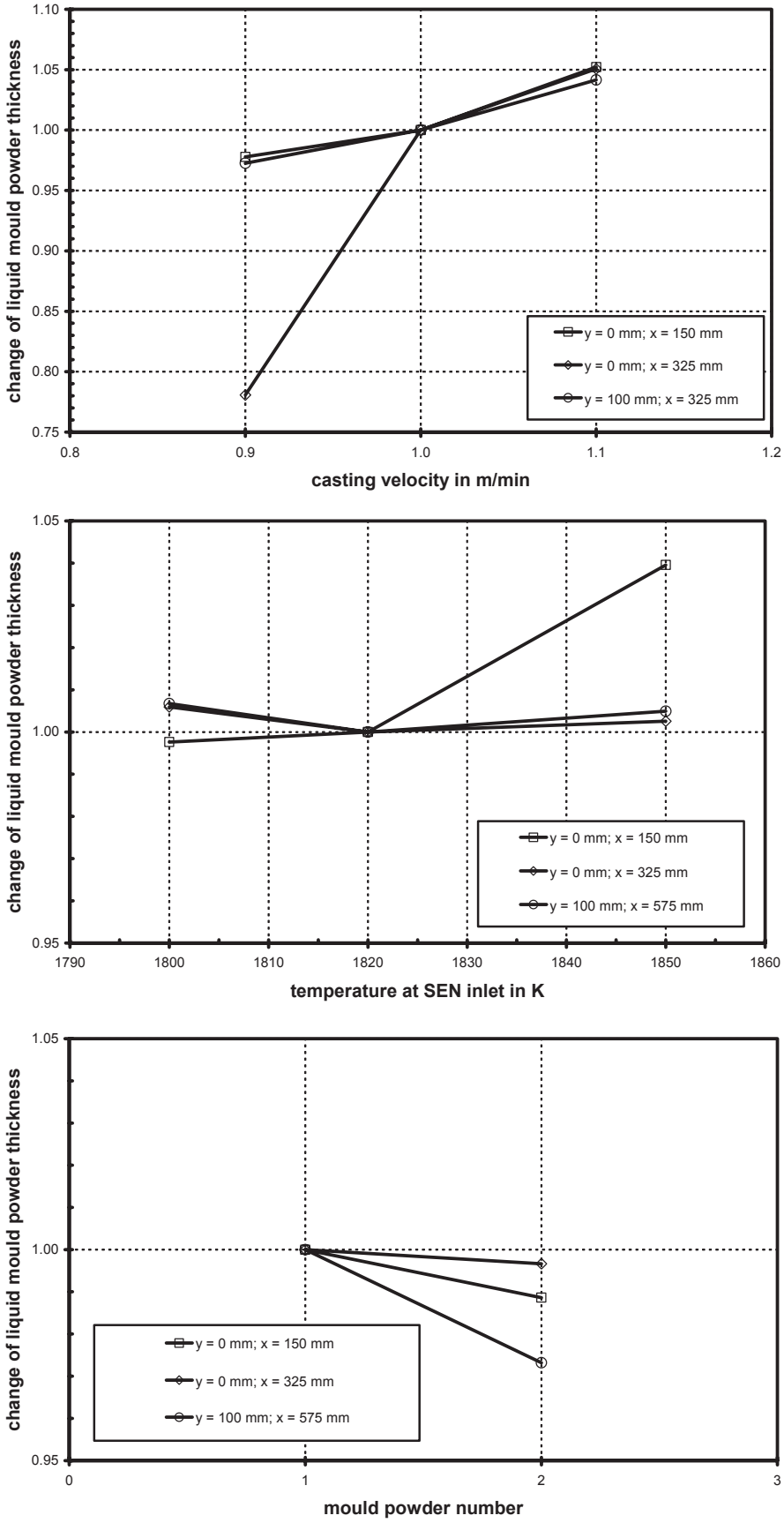

Figure 105 Numerical parameter variation performed at BFI – change of liquid mould powder

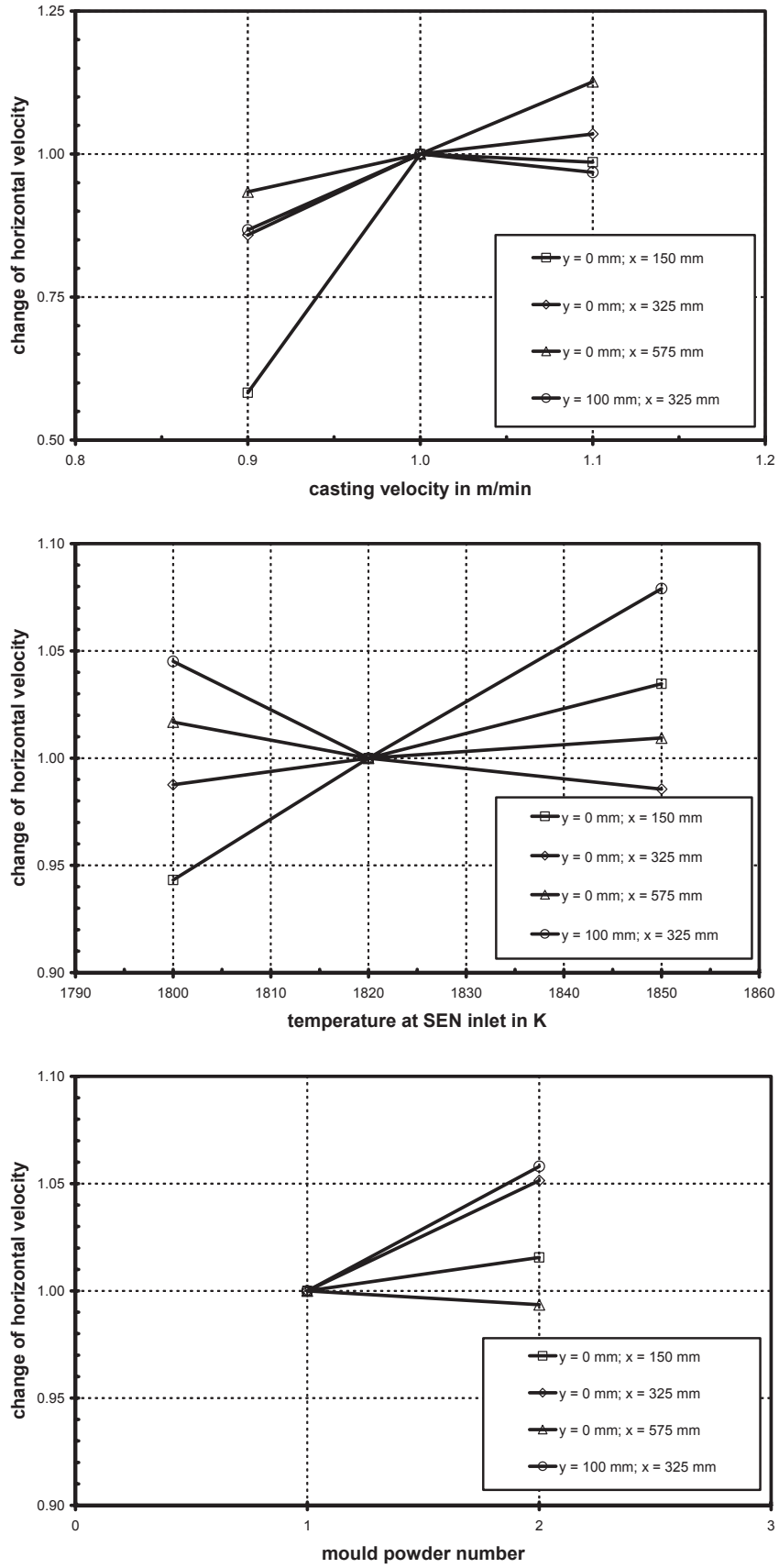

Figure 106 Numerical parameter variation performed at BFI – change of horizontal velocity

All the investigations described within this chapter provided information on the interrelations of casting parameters and flow conditions on wave formation at the interface steel melt/liquid flux as well as on near meniscus horizontal velocities for the operational situation at TKN.

The results of physical and numerical simulation could be validated and are in agreement with operational observations and results.

A great parameter variety was investigated concerning casting velocity, SEN immersion depth, melt superheat and type of casting powder.

Within the frame of the operational window investigated the casting velocity could be identified as a major influence with regard to melting of flux, wave formation and possible flux entrapment. The other parameters showed no significant influence. It can be concluded that under standard steady operational conditions no flux entrapment is expected. This could be confirmed by operational observations and results. So more strong unsteady events at the interface steel melt liquid flux are expected to be responsible for entrapment.

Moreover it can be concluded that further optimisation should also concentrate on the types (i.e. composition, morphology) of fluxes.

In order to set a link to the other partner producing flat products further numerical computations were performed concerning Arcelor España's operational conditions. Here these investigations were aiming at a comparison between a "clean" SEN and a SEN with depositions due to clogging. The latter will be further referred to as "clogged" SEN.

The computations were performed for a so called standard operational condition:

- Format: 1,400 mm x 235 mm
- Casting velocity: 0.95 m/min

Concerning the specifications of the "clean" and the clogged" SEN information as already described in chapter 2.3.2.1 was used.

Figure 107 shows on the left the geometrical set-up with the computational grid for the clean SEN. On the right side Figure 107 shows the situation for the "clogged" SEN with depositions in the port and the well region.

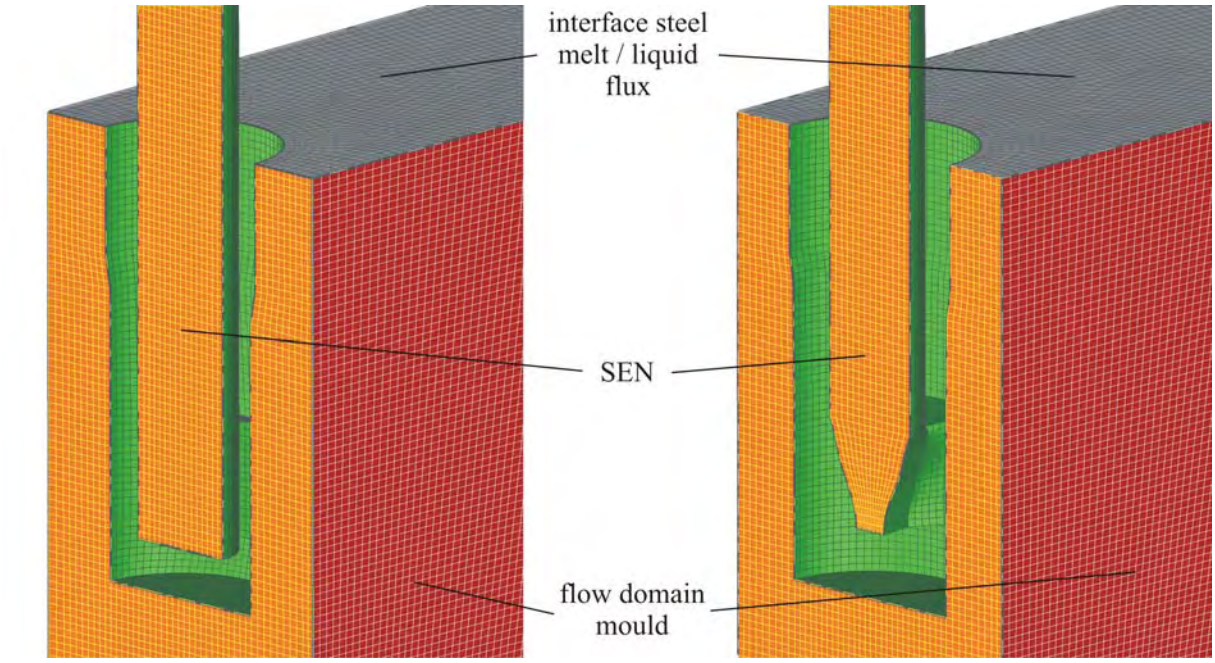

Figure 107 Geometrical set-up and computational grid for Arcelor España operational situation (BFI)

Figure 108 shows the computed flow field (left: velocity vectors; right: velocity contour) in the mould for both SEN configurations in a longitudinal slice (symmetry plane) for the standard case (i.e. 0.95 m/min casting velocity). The clogged situation is always on the left side of each plot, the clean situation on the right. The typical double roll flow structure can be seen for both configurations. The port jets are orientated more horizontally towards the narrow side for the clogged situation. This results in higher horizontal velocities near the interface steel melt/liquid flux.

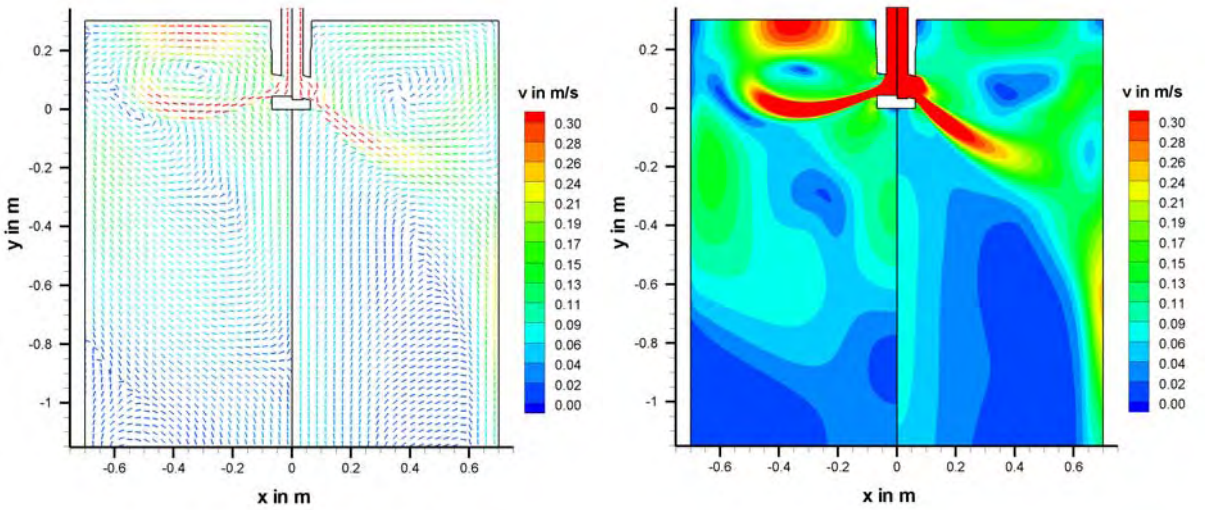

Figure 108 Computed flow field in the Arcelor España mould for a "clean" and a "clogged" SEN, longitudinal slice, symmetry plane (BFI)

Figure 109 shows the profile of the horizontal casting velocity along the mould width for a half mould (symmetry axis).

The typical course of this profile was already found in the previous computations (e.g. see Figure 98). One can see a maximum. The velocity values for the clogged situation are significantly higher than for the clean SEN. The computations had been performed for three casting velocities for each SEN configuration.

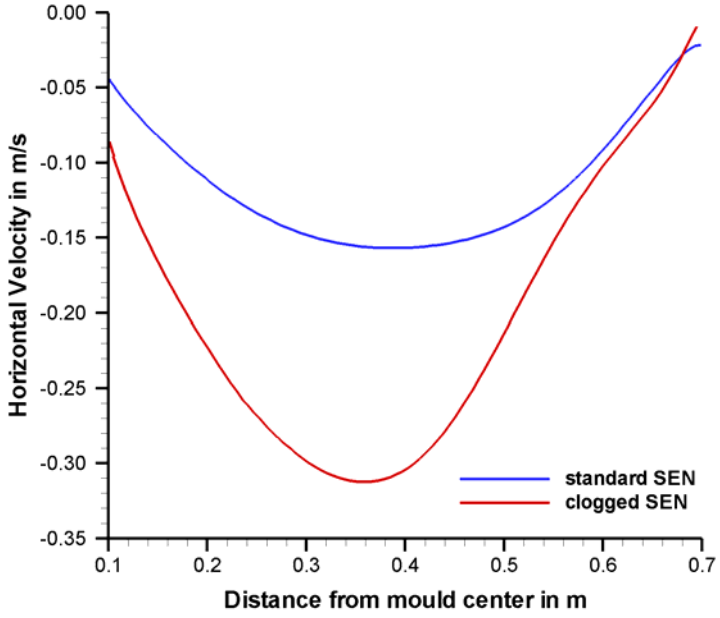

Figure 109 Profile of horizontal velocity in the mould of Arcelor España, half mould width, symmetry axis (BFI)

Figure 110 finally shows the influence of the casting speed on the maximum value of the horizontal flow velocity for two different distances beneath the interface steel melt/liquid flux (i.e. 10 mm and 30 mm). This influence is not so significant within each SEN configuration.

Summarizing it can be stated that there is a clear increase in the velocity value for the clogged SEN which is in accordance with the fact that Arcelor España found more entrapment defects for casts where a clogged SEN was found in the post mortem analysis.

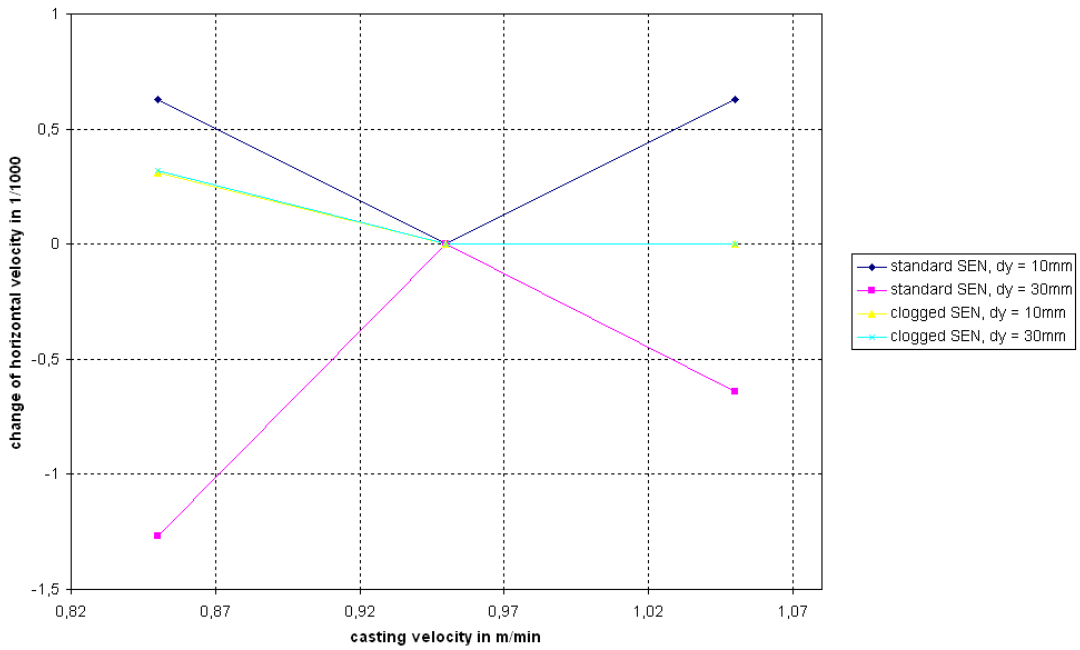

Figure 110 Variation of maximum horizontal velocity near the interface steel melt/liquid flux for different casting speeds ("clean" and "clogged")

2.3.4.5 Identification of optimum arrangements of parameters with regard to improved flux melting with no entrapment for relevant fluxes (Task 4.5)

The modelling investigations described in the previous section brought about indications on the most suitable value for the operating parameters during casting to improve flux melting conditions without leading to slag entrapment.

Optimum flow field

Basically, conditions leading to velocity at meniscus greater than a threshold value indicated by literature around 0.35 m/s should be avoided against risks of slag entrapment occurrence.

Long products. Apart from such a case related to improper nozzle design, flow conditions to be avoided to face slag entrapment occurrence are:

- at start casting (within, say, the first 10 minutes of casting, where the liquid slag layer is only few mm) velocity at meniscus able to induce waves of similar order of magnitude (corresponding to about 10 cm/s), that can break the poor liquid slag layer being formed;
- in steady-state conditions, by avoiding improper nozzle positioning, as nozzle misalignment with respect to mould axis, and not adequate nozzle design, namely:
  - nozzle later ports greater with respect to the central section (especially if rectangular with long size)
  - nozzle port angles not positive (= flow directed upwards, toward the meniscus)

Flat products. Within the frame of the investigated parameters the following parameter arrangements showed positive influence with regard to melting of flux, thickness development and minimisation/avoidance of flux entrapment.

- The main influence is the casting velocity. Here concerning melting and entrapment a value of 1.0 m/min seems to be suitable for the stainless steel. For carbon steel the casting velocity should be higher than 0.6 m/min but the casting rate should not exceed 2.6 to/min. But one has to keep in mind that always other production requirements can hinder a relevant parameter adjustment. This seems to be in accordance with the operational findings.
- The immersion depth of 140 mm seems also to be a good compromise between sufficient horizontal velocity concerning melting but no entrapment. Also this could be proved by slag layer measurements for the stainless steel. For carbon steel a suitable immersion depth here is between 180 mm and 210 mm.
- Argon flow rate should be lower than 15 l/min (carbon steel).
- Mould level variation should be less than 3.8 mm/s (carbon steel).
- Casting temperature (i.e. superheat) seems to be of minor influence.
- For the carbon steel it could be shown that the avoidance of clogging and therefore "keeping constant" the SEN geometry is important concerning the horizontal velocity and therefore the risk of entrapment.

Optimum performance of mould powder

Long products. This summary takes into account that:

- for 'optimum performance' is intended the powder capability to make harder slag entrapment according to the mechanisms identified (i.e., too high perturbation of steel-slag interface at meniscus and slag dragging into the steel being cast);
- the main casting step where such a drawback (slag entrapment) was preferably found to occur is start casting, with the time needed to the powder slag to attain the complete liquid layer thickness.

According to the physical system investigated:

- the liquid layer should be attained as rapidly as possible and as thick as possible (normally, respectively within 15-20 min and about 10-15 mm) = high melting rate. The parameters/quantities affecting melting rate are :

  - Free carbon content = should be as low as possible

  - Carbon particle size = should be as low as possible

The quantities depend on the specific working conditions. From Sidenor data, the thicker liquid pools are associated to free carbon contents greater than about 20%.

As refers to the operating practices to guarantee optimum powder feeding (=compensation between melting rate and consumption), the correlation holds:

$$\text{liquid pool consumption} = (\text{viscosity})^{0.5}/(\text{casting speed})^{0.75}$$

From the statement above mentioned, low viscosity is recommended (but below a certain value infiltration problems can occur). In particular, from the data considered in the frame of the research, viscosity values at least within 10 – 15 Poise are recommended.

Flat products. From the modelling results it can be concluded:

- The viscosity of the type of casting powder within the range investigated here is of minor influence.
- The free carbon content should not exceed a certain value.

2.3.5 Project coordination and reporting

Within the project the partners gained significant value from collaboration.

During the formal coordination meetings there were open discussions on the project activities and results obtained and advice and assistance offered where difficulties had been encountered. There were also free exchanges of data between the partners that aided progress of specific objectives. Data from the casting process at Arcelor España, CAS, Sidenor and TKN were used for the physical and numerical models of BFI and CSM and in return the models used to aid the interpretation of the data from industrial casts.
Formal project meetings were held at BFI (March 2004), Arcelor España (September 2004), CSM (February 2005), TKN (November 2005) and CAS (July 2006).

During the project the technical and financial reports demanded by the European Commission were written and sent to the commission and the TGS3 members as requested by the co-ordinator.

2.4 Conclusions

Extensive investigations concerning influences on and possibilities for controlling of flux melting and flux entrapment were performed.

Concerning detailed conclusions with regard to individual parameters and findings it is referred to chapters 2.3.2.3, 2.3.3.3 and 2.3.4.5. In this section here more general and summarising conclusions should be drawn.

In operational trials correlations between operational trials and flux related defects could be successfully elaborated. Various methods for quality inspection as well as tools for statistical evaluation were proved to be useful to provide the necessary information basis.

Physical and mathematical modelling approaches were developed and applied successfully with regard to simulation of:

- method of flux in terms of melting rate and layer thickness
- 3-dimensional fluid flow in the mould also taken into consideration electromagnetic stirring
- multiphase flow in the mould in terms of
  - evolution and formation of liquid flux layer
  - separation behaviour of entrapped flux droplets

A critical horizontal melt velocity was identified which should be avoided in order to minimise the risk of flux entrapment.

Measurement methods for assessment of flux layer thickness and flow velocity in an operational mould were provided and successfully applied.

The following mean guidelines with regard to sufficient melting of flux on the steel melt in the mould as well as to avoidance/minimisation of flux entrapment could be elaborated.

Flat products

Concerning *casting speed* and *immersion depth* an optimum could be found. In case of carbon steels the immersion depth, in the range investigated here is not so significant.

A changing in *SEN geometry* due to wear or due to clogging has to be minimised. For the stainless steel also a larger port exit area leads to better results.

Mould level stability should be guaranteed to avoid entrapment due to fluctuations.

Concerning mould powder a sufficient low *content of free carbon* should be provided. The *superheat* of the melt has also an influence but not so significant for stainless steel within the frame of these investigations.

Long products

Concerning *casting speed* and *immersion depth* an optimum could be found.

Concerning stainless steel a *SEN geometry* with a five hole design including an enlarged bottom hole could be identified as positive.

The *electromagnetic stirring* has minor influence.

Concerning mould powder a sufficient low *content of free carbon* should be provided.

The *oscillation stroke* should be below a certain limit.

Overall the investigations showed clearly that unsteady operating conditions are the main cause for flux entrapment. Such conditions are given of course during start of casting where the process needs time to achieve a certain stability. A high risk of entrapment is given when a necessary thickness of liquid flux is not provided or temporarily this thickness falls below the necessary value. Also strong flow fluctuations e.g. caused by fluctuations of casting parameters can result e.g. in horizontal flow velocities of the melt reaching the value identified as critical for flux entrapment.

These guidelines are principle ones. Concrete values or set-points for operational parameters, SEN designs and powder types have to be adjusted to the specific production portfolio and plant constellation.

Also other production requirements could limit the application of these guidelines. This project demonstrates how this concretisation for a specific casting situation could be achieved.

2.5 Exploitation and impact of the research results

The outcome of this research are guidelines for adjustment of operational parameters as well as of nozzle design with regard to a sufficient melting of the flux (e.g. sufficient liquid flux layer thickness) and to a minimisation/avoidance of flux entrapment.

Due to the fact that within the frame of these investigations producers of flat and long products casting carbon and stainless steels were involved the results should be useful for a wide range of European steel producers.

The producers involved in this project already have taken over the findings of this research where possible especially taking under consideration actual production requirements. Also plannings are now possible concerning plant or process modifications in order to exploit further results.

No patents were generated as outcome from this project.

References

[1] (7210-PR 272)

[2] Pete Chapman, Julian Clinton, Thomas Khabaza, Thomas Reinartz, and Rüdiger Wirth. CRISP-DM 1.0 step-by-step data mining guide. Technical report, CRISM-DM consortium, 2000. http://www.crisp-dm.org

[3] Kohonen, T: Self Organizing Maps, Ed. Springer, 1995

[4] Rackers, K G; Thomas, B G: "Clogging in continuous casting nozzles". 78th Steelmaking Conference Proceedings, Vol. 78, 1995, pp. 723 – 734.

[5] Huang, X; Thomas, B G: "Modelling of transient flow phenomena in continuous casting of steel", Canadian Metallurgical Quarterly, Vol. 37, 1998, N. 304, pp. 197 – 212.

[6] Hemy, P; Smylie, R; Srinivasan, C: "Analyzing Casting Problems by the On-line Monitoring of Continuous Casting Mold Temperatures", JOMe, Vol. 54, 2002, N. 1

[7] Najjar, F M; Thomas, B G; Hershey, D E: "Numerical study of steady turbulent flow through bifurcated nozzles in continuous casting", Metall. Mater. Trans. B, Vol. 26B, 1995, n. 4, pp. 749 – 765.

[8] Thomas, B G; Bai, H: "Tundish nozzle clogging: application of computational models", 18th Process Technology Division Conference Proceedings, Vol. 18, 200, pp. 895 – 912.

[9] Cramb, A W; Rastogi, R; Maddalena, R L; "Nozzle clogging", The Making, Shaping and Treating of Steel, Casting Volume, 2003, Chapter 9, pp. 1 – 17

[10] Dekkers, R: "Non-metallic inclusions in liquid steel", Ph.D. Thesis. Katholieke Universiteit Leuven, Chapter 9, 2002, pp. 125 – 132

[11] Ludlow, V. et. al.: Mould Powder Consumption, Melting and Lubrication and Its Effect on Mould Heat Transfer and Subsequent Surface Quanlity of Continuously Cast Slab

[12] Grunert, T.: Untersuchung der Veränderung des Gießpulvers während des Gießens Ti-stabilisierter Stähle; Diplomarbeit Universität-Gesamthochschule Duisburg 1990

[13] Solhed, H.: Efforts to Improve Steel Cleanness in the Tundish, Proceedings of the 5th International Conference (1997), pp. 1-10

[14] Mirkovas, A. C.; Argyropoulos, S. A.: A Novel Technique to Estimate Velocity in Liquid Steel and in Other High Temperature Liquid Metals, Transactions of the ISS (1993), pp. 85-94

[15] Normanton, A. et. al.: Detection and Measurement of Asymmetric Flow in the Mould and Assessment of Its Effect on Product Quality of Continuously Cast Slab, Final Report (2003), !Confidential!

[16] Iguchi, M., et. al.: A New Probe for Directly Measuring Flow Velocity in a Continuous Casting Mold, ISIJ International (1996), Vol. 36, pp. 190-193

[17] Hanao, M., et. al.: Influence of Molten Steel Flow Velocity Near the Meniscus in Continuous Casting Mold on Surface Quality of Slabs, ISM November 2000 (2000), pp. 55-60

[18] NKK: Development of Flow Velocity Sensor for Molten Steel, CAMP-ISIJ (1999), Vol. 12, pp. 64-65

[19] Andrezejewski, P.: Mould Flow Monitoring at No. 3 Slab Caster, Krupp Hoesch Stahl AG (1997), pp. 153-172

[20] Plas, D. W. et. al.: Combined Investigations of the EMBR Performance at Continuous Casters of Sollac Dunkerque and Hoogovens Ijmuiden, METEC Congress (1994), pp. 109-118

[21] Ishii, T. et. al.: Numerical prediction of magnetohydrodynamic flow in continuous casting process, Ironmaking and Steelmaking (1996), Vol. 23, pp. 267-272

[22] Moon, K. H. et. al.: Application of EMBR for the Control of Molten Steel Flow in the Continuous Casting Mold, Steelmaking Conference Proceedings (1997), pp. 173-181

[23] Kubo, N. et. al.: Two-phase Flow Numerical Simulation of Molten Steel and Argon Gas in a Continuous Casting Mold, ISIJ International (2002), Vol. 42, pp. 1251-1258

[24] Cervantes, M.: Velocity Measurements in Liquid Steel, La Revue de Metallurgie - ATS – JSI (1998), pp. 240-241

[25] Böcher G.; Berner K.: Einsatz einer elektromagnetischen Bremse an einer Stranggußanlage mit hohen Gießleistungen zur Verbesserung des Reinheitsgrades und er Oberfläche, Technische Forschung Stahl (1995)

[26] Wolf M., private communication in consultancy work.

[27] Mills, K.: Curso sobre Polvos Coladores y Colada Continua, IAS, 2003

[28] Iguchi, M. et al.: 'Model Study on the Entrapment of Mold Powder into Molten Steel', ISIJ International, vol. 40 (2000), n. 7, pp. 685 – 691

[29] Panaras, A. et al.: Metallurgical Trans. B, 1995, pp.1100 ÷1107

[30] Oeters, F.: Metallurgy of Steelmaking, Ed. Springer-Verlag, Berlin

[31] ECSC Agreement 7210/PR-273, 1999, Final report

[32] Mills, K.: 'Curso sobre Polvos Coladores y Colada Continua', August 2003, IAS, S. Nicolas, Argentina.

[33] ECSC Agreement n. 7210.CA/835-429-901-836-332-173-174-702-175, British Steel - CSM - BFI - IRSID - DDS - Krupp Hoesch- MPI -VDEh-Imperial College & University of Athens Final Report, June 1998

[34] Cramb, A. W.; Chung, Y.; Harman, J.; Sharan, A.; Jimbo, I.: 'The Slag-Metal Interface and Associated Phenomena', Molten Slags, Fluxes & Salts '97 Conference, pp. 35÷50

[35] Thomas, B.: http://ccc.me.uiuc.edu, chap. 14, 'Fluid flow in the Mold'.

[36] ISIJ International, vol. 37, (1997), n. 7, pp. 654 ÷ 658.

[37] Zhang, L.; Thomas, B. G.: ISIJ International, Vol. 43 (2003), No. 3, pp. 271–291

List of Tables and Figures

Figure 12 a.) Sample with entrapment of powder B; b.) Crack with powder entrapment (white); c.) transverse section of the defect (X 20); d.) close-up of the previous defect with CC powder entrapment (X 500) (CAS)

Figure 13 Typical on-line panel of the advanced mould monitoring system used at CAS billet caster

Figure 14 Wear of operational SEN's

Figure 15 Example of heat with mould powder entrapment (Heat No 57745, Strand #1) – Example of one heat with bad operational parameters stability (Sidenor)

Figure 16 Example of heat with mould powder entrapment (Heat No 23634, Strand #3) – Example with a fairly good result concerning meniscus stability (Sidenor)

Figure 17 Powder entrapment incidence for the reference caster mould powders (CAS)

Figure 18 Preliminary plant data: correlation between defect index, powder viscosity and melting rate (CAS)

Figure 19 Distribution of entrapment for ULC1 – entrapment density along time where each point represents one slab (right); distribution of slabs by entrapment density (left) (Aceralia)

Figure 20 Distribution of entrapment by slab face. Results for ULC1 in 2005 (a), and previous results (b) (Arcelor España)

Figure 21 Mould section (not drawn at scale) illustrating the preferential deposition of near-surface entrapments in the lower face of the slab (trajectories in black). By contrast deeper inclusions result preferably entrapped in the upper part of the slab (trajectories in blue) (Arcelor España)

Figure 22 Evolution of entrapments after increasing by 10 mm the mould level set point (around slab number 450). The depth of steel surface in mould is represented in green (Arcelor España)

Figure 23 Comparison of defects in slabs with the mould level curves for several slabs of the same heat. Each slab is represented with a different colour. The slab with most defects has also the most important mould level instabilities (Arcelor España)

Figure 24 SOM 2-D representation of the 12 variable problem formed by:

1. Percentage of slab affected by a very quick variation of mould level;
2. Percentage of slab affected by a quick variation of mould level;
3. Percentage of slab with non-automatic level control;
4. Velocity gradient of casting speed;
5. Superheating in tundish;
6. Life of the mould plates (number of heats);
7. Percentage of slab affected by ladle change;
8. Percentage of slab affected by SEN change;
9. Flow rate of gas injected at slide gate system;
10. Max-min mould level variation;
11. Mean-min mould level variation;
12. Entrapment density (Arcelor España)

Figure 25 Statistic correlations between process parameters and occurrence of defect

Figure 109 Profile of horizontal velocity in the mould of Arcelor España (half mould width, symmetry axis)

Figure 110 Variation of maximum horizontal velocity near the interface steel melt/liquid flux for different casting speeds ("clean" and "clogged")

European Commission

EUR 23182 — Enhanced steel product quality and productivity through improved flux performance in the mould by optimising the multiphase flow conditions and with special regard to melting and entrapment

R. Striedinger, L. F. Sancho, J. Díaz, M. De Santis, M. R. Ridolfi, A. Poli, A. Bennani, J. Laraudogoitia, J. Ciriza, J. Holzhauser, L. Ernenputsch

Luxembourg: Office for Official Publications of the European Communities

2008 — 153 pp. — 21 × 29.7 cm

Research Fund for Coal and Steel series

ISBN 978-92-79-07683-1

ISSN 1018-5593

Price (excluding VAT) in Luxembourg: EUR 20